UNIVERSITY COLLEGE LONDON

Department of Genetics, Evolution and the Environment

Development, characterisation and application of an inducible model of Alzheimer's Disease in the fruit fly, *Drosophila melanogaster*

Iain Rogers

September 2011

Thesis submitted for PhD award by University College London

Primary supervisor: Professor Dame Linda Partridge

Secondary supervisor: Professor John Hardy

Dedicated to my Grandma Rogers

'The most each generation can hope for is to reduce the error bars a little, and add to the body of data to which error bars apply' Carl Sagan

Abstract

Alzheimer's disease (AD) is the most common neurodegenerative disorder and the most prevalent form of senile dementia, affecting more than 26 million people worldwide. The amyloid-β42 peptide (Aβ42) has been suggested to play a central role in the pathogenesis of AD. Although the primary etiologic mechanism of AD is unknown, it has a clear association with age. However, is it ageing, the slow erosion of biological function, that is the cause of AD; or is ageing merely a measure of how long it takes to accumulate toxic levels of Aβ? To distinguish between age-dependent and age-independent effects on the rate and extent of AD pathogenesis, an inducible model of Aβ toxicity was developed in the fruit fly *Drosophila melanogaster*. This is a model system where expression of Aβ peptides can be induced for the first time, or turned off, at different ages.

Induced expression of the human Arctic mutant $A\beta_{42}$ peptide in *Drosophila* neural tissue resulted in flies with age-dependent locomotor and electrophysiology deficits and shortened lifespan. Conditional expression of Arctic Aβ42 at different ages was then used to show that ageing renders flies more vulnerable to Aβ42 toxicity. The results of this thesis also served to highlight the technical drawbacks of the GeneSwitch system and the complexities of measuring the effect of ageing interventions such as reduced insulin signalling and the drug rapamycin on Aβ toxicity in *Drosophila*.

Declaration

I can confirm that the work presented in this thesis is my own except where duly noted.

…….

Iain Rogers

Acknowledgements

First and foremost I would like to thank my wife, Beth, for being so patient, supportive and loving during this process. When times were difficult or testing she was always able to give me that extra bit of motivation and confidence to see me through. This work would have not been possible without her. I would also like to thank the Rogers and Brooks families for all their support, guidance and love.

I would like to thank Professor Linda Partridge for giving me this opportunity to work in such a wonderful, exciting lab and for her constant inspiration and encouragement. I would like to thank my second supervisor Professor John Hardy for invaluable feedback during the beginning of my PhD. I'm indebted to Dr. Fiona Kerr and Dr. Onyikan Sofola for 'showing me the ropes' of fly genetics, and for all their constant support and feedback. A big thanks goes to Dr. Hrvoje Augustin for all the electrophysiology work; Dr. Matt Piper for assistance with survivorship analysis; Dr. Ivana Bjedov for help with the radioactivity work; Dr Helena Cocheme for help on figures and answering my trivial questions and Dr Nazif Alic for his feedback and insight (and for making all the RU486). I would also like to thank everyone else at the IHA for making it such a lovely place to spend four-years of my life.

Finally, I would like to thank my sponsors, Eisai who funded the majority of this project. Without their support this PhD would have not been possible.

CHAPTER 1 GENERAL INTRODUCTION 17

1.1 *Alzheimer's disease* 18

1.1.1 Historical perspective and overview 18

1.1.2 Genetics of Alzheimer's disease 22

1.1.3 Neuropathological features of Alzheimer's disease 25

1.1.4 The origin of Aβ: APP metabolism 30

1.1.5 The amyloid cascade hypothesis 35

1.1.6 Framing Aβ toxicity: rise of the oligomer 38

1.2 *Using model organisms to study Alzheimer's disease* 41

1.2.1 Transgenic models of Alzheimer's disease 41

1.2.2 Transgenic models of AD in *Mus Musculus* 44

1.2.3 Transgenic models of AD in *Caenorhabditis elegans* 49

1.2.4 Transgenic models of AD in *Drosophila melanogaster* 51

1.2.5 *Drosophila* life cycle 53

1.2.6 *Drosophila* nomenclature 55

1.2.7 Modelling AD in the fly 56

1.2.8 Models of Aβ toxicity 58

1.2.9 Application of *Drosophila* models of AD 62

1.3 *Ageing as a risk factor for Alzheimer's disease* 63

1.3.1 Ageing and neurodegenerative disease 63

1.3.2 Ramifications of the evolutionary theory of ageing and the birth of modern biogerontology 66

1.3.3 Evidence linking ageing and neurodegeneration 68

1.4 *Thesis Outline* 71

CHAPTER 2 MATERIALS AND METHODS 72

2.1 *Drosophila melanogaster* stocks 73

2.1.1 Wild-type stocks 73

2.1.2 GeneSwitch driver stocks 74
2.1.3 UAS-stocks 75
2.1.4 *chico^{1}/CyO* 76
2.1.5 *w^{Dah}; Sp/CyO; TM6B/Mkrs* 76

2.2 *Food media* 77
2.2.1 Sugar yeast (SY) medium 77
2.2.2 RU486 (RU) SY 78
2.2.3 Rapamycin SY 79
2.2.4 Grape juice medium 79

2.3 *Fly husbandry and culturing* 80
2.3.1 Stock maintenance 80
2.3.2 Distinguishing males and females 81
2.3.3 Virgin Collection 81
2.3.4 Standard larval density 83

2.4 *Experimental procedures* 84
2.4.1 Once-mated females 84
2.4.2 Lifespan assay 85
2.4.3 Proboscis-extension assay during undisturbed conditions 85
2.4.4 Negative geotaxis (climbing) assay 86
2.4.5 Giant Fibre System (GFS) electrophysiology 89
2.4.6 Preparation of flies for molecular biology 89
2.4.7 RNA extraction, cDNA synthesis and Quantitative-PCR (Q-PCR) 90
2.4.8 Total, soluble and insoluble Aβ42 quantification 92
2.4.9 Liquid β-galactosidase quantitative assay 93
2.4.10 ^{35}S-methionine incorporation assay 93
2.4.11 Bradford assay 95
2.4.12 Weight analysis 95

CHAPTER 3 DEVELOPMENT AND CHARACTERISATION OF AN INDUCIBLE MODEL OF ALZHEIMER'S DISEASE 96

3.1 *Introduction*..... 97

3.2 *Results*..... 102

3.2.1 Development of the model 102

3.2.2 Characterisation of elavGS induction kinetics..... 105

3.2.3 Arctic Aβ42 expression can be induced in adult *Drosophila* neurons 107

3.2.4 Induced Arctic Aβ42 protein rapidly aggregates in adult neurons..... 110

3.2.5 Over-expression of Arctic Aβ42 peptide in adult neurons increases mortality and induces neuronal dysfunction in *Drosophila*, without evidence of neuronal cell loss 111

3.3 *Discussion* 120

3.3.1 Induction with the GeneSwitch system is robust but declines with age 120

3.3.2 Transgene expression in the absence of RU486 is a feature of the GeneSwitch system..... 122

3.3.3 The inducible AD model in relation to other fly models of Aβ42 toxicity 123

CHAPTER 4 TESTING THE INTERACTION BETWEEN AGEING AND AD USING AN INDUCIBLE MODEL OF AD..... 127

4.1 *Introduction*..... 128

4.2 *Results*..... 131

4.2.1 Dynamics of Arctic Aβ42 transcript and protein expression using the elavGS-UAS system..... 131

4.2.2 Aβ42-mediated toxicity correlates with total Arctic Aβ42 concentration in young flies 134

4.2.3 The challenges of measuring the effect of ageing on Arctic Aβ42-mediated toxicity 140

4.2.4 Arctic Aβ42 transcript expression equalisation in young and old flies 140

4.2.5 Ageing increases Aβ42 peptide accumulation and toxicity when Arctic Aβ42 transgene expression is normalised between young and old flies 144

4.2.6 Ageing increases neuronal vulnerability to equivalent concentrations of Arctic Aβ42 peptide in young versus old flies 148

4.2.7 Older flies are more vulnerable to chronic Arctic Aβ42-mediated toxicity 163

4.3 *Discussion* 169

4.3.1 The dynamics of Aβ42 expression 169

4.3.2 Aβ42 toxicity is a dose-dependent in *Drosophila* 171

4.3.3 Older neurons are more vulnerable to Aβ42 toxicity 174

4.3.4 Discussion of the Ling *et al*. (2011) study 176

CHAPTER 5 TOR PATHWAY INHIBITION DELAYS AGEING BUT NOT NEURONAL DYSFUNCTION IN AN ADULT-ONSET MODEL OF ALZHEIMER'S DISEASE 179

5.1 *Introduction* 180

5.2 *Results* 184

5.2.1 Rapamycin has no effect on lifespan or neuronal dysfunction in *UAS-Arctic Aβ42/+;elavGS/+* flies in the w^{1118} genetic background 185

5.2.2 Rapamycin delays ageing but has no effect on neuronal dysfunction in *UAS-Arctic/+;elavGS/+* flies in the w^{Dah} genetic background 188

5.3 *Discussion* 196

5.3.1 The effects of rapamycin were inconclusive in the w^{1118} genetic background 196

5.3.2 Rapamycin delays ageing but not neuronal dysfunction in the w^{Dah} genetic background 197

5.3.3 The effects of rapamycin in other AD models 200

CHAPTER 6 INVESTIGATING THE INTERACTION BETWEEN REDUCED INSULIN SIGNALLING AND AB42 TOXICITY IN *CHICO*^{1} MUTANTS 204

6.1 *Introduction*..... 205

6.2 *Results*..... 207

6.2.1 Stock generation 207

6.2.2 Arctic Aβ42-mediated toxicity is suppressed in *chico*^{1} homozygotes..... 212

6.2.3 Arctic Aβ42 expression is reduced in *chico*^{1} homozygotes..... 217

6.3 *Discussion* 221

6.3.1 The suppression of Arctic Aβ42-mediated toxicity in *chico*^{1} homozygotes is an artefact of reduced feeding..... 221

6.3.2 The pitfalls of the GeneSwitch system and possible future resolutions 222

CHAPTER 7 OVERALL CONCLUSIONS AND FUTURE WORK..... 227

7.1 *Summary of findings*..... 228

7.2 *Future work*..... 231

REFERENCES..... 233

APPENDIX..... 250

List of Figures

Chapter 1

FIGURE 1.1. A PHOTOGRAPH OF AUGUSTE DETER 19

FIGURE 1.2. PREVALENCE OF ALZHEIMER'S DISEASE AS A FUNCTION PROJECTED TOTAL NUMBER OF CASES OVER TIME 20

FIGURE 1.3. ATROPHY OF THE BRAIN DURING ALZHEIMER'S DISEASE 26

FIGURE 1.4. NEUROPATHOLOGY OF AD 28

FIGURE 1.5. SCHEMATIC SHOWING AMYLOIDOGENIC AND NON-AMYLOIDOGENIC PROCESSING OF APP34

FIGURE 1.6. THE HYPOTHETICAL SEQUENCE OF PATHOGENIC EVENTS LEADING TO AD PROPOSED BY THE AMYLOID CASCADE HYPOTHESIS 36

FIGURE 1.7. THE *DROSOPHILA* LIFE CYCLE 54

FIGURE 1.8. THE PREVALENCE OF AD HAS A FUNCTION OF AGE 64

Chapter 2

FIGURE 2.1. A PHOTOGRAPH OF THE GLASSWARE AND PLASTICWARE USED FOR STOCK MAINTENANCE AND EXPERIMENTS 78

FIGURE 2.2. PHOTOGRAPH OF GRAPE PLATES USED TO EASILY TRACK AND IDENTIFY EGG LAYING 80

FIGURE 2.3. A PHOTOGRAPH OF THE APPARATUS USED FOR CLIMBING ASSAYS 88

Chapter 3

FIGURE 3.1. A SCHEMATIC REPRESENTATION OF THE CROWTHER *ET AL* (2005) AB MINI-GENE MODEL AND THE GAL4/UAS SYSTEM 99

FIGURE 3.2. A SCHEMATIC REPRESENTATION OF THE GENESWITCH-UAS EXPRESSION SYSTEM 104

FIGURE 3.3. INDUCED β-GALACTOSIDASE ACTIVITY WITH ELAVGS AND ELAVGS302.1 106

FIGURE 3.4. ADULT-ONSET INDUCTION OF ARCTIC AB42 PEPTIDE IN FLY NEURONS 108

FIGURE 3.5. ARCTIC AB42 PEPTIDE IN THE ADULT *DROSOPHILA* NEURONS WAS MOSTLY IN AN INSOLUBLE STATE 111

FIGURE 3.6. EXPRESSION OF ARCTIC AB42 SPECIFICALLY IN ADULT NEURONS SHORTENED LIFESPAN 113

FIGURE 3.7. ARCTIC AB42 PEPTIDES INDUCED PROGRESSIVE, ADULT-ONSET NEURONAL DEFECTS IN *DROSOPHILA* 115

FIGURE 3.8. EXPRESSION OF ARCTIC AB42 PEPTIDES IN THE ADULT FLY NERVOUS SYSTEM CAUSED LOCOMOTOR DYSFUNCTION 117

FIGURE 3.9. NEURONAL CELL LOSS WAS NOT EVIDENT IN FLIES OVER-EXPRESSING ARCTIC AB42 PEPTIDE IN ADULTHOOD 118

Chapter 4

FIGURE 4.1. THE EFFECT OF RU486 REMOVAL ON β-GALACTOSIDASE ACTIVITY 132

FIGURE 4.2. REMOVAL OF RU486 RESULTS IN A ROBUST DECLINE IN UAS-ARCTIC AB42 MRNA EXPRESSION 134

FIGURE 4.3. TOTAL AB42 PROTEIN LOAD INCREASES WITH RU486 EXPOSURE TIME 137

FIGURE 4.4. LOCOMOTOR DYSFUNCTION INCREASES WITH RU486 EXPOSURE TIME 138

FIGURE 4.5. MORTALITY INCREASES WITH RU486 EXPOSURE TIME 139

FIGURE 4.6. ARCTIC AB42 MRNA EXPRESSION EQUALISATION IN YOUNG AND OLD FLIES 142

FIGURE 4.7. AB42 TRANSCRIPT EQUALISATION REDUCES LIFESPAN IN OLD FLIES ONLY 145

FIGURE 4.8. ARCTIC AB42 TRANSCRIPT EQUALISATION HAS DIFFERENTIAL EFFECTS ON PROTEIN EXPRESSION IN YOUNG AND OLD FLIES 146

FIGURE 4.9. PROTEIN TRANSLATION DECREASES WITH AGE 148

FIGURE 4.10. ARCTIC AB42 PROTEIN EXPRESSION LEVELS WITH AGE FOLLOWING CONDITIONAL RU486 TREATMENTS 150

FIGURE 4.11. HYPOTHETICAL PLOTS ILLUSTRATING THE POSSIBLE EFFECTS OF AGEING ON ARCTIC AB42 TOXICITY 153

FIGURE 4.12. OLDER FLIES ARE MORE VULNERABLE WHEN COMPARING THE EFFECT OF EQUALISED ARCTIC AB42 EXPRESSION IN 5-DAY AND 20-DAY TREATED FLIES 156

FIGURE 4.13. OLDER FLIES ARE MORE VULNERABLE TO ARCTIC AB42 WHEN COMPARING THE EFFECT OF EQUALISED ARCTIC AB42 PROTEIN EXPRESSION IN 20-DAY AND 30-DAY TREATED FLIES 158

FIGURE 4.14. OLDER FLIES ARE MORE VULNERABLE WHEN COMPARING THE EFFECT OF EQUALISED ARCTIC AB42 EXPRESSION IN 5-DAY, 20-DAY AND 30-DAY TREATED FLIES 161

FIGURE 4.15. ARCTIC AB42 EXPRESSION LEVELS IN RESPONSE TO CHRONIC RU486 TREATMENT IN YOUNG AND OLD FLIES 165

FIGURE 4.16. OLDER FLIES ARE MORE VULNERABLE TO CHRONIC ARCTIC AB42-EXPRESSION 167

Chapter 5

FIGURE 5.1. RAPAMYCIN HAS NO EFFECT ON AB42-MEDIATED NEURONAL DYSFUNCTION 186

FIGURE 5.2. RAPAMYCIN TREATMENT MAY DELAY AGEING IN FLIES OVEREXPRESSING AB42 187

FIGURE 5.3. RAPAMYCIN EXTENDS LIFESPAN IN W^{DAH} WILD-TYPE FEMALE FLIES 189

FIGURE 5.4. RAPAMYCIN HAS NO EFFECT ON AB42-MEDIATED NEURONAL DYSFUNCTION BUT DOES DELAY SENESCENT-RELATED DECLINE IN LOCOMOTOR FUNCTION 190

FIGURE 5.5. RAPAMYCIN TREATMENT DELAYS AGEING IN FLIES OVEREXPRESSING AB42 192

FIGURE 5.6. RAPAMYCIN HAS NO EFFECT ON TOTAL AB42 PROTEIN LEVELS. 194

FIGURE 5.7. DELAYED SENESCENCE OF NEGATIVE GEOTAXIS IN *CHICO*^{1} HOMOZYGOUS MUTANTS 198

Chapter 6

FIGURE 6.1. CROSSING SCHEME USED TO ESTABLISH THE INDUCIBLE AD MODEL IN A *CHICO*^{1} HOMOZYGOUS GENETIC BACKGROUND 207

FIGURE 6.2. CROSSING SCHEME USED TO GENERATE *CHICO*^{1}/CY*O*; ELAVGS/+ FLIES 209

FIGURE 6.3. CROSSING SCHEME FOR GENERATING *UAS-ARCTIC AB42, CHICO*^{1} RECOMBINANTS 210

FIGURE 6.4. BODY SIZE REDUCTION IN *CHICO1* HOMOZYGOTES 212

FIGURE 6.5. AB42-MEDIATED NEURONAL DYSFUNCTION IS AMELIORATED IN FLIES HOMOZYGOUS FOR *CHICO*^{1} 214

FIGURE 6.6. AB42-MEDIATED AGEING IS DELAYED IN A *CHICO*^{1} HOMOZYGOUS BACKGROUND 216

FIGURE 6.7. ARCTIC AB42 EXPRESSION IS REDUCED IN *CHICO*^{1} HOMOZYGOTES 219

FIGURE 6.8. FEEDING FREQUENCY IS REDUCED IN *CHICO*^{1} HOMOZYGOTES 220

FIGURE 6.9. THE TARGET SYSTEM 225

List of tables

TABLE 1. OVERVIEW OF THE VARIOUS FAD-CAUSING MUTATIONS AND THEIR EFFECTS ON APP PROCESSING AND THE PROPERTIES OF AB 24

TABLE 2. THE VARIOUS RU486 PULSES USED IN SWITCH-OFF EXPERIMENTS 135

Publications arising from this thesis

Appendix

Sofola, O., Kerr, F., Rogers, I., 2010. Inhibition of GSK-3 ameliorates Abeta pathology in an adult-onset Drosophila model of Alzheimer's disease. *PLoS genetics*, 6(9).

Abbreviations

AD	Alzheimer's Disease
APP	Amyloid Precursor Protein
Aβ	Amyloid-β
d	Days
elavGS	Embryonic lethal abnormal vision GeneSwitch driver
ELISA	Enzyme-linked immunoabsorbent assay
FAD	Familial Alzheimer's disease
HD	Huntington's disease
hrs	Hours
IIS	Insulin/Insulin-like signalling
ml	Milli litre
mM	Milli molar
NMJ	Neuromuscular junction
PD	Parkinson's disease
PI	Performance index
Q-PCR	Quantitative polymerase chain reaction
RNAi	RNA interference
RU	RU486
SY	Sugar-yeast medium
TOR	Target of rapamycin
UAS	Upstream activating sequence
w^{Dah}	White Dahomey flies
µM	Micro molar

Chapter 1 General Introduction

1.1 *Alzheimer's disease*

1.1.1 Historical perspective and overview

In 1901, a German psychiatrist and neuropathologist, Alois Alzheimer (1864-1915), admitted a 51-year-old woman, Auguste D., to the state asylum in Frankfurt. She was suffering from an assortment of strange behavioural symptoms including short-term memory loss, language deficits, auditory hallucinations, delusions, paranoia and aggression. After her death in 1906, her brain was sent for examination to the Munich medical school, where Alzheimer had moved in 1903 to work under Emil Kraepelin – one of the foremost German psychiatrists of the era. With the aid of a new silver staining method developed by Max Bielschowsky 4 years earlier, Alzheimer identified two unique lesions in Auguste's brain: amyloid plaques and neurofibrillary tangles.

On the 3rd November 1906, at the 37th meeting of the Society of Southwest German Pyschiatrists in Tubingen, Germany, Alzheimer presented the clinical and neuropathological features of Auguste's case and the following year his talk was published. Auguste's condition remained nameless until Kraeplin, writing in the eighth edition (1910) of his Handbook of Psychiatry, coined the term 'Alzheimer's disease'.

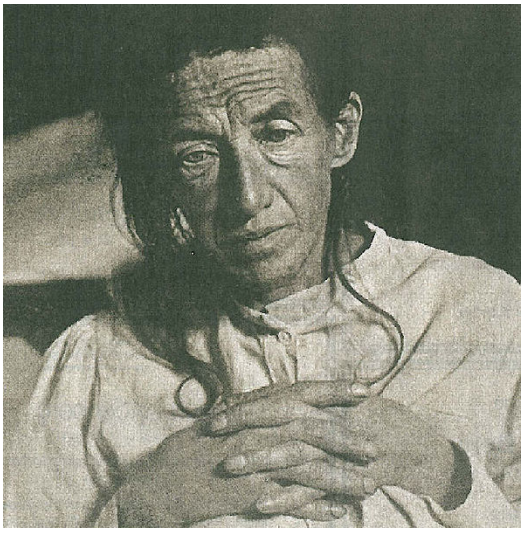

Figure 1.1. A photograph of Auguste Deter. During her time at the Frankfurt state asylum she was often recorded saying, 'I think I have lost myself'.

In over a 100 years since, Alzheimer's disease (AD) has become the most common cause of senile dementia and 7th leading cause of death (www.alz.org), currently affecting more than 26 million people worldwide (Brookmeyer *et al*. 2007). It is a progressive, genetically heterogeneous and fatal neurodegenerative disorder of uncertain etiology, the risk of which dramatically increases in individuals beyond the age of 65. With a rapidly ageing population in the developed world and increasing life expectancy in the developing world, the social and economic burden of AD is set to explode, with some predicting the current prevalence to quadruple by 2050 (see **Figure 1.2**; Ferri *et al*. 2005; Brookmeyer *et al*. 2007).

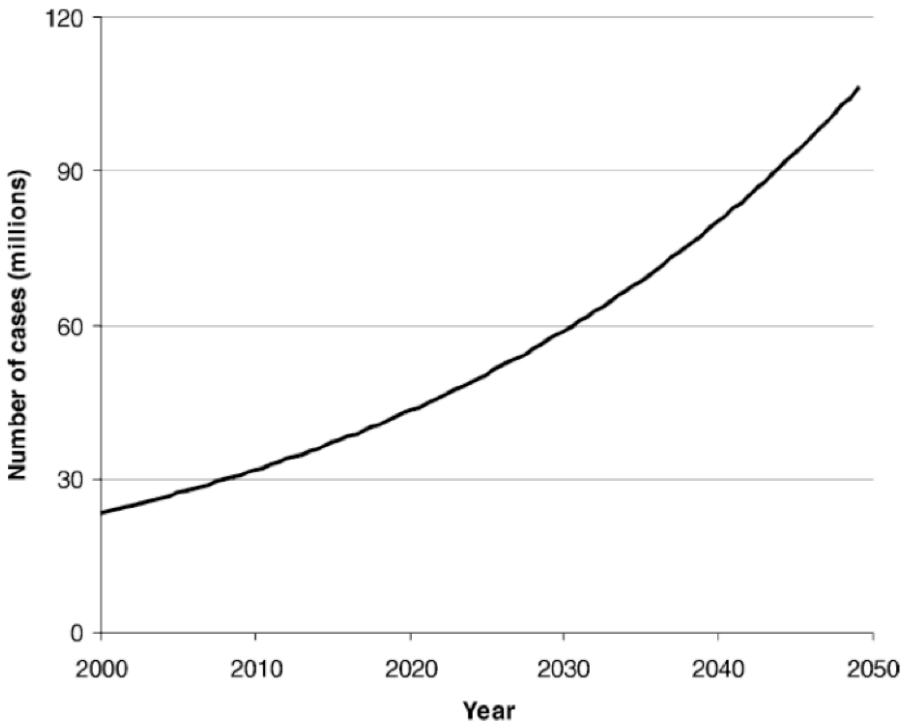

Figure 1.2. Prevalence of Alzheimer's disease as a function projected total number of cases over time. Figure taken from Ferri *et al*. (2005**)**.

The disease is broadly categorised into two subtypes: early onset familial AD (FAD) and late-onset sporadic AD (see section **1.1.2)**. Despite the difference in age of onset, familial and sporadic AD is clinically and histologically identical, characterised by a progressive, global, cognitive decline, involving memory, orientation, judgement and reasoning. Typically, the disease starts with insidious memory problems, advancing to the terminal stages 8-10 years later, where there is complete memory loss of all life-time events together with deficits in verbal and motor control. However, definitive confirmation of the disease requires histological examination of post-mortem brain tissue and the presence of both extracellular amyloid-β (Aβ) plaques and intraneuronal neurofibrillary tangles (NFTs). The neuropathology of AD is covered in more detail in section **1.1.3**.

Amyloid-plaques have long represented one of the hallmark features of AD. However, it took almost 80 years before Aβ was purified and identified as the primary component of meningovascular (blood vessel) amyloid deposits in AD and Down's syndrome (Glenner & Wong. 1984a; Glenner & Wong. 1984b). A year later, the same peptide was recognized as the primary component of senile (neuritic) plaques isolated from AD brain tissue (Masters & Simms. 1985). Around the same time, the microtubule-associated protein tau was identified as the main constituent of the NFTs that accumulate inside many neurons and their processes in AD brains (Grundke-Iqbal *et al*. 1986; Kosik & Joachim. 1986; Nukina *et al*. 1986).

Soon after, the gene encoding APP, of which Aβ is part, was mapped to chromosome 21 (Kang *et al*. 1987). These seminal discoveries marked the beginning of the modern era of AD research, paving the way for the discovery of AD causative genes, the development of the paradigmatic amyloid cascade hypothesis, which accuses Aβ as main villain in AD, and the subsequent engineering of many different transgenic disease models. Unfortunately, although much has been learnt from genetic studies of FAD, the precise molecular events underlying the initiation and progression of AD remain unclear, particularly for sporadic forms of the disease. As a result, no biological markers or specific disease modifying treatments for AD are available and current therapies are palliative at best. With ageing representing one of major risk factors for AD, understanding the link between the ageing process and AD may hold the key to successfully treating the disease.

1.1.2 Genetics of Alzheimer's disease

Genetically, AD is heterogeneous and complex, displaying no single or simple mode of inheritance. Rare, early-onset forms of the disease (FAD) account for less than 5% of all cases and typically affect patients in their 4th or 5th decade. FAD is caused by the inheritance of autosomal-dominant mutations in one of three genes: APP (chromosome 21), which encodes the amyloid precursor protein; and PSEN1 (chromosome 1) and PSEN2 (chromosome 14) which encode the presenillins 1 and 2, respectively. Notably, all these mutations affect APP processing and act to either increase the total amount of Aβ, increase the Aβ42/Aβ40 ratio or to increase the propensity for Aβ to aggregate (**Table 1**). Up-to-date information regarding FAD-causing mutations can be found at the Alzheimer's Disease Mutation Database (www.molgen.ua.ac.be/ADMutations).

Mutations in the APP gene were the first to be identified (Goate *et al*. 1991) and to date 37 unique, missense mutations have been discovered in 89 families (www.molgen.ua.ac.be/ADMutations). The effect of each APP mutation depends in part on its position in the molecule. Mutations found near the N-terminal site (beta-secretase cleavage site) of the Aβ peptide such as the Swedish mutation, a double K670M/N671L substitution (Mullan *et al*. 1992), can result in increased Aβ production (Citron *et al*. 1992). Mutations within the Aβ domain, such as the Arctic mutation, a Glu22Gly amino acid substitution, typically increase the propensity of Aβ to aggregate (Nilsberth *et al*. 2001; Murakami *et al*. 2002) Additionally, mutations found near the C-terminus, such as the London mutation, a V717I substitution (Goate *et al*. 1991), result in increased production of Aβ42 relative to Aβ40 (Suzuki *et al*. 1994; Tamaoka *et al*. 1994).

APP gene dosage can also have an effect. In Down's syndrome (trisomy 21) patients, who have an extra copy of APP, Aβ42 levels are significantly higher (Tokuda *et al*. 1997) and invariably lead to AD-like pathology. Moreover, in an extremely rare example, five familial cases of AD and congophillic amyloid angiopathy (CAA), an amyloid disease where Aβ is deposited in nervous system blood vessels, were recently discovered to be a result of duplication of the APP locus (Rovelet-Lecrux *et al*. 2006).

Mutations in APP only account for 1% of all familial cases (Brouwers *et al*. 2008). The majority of familial cases are caused by mutations in the genes encoding presenilin-1 (PS1) and presenilin-2 (PS2), the two proteins that provide the catalytic core of γ-secretase. To date, 182 FAD mutations have been identified in PS1 and 13 FAD mutations in PS2 (www.molgen.ua.ac.be/ADMutations). Mutations in PSEN1 and PSEN2 are scattered across the protein but typically result in an increase in the Aβ42/Aβ40 ratio.

Gene	Type of mutations	Location of mutations	Effect of mutations
APP	missense	N-terminal of Aβ peptide (β-secretase site)	enhanced β-secretase cleavage → increased Aβ production
APP	missense	Aβ peptide encoding region	alteration of the Aβ sequence and its properties → increased aggregation propensity → increased protofibril and/or fibril formation reduced α-secretase cleavage → increase in β-secretase substrate
APP	missense	C-terminal of Aβ peptide (γ-secretase sites)	decreased cleavage at $A\beta_{40}$ and/or increased cleavage at $A\beta_{42}$ → relative increased production of $A\beta_{42}$ compared to $A\beta_{40}$
APP	gene/locus duplication	whole gene	increased levels of APP as substrate for Aβ production; relatively increased production of $A\beta_{42}$ compared to $A\beta_{40}$
APP	promoter mutations	5′ regulatory region	increased levels of APP as substrate for Aβ production
PSENs	missense mutations—insertions/deletions—genomic deletions	scattered over the protein	decreased γ-secretase activity alterations in the position of the cleavage site → relative increased production of $A\beta_{42}$ compared to $A\beta_{40}$

Table 1. Overview of the various FAD-causing mutations and their effects on APP processing and the properties of Aβ. Figure taken from Brouwers *et al*. (2008).

By contrast, sporadic forms of AD, which account for the majority of cases and typically affect patients in their 7th decade, have a multifactorial etiology in which a wide range of genetic polymorphisms have been identified as predisposing factors. The most robust findings are for the gene encoding apolipoprotein E, particularly the ε4 allele, which has been shown to increase the risk of developing sporadic AD (Corder *et al*. 1993). Conversely, it has been shown that the ε2 allele may confer some protection (Corder *et al*. 1994). Although the exact mechanism is unclear, there is evidence that ApoE may alter Aβ levels through modulation of γ-secretase activity (Irizarry *et al*. 2004). Many other disease-predisposing genetic polymorphisms have been identified including: insulin-degrading enzyme (IDE), which plays a role in the catabolism of Aβ; ubiquillin-1 (UBQLN1), which affects intracellular APP trafficking; sortilin-related receptor 1 (SORL1); and α2-macroglobin The exact details of

these polymorphisms are beyond the scope of this thesis, but a comprehensive review can be found in Brouwers *et al*. (2008).

As with other age-related diseases (cardiovascular diseases, diabetes, cancer and so on) sporadic AD is associated with a host of dietary, behavioural and other environmental risk factors. Advancing age is the most prominent, with incidence in the general population rising from 6% in those over 65 years to 30% in those over 85 years (Ferri *et al*. 2005). Other studies have linked cerebral microvascular pathology, such as reduced blood supply to the brain or disrupted microvascular integrity in cortical regions, to the development of sporadic AD (for review see Farkas & Luiten. 2001). A low education level (Koepsell *et al*. 2007), traumatic brain injury (Van den Huevel *et al*. 2007), depression (Ownby *et al*. 2006), consumption of high-calorie, high-fat diets and a sedentary lifestyle have all been highlighted as potential risk factors (Mattson. 2004).

1.1.3 Neuropathological features of Alzheimer's disease

Because memory loss is a symptom with many underlying pathologies, definitive diagnosis of AD requires post-mortem examination of the brain. Macroscopically, AD is characterized by synaptic degeneration and neuron loss in the cerebral cortex (the outermost layer of the brain associated with higher-order functions) and certain sub-cortical regions. This results in gross cortical atrophy, particularly in the frontal, parietal and temporal lobes (**Figure 1.3**). The temporal lobes are the location of the hippocampus and the entorhinal cortex, two areas critically important in the formation of new memories. Notably, these structures are two of the first to suffer damage during AD. Interestingly, there is

relative sparing of occipital, and primary motor and sensory regions. The ventricular system, cavities in the brain containing cerebrospinal fluid that provide mechanical support to the brain, are also frequently found enlarged.

Mere changes in the anatomical structure of the brain are not sufficient for diagnosis, since these features are not specific to AD (Mott & Hulette. 2005). A definitive diagnosis requires histopathological examination of brain tissue, which must contain a sufficient number of senile plaques and neurofibrillary tangles (**Figure 1.4**).

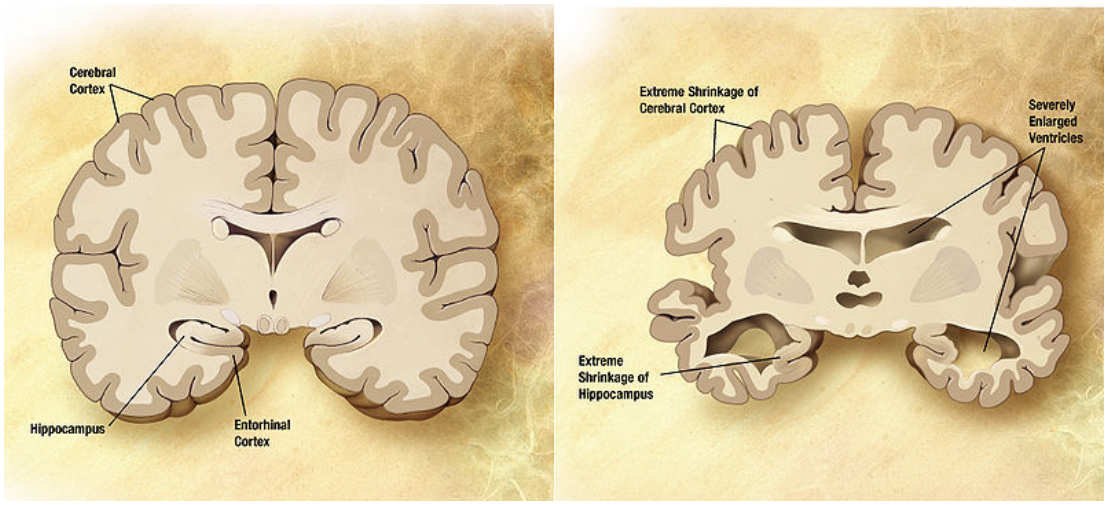

Figure 1.3. Atrophy of the brain during Alzheimer's disease. The image on the left represents a normal, healthy brain whereas the image on the right represents typical gross changes to the brain in severe AD (image taken from www.nia.nih.gov/Alzheimers/Resources/HighRes.htm).

Senile, or amyloid, plaques are extracellular deposits of fibrillar and amporphous aggregates of amyloid-beta peptides (Aβ) (Glenner & Wong. 1984b; Masters *et al*. 1985) that occur principally in a filamentous form, i.e., as star-shaped masses

of Aβ fibrils rich in β-pleated sheet structure (Selkoe. 2001). Senile plaques are complicated and heterogeneous lesions ranging between 10-160μm in diameter and may either be 'cored', with a dense core of fibrillar Aβ (**Figure 1.4a**), or diffuse (**Figure 1.4b**). Cored plaques are typically found in limbic structures and the association neocortex (outermost part of frontal cortex) and are often neuritic, surrounded by dystrophic neurites (degenerated axons and dendrites) and glial (reactive astrocytes and active microglia) cellular elements. Much of the fibrillar Aβ found in neuritic plaques is Aβ42 (Iwatsubo *et al*. 1994), the slightly longer and more hydrophobic form that is prone to aggregation (Jarret *et al.* 1993). However, Aβ40 has also been shown to co-localise to a lesser extent with Aβ42 in plaques, particularly those of the mature type (Iwatsubo *et al*. 1994; Iwatsubo *et al*. 1995).

Diffuse plaques, commonly referred to as 'pre-amyloid deposits', were first identified in the late 1980's (Joachim *et al*. 1989; Tagliavini *et al*. 1988) following the sequencing of Aβ and subsequent development of antibodies sensitive to endogenous and synthetic Aβ. Diffuse plaques demonstrate light, amorphous Aβ-immunoreactivity without a clearly fibrillar, compacted centre (**Figure 1.4b**). They are mainly composed of Aβ42, rather than a mix of Aβ40, as seen in neuritic plaques, and are associated with little or no neuritic dystrophy. They are found in areas typical of neuritic plaques (limbic and association cortices) but also in areas not clearly implicated in the symptomatology of AD, such as the thalamus and cerebellum (Joachim *et al*. 1989). These observations led to the idea, diffuse plaques may represent immature lesions - the beginnings in the formation of neuritic, cored plaques. Aβ deposits can also be found in

blood vessel walls, in the form of congophillic amyloid angiopathy (CAA) (**Figure 1.4c)**.

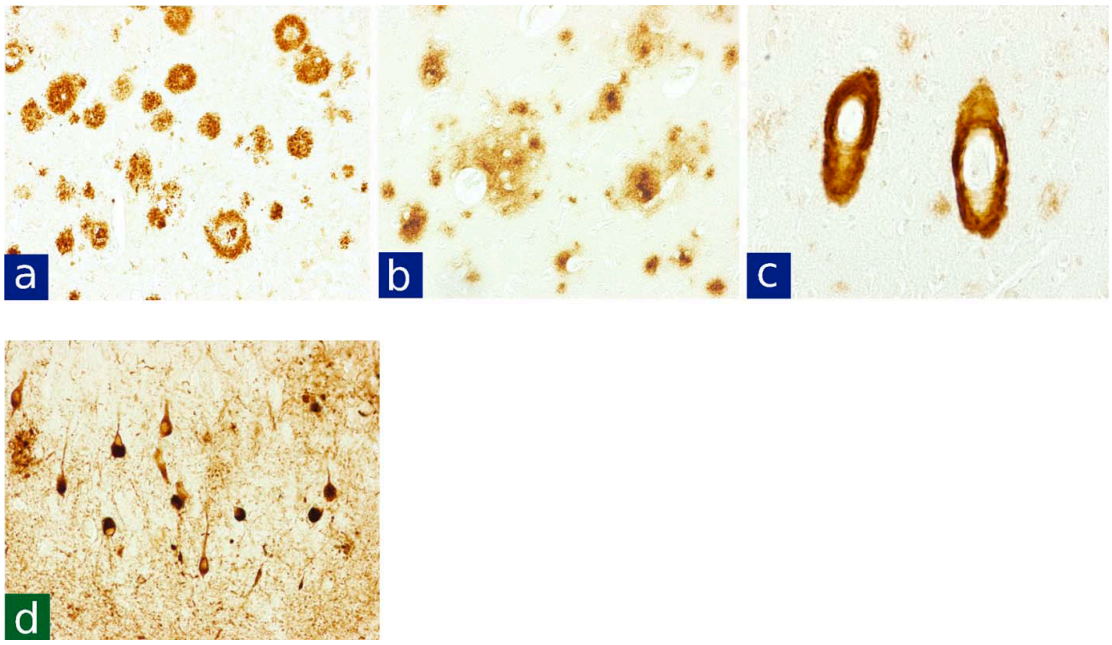

Figure 1.4. Neuropathology of AD. Immunohistochemistry with antibodies to Aβ: senile plaques (a), preamyloid deposits (b), and amyloid angiopathy (c). Immunohistochemistry for phosphorylated tau in NFTs (d). Figure taken from Minati *et al*. (2009).

Many neurons of the brain associated with plaque pathology are found to contain intraneuronal, non-membrane bound bundles of abnormal fibres. These fibres consist of pairs of ~10-nm filaments wound in helices, otherwise known as paired helical filaments (PHFs). PHFs are themselves composed of insoluble fibrillar aggregates of the microtubule-binding protein tau (Grundke-Iqbal. 1986; Kosik *et al*. 1986; Nukina & Ihara. 1986), which is found to be in a hyperphosphorylated state (Hanger *et al*. 1991). These neurofibrillary tangles (NFTs) (**Figure 1.4d**) are the other defining feature of AD neuropathology and

their accumulation in the brain follows a defined pattern as the severity of the disease progresses (Braak and Braak. 1991). Initially, they are confined to the entorhinal cortex and hippocampus in what is known as Braak and Braak stages I-II, before spreading throughout all neocortical association areas during Braak and Braak stages III-IV.

It is still unclear how the neuropathological features of AD relate to each other and more importantly, to the emergence of cognitive impairments. Memory deficits occurring early in the disease process appear to correlate best with synaptic loss, prior to overt neuronal loss (Terry *et al*. 1991) and possibly to the number of NFTs (Arriagada *et al*. 1992). Interestingly, it has been found that the number of plaques in the brain correlates weakly with the degree of dementia experienced in life (Terry *et al* 1991; Arriagada *et al*. 1992). This is exemplified by the fact that healthy, cognitively normal humans can have substantial amounts of Aβ amyloid present at death (Katzman *et al*. 1988; Delaere *et al*. 1990). These observations have been confirmed in transgenic mouse models of AD, where overexpression of FAD-associated mutant APP causes memory and cognitive deficits prior to the detection of plaque pathology (Mucke *et al*. 2000; Oddo *et al*. 2003; Billings *et al*. 2005; Lesné *et al*. 2008). Furthermore, studies in transgenic mice that overexpress APP have indicated that the accumulation of insoluble Aβ is accompanied by minimal neuron loss (Irizarry *et al*. 1997a; Irizarry *et al*. 1997b) and that the relationship between plaque load and the degree of memory impairment is relatively weak (Holcomb *et al*. 1999; Westerman *et al*. 2002). Following the development of sensitive Aβ enzyme linked immunoabsorbent assays (ELISA), it was found that the degree of

dementia in AD correlates much better with the concentration of soluble Aβ species (Lue *et al*. 1999; Wang *et al*. 1999). This observation and further studies have led to the suggestion; small soluble, oligomeric assemblies of Aβ are the ultimate cause of synaptic dysfunction and memory impairment in early AD (see **1.1.5**)

1.1.4 The origin of Aβ: APP metabolism

Aβ peptides are derived from endoproteolysis of the parental amyloid precursor protein (APP). APP is a ubiquitously expressed type I transmembrane protein with a large, extracellular, glycosylated N-terminus, a single trans-membrane domain and a shorter cytoplasmic C-terminus (Kang *et al*. 1987). The Aβ region is located at the cell surface (or the lumenal side of the endoplasmic reticulum (ER) and Golgi membranes) with part of the peptide embedded in the membrane. As a consequence of alternative splicing, several isoforms of APP exist, ranging in length between 695 and 770 amino acids (Selkoe. 2001). APP751 and APP770 are widely expressed in non-neuronal cells and neuronal cells (Selkoe. 2001). The APP695 isoform however, is the most abundant in neurons (Tanzi *et al*. 1987) and differs by the lack of a Kunitz-type protein inhibitor (KPI) sequence in its extracellular domain. Interestingly, the relative expression of each APP isoform may be important for the development of AD. It has been reported that there is a shift in expression from APP695 to KPI-containing APP isoforms in AD and that this shift correlates with higher soluble Aβ levels (Matsui *et al*. 2007).

APP is now known to be a member of a larger gene family, the amyloid

precursor-like proteins (APLPs), which includes APLP1 and APLP2 in humans, the fly homolog Appl (Rosen *et al*. 1989) and the worm homolog apl-1 (Daigle & Li. 1993). All genes in this family encode type 1 membrane proteins with a large extracellular domain and short cytoplasmic region and undergo processing similar to APP. Notably, only APP contains the sequence encoding the Aβ domain. The biological function of this family, particularly APP, is unclear. There is some confusion as to whether APP functions as a *bona fide* signalling receptor and/or adhesion molecule or whether the physiological function derives from the proteolytic fragments generated in its metabolism. Either way, APP has been implicated in a variety of important roles ranging from cell adhesion and cell movement to synaptic plasticity and insulin and glucose homeostasis (Review in Jacobsen & Iverfeldt. 2009). Whatever its exact function, APP clearly has a subtle role. APP-deficient mice ($APP^{-/-}$) are viable and fertile, displaying only minor abnormalities such as impaired locomotor function and gliosis (Zheng *et al*. 1995).

APP is subject to cleavage by a group of proteases known as alpha-secretase, beta-secretase and gamma secretase. The precise identity of the α-secretase is unclear but studies have identified several enzymes belonging to the ADAM (A disintegrin and metalloproteinase) family of proteases, including ADAM9 (Koike *et al*. 1999), ADAM-10 (Lammich *et al*. 1999) and tumour necrosis factor-alpha converting enzyme (TACE)/ADAM-17 (Buxbaum *et al*. 1998). It has been shown in cell culture that endogenous alpha-secretase activity may be composed of several ADAM enzymes (Asai *et al*. 2003). Beta-secretase has been identified as a novel transmembrane aspartyl protease, now termed the beta-site

APP cleaving enzyme-1 (BACE1) (Vassar *et al*. 1999). Since mice deficient in BACE-1 do not produce any Aβ (Luo *et al*. 2001), BACE-1 is thought to be the only *in vivo* protease with clear beta-secretase activity. Interestingly, these mice are healthy, fertile and phenotypically normal (Luo *et al*. 2001), raising the potential of BACE-1 inhibition as a viable therapeutic intervention. Gamma-secretase has been identified as a multi-protein complex consisting an array of proteins including presenillin 1 or 2, nicastrin, Aph-1 and Pen-2. The presenillins function within this group to provide the catalytic core of the protein (Wolfe *et al*. 1999).

APP can be processed in two ways (**Figure 1.5**). In the prevalent, non-amyloidogenic pathway, which precludes Aβ generation, APP is first cleaved within the Aβ domain by α-secretase, releasing a large N-terminal ectodomain (sAPPα) into the extracellular/lumenal medium. Interestingly, sAPPa has been reported to have neurotrophic and neuroprotective properties (Furukawa *et al*. 1996; Meziane *et al*. 1998). Following α-secretase cleavage, the resulting 83-amino acid C-terminal membrane stub (C83) is then cleaved by γ-secretase, producing a fragment known as p3. P3 is believed to be benign or even neuroprotective (p3 is not found in compact amyloid plaques, reviewed in Dulin *et al*. 2008).

The amyloidogenic pathway involves the sequential cleavage of APP by β- and γ-secretase at the N and C termini respectively and leads to the release of Aβ peptides. APP is first cleaved by β-secretase, releasing sAPPβ into the extracellular space, leaving a 99-amino-acid C-terminal stub (C99). Unlike the

neuroprotective effects of sAPPα, sAPPβ appears to have a proapoptotic function. Nikolaev *et al*. (2009) demonstrated that sAPPβ can be further processed (by a currently unknown protease) to generate an N-terminal derivative that binds to the death receptor DR6, resulting in axonal pruning and apoptosis during development.

Following beta-secreatase cleavage, C99 is cleaved within the membrane by γ-secretase. Depending on the exact point of cleavage by γ-secretase, three principal forms of Aβ, comprising 38, 40 or 42 amino acids, are produced. The relative amount of Aβ42 formed is particularly noteworthy, because this longer form of Aβ is more hydrophobic and far more prone to oligomerise and form amyloid fibrils (Jarret *et al*. 1993) than the more abundantly produced Aβ40. This is particularly exemplified by the fact Aβ42 is the predominant isoform found in both amyloid and diffuse plaques (Iwatsubo *et al*. 1994).

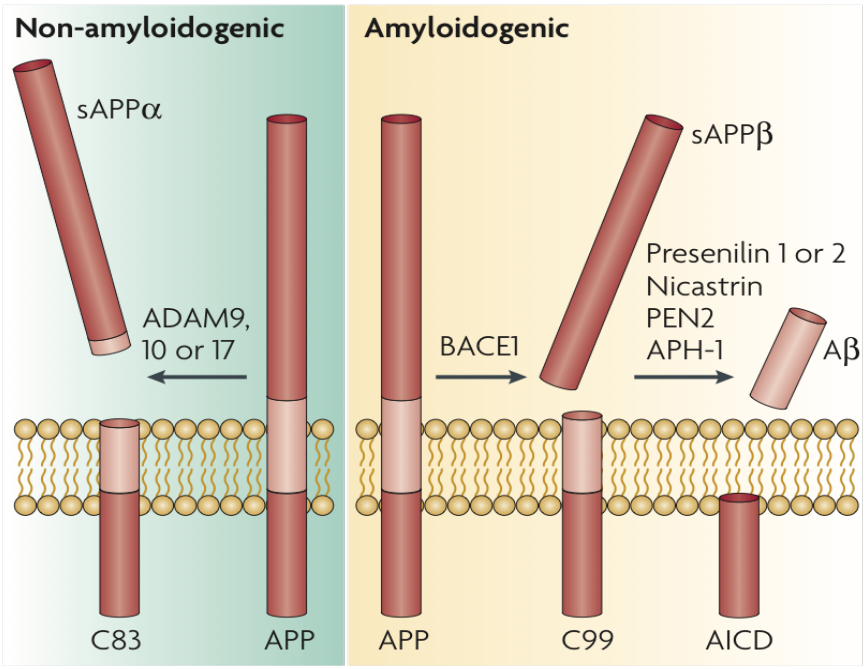

Figure 1.5. Schematic showing amyloidogenic and non-amyloidogenic processing of APP. Figure taken from Laferla *et al*. (2007).

For many years Aβ production was considered a pathological event. It was thought cleavage of C99 could only occur following some preexisting membrane injury – the idea of cleavage occurring within the plane of the membrane was unheard of (Selkoe. 2001). Hence, there was much surprise when it was demonstrated that Aβ production is a normal, physiological event as exemplified by the detection of Aβ in cell culture (cells overexpressing APP) (Haas et al, 1992) and in the brains and human cerebrospinal fluid (CSF) of healthy humans throughout life (Seubert *et al*. 1992; Shoji *et al*. 1992; Busciglio & Gabuzda. 1993).

After APP is synthesized in the endoplasmic reticulum (ER), the mature glycosylated form of APP in the trans-Golgi network (TGN) is transported to the plasma membrane, where it is rapidly processed – the half-life of APP in cell culture is typically 45-60 minutes (Selkoe. 2001). Any unprocessed APP can be reinternalised into endosomal compartments through clathrin-coated pits (Nordstedt *et al*. 1993), then either recycled back to the cell surface or transported to the endosomal/lysosomal system for degradation (Haass *et al*. 1992). Theoretically, APP processing could occur in many cellular compartments, giving rise to both secreted and intracellular forms of Aβ (i.e. secreted into vesicle lumens). Although it is widely accepted the vast majority of Aβ is secreted, it is suspected the main source of extracellular Aβ is APP processed from an intracellular location such as the ER, TGN and the endosomal/lysosomal system rather than the plasma membrane (where the

majority of alpha-secretase cleavage is believed to occur (Parvathy *et al*. 1999). In fact, evidence seems to implicate the endosomal/lysososomal pathway as the main source of intracellular Aβ, because this is where the majority of beta- and gamma-secretase cleavage of APP occurs, following re-internalisation of APP (Pasternak *et al*. 2004). Morever, the low pH of endosomal/lysosomal pathways is optimal for BACE1 cleavage of APP (Laferla *et al*. 2007) and it has been shown that low pH favours Aβ aggregation (Carrotta *et al*. 2005). Also, prior to extracellular Aβ deposition, the intracellular pool of soluble Aβ rises substantially in endosomal-lysosomal compartments (Cataldo *et al*. 2004; Takahashi *et al*. 2004) and remains substantial even in the heavily plaque-laden AD brain (Näslund *et al*. 2000).

1.1.5 The amyloid cascade hypothesis

Although the exact etiology of AD remains elusive, the amyloid cascade hypothesis remains the best-defined and most studied conceptual framework for AD. In essence, the amyloid cascade hypothesis proposes that increased production or decreased clearance of Aβ42 peptides is the primary influence driving all forms of AD (Hardy and Selkoe. 2002). The hypothesis outlines a linear pathological cascade beginning with an increase in Aβ production and accumulation and the formation of soluble Aβ oligomers. This culminates in a series of downstream pathological events including synaptic injury, inflammation, oxidative damage and tau dysfunction that in turn result in widespread neuronal dysfunction and cell death (see **Figure 1.6**)

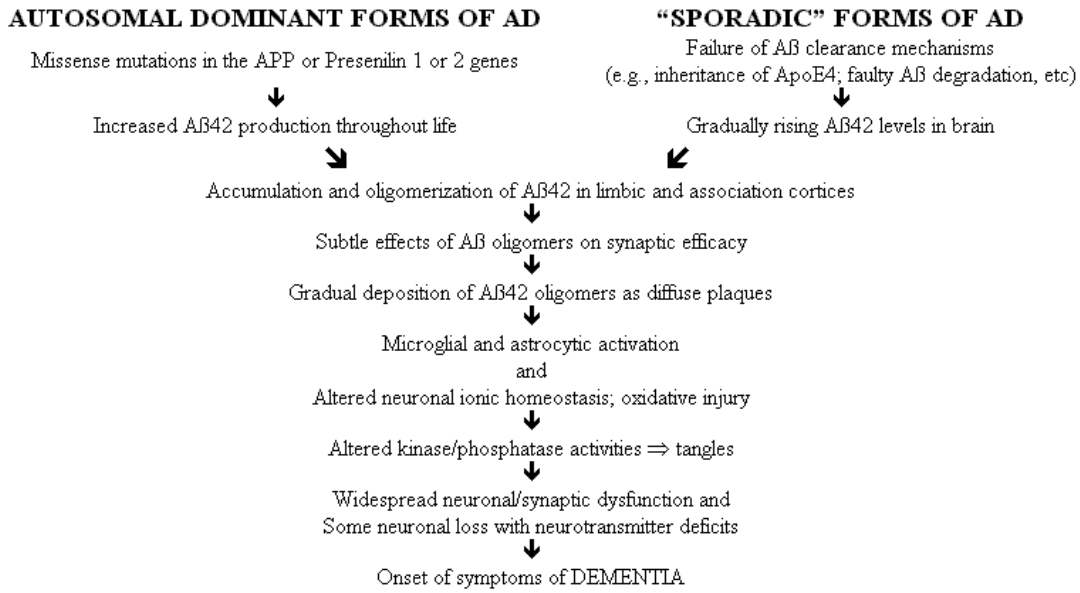

Figure 1.6. The hypothetical sequence of pathogenic events leading to AD proposed by the amyloid cascade hypothesis. Figure taken from Hardy and Selkoe. (2002).

Support for a causal role for Aβ in AD is overwhelming. The first major piece of evidence came from the localisation of the APP gene to chromosome 21 (Kang *et al*. 1987). Since 1969, it had been known that middle-aged patients with Down's syndrome (trisomy 21), invariably develop AD-like pathology (Olson & Shaw. 1969) and that the amyloid plaques found in these patients are predominantly composed of Aβ (Glenner & Wong 1984a; Masters *et al*. 1985). Thus, the mapping of APP to chromosome 21 was significant because it hinted that the extra copy of APP was to blame for the development of AD-like pathology in Down's. Moreover, Down's patients have higher total levels of Aβ, as would be expected with an extra copy of the APP gene (Tokuda *et al*. 1997). This

relationship was further strengthened by the detection of a rare case of Down's syndrome in which the distal location of the chromosome 21q breakpoint left the patient diploid for the APP gene (Prasher *et al*. 1998). This individual displayed no signs of dementia, and amyloid deposition was essentially absent from the brain upon death. Conversely but in a similar vein, five familial cases of AD and CAA were recently identified to be exclusively the result of duplication of the APP locus (Rovelet-Lecrux *et al*. 2006).

Perhaps the strongest support for the amyloid cascade hypothesis comes from genetic studies, which have demonstrated that all FAD causing mutations in APP, PS1 and PS2 (for which there are now over 200) either result in increased production of Aβ, increased production of Aβ42 relative to Aβ40, or an increased propensity for Aβ42 to aggregate (for details see **1.1.2.**). These genetic data are supported by the many mouse models of AD that develop Aβ plaques and exhibit memory deficits (covered in more detail in **1.2.1**). These transgenic mouse models are typically based on overexpression of FAD mutant APP or PS1 (or both). Furthermore, similarly designed models in the fruit fly *Drosophila* and the nematode worm *Caenorhabditis elegans* have demonstrated that APP and Aβ overexpression result in an age-dependent accumulation of Aβ, neuronal dysfunction and increased mortality (see section **1.2**.).

Neurofibrillary tangles represents the other major neuropathological hallmark of AD yet mutations in tau, the major constituent of NFTs, do not cause AD but instead have been linked to frontotemporal dementia (FTD) with parkinsonism (Hutton *et al*. 1998). Moreover, this neurodegenerative disorder is characterized

by severe deposition of tau in NFTs in the brain but no deposition of amyloid. Thus, the implication is that even the most severe disruptions to tau metabolism – profound NFT formation leading to fatal neurodegeneration – are insufficient to induce AD pathology. Consequently, it is argued that the wild-type tau NFT pathology see in AD must be a consequence of prior changes in Aβ metabolism, rather than a cause of them (Hardy & Selkoe. 2002). This is further supported by studies where injection of synthetic Aβ into the brains of tau transgenic mice (Götz *et al*. 2001) or the co-expression of mutant APP with mutant tau (Lewis *et al*. 2001; Oddo *et al*. 2003; Santacruz *et al*. 2005) accelerates tau hyperphosphorylation and leads to tangle formation reminiscent of the other hallmark lesion that characterises AD.

1.1.6 Framing Aβ toxicity: rise of the oligomer

Despite the overwhelming support for the amyloid cascade hypothesis, the pathogenic role of Aβ remains controversial, with two main issues: (1) the exact nature of the toxic Aβ species and (2) whether Aβ mediates its effects from an intracellular or extracellular location. Originally, when the hypothesis was first proposed in the early 90's, it was believed extracellular Aβ in the form of amyloid plaques represented the major toxic moiety. This was duly supported by studies demonstrating that fibrillar forms of Aβ, as found in plaques, are toxic to neuronal cells in culture (Yankner *et al*. 1990; Busciglio *et al*. 1992).

Nevertheless, the pathogenic role of Aβ plaques has been questioned because of their presence in healthy, cognitively normal individuals (Katzman *et al*. 1988) and the poor correlation between amyloid load and cognitive impairment in

individuals with AD (Terry *et al*. 1991; Arriagada *et al*. 1992). This is exemplified by the many mouse models of AD that display behavioural deficits prior to the detection of plaque pathology (Mucke *et al*. 2000; Oddo *et al*. 2003; Billings *et al*. 2005; Lesné *et al*. 2008). However, proponents of the amyloid cascade hypothesis argue that the plaques detected in normal individuals are almost exclusively of the diffuse type, which are not associated with surrounding neuritic and glial pathology (Hardy & Selkoe. 2002) and that the quantitative correlations between histologically determined plaque counts (which are counted manually) and cognitive impairment are imprecise and fraught with methodological challenges (Haass & Selkoe. 2007).

The advent of Aβ-specific ELISA, combined with western blotting and mass spectrometry has provided a much more precise means of biochemically assessing Aβ levels and has led to the observation that total Aβ levels, particularly soluble Aβ levels, correlate much better with dementia than does plaque count (Lue *et al*. 1999; Wang *et al*. 1999). These findings led to the idea that soluble oligomers of Aβ, not monomers or insoluble amyloid fibrils, are the primary neurotoxic species in AD (Walsh & Selkoe. 2007). However, the term 'soluble oligomer' casts a wide net, describing any Aβ species (except monomers) that does not pellet following high-speed centrifugation. Consequently, there remains much confusion as to which particular species of soluble Aβ oligomer is ultimately responsible for toxicity.

Many groups have generated/isolated synthetic/natural Aβ oligomers and have shown them to be toxic *in vitro* and *in vivo*. The list includes secreted dimers and

trimers, protofibrils, annular structures, Aβ-derived diffusible ligands (ADDLs) (Lambert *et al*. 1998) and Aβ*56, an endogenous dodecameric form of Aβ (Pimplikar. 2009).

1.2 *Using model organisms to study Alzheimer's disease*

1.2.1 Transgenic models of Alzheimer's disease

With the incidence of AD set to grow, pressure is mounting on the scientific community to develop effective treatments. Other age-related diseases such as heart disease and cancer can now be effectively treated and in some cases cured, whereas treatments of AD, and indeed of other age-related neurodegenerative disorders such as Parkinson's Disease, are palliative at best. In part, this is due to a poorer understanding of AD, a consequence of the complexity of the brain and its relative inaccessibility, but it is also through a dearth of 'natural' disease models. For instance, the dog naturally reproduces some features of AD including Aβ cortical pathology, neuronal degeneration and learning and memory deficits, but it does not develop neuritic plaques and NFTs (Sarasa & Pesini. 2009). Also, although rodents will readily develop cancer, the sporadic formation of plaques and NFTs has never been reported (Link. 2005).

Thus, transgenic models of AD have enabled researchers to overcome the lack of a convenient natural model. Since the study of AD in humans is methodologically and ethically complicated, transgenic animal models of AD provide a powerful means to further understanding of AD pathogenesis, to identify new biomarkers and to design new treatments. In addition, transgenic animal models allow investigation of the early stages of the disease, something that is difficult with human post-mortem tissue, which typically reflects the terminal stages of pathogenesis (Wentzel and Kretzchimer. 2010). Human studies, particularly drug trials, are further complicated by the fact AD patients are often suffering from a range of other age-related problems.

The aims of developing a transgenic model are to replicate as much of the natural human pathology as possible whilst also providing opportunities to test candidate compounds and other interventions at all points along the pathogenetic cascade. With AD, this is further complicated by disagreement in the literature on exactly what the pathogenic cascade is. The amyloid cascade hypothesis remains the most widely supported and tested mechanism and has thus formed the basis of almost all transgenic models; that is, they are engineered to overproduce Aβ42. This has been achieved either through the overexpression of FAD-associated mutant APP (with or without FAD-associated PSEN-1) or via the direct expression of Aβ mini-genes in the nervous system.

The success of a model system depends on the degree of homology at the molecular, cellular and tissue level between the human and candidate organism. In this light, the most appropriate animal for modelling AD is probably the aged primate, but this is all but ruled out on ethical grounds. As a consequence, most studies have favoured murine models of AD, mainly because mice are mammals and have well-established systems for genetic and other types of experimental manipulation and phenotypic characterisation. However, due to various limitations of the mouse, there has been a move in recent years towards using invertebrate models such as *Drosophila melanogaster* and *Caenorhabditis elegans*.

These two organisms offer two major advantages: first, experiments can in general be conducted much more rapidly than in the mouse and with much larger numbers of animals and, second, these invertebrate models organisms can be

rapidly screened for with both mutations and chemicals, allowing investigation of processes involved in AD from a unbiased perspective, something that is challenging in mammalian systems.

Flies and worms are phylogenetically further from humans than are rodents, and lack some of the complexity of nervous system and behavioural of mammals as well as some biological processes that are likely to play a role in AD pathology (e.g. a closed blood circulation). Modelling of some diseases, which affect specific tissues that are absent in the invertebrates, such as Cystic fibrosis and the lungs, would obviously be inappropriate in invertebrates. However, despite these limitations, results of both classic genetic analyses and transgenic manipulation of these invertebrates (discussed below) appear to validate their use as model platforms for the study of AD.

The production of different transgenic models in a variety of model organisms raises the question of which is the 'right' model. It is important to emphasise that, although each particular model system recapitulates one or various aspects of disease, to date, not one has completely reproduced all features of the disease. Caution must therefore be taken when making conclusions from any model system and these conclusions must be made with an appreciation of other systems, and always, above all, to the pathology seen in humans.

1.2.2 Transgenic models of AD in *Mus Musculus*

The formulation of the amyloid cascade hypothesis in the early 90's prompted many groups to attempt to replicate AD pathology in the house mouse *Mus musculus* by overexpressing human APP (wild-type, FAD associated mutations in APP or fragments of Aβ) under neuron specific promoters. Despite largely unsuccessful attempts in the early 1990's (McGowan *et al*, 2006) the field has grown enormously, and to date, over a dozen different models exist that develop amyloid and tangle pathology (for review see McGowan *et al*, 2006). For the sake of brevity, only the most popular models, and those particularly relevant to this thesis will be discussed.

The first significant developments were publication of the PDAPP (Games *et al*. 1995), followed in subsequent years by the Tg2576 (Hsiao *et al*. 1996) and APP23 (Stürchler-Pierrat *et al*. 1997) mouse models, currently the most widely used amyloidosis models in AD-related research. PDAPP mice overexpress a human APP minigene, encoding the FAD-associated V717F mutation (Murrel *et al*. 1991) under the control of the platelet derived growth factor β promoter (PDGFβ). Both the Tg2576 mouse and the APP23 mice overexpress a human APP minigene, encoding the FAD-associated double Swedish mutation (K670M/N671L) (Mullan *et al*. 1992), under the control of the hamster prion protein promoter (PrP) and murine thy-1 promoter, respectively. All these mice develop robust age- and brain region specific AD pathology (from 6-9 months in PDAPP and APP23, 9 months in Tg2576) including Aβ deposition in both neuritic and diffuse plaques, dystrophic neurites, synapse loss and extensive gliosis. Although tau was found in a hyperphosphorylated state in these mice

(Games *et al*. 1995, Hsiao *et al.* 1996), no NFTs were detected nor was there evidence of widespread neuronal loss or brain atrophy.

Mutant APP mice do develop a range of behavioural and cognitive deficits but the correlation between specific pathological lesions and memory deficits is unclear. Furthermore, the use of subtlely different behaviour and learning paradigms makes comparison between different studies difficult. For instance, spatial discrimination in PDAPP mice, as tested using a radial arm maze (which assesses spatial learning and memory), is impaired at ages between 3 and 10 months, a period both before and after the development of amyloid deposits (6-9 months) in this model. However, when using the Morris water maze to assess spatial learning and memory, deficits were not observed until 13-15 months, well after the emergence of Aβ deposits (Chen *et al*. 2000). On one side we have emergence of cognitive deficits before plaque pathology, which argues against plaques as the primary toxic moiety in AD, whereas in the other case we see cognitive deficits emerging after plaque formation.

There is a similar story with Tg2576 mice. It was originally demonstrated that these mice develop memory deficits, as assessed by the water maze (Hsiao *et al*. 1996) and T-maze (Chapman *et al*. 1999), by 10 months of age (no deficits were observed at 3 months). Since there is no widespread neuronal loss in this model, these cognitive deficits are believed to be the result of impaired synaptic plasticity (Chapman *et al.* 1999). However, when assessed over a broader age range (4-22 months) Tg2576 mice failed to show any overall correlation between

memory function and levels of insoluble Aβ, although a correlation was observed within individual age groups (Westerman *et al*. 2002).

The discovery of FAD associated mutations in PSEN1 and PSEN2 prompted many groups to cross APP mutant mice with mice expressing mutant PSEN transgenes (PSAPP mice). PSAPP mice display an increased Aβ42/Aβ40 ratio and dramatically accelerated Aβ pathology (compared to the single APP model they are respectively based on) and thus support the modifying role of PSEN mutations. For example, Holcomb *et al* (1998) crossed the Tg2576 line with a mutant PSEN1 (M146L) transgenic line. The double transgenic progeny developed large numbers of fibrillar Aβ deposits in the cerebral cortex and hippocampus far earlier than in their singly transgenic Tg2576 littermates (at 6 months compared to 9 in Tg2576). Furthermore, these mice showed a selective 41% increase in Aβ42 levels, when compared to Tg2576 mice. Interestingly, these mice showed cognitive deficits, as assessed using a T-maze, as early as 3 months; well before Aβ could be detected (Holcomb *et al*. 1999).

The major caveat of these particular models however, is the notable absence of NFT pathology and widespread neuronal loss. This was partly overcome by the development of mutated human tau mice and the subsequent crossing of tau and APP (Lewis *et al*. 2001a). JNPL3 mice over-express a mutant form of tau and display marked tangle pathology and neuronal loss. Crossing these mice with Tg2576 increased tau forebrain pathology relative to the singly transgenic JNPL3 mice, suggesting that mutant APP and or Aβ can influence downstream tau

pathology. In another study, Aβ42 fibrils injected into JNPL3 mice, accelerated NFT pathology, further implicating the primacy of Aβ (Götz *et al*. 2001).

The most complete mouse model of AD is probably the triple transgenic (3xTg) mouse (Oddo *et al*. 2003). These mice express human APP, encoding the Swedish mutation; and human tau with the P301L mutation (like the JNPL3 mice) in a PSEN1 (M1646V) knockin background. Rather than crossing independent mutant mouse lines, two transgenic constructs (mutant APP and tau) were microinjected into single-cell embryos from homozygous mutant PSEN1 mice, thereby preventing segregation of APP and tau genes in subsequent generations. In accordance with the amyloid cascade hypothesis, 3xTg mice develop Aβ plaques prior to NFT pathology with a temporal and spatial profile equivalent to AD, in addition to inflammation, synaptic dysfunction, and cognitive decline.

Of particular relevance to this thesis are transgenic mouse models that directly overexpress Aβ isoforms in the absence of APP processing, since this is the favoured approach to modelling AD in *Drosophila*. LaFerla *et al* (1995) used a strong neuron-specific promoter, neurofilament-light (NF-L), to drive expression of murine Aβ42 in the brains of mice. The construct was engineered so that Aβ would accumulate intracellularly - a decision based on the authors' belief that Aβ neurotoxicity is mediated from an intracellular location, for which there is now much evidence. These mice display extensive neuronal degeneration, suggested to be a result of apoptosis; reactive gliosis and a 50% reduction in lifespan. However, although some extracellular Aβ deposits were detected using

immunohistochemical techniques, no plaque or tangle pathology was observed in these mice. Furthermore, this study did not include a negative control peptide such as Aβ40 or GFP, therefore casting doubt on the specificity of Aβ42 toxicity implied in this model.

McGowan *et al* (2005) similarly generated mice that express Aβ42 and Aβ40 in the absence of APP processing. Their approach was slightly different. They used cDNAs that expressed fusion proteins between the transmembrane protein BRI, which is involved in amyloid deposition in Familial British Dementia (FBD) and Familial Danish Dementia (FDD), and human Aβ40 or Aβ42. It was previously shown that transfection of BRI-Aβ in cell culture results in high levels of expression and secretion of Aβ peptides, following cleavage of the fusion protein (Lewis *et al.* 2001). The efficient secretion of Aβ in these mice and the use of Aβ40 are the major differences to the approach taken by LaFerla *et al* (1995), who instead specifically aimed to generate high levels of intracellular Aβ.

Cleavage of the fused BRI-Aβ protein in BRI-Aβ40 and BRI-Aβ42 mice resulted in efficient production and secretion of Aβ40 and Aβ42, respectively. Soluble fractions of both peptides accumulated with age, quantified using Aβ sandwich ELISA over a period of 3-22 months. However, only BRI-Aβ42 mice accumulated insoluble Aβ42 and developed compact amyloid plaques, diffuse Aβ deposits and extensive CAA with age. This is despite BRI-Aβ40 mice having significant higher levels (~5-10 fold relative to Aβ42) of Aβ40 expression. Despite overt amyloid plaque pathology in BRI-Aβ42 mice, there was no evidence of NFT pathology or widespread neuronal loss. Interestingly,

endogenous murine Aβ42 was found to co-localise with human Aβ42 in a subset of plaques. This was further evidence demonstrating that different Aβ sequences can aggregate and form plaques.

More importantly, this study demonstrated that Aβ42 is essential for amyloid deposition in the brain parenchyma and also in vessels. It also provides further evidence for the primacy of Aβ42 toxicity in AD, as posited by the amyloid cascade hypothesis.

1.2.3 Transgenic models of AD in *Caenorhabditis elegans*

Caenorhabditis elegans or *C. elegans* are small (~1.2mm), transparent, soil-dwelling nematode worms first used to study molecular and developmental biology by Syndey Brenner in the 1970's (Brenner. 1974). This invertebrate was the first animal for which an entire genome was sequenced (*C. elegans* Sequencing Consortium. 1998) and has recently become one of the most popular models organisms to study neurodegenerative disease, as demonstrated by the development of numerous transgenic disease models including for Alzheimer's Disease (discussed below), Parkinson's Disease (Lakso *et al*. 2003; Ved *et al*. 2005; Kuwahara *et al*. 2006), Huntington's Disease (Faber *et al*. 2002), and Amyotropic Lateral Sclerosis (Oeda *et al*. 2001).

C. elegans provide a variety of practical advantages for studying age-related neurodegenerative disease. They are cheap and easy to maintain in large numbers (on plates of *E. coli* bacteria on which the worms feed), they have a complete cell lineage, a simple well-mapped nervous system, a short development time (egg to

adult in three days) and a short lifespan (18 days at 20°C). In addition, they are amenable to RNA interference, a technique for down-regulating the expression of a particular gene of choice. RNAi involves feeding worms bacteria that express double stranded RNA copies of the gene of interest (Carthew. 2001), which, once ingested by the worm, interfere with the mRNA transcript of the gene thereby preventing translation and expression of the respective protein. Bacterial libraries of strains that allow RNAi of all known *C. elegans* coding sequences are available and can be used for genome-wide screens for phenotypes of interest.

Models of AD in the worm have been almost exclusively developed and studied by the laboratory of Christopher D. Link. Their first model, which was in fact the first attempt at modeling AD in an invertebrate, involved expressing a signal peptide:human Aβ42 mini-gene in the body wall muscle of the worm (they used the unc-54 promoter which encodes a body-wall muscle myosin) (Link. 1995). The expression of the Aβ42 mini-gene resulted in muscle-associated thioflavin S-reactive deposits and a clear progressive paralysis phenotype. Interestingly, despite the inclusion of a signal peptide, Aβ was not secreted in this model. Immunoreactive amyloid deposits were only detected inside the muscle (Link. 2001). Owing to the lack of Aβ expression in the nervous system, this is perhaps a more useful model for the progressive muscle disease Inclusion Body Mitosis (IBM), which is associated with the intracellular accumulation of Aβ (Askanas & Engel. 2001) rather than AD.

One concern prior to the development of this worm AD model was that the short

lifespan of the worm would not allow enough time for the development of Aβ deposits. On the contrary, this early study demonstrated the Aβ could rapidly (~2 days) accumulate into amyloid-like deposits *in vivo* as well as producing a clear and practical phenotype amenable to genetic screens. This model was further used to study effects of Aβ sequence on its propensity to aggregate. Fay *et al* (1998) engineered worms to express wild type and single amino acid variants of Aβ42 in the muscle cell wall. They identified Leu17 and Met35 as key residues for *in vivo* amyloid formation, since their substitution blocked the formation of amyloid deposits.

The original Link model (1995) was then later adapted for a temperature-inducible Aβ expression system (Link *et al*. 2003; Drake. 2003), in which Aβ42 is only expressed at a non-permissive temperature of 23°C. Movement to the higher temperature resulted in increased oxidative stress, evidenced by increased protein oxidation, in the absence of Aβ42 fibril formation (Drake. 2003). Thus, this study adds further weight to the notion the toxic species in Aβ toxicity and AD is pre-fibrillar in nature (i.e. soluble oligomers).

1.2.4 Transgenic models of AD in *Drosophila melanogaster*

Drosophila melanogaster are the most commonly used species of *Drosophila* in the laboratory. Their use in the modelling of human neurodegenerative disease is predominantly based on the inherent presumption that the fundamental aspects of cell biology are conserved throughout evolution in higher organisms. This is supported by the fact approximately 75% of human disease-related genes have

homologs in *Drosophila* (Reiter *et al*. 2001), suggesting that molecular mechanisms underlying disease in humans may be conserved in the fly.

There are many compelling reasons to studying AD in the fly. The fly brain is estimated to have in excess of 300,000 neurons and, similarly to mammals, is organized into areas with separate, specialized functions such as learning, memory, olfaction and vision. Flies are also highly practical; they have a short generation time (10 days), are inexpensive to keep (although, unlike *C. elegans* and mice, they cannot be recovered alive from freezing) and relatively short-lived. Although one could argue the fly's maximum lifespan of 50-80 days is significantly greater than that of the worm (~18 days), it is still much shorter than that of the mouse (2-3 years), making it ideal for studying a progressive age-related disease such as AD.

In addition, the fly has an unrivalled battery of genetic tools, including a fully sequenced genome; an extensive library of mutant stocks including RNA interference (RNAi) and knock out (KO) lines; sophisticated transposon based methods for gene manipulation; systems for spatial- and temporal-specific ectopic gene expression; and balancer chromosomes. Balancer chromosomes are unique composed of multiple inversions that prevent recombination, together with dominant lethal visible and markers. They allow the maintenance in long-term culture of lethal or deleterious mutations in heterozygotes, without any necessity to set up specific crosses.

The combination of such extensive genetic tools and practicality makes the fly ideal for genetic screening. A variety of screening methods are available in the fly, involving chemical mutagenesis (EMS), genetic deletion kits or mobile genetic elements (P-, EP-, GS-elements). Genetic screens are powerful experiments providing an unbiased forward genetics approach, which allows the discovery of genes or metabolic pathways not immediately apparent in the pathogenesis of AD.

1.2.5 *Drosophila* life cycle

The *Drosophila* life history is divided into four distinct morphological phases (see **Figure 1.7**). Periods of growth and development can be easily distinguished from sexual maturity and the adult phase. Development time from egg to adult is approximately 10 days at 25ºC, although this can change depending on the mutant being used. For instance, flies mutant for the insulin receptor substrate protein, *chico*, typically take 12 days to develop whereas mutants lacking the *Drosophila* insulin-like peptides 2,3 and 5 (*dilp 2,3-5*) can take up to 18 days to develop (Grönke *et al*. 2010).

Once fertile eggs are laid, larvae start to emerge around 24 hours later and then enter three distinct stages of growth or instars known as L1, L2 and L3. L1 and L2 last for 24 hours each whereas the L3 stage lasts for 48 hours. During L2 the larvae become larger in size and switch from feeding on the surface of the food to burrowing down into the food. Feeding can last ~100 hours before larvae leave the food medium and crawl up the sides of the vial or bottle to pupariate. The pupal period lasts approximately 4 days, during which time pupae undergo

metamorphosis before eclosion into adult flies. Adult flies consist almost entirely of post-mitotic, fully differentiated cells, with the exception of cells in the gonad and some cells in the gut and Malphigian tubule (fly equivalent of the mammalian kidney), which continue to divide.

Freshly eclosed flies have shrivelled wings and are pale with a dark spot on their abdomen, as a result of their last feed as L3 larvae. Wings expand within an hour, followed by pigmentation. Female virgin flies will not mate within the first 8 hours post-eclosion. After mating, females commence a heavy egg-laying period that peaks after 5 days post-copulation. Virgin flies also lay eggs but fewer and in a different pattern.

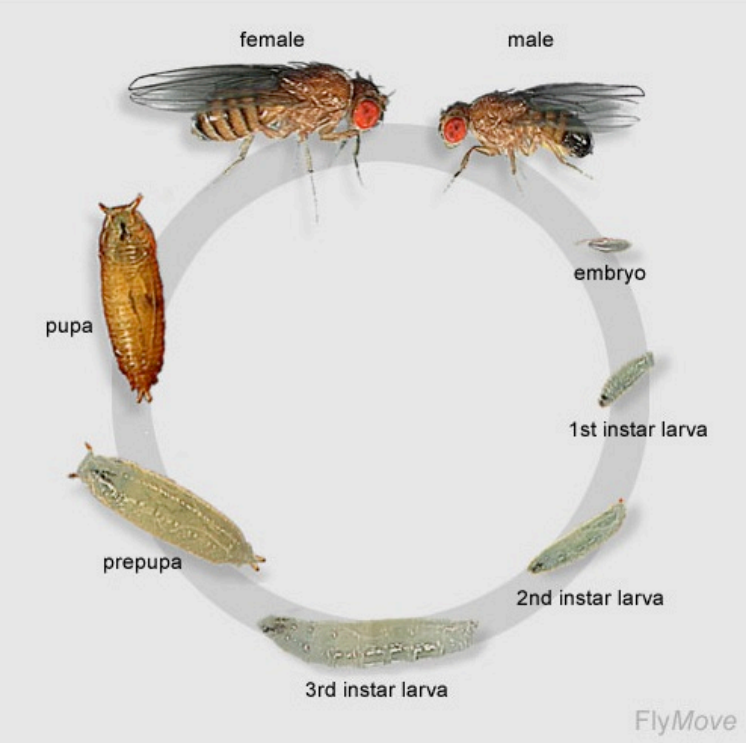

Figure 1.7. The *Drosophila* life cycle. The development of a fertile egg to an adult fly over a 10-day period at 25ºC. Following hatching (eclosion), larvae go through three instars before reaching pupariation at which time metamorphosis

takes place resulting in the emergence of an adult fly. Figure taken from FlyMove (http://flymove.uni-muenster.de).

1.2.6 *Drosophila* nomenclature

Drosophila melanogaster have four pairs of chromosomes: X; 2nd; 3rd; and 4th. In *Drosophila* sex is determined by the ratio of X to autosomes. Thus, males contain a single X and a Y chromosome. For most practical purposes the fourth chromosome is ignored because of its relatively small size (it is a fifth of the size of any other chromosome).

To fully understand a genetic cross, the specific nomenclature that the geneticists uses must be understood. There are a few general rules. When describing a stock genes on the same chromosome are separated by a space and genes on homologous chromosomes by a slash; a semi-colon separates genes on non-homologous chromosomes. Wild-type alleles are typically signified by +. Hence, a wild-type fly would be written as such:

+/+ ; +/+ ; +/+ ; +/+

If there are no mutations or alterations to a chromosome then generally nothing is shown. However, if a cross potentially results in progeny with altered chromosomes then + will be used. If the fly is homozygous for a mutation or insertion then only one line is usually shown. Gene names are often descriptive of the gene function or mutant phenotype such as *Curly* (curly winged flies) or *chico* (little boy in Spanish), the latter describing the dwarf phenotype of a

mutant in a gene encoding the insulin receptor substrate protein. When a gene is an orthologue of a gene previously discovered in another organism, a "d" is added to the front of the gene name, for example, dFOXO. In addition, the genotype, mutant and gene name are always italicized. If the mutant phenotype is dominant to the wild-type then the first letter is capitalized, but not when it is recessive.

One of the most commonly used stocks in this thesis is:

w^{1118};UAS-Arctic Aβ42/+;elavGS/+

This stock is therefore homozygous for the w gene in the 1118 background on chromosome 1, heterozygous for the UAS-insertion on chromosome 2 and heterozygous for the elavGS insertion on chromosome 3.

1.2.7 Modelling AD in the fly

As has been previously described, AD is characterised by two major neuropathological mechanisms, the development of extracellular amyloid-β (Aβ) plaques and intraneuronal neurofibrillary tangles, and fly models of AD can be broadly grouped according to these. Thus, *Drosophila* models of AD typically aim to either overexpress Aβ or tau, respectively. Here, I will largely concentrate on models of Aβ toxicity since the same approach was used to develop an inducible model of AD in this thesis.

Modelling Aβ toxicity in the fly has proved to be challenging because not all the components of APP proteolytic processing machinery are conserved. Flies do

possess an APP homologue, Appl (Rosen *et al*. 1989), and like mammalian APP, it is expressed specifically in neuronal tissue (Luo. 1990). Interestingly, it has been shown that APPL may function as a vesicular receptor for kinesin 1, a motor mediating anterograde vesicle trafficking. Flies lacking APPL or overexpressing human APP and *Drosophila* APPL constructs have axonal transport defects, which are enhanced by reductions in kinesin 1 expression. Moreover, over-expression of the Aβ-domain-containing APP, but not APPL, induced neuronal apoptosis (Torroja *et al*. 1999a; Gunawardena & Goldstein. 2001). APPL also been implicated in promoting synaptic formation at the neuromuscular junction (NMJ) (Torroja *et al*. 1999b).

The main problem in modelling Aβ toxicity is that the equivalent of the Aβ domain in APPL shows low evolutionary conservation with that of mammals (Rosen *et al*. 1989). Furthermore, there is confusion as to whether a functioning β-secretase exists in the fly. When using full length human APP695, Fossgreen *et al* (1998) failed to detect any Aβ, leading them to conclude that the 'postulated β-secretase might somehow be altered in insects or might cleave APP to a non-detectable extent'. However, Greeve *et al* (2004) showed that human APP is cleaved in the fly, in the absence of human BACE1. Adding fuel to the fire was a recent study reporting that APPL could be cleaved by an endogenous β-secretase-like enzyme, or by human BACE1 to generate Aβ fragments known as dAβ. These APPL-derived Aβ fragments were shown to accumulate, causing behavioural deficits and neurodegeneration (Carmine-Simmen *et al*. 2009).

On the other hand, *Drosophila* does definitely possess a functional γ-secretase. Using a truncated form of human APP (SPA4CT), Fossgreen *et al* (1998) first

demonstrated Aβ release in flies and fly-tissue culture indicating endogenous γ-secretase activity.

1.2.8 Models of Aβ toxicity

Two approaches have been used to work round the lack of endogenous Aβ production in the fly. The first aims to reconstitute the human APP/secretase system in the fly, whereas the second directly investigates the downstream consequences of Aβ production.

Greeve *et al*. (2004) reconstituted the human APP/secretase system in the fly eye, by generating flies transgenic for both human APP and human BACE. The advantage of this approach is that it makes fewer assumptions about causality, allowing investigation into APP processing, in addition to the mechanism of Aβ toxicity. As expected, flies expressing APP and BACE produced Aβ40 and Aβ42, demonstrating that human BACE appropriately functions in the fly and that the endogenous fly Psn gene (single fly homolog of human presenilin) can provide the γ-secretase activity necessary to produce Aβ. Interestingly, the expression of human APP alone resulted in the production of an Aβ-like peptide containing a 13-amino acid N-terminal extension. In addition, expression of APP in the eye alone or in combination with human BACE resulted in an age-related degeneration of the retina and the underlying neurons of the optic pathway. Both phenotypes were absent when human BACE was expressed alone. The introduction of loss-of-function Psn alleles suppressed this APP transgene-dependent phenotype, and the addition of Psn alleles with FAD-associated

mutations enhanced it. This strongly argued that the production of Aβ was responsible for the observed pathology.

Following this study, a number of groups adopted a more focused approach, directly overexpressing Aβ peptides fused to secretion signal peptides, because it is believed the majority of Aβ in humans is eventually secreted. Finelli *et al* (2004) and Iijima *et al* (2004) generated flies engineered to overexpress human $A\beta_{40}$ and $A\beta_{42}$ mini-genes conjugated to the pre-proenkephalin signal to ensure secretion of the peptides.

Expression of $A\beta_{42}$ in photoreceptor cells (by using the eye-specific GMR-Gal4 driver) led to a range of eye abnormalities not seen in multiple $A\beta_{40}$ lines (Finelli *et al*., 2004). The severity of the eye-phenotypes was dose-dependent and increased with age. Flies solely expressing the GMR driver, aged in parallel, did not show any age-dependent rough-eye phenotypes. The rough-eye phenotype is a non-progressive, developmental abnormality of the ommatidia that constitute the compound eye of the fly. Toxic transgene products may produce a range of irregularities in the eye, from subtle misalignments of ommatidia, through fusion of ommatidia to the development of necrotic patches. Consequently, the rough eye phenotype can be used as a qualitative measure of neurodegeneration

Pan-neuronal expression of Aβ42 (using the elav-$Gal4^{C155}$) resulted in a ~50% reduction in life span. Finelli *et al* (2004) also screened for genetic modifiers of the $A\beta_{42}$-induced rough-eye phenotype. The screen identified a mutation that up-regulates expression of nep2, a neprilsyin homolog. Neprilsyin is a plasma-

membrane bound protein capable of catabolising Aβ. Appropriate tissue-specific expression of this gain of function mutation both decreased Aβ-dependent eye abnormalities and partially rescued the premature death phenotype.

Iijima and colleagues (2004) furthered these studies by measuring behavioural phenotypes (olfaction and locomotor ability) as well as neurodegeneration in the brain. However, unlike the situation in photoreceptor cells, both Aβ40 and Aβ42 accumulated, although only Aβ42 flies formed sodium dodecyl sulfate (SDS)-insoluble aggregates (insoluble Aβ42 refers to higher order aggregates, fibrils etc.). Both Aβ40 and Aβ42 lines showed age-dependent olfactory learning deficits, but only the Aβ42 flies demonstrated age-dependent climbing phenotypes and shortened lifespan.

Crowther *et al* (2005) followed with the same direct approach and engineered a series of flies overexpressing Aβ40, wild-type Aβ42 and the Arctic mutant form of Aβ42 but conjugated to a different secretion signal peptide, *Drosophila* necrotic. The Arctic mutation is a Glu22Gly amino acid substitution that causes more rapid protofibril formation with increased neurotoxicity and results in early-onset *Alz*heimer's disease (Nilsberth *et al*. 2001; Murakami *et al*. 2002). Expression of these peptides was driven by the pan-neuronal driver elav-Gal4C155. Aβ40 was used as a control and over-expression produced no survival or climbing phenotypes, consistent with the idea that Aβ42 represents the toxic moiety in AD. On the other hand, expression of Aβ42 and Aβ42 (Arctic) resulted in age-dependent and dose-dependent neurodegeneration, reduced longevity and locomotor deficits. Expression of the more aggregation

prone Aβ42 (Arctic) accelerated these phenotypes, consistent with the early-onset of AD in humans harbouring this mutation. This model was then subsequently used to confirm that a modifier of Aβ42 aggregation, neuroserpin, interacts with Aβ42 *in vivo* (Kinghorn *et al*. 2006).

One source of concern regarding these models is whether they are all examining the same toxic process. The contribution of intracellular Aβ in human remains controversial and, although the Aβ peptides were fused to secretion signals, the intracellular/extracellular distribution of Aβ *in vivo* was not determined. Finelli *et al* (2004) demonstrated that the signal peptide (as used by Iijima *et al*. 2004) is efficiently cleaved from Aβ in the fly model and showed that in *Drosophila* S2 cells the Aβ transgenes can produce secreted Aβ. In addition, the suppression of Aβ-dependent phenotypes by nep2 up-regulation suggests Aβ is secreted in this model. However, Crowther *et al* (2005), who also used S2 cell lines, claimed that, although Aβ42 correctly entered the secretory pathway, the majority of Aβ42 and all the Arctic Aβ42 were retained within the cell as a monomer or soluble oligomers. This could be attributed to use of a different secretion signal peptide. Furthermore, they observed that in brain sections from young transgenic flies, Aβ is initially intracellular and only later are extracellular deposits observed. Hence, Crowther *et al* (2005) used their model as evidence for a role of intraneuronal Aβ aggregation in causing toxicity.

1.2.9 Application of *Drosophila* models of AD

A major advantage of using invertebrates such as *Drosophila* is the power to perform unbiased genetic screens to identify novel modifiers of AD phenotypes. To date, two such screens have been published (Cao *et al*. 2008; Rival *et al*. 2009). Cao *et al* (2008) searched for modifiers of the rough eye phenotype, caused by Aβ over-expression in the eye of the fly (Finelli *et al*. 2004). They screened for dominant modifiers of the phenotype in a library of flies with 1963 unique insertions of mobile transposon constructs (EP-elements) that enhance expression of neighbouring genes. Rival *et al* (2009) used a slightly different approach. They use EP-like elements to generate up-regulation of a random set of genes in flies over-expressing Aβ in the nervous system, and subsequently measured differences in lifespan to look for disease modifiers.

Both screens identified a strong role for the transition metals copper (Cao *et al*. 2008) and iron (Rival *et al*. 2009) amongst genes for vesicle transport, protein degradation, stress response and chromatin structure (Cao *et al*. 2008). The most powerful modifying genes in the Rival *et al* (2009) screen were those encoding iron binding proteins such as the heavy and light chains of the iron storage protein ferritin. Furthermore, co-expression of heavy chain ferritin with Aβ in a Aβ-mini gene model (Crowther *et al.* 2005) suppressed longevity and behavioural phenotypes, and reduced oxidative damage, despite an increase in the Aβ load in the brains of these flies. The researchers went further to suggest the free-radical generating Fenton reaction therefore might play a role in Aβ toxicity.

1.3 *Ageing as a risk factor for Alzheimer's disease*

1.3.1 Ageing and neurodegenerative disease

Late-onset is the most striking common feature of human neurodegenerative disorders including Alzheimer's disease (AD), Parkinson's disease (PD) Huntington's disease (HD) (and other polyglutamine diseases) and prion disease. In the case of AD and PD, rare individuals that carry familial-associated mutations develop the disease in their fifth decade, whereas the sporadic forms manifest during the seventh decade of life (Amaducci and Tesco. 1994). HD is a familial, monogenic disorder that similarly to other familial neurodegenerative disorders onsets during the patients fifth decade. The common pattern of onset between these disparate maladies defines ageing as a major risk factor for the development of neurodegenerative disease (Amaducci and Tesco. 1994). With sporadic AD, the association between ageing and onset could not be clearer – beyond the age of 65, the prevalence doubles approximately every 5 years (see **Figure 1.8**).

At this point it will be important to discuss exactly what 'ageing' is. The term itself is rather vague and can be colloquially used to describe almost any change over time, be it a positive, negative or indifferent one. For example, the ageing of red wine is believed to improve its quality whereas the hardening of the arteries with advancing age can be life threatening. On the other hand some changes such as the greying of hair carry no positive or negative ramifications for health. From a biological perspective ageing is defined as an intrinsic decline in function during adulthood that reduces fecundity and increases the probability of death (Partridge. 2010). This decline in function is thought to be the result of

accumulation of multiple forms of tissue-specific molecular damage over time. Thus, ageing represents a highly complex, multifaceted process.

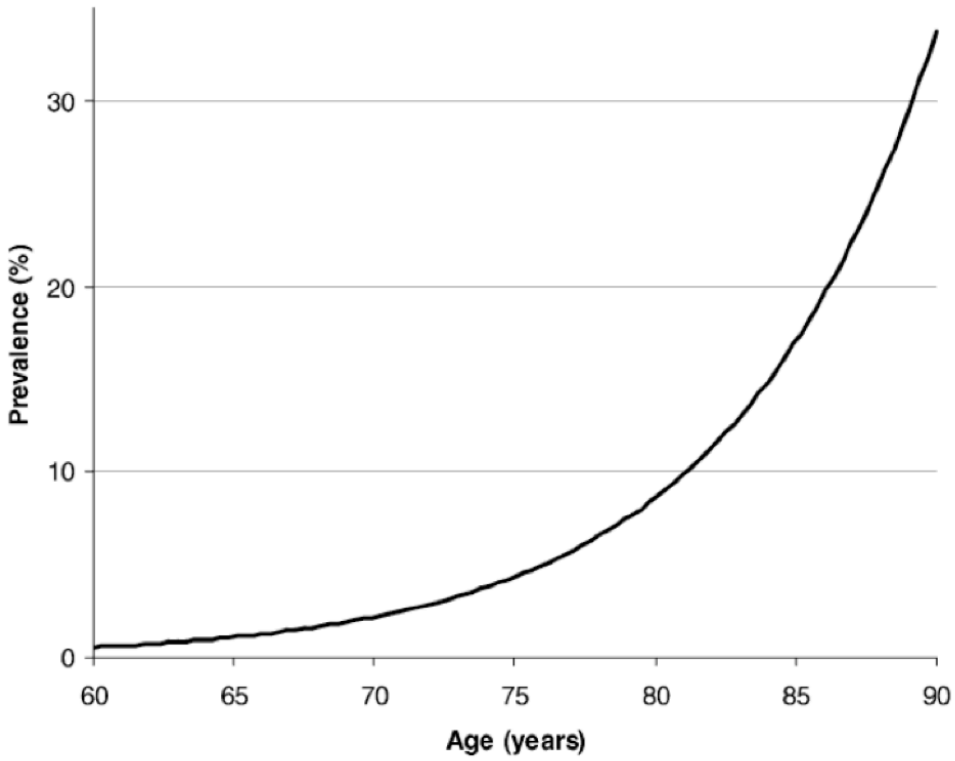

Figure 1.8. The prevalence of AD has a function of age. Figure taken from Ferri *et al*. (2005).

Aside from late-onset, neurodegenerative diseases are also defined by the aggregation, accumulation and deposition of abberantly folded proteins. As has been extensively discussed, Aβ aggregation is believed to underlie pathology in AD. Similarly, PD is caused by aggregation of α-synuclein, whereas in HD, a mutated form of the Huntington (Htt) protein, bearing an abnormally long polyglutamine (CAG) stretch causes the disease. Furthermore, aggregation of the prion protein (PrP) leads to prion disorders.

There is now much evidence implicating the soluble oligomeric forms of these various proteins as the primary toxic species. The remarkable fact these soluble oligomers share a common structure (Kayed *et al*. 2003) implies that these diseases may all share a common pathogenic mechanism. Furthermore, the fact these diseases share a common risk factor points towards the ageing process as a fundamental aspect of this 'common pathogenic mechanism' and ultimately raises an important question: why do such different diseases, each with distinct underlying pathologies, occur late in life? Is there a causal relationship between ageing and protein-mediated neurodegeneration?

One idea suggests that the production and accumulation of toxic aggregates is a stochastic process, requiring many years to initiate disease. So in fact, it is not ageing per se, that increases the risk of neurodegenerative disease, rather, the time it takes for an initially asymptomatic protein to accumulate to toxic levels. Alternatively, it has been proposed that the ageing process - the increase in neuronal vulnerability and the decline in the cell's ability to defend against protein aggregates – plays an active role in enabling the onset of neurodegenerative disease (Cohen *et al*. 2006). In other words, this theory predicts that neurodegeneration, or in the context of this thesis, Aβ-mediated toxicity, is age dependent.

Distinguishing between these two scenarios has been difficult for two reasons. Firstly, the development of effective and practical transgenic models of AD has only occurred in the last twenty years. Secondly, and more importantly, the

ageing process was, until recently, intractable - a kind of genetic 'black box'. This idea was a natural consequence of work on evolution of ageing.

1.3.2 Ramifications of the evolutionary theory of ageing and the birth of modern biogerontology

At first sight ageing requires no special explanation. It is simply a consequence of the second law of thermodynamics - biological wear and tear. However, despite showing a broad phylogenetic distribution, ageing is not universal. For instance, the simple fresh-water animals Hydra were reported to show no increases in mortality when assayed over a four-year period (Martínez. 1998). If biological wear and tear were the cause of ageing we would expect similar organisms to age at roughly similar rates but this is not so. For example, as a group, bats live 3.5 times as long as nonflying mammals of the same size (Austad. 2005), and within the bat species itself there are huge differences in lifespan despite roughly identical body sizes. The rate at which organisms age can therefore, evolve. This presents somewhat of an evolutionary paradox and is why evolutionary biologists are so fascinated by ageing. According to Darwinian theory, natural selection acts to remove deleterious traits from populations through the differential survival and reproductive success (fitness) of individuals. Ageing is unconditionally deleterious – it results in damage, lowered fertility and death- yet is believed no genes have evolved to cause ageing (Partridge. 2010).

Early evolutionary biologists such as Alfred Russel Wallace and August Weismann first debated the evolution of ageing in the late 19th century. They posited that ageing is an evolved trait for the good of the species, not the

individual. They believed ageing removes the old so to increase the fitness of the young (i.e. through reallocation of resources). Although a logical explanation, this idea has now been discredited. This is because there is little evidence to suggest ageing contributes to mortality in the wild (Kirkwood & Austad. 2000). In fact, natural mortality is mostly due to extrinsic hazards such as infection, predation and accidents. A key realisation was the idea the force of natural selection declines with age (Haldane. 1941; Medawar. 1952). Extrinsic hazard makes it unlikely for individuals to grow old therefore the greatest contribution in creating a new generation comes from the young. This idea is central to contemporary evolutionary theory of ageing, which proposes that ageing evolves as a side effect, either of pressure of new mutations that reduce fecundity or survival probability later in life or of mutations that have beneficial effects in the young (Medawar. 1952; Williams. 1957; Partridge & Gems. 2006). These ideas led to the assumption that ageing is a non-adaptive, highly polygenic trait, too complex for experimental manipulation. The idea single-gene mutations could affect ageing was unheard of.

Thus, there was great surprise when Klass isolated the first long-lived mutants in *C. elegans* (Klass. 1983). He himself seemed surprised suggesting it was 'most likely due to reduced caloric intake' and that lifespan could be controlled in a polygenic manner. However, these were later verified and these worms were found to have a mutation in the *age-1* gene. Kenyon and colleagues (1993) then isolated *daf-2* mutant worms that exhibited a lifespan double that of wild-type worms. It was discovered that these mutations occurred in the dauer formation (Daf) pathway and that animals with weak alleles of the *daf-2* or *age-1* genes

could bypass the dauer state and show significant longevity gains that were dependent on *daf-16* (Kenyon *et al*. 1993) - a downstream transcription factor. It was later determined that the effects of *daf-2* are also dependent on another downstream target encoded by the *hsf-1* gene (Hsu *et al*. 2003). The mutated genes were discovered to encode components of an invertebrate insulin/insulin-like growth-factor-like signalling (IIS) pathway and mutations in IIS pathway components that increase lifespan were soon found in flies and mice. These discoveries marked the beginning of the modern biogerontology era and the ability to manipulate the rate of ageing experimentally.

1.3.3 Evidence linking ageing and neurodegeneration

As previously discussed, a major question in the neurodegenerative field concerns the nature of the association between ageing and susceptibility to protein-mediated toxicity. The discovery of single-gene mutations that extend lifespan have allowed this issue to be properly explored. In the age-dependent role model of toxicity, one would expect interventions that increase lifespan to also rescue protein-mediated toxicity. Increasing evidence is in support of this, suggesting that the IIS pathway might be the mechanistic link between ageing and protein-mediated toxicity.

The IIS pathway is an evolutionary conserved pathway that is ubiquitous in multi-cellular animals (Skorokhod *et al*. 1999). In fact, it is believed to have played a central role in the evolution of multi-cellularity itself (Skorokhod *et al*. 1999). The IIS pathway has a multitude of functions, exemplified by studies showing that modulation of IIS activity can affect growth, development,

metabolic homeostasis, fecundity and, of particular relevance to this thesis, lifespan. The role of IIS signalling in regulating lifespan appears to be evolutionary conserved since reductions in IIS signalling yield stress-resistant, long-lived worms (Kenyon *et al*. 1993), flies (Tatar *et al*. 2001; Clancy *et al*. 2001; Giannakou & Partridge. 2007) and mice (Blüher *et al*. 2003; Holzenberger *et al*. 2003).

Several studies performed in *C. elegans* and mouse models of neurodegenerative disease support the role of IIS in mediating toxic protein aggregation. In a worm model of Huntington's disease (HD), it was found that poly-glutamine (polyQ) aggregation and toxicity was reduced in age-1 mutants (Morley *et al*. 2002). This protection was dependent on *hsf-1* yet this study failed to determine whether IIS was acting at the level of protein synthesis or polyglutamine solubility. Cohen *et al*. (2006) similarly demonstrated in a worm model of AD (Link *et al*. 1995), that Aβ toxicity (as measured by survival and motility) was ameliorated in worms treated with *daf-2 RNAi*. This was also found to be dependent on *daf-16* and *hsf-1*.

These findings were confirmed in various mouse models of AD, where it was shown that deficiencies in IRS-2, neuronal IGF and the neuronal insulin receptor delayed mortality and decreased Aβ accumulation through reduced amyloidogenic processing (Freude *et al*. 2009). This same effect was also seen in IRS-2 null mice (Killick *et al*. 2009) and IGF-1 receptor heterozygous mice (Cohen *et al*. 2009). In the latter study, it was found that reduced IIS resulted in fewer amyloid plaques of higher density, which resulted in decreased steady state

levels of soluble Aβ oligomers. This is evidence for the protective effects of amyloid formation as a means of removing the toxic soluble oligomers.

One of the other major pathways controlling lifespan is dietary restriction (DR). DR describes a reduction in food intake that falls short of starvation or malnutrition and has been shown to extend lifespan in organisms from yeast to mammals (for review see Mair & Dillin. 2008). Interestingly, DR delays protein mediated toxicity in *C.elegans* models of poly-glutamine disease and Aβ toxicity (Steinkraus *et al*. 2008). This was apparently due to a mechanism distinct from reduced IIS, which was dependent on hsf-1. Interestingly, in a *Drosophila* model of AD, DR had no effect on neuronal dysfunction but did delay ageing (Kerr *et al*. 2009).

Thus, these studies point towards a strong link between the ageing process and protein-mediated toxicity.

1.4 *Thesis Outline*

The aims of this thesis were to investigate the association between ageing and neurodegeneration using a *Drosophila* model of Alzheimer's disease. In particular, the aim was to determine whether ageing increases the vulnerability to Aβ42-mediated toxicity. This was achieved using a novel inducible model of Aβ42 toxicity to conditionally express Aβ42 peptides at different ages and by using genetic and pharmacological interventions known to extend lifespan.

The specific aims were to:

1) To refine existing fly models of AD with the aim of developing an inducible model of Aβ toxicity and to fully characterise this model using well-established markers of toxicity (Chapter 3).

2) To further characterise and exploit the features of this particular model system to investigate: a) the dynamics of Aβ42 toxicity and b) whether ageing plays an active mechanistic role in enabling neurodegeneration (Chapter 4).

3) To measure the effect of lifespan-extending pharmacological (rapamycin, Chapter 5) and genetic interventions (reduced IIS signalling, Chapter 6) on Aβ-mediated toxicity.

Chapter 2 Materials and Methods

2.1 *Drosophila melanogaster* stocks

2.1.1 Wild-type stocks

The majority of experiments were performed in the wild-type inbred *white*^{1118} (3605), background. However, in some instances the *white*^{Dahomey} background was used and this has been clearly noted.

2.1.1.1 white^{1118} (*w*^{1118})

w^{1118} was originally obtained from the Bloomington stock centre at Indiana University, and has been maintained in bottles containing standard sugar yeast medium with overlapping generations on a 12-hour light/dark cycle at 25°C and 65°C in a controlled temperature (CT) room. *w*^{1118} is an inbred isogenic strain with white eyes due to a deletion in the sex-linked white gene (*w*). This strain also lacks the intracellular bacterium Wolbachia.

2.1.1.2 white^{Dahomey} (*w*^{Dahomey})

w^{Dahomey} were generated by backcrossing *w*^{1118} flies into the outbred Dahomey wild-type background. The Dahomey wild-type stock was originally collected in 1970 in the Republic of Dahomey (now Benin), West Africa, and have since been maintained in population cages (measuring 20 x 21 x 30cm) at 25°C at 0% humidity under a 12-hour light/dark cycle with overlapping generations. Unlike discrete culture, this method has been shown to maintain lifespan and fecundity at levels observed with flies freshly collected from the wild (Sgrò & Partridge. 2001). Flies in population cages had constant access to 12 bottles of standard Sugar-Yeast (SY) food medium, with the three oldest bottles being replaced with

fresh medium every week. Naturally, Dahomey and $w^{Dahomey}$ strains both carry the intracellular bacterium Wolbachia.

2.1.2 GeneSwitch driver stocks

Two pan-neuronal GeneSwitch drivers were used throughout this thesis. They consist of the cloned promoter of the pan-neural ELAV (embryonic lethal, abnormal vision) gene upstream of the gene encoding a RU486-dependent GAL4-progesterone-receptor fusion protein called GeneSwitch, which can be used for spatially and temporally restricted UAS-linked transgene (see UAS-stocks below) expression (Osterwalder *et al*. 2001). All drivers were backcrossed at least six times into the w^{1118} and $w^{Dahomey}$ genetic backgrounds.

2.1.2.1 elavGS301.2

This is the original line created by Osterwalder and colleagues and was obtained from the Bloomington stock centre.

2.1.2.2 elavGS

This is a more potent line (see results section **3.2.2**) derived from the original elavGS301.2 line. Latouche *et al* (2007) generated this line to develop an adult-onset *Drosophila* model of spinocerebellar ataxia (SCA) (Latouche *et al*. 2007) and it was obtained as a generous gift from Dr H. Tricoire (CNRS, France).

2.1.3 UAS-stocks

All UAS stocks contain a GAL4 binding site or Upstream Activating Sequence (UAS) upstream of the transgene. All UAS lines were backcrossed at least six times into the w^{1118} and $w^{Dahomey}$ genetic backgrounds.

2.1.3.1 UAS- Arctic Aβ42

This strain encodes the human Aβ42 peptide (MASKVSILLLLTVHLLAAQTFAQDAEFRHDSGYEVHHQKLVFFA EDVGSNKGAIIGLMVGGVVIA) fused to a secretion signal peptide from the *Drosophila necrotic* gene (Crowther *et al*. 2005). This mutant form of Aβ42 contains the FAD-associated Arctic mutation (Glu22Gly) that leads to rapid aggregation of the peptide and early-onset AD (Nilsberth *et al*. 2001).

2.1.3.2 UAS-Aβ40

This strain encodes the human Aβ40 peptide (MASKVSILLLLTVHLLAAQTFAQDAEFRHDSGYEVHHQKLVFFA EDVGSNKGAIIGLMVGGVV) fused to the same a secretion signal peptide as above.

Both UAS stocks were obtained as kind gift from Dr D. Crowther (University of Cambridge, UK) and were previously used to develop a *Drosophila* model of AD (Crowther *et al*. 2005).

2.1.3.3 UAS-lacZ

This strain encodes the product of the *E. coli lacZ* gene, β-galactosidase. β-galactosidase catalyses the hydrolysis of a variety of β-galactosides including CPRG that is used in this thesis (see section **2.4.9**). This is one of the most extensively used reporter strains in *Drosophila* research. *UAS-lacZ* flies were obtained form the Bloomington stock centre at Indiana University.

2.1.4 *chico^{1}/CyO*

These flies are heterozygous for a null mutation in the *Drosophila* insulin receptor substrate gene, *chico*, which is a component of the IIS pathway. *chico^{1}* was maintained in a heterozygous state over a chromosome 2 balancer carrying the dominant *CyO* marker. Thus, the majority of flies in this stock had curly wings, although a small proportion were homozygous for *chico^{1}*.

chico^{1} homozygotes are sterile, less than half the size of wild-type flies, owing to fewer and smaller cells, (although they do have higher lipid levels) and exhibit an increase in median and maximum lifespan (Böhni *et al*. 1999; Clancy *et al*. 2001). These flies were obtained as a kind gift from Ivana Bjedov, who acquired them from Ersnt Hafen. They were backcrossed at least 6 times into the *w^{Dah}* background.

2.1.5 *w^{Dah}; Sp/CyO; TM6B/Mkrs*

This stock carried multiple balancers on the 2nd and 3rd chromosomes and was obtained from the Bloomington stock centre at Indiana University.

2.2 *Food media*

2.2.1 Sugar yeast (SY) medium

SY medium contained per litre: 100g autolysed Brewer's yeast powder (MP Biomedicals, Solon, OH, USA), 50g sucrose (Tate and Lyle Sugars, London, UK), 10g agar (Sigma-Aldrich, UK), 30ml nipagin (100g/L methyl 4-hydroxybenzoate in 95% ethanol) (Clariant UK Ltd, Pontypridd, UK), 3ml propionic acid (Sigma-Aldrich, UK) and distilled water to 1 litre. Nipagin and Propionic acid were added as preservatives and anti-fungal reagents.

To prepare the medium 700ml of distilled water and 15g of agar were mixed in a saucepan and brought to the boil. The sugar and yeast were then added and mixed thoroughly. The mixture was then returned to the boil and the heat removed. Once the food had settled, the remaining 170ml of water were added and the mixture was left to cool. Following cooling to 60°C, both the nipagin and propionic acid were added.

The medium was dispensed into glass vials or glass bottles (see **Figure 2.1**) in aliquots of 7ml and 70ml respectively using a motorized pump. SY medium was left to solidify and dry overnight. The vials or bottles were then plugged with cotton wool and stored at 4°C for no longer than 3 weeks.

It is important to note glassware was used for stock maintenance whereas plastic vials were used for all experiments involving drug-based SY mediums (see below). This was necessary to prevent contamination of the communal glassware (which is autoclaved, washed and recycled after each use). Plastic vials were

disposed of immediately after use. To prevent any contamination of the pumping apparatus, drug based SY medium was manually dispensed using 1L plastic 'ketchup bottles' at ~3ml a vial.

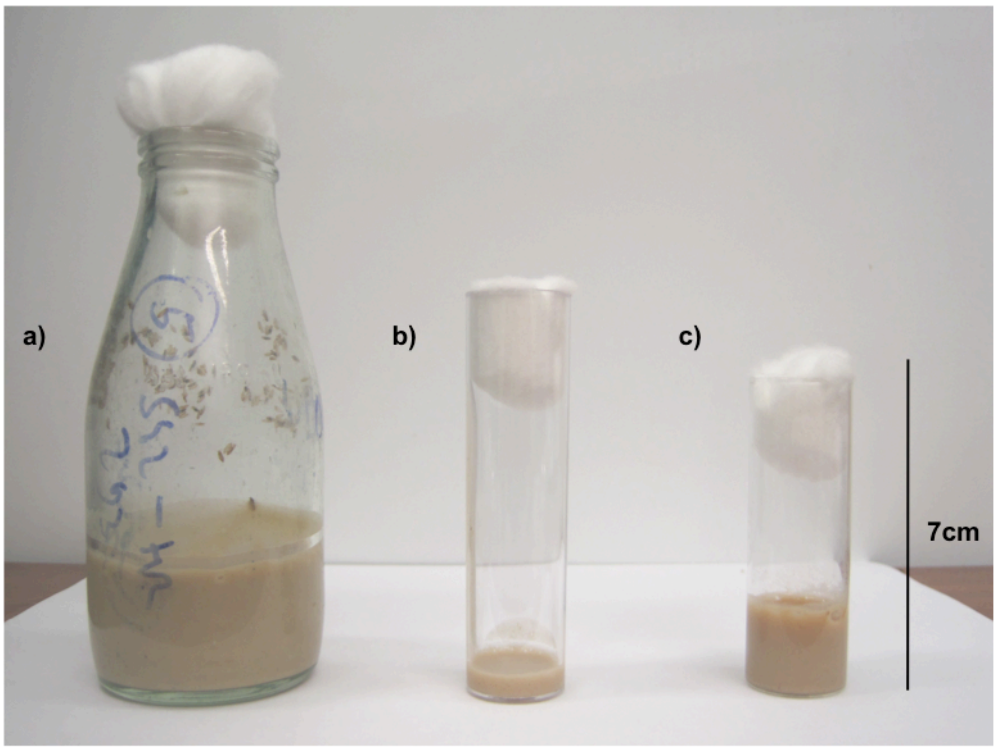

Figure 2.1. A photograph of the glassware and plasticware used for stock maintenance and experiments: a) UK half-pint glass bottle containing 70ml SY b) plastic vial containing ~3ml SY and c) glass vial containing 7ml SY.

2.2.2 RU486 (RU) SY

A 100mM RU working stock was made by dissolving RU powder in 95% ethanol at a concentration of 43mg/ml. 2ml of this 100mM stock was then added to 998mL SYA, prior to dispensing, to give a final concentration of 200µM RU per litre. To obtain other RU SY concentrations, the volume of RU working stock was changed accordingly (e.g. 1ml in 1L to give a final concentration of

100µM or 4ml in 1L to obtain a final concentration of 400µM). For control food (-RU), the equivalent volume of ethanol alone was added. All concentrations of RU SY medium, including -RU, were dispensed into plastic vials at ~3ml per vial.

It is important to note that RU486 is a synthetic steroid with antiprogestational effects. It is commercially used with the name of Mifeprex to give abortions in the case of unwanted early pregnancies. The usual dose for terminating pregnancy is 200mg, however it has been reported that a dose of 1mg/kg of body weight can have effects on uterus implantation and the absorption of 300ug/kg can severely disrupt the estrus cycle. Thus, RU SY must be dispensed under a fumehood and be clearly labelled when drying or in storage.

2.2.3 Rapamycin SY

1g of rapamycin (LC Laboratories) was dissolved in 100% ethanol and vortexed. 2.4ml were then added to a final volume of 600ml SY medium (+/- RU), prior to dispensing, to give a final concentration of 200µM. For rapamycin-free control food (-rapa), the equivalent volume of ethanol alone was added. All concentrations of rapamycin SY medium, including -rapa, were dispensed into plastic vials at ~3ml per vial.

2.2.4 Grape juice medium

Grape juice medium consisted of 500ml distilled water, 25g agar, 300ml grape juice, 50ml extra water and 21ml nipagin (100g/L). Water and agar were first

brought to the boil, at which point all the grape juice was added. The mixture was then returned to the boil and allowed to cool. Once below 60°C, the extra water (used to rinse the cylinder containing the residual grape juice) and nipagin were both added. The medium was then poured into small or large petri dishes, otherwise known as grape plates (**Figure 2.3**). Grape plates were used during standard larval density preparations to promote and track egg laying.

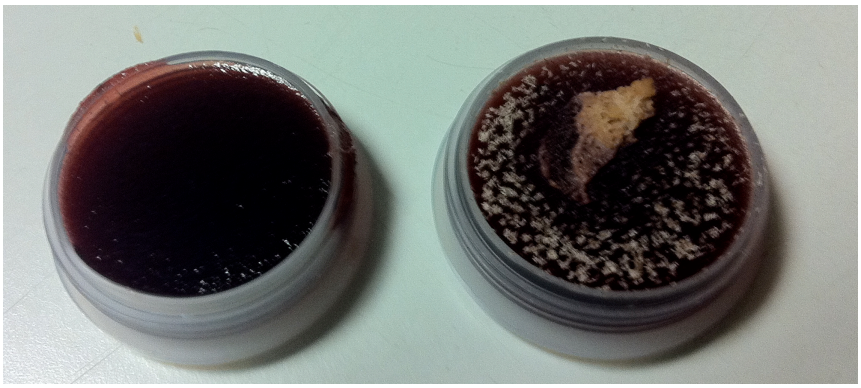

Figure 2.2. Photograph of grape plates used to easily track and identify egg laying. On the plate in the right of the image eggs are visible around the circumference of the plate. A globule of yeast paste is also visible in the middle of the plate.

2.3 *Fly husbandry and culturing*

2.3.1 Stock maintenance

All stocks were maintained at 18°C or 25°C on a 12 hour light/dark cycle at constant humidity (65%) on SY medium. Stocks were maintained in glass, half-pint UK milk bottles or glass-shell vials (**Figure 3.1**). Stocks at 18°C were transferred to fresh medium roughly every 4 weeks, whereas stocks at 25°C were

transferred every 10 days. Stocks were transferred or 'tipped' from old bottles/vials to fresh ones by quickly banging the flies into the fresh bottle/vial, with the aid of a funnel to prevent any flies escaping. In some instances light CO2 anesthesia was used to confirm the phenotype of the stock or to select a standard number of flies to transfer to a fresh bottle.

2.3.2 Distinguishing males and females

The sex of flies can easily be distinguished, while anaesthetised with CO_2, under a light microscope. Males are generally smaller than females and have a rounder abdomen that is dark dorsally compared with the striped tip of the female abdomen (Roberts. 1998). These differences are so clear that one can often tell the difference with the naked eye, especially with the abdomen. However, both shape and colour may be deceptive in newly eclosed flies. When in doubt, males were unambiguously identified by the presence of sex combs, a row of thick dark bristles on the tarsus on the first pair of legs (Roberts. 1998). Males and females were sorted with the use of a fine paintbrush on a CO_2 pad to avoid any structural damage.

2.3.3 Virgin Collection

For all experimental crosses it was essential to use virgin females. This is because mated females store sperm in the ventral receptacle and spermatheca. This stored sperm is sufficient to enable females to lay up to 100 eggs per day for many days in ideal conditions (Roberts. 1998). Because males and females emerge from the same bottle, brother-sister mating can occur potentially

confusing the results of crosses. Using virgin females therefore ensures crosses produce progeny at expected Mendelian ratios.

Female *Drosophila* will not mate within 8 hours after eclosion at 25°C. Thus, the following routine was followed to ensure successful virgin collection. First, bottles with emerging flies were emptied first thing in the morning, preferably before lights on (when flies are more likely to start emerging). It was extremely important to remove all flies, particularly those stuck on the side of the bottle. A paintbrush was used to scrape any rogue males off the sides. Alternatively, the cotton plug (the site of most pupation in a bottle) was removed and placed in a fresh bottle. This prevented flies getting stuck in the old 'churned' medium. Females were then collected at the end of the day/within 8 hours and stored at a density of 10-20 virgins per vial. Virgin flies can be distinguished by their pale body colour and the presence of a dark spot or meconium in the gut, visible through the ventral abdominal wall. It is important to use very light CO_2 anaethesia, or preferably ice anaethesia, when sorting virgin females since excess CO_2 exposure can cause visible bloated abdomens, which often results in premature death. Males were either disposed or stored at a density of 25 males per vial. Collection bottles were kept at 18°C overnight to slow the rate of eclosion until the morning, from when the bottles were brought back to 25°C. This cycle was repeated until the desired number of virgins was collected.

2.3.4 Standard larval density

Maintaining standard density in larvae is important since larval density can affect longevity (Priest & Mackowiak. 2002). Since longevity was used as a surrogate marker of Aβ toxicity throughout this thesis, it was essential to control for this. Furthermore, overcrowding of larvae results in smaller flies. The size of a fly can negatively affect negative goeotaxis, another marker of disease used in fly AD models, since smaller flies have to effectively climb farther than normal sized flies. To ensure standard larval density, the following technique developed by Kennington and Clancy (2001) was used when setting up all experimental crosses.

To rear flies at a constant density, crosses were set up in plastic population cages at a virgin female:male ratio of 2:1. Each cage contained a single petri-dish containing grape juice medium, otherwise known as a grape plate (see grape juice medium), supplemented with live yeast paste. Larger cages also included a vial of water plugged with a damp cotton bud, to provide humidity. Flies were left to lay eggs for a maximum of 22 hours. It was often necessary to carry out a 'pre-lay' whereby the plates were supplemented with lots of yeast paste to encourage sufficient egg laying. After a sufficient number of eggs were laid the eggs were washed off with phosphate buffered saline (PBS) into a Falcon tube with the aid of a paintbrush. Eggs were allowed to settle and the remaining supernatant was poured off. Using a Gilson pipette, 20µl of the eggs were aspirated from the solution and squirted into 200ml glass bottles containing 70ml SYA medium, typically resulting in a standard density of 300-350 eggs per bottle (Kennington. 2001).

2.4 *Experimental procedures*

2.4.1 Once-mated females

For all experiments, flies were raised at a standard density on 70ml of standard SY medium in 200mL glass bottles. Flies emerging over a 24-hour period were transferred to fresh bottles for a period of 48 hours following eclosion. This ensured all females had mated at least once. Once-mated females were then sorted into vials (at a density necessary for the specific experiment) and the males discarded. Once-mated females were used for experiments for two key reasons. Because I decided to use the 'in-food' RU486 delivery approach, it was essential for flies to feed to induce UAS-transgene expression. Since females are known to feed at a higher level than males, using females ensured UAS-transgene would be more robust owing to a higher rate of RU486 ingestion.

Females were once-mated mainly for practical reasons. Having them one-mated was a means of standardising the female population, which was especially important when assaying behavioural phenotypes and survival. Virgins are thought to live twice as long as mated females (Smith. 1958) possibly due to higher egg production and the cost of mating in mated flies, both from physical damage and the transfer of seminal fluid from males, which has been shown to reduce lifespan (Trevitt and Partridge. 1991). Contrastingly, overexposure to males can shorten lifespan (Fowler and Partridge. 1989). Thus, using once-mated females ensured the female population was fairly homogenous rather than an assortment of virgins and mated females. Furthermore, it was more practical to collect mated females rather than virgins since strict timings did not need to be adhered to.

2.4.2 Lifespan assay

Once-mated females were transferred to experimental plastic vials containing ~3ml of SYA medium (with or without specified drug where applicable) at a density of 10-15 flies per vial. Flies were transferred to fresh food every 2-3 days, at which point, deaths or censors were scored. Dead flies were typically motionless with curled legs and shriveled bodies. A record was made of any dead flies carried over into the fresh vial. Censored flies included those that escaped during transfer, that had been accidentally damaged (eg. crushed between the cotton wool and vial) or any that were stuck to the food. Data are presented as survival curves and statistical comparisons of survival were performed using log-rank tests.

2.4.3 Proboscis-extension assay during undisturbed conditions

For undisturbed observations of feeding, 7-day-old mated flies of the same sex, were transferred to new food at a density of 5 per vial on the evening before the assay. Vials were coded and placed in a randomised order in rows on viewing racks at 25ºC overnight. The assay occurred with minimal noise and physical disturbance to the flies. To avoid recording disturbed fly feeding behaviour, 30 minutes was allowed between the arrival of the observer and commencement of the assay.

Observations were performed ‘‘blind’’ the next day for 90 minutes, commencing one hour after lights-on. In turn, each vial was observed for approximately 3 seconds during which the number of flies feeding was noted. A feeding event was scored when a fly had its proboscis extended and touching the food surface

while performing a bobbing motion. Once all vials in the experiment had been scored in this way, successive rounds of observations were carried out in the same way for the whole 90 minutes of the assay, which, depending on the size of the experiment meant that each vial was observed once every 2 to 5 minutes. At the end of the assay, the vial labels were decoded and the feeding data expressed as a proportion by experimental group (sum of scored feeding events divided by total number of feeding opportunities, where total number of feeding opportunities = number of flies in vial*number of vials in the group*number of observations). For statistical analyses, comparisons between experimental groups were made using log rank test.

2.4.4 Negative geotaxis (climbing) assay

Negative geotaxis is a commonly assessed behaviour in *Drosophila* that is used as a proxy measure of neuronal dysfunction. It is an innate escape response mechanism elicited by banging flies to the bottom of a container; the flies respond to the mechanical stimulation by climbing up the container wall.

Once-mated females were transferred to plastic vials containing ~3ml of SYA (+/-drug) medium at a density of 15 flies per vial. 3 vials of 15 flies were typically set up per genotype/condition. Climbing ability was then assayed every 2-3 days post-drug treatment. All assays were performed blind at the same time of day and under constant conditions (25°C, no humidity, no CO_2 exposure prior to assay). Flies were moved to the CT room at least an hour prior to the beginning of each assay to allow the flies to adjust to changes in the environment.

For the assay, 15 adult flies were transferred to a vertical column (25cm long, 1.5cm diameter) with a conic bottom end (i.e. a 25ml pipette, see Figure 2.4) tapped to the bottom of the column, and their subsequent climb to the top of the column was analysed. Flies reaching the top and flies remaining at the bottom of the column after a 45s period were counted separately, and three trials were performed at 1 min intervals for each experiment. A 45s training tap was performed before each trial. Scores recorded were the mean number of flies at the top (ntop), the mean number of flies at the bottom (nbottom) and the total number of flies assessed (ntotal). The Performance Index (PI) was calculated as 0.5(ntotal + ntop – nbottom)/ntotal. Data are presented as the mean PI ± SEM obtained in three independent experiments for each group, and analysis of variances (ANOVA) and post hoc analyses were performed using JMP 7.0 software.

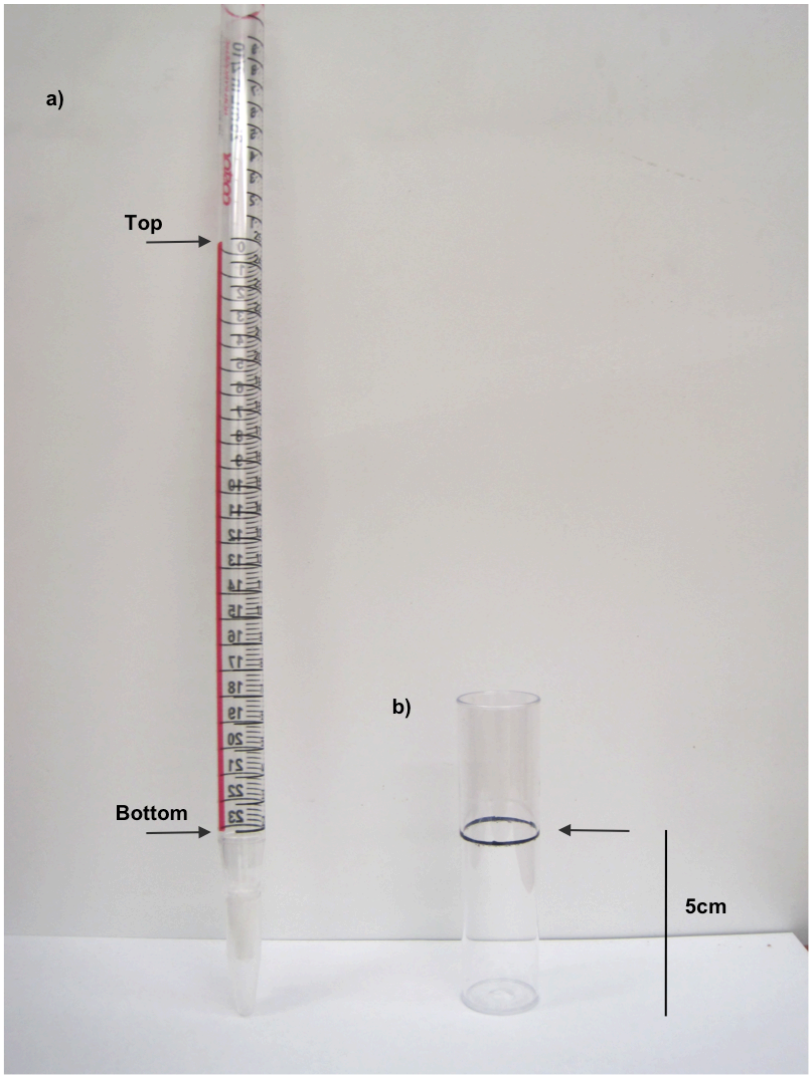

Figure 2.3. A photograph of the apparatus used for climbing assays. a) 25ml pipette assay and b) plastic vial assay. In the 25ml pipette assay the number of flies reaching the top, middle (area between top and bottom) and remaining at the bottom were scored after 45s. With the vial assay, the number of flies reaching the 5cm (labelled on vial) was recorded after 18s.

2.4.5 Giant Fibre System (GFS) electrophysiology[1]

Recordings from the giant fibre system (GFS) of once-mated female flies were made as described in (Allen *et al*. 1999). Flies were anaesthetized by cooling on ice and secured in wax, ventral side down, with the wings held outwards. A tungsten earth wire (ground electrode) was placed into the abdomen; tungsten electrodes were pushed through the eyes and into the brain to deliver a 40 V pulse for 0.03ms using a Grass S48 stimulator. Recordings were made from the tergotrochanteral muscle (TTM) and contralateral dorsal longitudinal muscle (DLM) using glass microelectrodes (resistance: 40–60 M). The electrodes were filled with 3M KCl and placed into the muscles through the cuticle. Responses were amplified using Getting 5A amplifiers (Getting Instruments, USA) and the data digitized using an analogue-digital Digidata 1320 and Axoscope 9.0 software (Axon Instruments, USA). For response latency recordings, at least 5 single stimuli were given with 5s rest periods between each stimulus; trains of 10 stimuli, at either 100, 200 or 250 Hz, were given with a 5s rest interval between each train.

2.4.6 Preparation of flies for molecular biology

Once-mated females were transferred to plastic vials containing ~3ml of SYA (+/- drug) medium at a density of 15-25 flies per vial and 5 vials per condition. Flies were transferred to fresh food every 2-3 days until the desired age. Flies were then transferred, under ice anaesthesia, from the vial to a 1.5ml eppendorf, snap frozen in liquid nitrogen and stored at-80°C. The majority of molecular

[1] All electrophysiology work was carried by H. Augustin.

work exclusively used fly heads. To decapitate the flies, the eppendorf was dipped in liquid nitrogen and then shaken vigorously, shearing the heads from the intact abdomen and thorax. The heads were then sorted from the bodies using a custom-made sieve. Once separated, the heads were immediately used or snap frozen in liquid nitrogen and stored at -80°C. However, repeated freeze/thaw cycles were generally avoided.

2.4.7 RNA extraction, cDNA synthesis and Quantitative-PCR (Q-PCR)

Total RNA was extracted from 20–25 fly heads (at least three independent head extraction per genotype) using Trizol (GIBCO) according to the manufacturer's instructions. The concentration of total RNA purified for each sample was measured using an eppendorf biophotometer. To prevent amplification of contaminating genomic DNA, 1mg of total RNA was subjected to DNA digestion using DNAse I (Ambion). This was necessary because the Aβ primers were designed within one exon (because the UAS-Aβ mini-gene was so small) and therefore off-target genomic DNA could serve as a template for PCR amplification.

DNase treated RNA samples were then subject to reverse transcription using the Superscript II system (Invitrogen) with oligo (dT) primers. To evaluate the level of genomic DNA in my RNA samples, reverse transcription was performed in the absence of reverse transcriptase (negative control). Amplification of this sample during Q-PCR represented the level of genomic DNA contamination. This was found to be neglibile. Q-PCR was performed using the PRISM 7000

sequence-detection system (Applied Biosystems), SYBR Green (Molecular Probes), ROX Reference Dye (Invitrogen), and Hot Star Taq (Qiagen, Valencia, CA) by following manufacturers' instructions. cDNA was amplified using two-pairs of PCR primers, one specific to UAS-Aβ42/Aβ40 and a second set specific to the endogenous control RP49. The primers for the Aβ42 and Aβ40 transgenes were directed to the 5' end and 3' end of the Aβ coding sequence: forward GATCCTTCTCCTGCTAACC; reverse CACCATCAAGCCAATAATCG. The RP49 primers were as follows: forward ATGACCATCCGCCCAGCATCAGG; reverse ATCTCGCCGCAGTAAACG. Cycle numbers were optimised for each primer set to ensure the reaction was within the linear range and each reaction terminated before reagents became limiting.

Aβ expression levels were quanitified using the relative standard curve method (Broughton *et al*. 2005) and normalised to RP49 (to control for variation in the amount and quality of RNA between different samples). Standard curves were prepared for both Aβ and RP49. For each experimental sample, the amount of Aβ and RP49 was determined from the relevant standard curve. Then, each Aβ amount was dividied by the respective RP49 amount to obtain a normalised Aβ value. This value was then expressed relative to a normalised calibrator sample (this division removed any units). In most instances this was the normalised Aβ amount in the negative w^{1118} control. Therefore, Aβ42 expression levels were presented as normalised expression levels relative to w^{1118}.

2.4.8 Total, soluble and insoluble Aβ42 quantification

To extract total Aβ42, five fly heads (per replicate) were homogenised in 50µl GnHCl extraction buffer [5M Guanidinium HCl, 50mM Hepes pH 7.3, protease inhibitor cocktail (Sigma, P8340) and 5mM EDTA], centrifuged at 21,000 g for 5 min at 4^0C, and the cleared supernatant retained as the total fly Aβ42 sample. Alternatively, soluble and insoluble pools of Aβ42 were extracted using a protocol adapted from previously published methods (Burns *et al*. 2003): 200 fly heads were homogenised in 200µl tissue homogenisation buffer [250mM sucrose, 20mM Tris base, 1mM EDTA, 1mM EGTA, protease inhibitor cocktail (Sigma)] then mixed further with 200µl DEA buffer (0.4% DEA, 100mM NaCl and protease inhibitor cocktail). Samples were centrifuged at 135,000g for 1 hour at 4°C (Beckman Optima^{TM} Max centrifuge, TLA120.1 rotor), and supernatant retained as the soluble Aβ42 fraction. Pellets were further resuspended in 400µl ice-cold formic acid (70%), and sonicated for 2 × 30 sec on ice. Samples were re-centrifuged at 135,000g for 1 hour at 4°C, then 210 µl of supernatant was diluted with 4ml FA neutralisation buffer (1M Tris base, 0.5M Na_2HPO_4, 0.05% NaN_3) and retained as the insoluble, formic acid-extractable Aβ42 fraction.

Total, soluble or insoluble Aβ42 content was measured in Arctic Aβ42 flies and controls using the hAmyloid β42 ELISA kit (HS) (Millipore). Total Aβ42 samples were typically diluted 1:10 or 1:100, and soluble versus insoluble Aβ42 samples diluted 1:10 in sample/standard dilution buffer, then ELISA performed according to the manufacturer's instructions. Protein extracts were quantified using the Bradford protein assay and the amount of Aβ42 in each sample expressed as a ratio of the total protein content (pmoles/g total protein). Data are

expressed as the mean pmol Aβ42/g total protein ± SEM obtained in at least three independent experiments for each genotype. ANOVAs and post-hoc analyses were performed using JMP 7.0 software.

2.4.9 Liquid β-galactosidase quantitative assay

Whole flies were weighed (see **2.4.12**) then homogenised in assay buffer (50mM K_2HPO_4, 1mM $MgCl_2.6H_2O$) in 96-square well blocks (Qiagen S block) with 2 flies per well. After spinning down, 15µl of homogenate was extracted and added to a flat-bottomed 96-well plate containing 30µl chlorophenol red-b-D-galactopyranoside (CPRG). Hydroloysis of CPRG by β-galactosidase turns the yellow substrate solution yellow to a dark red product. Plates were then mixed and allowed to develop in the dark at 25°C for 1 hour. 180µl MilliQ water was then added to each well and mixed. Absorption was then immediately measured at 574nm. Data are presented as the mean arbitary β-gal activity +/- SEM (n = 8-10) and were compared using Student's t-test.

2.4.10 ^{35}S-methionine incorporation assay

This assay was used to measure the rate protein translation and was adapted from a previously used method (Bjedov *et al*. 2010) for the use with fly head extracts. SY medium was first supplemented with 100µCi 35S methionine/ml of food (American Radiolabeled Chemicals 1mCi/37MBq ARS0104A)

15 flies were transferred to each vial containing 1ml radioactive SY medium. After three-hours of feeding, flies were transferred to non-radioactive SY for

30min in order to purge any undigested radioactive food from the intestines. Flies that were in contact with the radioactive food for 1 minute were used as a background control. Flies were then decapitated using liquid nitrogen and the heads were homogenized in 200μM 1% SDS and heated for 5 minutes at 95°C. At this stage aliquots were taken and mixed with 3ml scintillant. These samples represented the total radioactivity in fly head homogenates prior to protein extraction.

Samples were then centrifuged for 2x5 mins at maximum speed and supernatant retained. Proteins were precipitated by the addition of the same volume of 20% cold TCA (10% TCA final concentration) and incubated for 15 minutes on ice. Samples were then centrifuged at 16,000 g for 15 minutes, the pellet washed twice with acetone and then resuspended in 200μl of 4M guanidine-HCl. Samples (100μl) were mixed with 3ml of scintillant (Fluoran-Safe 2, BDH) and radioactivity counted in a liquid scintillation analyzer (TriCarb 2800TR, Perkin Elmer), with appropriate quench corrections. At the same, time the earlier total fly head homogenate samples were also measured. Measurements were normalized to total protein for each sample, as determined using the Bradford assay. Data are presented as the mean translation index ± SEM (n = 4) and were compared using Student's t-test.

The translation index was calculated as followed:

(TCA protein cpm/total cpm)/μg protein per sample.

2.4.11 Bradford assay

This assay was used to measure the total protein content in whole and head fly samples. BioRad reagent (5x) [Bio-Rad protein assay reagent, Bio-Rad Laboratories (UK) Ltd, Hemel Hempstead] was first diluted 1/5 in dH_20. 200µl was then added per well in a flat-bottomed 96-well plate. 2µl of sample was then added to each well. Plates were then mixed and absorbance was measured at 595nm. Absolute protein concentrations were determined using known volumes of bovine serum albumin (BSA) as a standard.

2.4.12 Weight analysis

Body weight of individual female flies (N = 10) was measured with a precision scale (range 0.001 – 10mg). Flies were reared at standard larval density and were age-matched (typically two-days post eclosion) before weighing. Data are presented as the mean mg wet weight per fly +/- SEM (n = 10). Means were compared using Student's t-test.

Chapter 3 Development and characterisation of an inducible model of Alzheimer's Disease

3.1 *Introduction*

Over the past several years, there has been a move towards using invertebrate models such as *Drosophila* to investigate a host of neurodegenerative diseases, including Alzheimer's disease (AD) (reviewed in Lu & Vogel. 2009). Although murine models remain the most popular, they often fail to recapitulate all of the pathological features associated with the disease, and the behavioural phenotypes can be laborious to characterise (Westerman *et al*. 2002). Moreover, the relative time and expense of modelling AD in the mouse permits little flexibility in experimental design. These issues combined with the relative practical advantages of *Drosophila* (see section **1.2.4**) the power and speed to perform large, unbiased experiments – have led to the development and application of many fly models of AD.

As has been previously described, AD is characterised by two major neuropathological mechanisms, the development of extracellular amyloid-β (Aβ) plaques and intraneuronal neurofibrillary tau tangles, and fly models of AD can be broadly grouped according to these. Because of the hypothesised causative role of Aβ in AD pathogenesis, the aim of many groups has been to overexpress Aβ peptides in fly neurons either by reconstituting the human APP/secretase system (Greeve *et al*. 2004) or by directly overexpressing wild-type and mutant Aβ as secreted peptides of different lengths (eg. 1-40 and 1-42) (Finelli *et al*. 2004; Iijima *et al*. 2004; Crowther *et al.* 2005). In either case, overexpression of Aβ42 but not Aβ40 caused neurodegeneration in a dose-dependent and age-dependent manner, reduced longevity, and caused locomotor deficits. All these features were associated with the progressive accumulation of Aβ42, replicating

a key feature of the human disease and further strengthening the validity of the fly as a model system. In addition, all three Aβ mini-gene models (Finelli *et al*. 2004; Iijima *et al*. 2004; Crowther *et al.* 2005) displayed clear phenotypes in the absence of amyloid-like deposits of Aβ, demonstrating that neuronal dysfunction and neuronal loss in *Drosophila* do not require the presence of β-amyloid plaques – a feature also demonstrated in worm and various mouse models.

The GAL4/UAS system represents the most widely used system for generating spatially restricted transgene expression in *Drosophila*, and it has been used to restrict expression of key AD disease genes to the fly nervous system. It is a bipartite system consisting of the yeast transcriptional activator GAL4 and its target sequence, the Upstream Activating Sequence or UAS (Brand and Perrimon. 1993). Essentially, any line showing tissue-specific expression of GAL4 can be used to drive similar tissue-specific expression of any cloned gene of interest (effector gene) that is fused to a promoter carrying a UAS. In practice, this involves crossing the appropriate GAL4 line to a second line carrying the UAS-effector fusion. This produces F1 individuals that carry both constructs and express the transgene in a spatially restricted manner as determined by the GAL4 promoter. In the case of modelling AD, the pan-neuronal elav-GAL4 or eye-specific GMR-GAL4 drivers have been used to drive either UAS-APP/UAS-BACE or UAS-Aβ transgenes. An example of the use of the GAL4/UAS system to model AD is shown below (**Figure 3.1**).

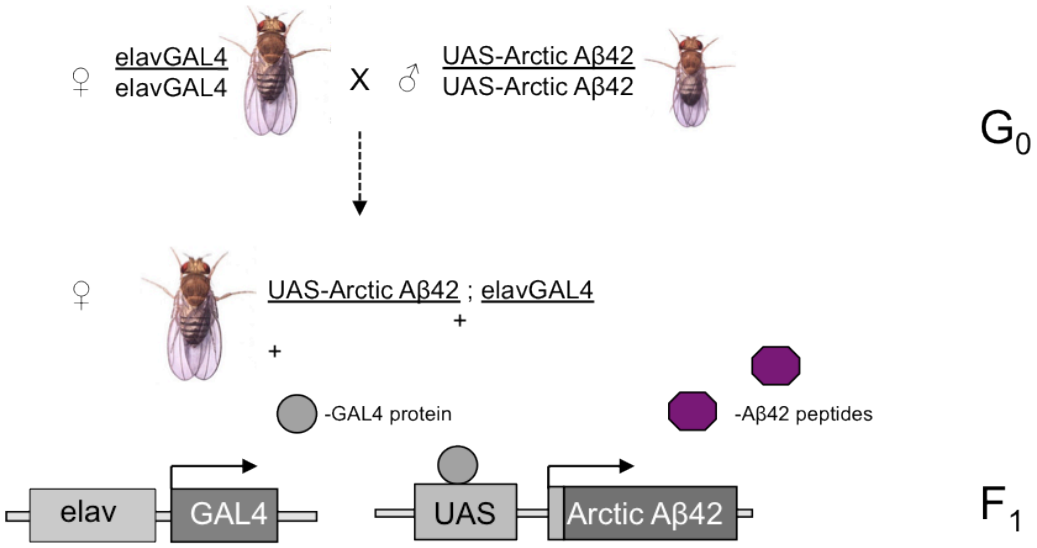

Figure 3.1. A schematic representation of the Crowther *et al* (2005) Aβ mini-gene model and the GAL4/UAS system. Driver lines expressing the transcriptional activator GAL4 under control of the neuron-specific elav promoter (elavGAL4) are crossed to flies expressing an Arctic Aβ42 transgene fused to a GAL4-binding upstream activation sequence (UAS-Arctic Aβ42). Aβ42 peptides are therefore expressed in the same cells where GAL4 is present.

A major drawback of the GAL4/UAS system when modelling age-related neurodegenerative disease is that it does not provide any temporal control over transgene expression. This is because most promoters and enhancers that drive GAL4 expression are active at multiple stages of development. This raises the issue of whether the phenotypes seen in fly AD models actually represent developmental defects brought on by toxic Aβ42 overexpression. For instance, Crowther *et al* (2005) observed a rough-eye phenotype, a commonly described mild developmental abnormality of the corneal lens of the compound eye, in all flies expressing Aβ42 peptides but not Aβ40.

Ideally, it would be much better to express Aβ peptides, for the first time, in the adult-fly to better replicate the natural progression of the disease in humans (i.e. pathology is not present at birth). The advent of inducible transgene systems has provided a means of circumventing this problem, allowing spatial and temporal control over transgene expression. Conditional systems use an environmental stimulus, such as light, temperature or a drug, to activate expression of a target gene. Therefore, one can choose when in the life cycle to turn transgene expression on and off by adding or removing the stimulus. A further advantage is that experimental and control groups are genetically identical - produced from the same cross and sharing the same developmental conditions. Ideally, the only variable during an experiment should be the absence or presence of the stimulus.

A variety of different conditional systems exist in *Drosophila*. The use of heat shock promoters has proved to provide temporal control but these promoters are limited because of their lack of tissue-specificity. Other approaches have included light-induced activation of caged GAL4 (Cambridge *et al*. 1997) and the use of tetracycline-dependent 'tet-off' (Bello & Resendez-Perez. 1998; Stebbins 2001) or 'tet-on' (Bieschke *et al*. 1998) transactivation systems, which are based on binding of the tetracycline operator (tetO) sequences (upstream of target gene), either by the tetracycline repressor protein (tetR) in the absence, or by a mutant tetracycline repressor (rTA) in the presence, of tetracycline or derivatives such as doxycycline.

Although the 'tet-on' and 'tet-off' systems have proven to be effective, they do not take advantage of the huge library of pre-existing UAS lines, therefore

requiring new tetR or rTA drivers and tetO responsive fly stocks to be generated. The GeneSwitch system, on the other hand, is compatible with pre-existing UAS lines. Essentially, it is an extension of the GAL4/UAS system, permitting spatial and temporal control with a RU486-dependent GAL4-progesterone-receptor fusion protein called 'GeneSwitch' (Osterwalder *et al.* 2001; Roman *et al*. 2001). With this system, transgene expression can be initiated at any time, simply by adding the drug, mifepristone (RU486) to the fly food before feeding. Once activated, GeneSwitch mediated transgene expression can be turned off by shifting animals to RU486-free food.

In this chapter I set out to develop a novel adult-onset model of AD in the fruit fly *Drosophila melanogaster* by using the inducible GeneSwitch system to spatially and temporally restrict the expression of human Aβ peptides in fly neurons, for the first time in adult flies. Aβ expression, following induction, was first confirmed and characterised. The effect of Aβ overexpression was then measured and profiled with the use of established markers of neuronal function and toxicity. The overall aim in developing this model was to investigate the direct consequences of Aβ production, in the absence of APP processing or endogenous Aβ production, exclusively in the adult fly, thereby bypassing any potential developmental defects.

3.2 *Results*

3.2.1 Development of the model

To establish the model, a pan-neuronal elav GeneSwitch (elavGS) driver line (Osterwalder *et al*. 2001) that has been previously used to develop an adult-onset, *Drosophila* model of spinocerebellar ataxia (SCA) (Latouche *et al*. 2007) was used to direct expression of a UAS-Arctic Aβ42 mini-gene (Crowther *et al*. 2005) both spatially and temporally, to neurons in the adult fly (**Figure 3.2**) The Arctic mutation, which causes early-onset familial AD (FAD) in humans, encodes a Glu22Gly amino acid substitution within the Aβ domain that increases the propensity of the peptide to aggregate (Nilsberth *et al*. 2001; Murakami *et al*. 2002). Expression of the Arctic mutant form of Aβ42 is more toxic to flies than wild-type Aβ42 (Crowther *et al*. 2005). Thus, the decision to overexpress Arctic Aβ42 was made to ensure a robust phenotype could be detected. A UAS-Aβ40 line (Crowther *et al*. 2005) was used as a control for over-expression of non-toxic forms of Aβ in fly neurons, since this form of the peptide has previously been shown to have no detrimental effect in flies (Finelli *et al*. 2004; Iijima *et al*. 2004; Crowther *et al*. 2005).

Notably, because the same UAS-Aβ lines were used, this model can be effectively viewed as an extension of the Crowther *et al* (2005) Aβ mini-gene model. To reiterate, this model investigated the downstream consequences of Aβ production (rather than APP processing) by overexpressing Aβ peptides fused to the *Drosophila* netrotic secretion signal peptide under the control of the pan-neuronal driver elav-GAL4^{C155}. In this study expression of Aβ42 and Arctic

Aβ42 resulted in age-dependent and dose-dependent neurodegeneration, reduced longevity and locomotor deficits, with the Arctic mutation accelerating these phenotypes. In addition, it was reported that much of the Aβ42 and all of the Arctic Aβ42 were retained within the cell as monomers or SDS-resistant oligomers in *Drosophila* S2 cells. Similarly in the brain tissue of young flies Aβ was first found to accumulate intracellularly, only later forming extracellular non-amyloid deposits. These deposits resembled the diffuse plaques found in human AD. So in some ways, this model system better represents the effects of intraneuronal Aβ42-mediated toxicity.

To generate flies for use in experiments, parental flies were crossed as follows: *UAS-ArcticAβ42/UAS-ArcticAβ42* males were crossed to female *elavGS/elavGS*. The decision to use female elavGS was mainly practical – the reciprocal cross would have been equally valid. However, as it was necessary to cross elavGS to many different UAS-lines, using elavGS females minimised the time and media required for collecting virgins. Adult-onset expression in neurons was then induced in *UAS-Arctic Aβ42/+;elavGS/+* once-mated female progeny by adding RU486 to SY medium, typically at two-days post eclosion (**Figure 3.2**). The same crossing scheme applied when using other UAS-lines and driver lines in experiments described below.

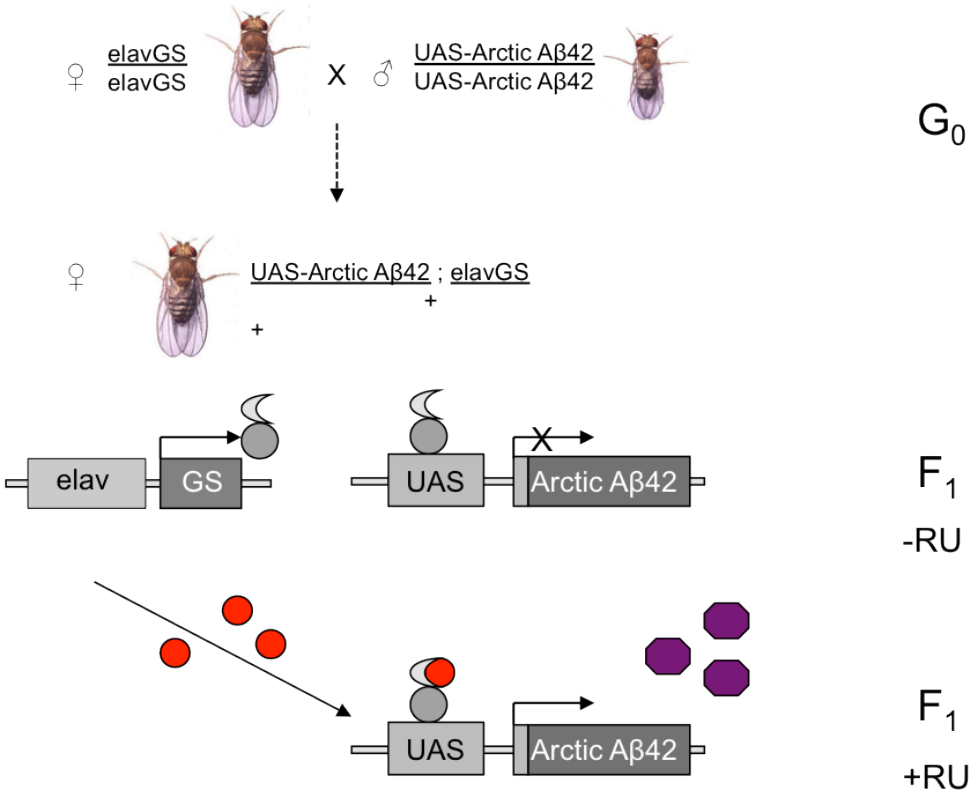

Figure 3.2. A schematic representation of the GeneSwitch-UAS expression system. The GeneSwitch system, a modified version of the GAL4/UAS system permits spatial and temporal control of transgene expression with a RU486-dependent GAL4-progesterone-receptor fusion protein called 'GeneSwitch (GS) (Osterwalder *et al*. 2001). Driver lines expressing the transcriptional activator GeneSwitch under control of the neuron-specific elav promoter (elavGS) are crossed to flies expressing an Arctic Aβ42 transgene fused to a GAL4-binding upstream activation sequence (UAS-Arctic Aβ42). In the absence of the activator mifepristone (RU486; -RU), the GeneSwitch protein is expressed in neurons but remains transcriptionally silent, so that Arctic Aβ42 is not expressed. Following treatment with RU486 (+RU; red) the GeneSwitch protein is transcriptionally activated, binds to UAS and thus mediates expression of Aβ peptide (purple) specifically in fly neurons. With this system, UAS-linked transgene expression can be initiated at any time, by adding RU486 to SY medium prior to feeding. Likewise, expression can be switched off by removal of RU486 from the SY medium.

3.2.2 Characterisation of elavGS induction kinetics

Before establishing the AD model, it was necessary to characterise the kinetics of the *elavGS* driver. The *elavGS* driver line was derived from the *elavGS302.1* strain, originally published by Osterwalder *et al* (2001), and has been reported to induce relatively higher levels of expression, equal to that obtained with the constitutive *elav^{C155}-GAL4* line (Latouche *et al*. 2007) used in previous fly models of AD (Iijima *et al*. 2004; Crowther *et al*. 2005). However, because this information was not published, it was important to validate and further characterise the driver before adopting it for use in modelling AD. Driver kinetics were characterised using a UAS-lacZ reporter construct accompanied with quantitative β-galactosidase (β-gal) liquid assays. β-galactosidase activity was therefore used as a proxy of gene expression. Because the half-life of β-gal and Aβ were likely to differ, this characterisation was merely to get a quick evaluation of the efficacy of the new driver.

Homozygous *elavGS or elavGS302.1* females were crossed with homozygous *UAS-lacZ* males. Adult-onset neuron expression of β-galactosidase was then induced in *UAS-lacZ/+;elavGS/+* or *UAS-lacZ/+;elavGS302.1/+* female progeny by adding RU486 to SY medium.

To assess the immediate short-term response of the driver lines to RU486, β-galactosidase activity was measured in *UAS-lacZ/+;elavGS* and *UAS-lacZ/+;elavGS302.1* flies treated with 200μM RU486 from two-days post eclosion. β-galactosidase activity was then measured up to 48-hours into

treatment. Non-RU-treated controls (-RU) were also assayed for each genotype at every time point (**Figure 3.3**).

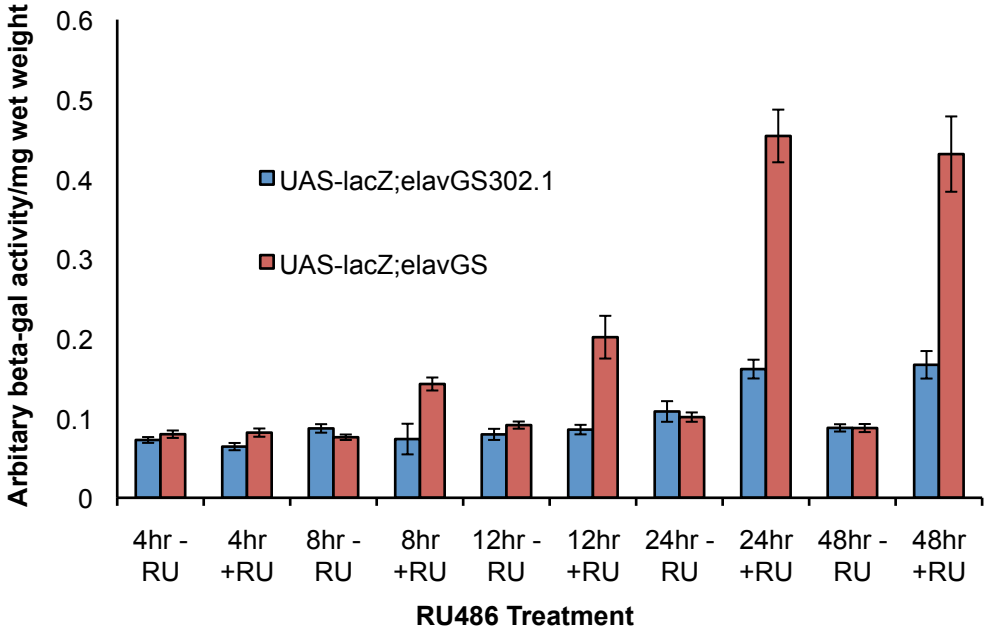

Figure 3.3. **Induced β-galactosidase activity with elavGS and elavGS302.1.** β-galactosidase assays were performed on once-mated, female *UAS-lacZ/+;elavGS/+* and *UAS-lacZ/+;elavGS302.1/+* flies treated with +RU (200μM) and –RU (0μM) from two-days post eclosion for 4, 8, 12, 24 and 48 hours. Data are presented as the mean arbitrary β-gal activity/mg wet weight +/- SEM (n = 5 for each group). Activity levels between treatments were compared within each genotype and between genotypes using Student's t-test.

β-galactosidase activity levels were significantly higher in *elavGS* flies, when compared to *elavGS302.1* and non-RU-treated controls, following 8, 12, 24 and 48 hours of induction ($p<0.01$ in all cases, Student's t-test). Activity levels significantly higher than the –RU controls were first detected after 8-12 hours in *elavGS* ($p<0.01$, Student's t-test), and after 12-24 hours in *elavGS302.1* ($p<0.01$, Student's t-test). 4 hours induction did not significantly increase β-galactosidase

activity in either line, highlighting a minimum period of RU treatment necessary for induction. Interestingly, a low level of β-galactosidase activity in the absence of RU486 (-RU) was also observed at all timepoints. This basal activity did not significantly change over the 48-hour period and it did not differ between *elavGS* and *elavGS302.1* flies. Nonetheless, it indicated there was a significant, albeit low, basal expression of the UAS-transgene in the absence of RU486.

3.2.3 Arctic Aβ42 expression can be induced in adult *Drosophila* neurons

The first goal in establishing the inducible model was to confirm RU treatment could induce Arctic A*β*42 expression in the adult neurons. This was assessed by measuring Aβ42 mRNA and protein levels in the heads of *UAS-Arctic Aβ42/+;elavGS/+* flies chronically treated with RU486 (+RU) from two-days post eclosion. mRNA and protein expression levels were measured four- and 21-days into RU486 treatment using RT-PCR and Aβ42-specific sandwich ELISA, respectively (**Figure 3.4**). Non-RU-treated (-RU) *UAS-Arctic Aβ42/+;elavGS/+* flies were used as a control for expression in the absence of inducer. In addition, Aβ40 mRNA and protein levels were assayed in *UAS-Aβ40/+;elavGS/+* flies at both timepoints.

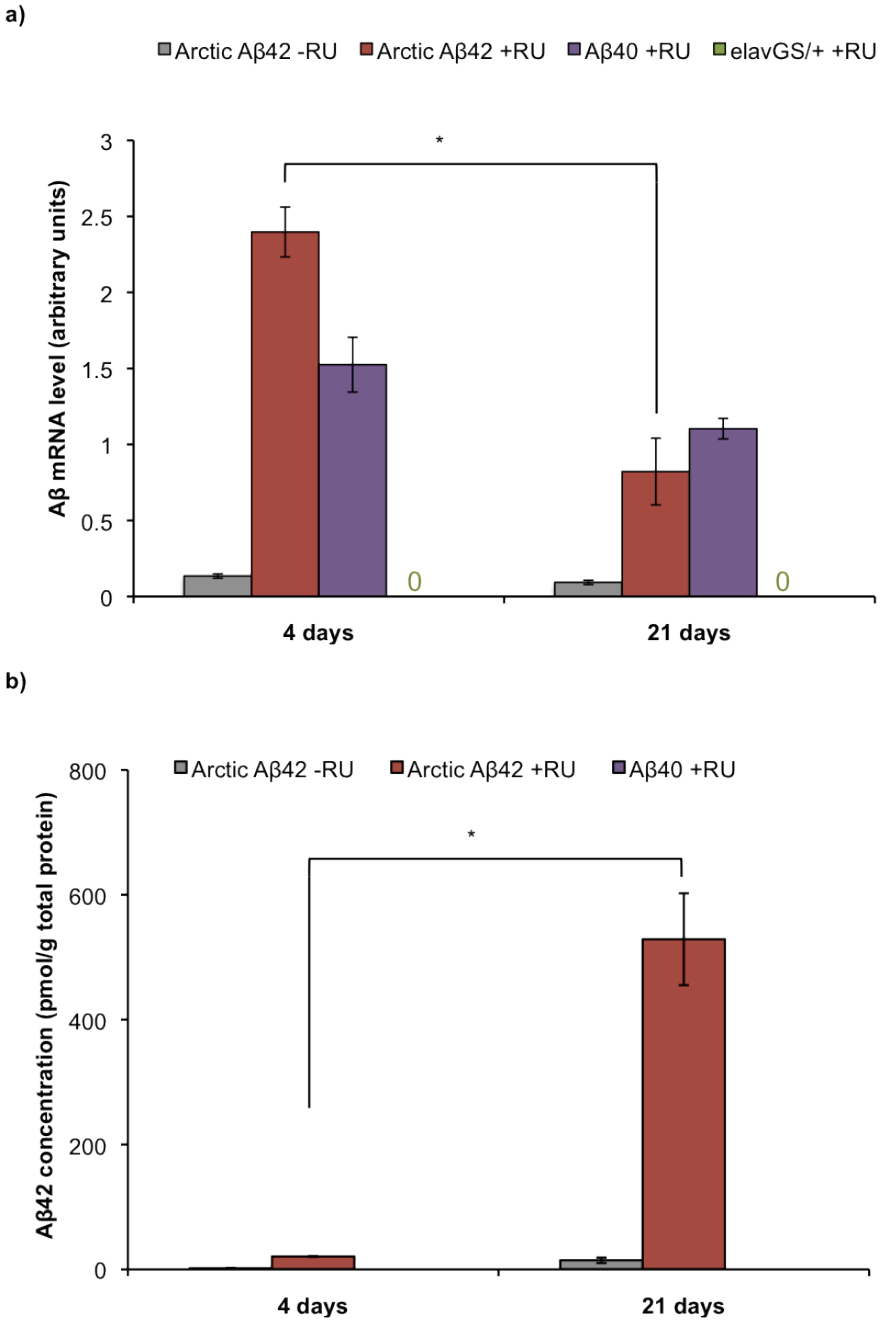

Figure 3.4. Adult-onset induction of Arctic Aβ42 peptide in fly neurons. Arctic Aβ42 and Aβ40 mRNA (relative to w^{1118} controls) and protein levels were quantified at four days and 21 days into-RU486 treatment. Data are presented as means +/- SEM (n = 4 for each group) and were analysed by Student's t-test (* = P<0.01).

Aβ42 transcripts were clearly elevated in RU-treated *UAS-Arctic Aβ42/+;elavGS/+* flies in comparison with untreated (-RU) flies at four-days ($P<0.01$, Student's t-test) and 21-days ($P<0.01$, Student's t-test). Moreover, Aβ42-specific sandwich ELISA confirmed that Aβ42 protein was elevated in RU-treated flies compared to untreated (-RU) control flies at both timepoints ($p<0.01$, Student's t-test) and that the level of protein increased from four-days to 21-days of age ($p<0.01$, Student's t-test). The increase in Aβ42 protein by 21-days contrasted with a significant decrease in Aβ42 mRNA over the same period ($P<0.01$, Student's t-test). The decline in Aβ42 mRNA expression could have been attributable to a decline in RU consumption, an idea consistent with the reduction in feeding behaviour with age previously reported for wild-type flies (Wong *et al*. 2009). The relatively higher Aβ42 protein levels at 21-days indicated a significant accumulation of the Arctic Aβ42, despite a reduction in Aβ42 mRNA. Again, as in the case when driving UAS-lacZ, Aβ42 mRNA and protein transcripts were both detected in the absence of RU486, indicating a slight leak in the control of expression. At the transcript level, leakiness was constant; evident by the fact Aβ42 mRNA levels in untreated flies (-RU) did not change over time. However, Aβ42 protein levels did increase over the same period ($P<0.05$, Student's t-test), indicating that Aβ42 protein was accumulating in uninduced flies, albeit at a very low level relative to RU-treated flies.

Aβ40 transcripts were also elevated in *UAS-Aβ40/+;elavGS/+* flies treated with RU at both timepoints ($P<0.01$, Student's t-test). At day 4, Aβ40 mRNA levels were significantly lower than Aβ42 levels ($P<0.01$, Student's t-test) but by day 21 these levels were equivalent. Similarly to Aβ42-expressing flies, Aβ40

mRNA levels decreased from four-days to 21-days. This result is in keeping with the idea of reduced RU486 ingestion over time. Unsurprisingly, no Aβ40 was detected in the Aβ42-specific ELISA, highlighting the specificity of this particular assay kit.

3.2.4 Induced Arctic Aβ42 protein rapidly aggregates in adult neurons

Next, I assessed the state of aggregation of Aβ42 protein in the mutant flies by separating soluble and insoluble protein fractions from fly head extracts. Soluble Aβ is defined as any species that does not pellet and is retained in the supernatant following high-speed centrifugation. At day 15, when the first signs of pathology were observed in *UAS-Arctic Aβ42/+;elavGS/+* flies (see climbing data below), most of the Aβ42 had accumulated in an insoluble form (**Figure 3.5**), consistent with the aggregation-promoting effects of the Arctic mutation. Interestingly, all the Aβ42 in non-RU-treated flies was found in a soluble state.

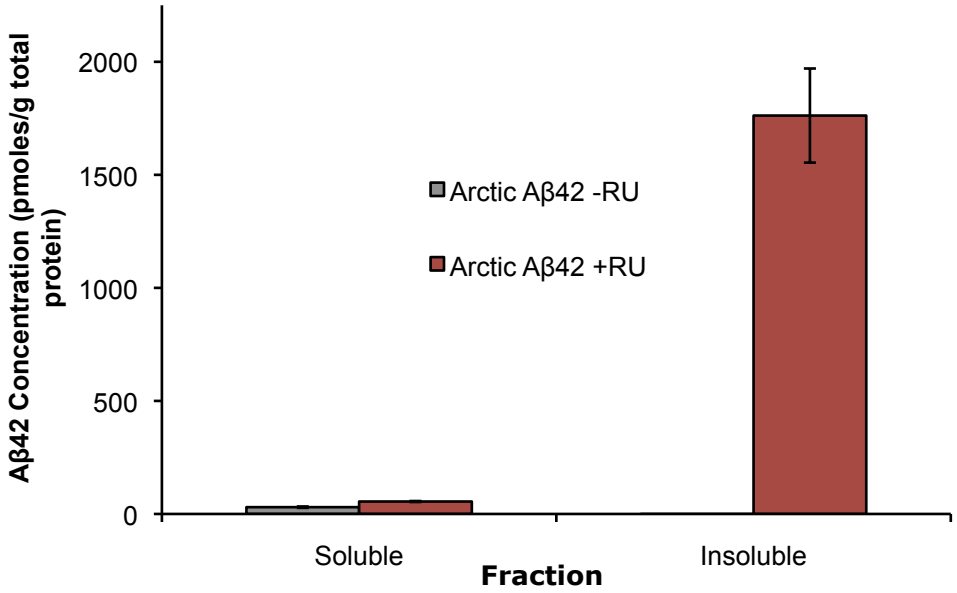

Figure 3.5. Arctic Aβ42 peptide in the adult *Drosophila* neurons was mostly in an insoluble state. In the absence of the RU486 (-RU) a negligible amount of soluble protein was observed at day 15. Following treatment with RU486 (+RU; red) the Aβ peptide expression was seen in both soluble and insoluble fractions, with a significant proportion observed in the insoluble fraction. Data are presented as means +/- SEM (n = 3) and were analysed by Student's t-test. $P<0.01$ when mean protein levels of soluble and insoluble fractions of Aβ42 expressing flies (+RU) were compared.

3.2.5 Over-expression of Arctic Aβ42 peptide in adult neurons increases mortality and induces neuronal dysfunction in *Drosophila*, without evidence of neuronal cell loss

Previously published studies have shown that constitutive expression of Arctic Aβ42 peptide in fly neurons significantly shortens lifespan, induces behavioural impairments and causes neuronal death (Finelli *et al*. 2004; Iijima *et al*. 2004; Crowther *et al*. 2005). To determine whether adult-onset expression of Arctic

Aβ42 peptide in neurons causes similar phenotypes, I examined survival, and neuronal and behavioural dysfunction in *UAS-Arctic Aβ42/+;elavGS/+* flies.

First, the effect of Arctic Aβ42 over-expression on lifespan was measured by treating *UAS-Arctic Aβ42/+;elavGS/+* and *UAS-Aβ40/+;elavGS/+* flies with 200μM RU from two days-post eclosion and recording their survival (**Figure 3.6**). Flies maintained on SY medium containing no RU (-RU) were used as controls. Induced expression of Arctic Aβ42 in adult neurons significantly shortened median lifespan by about 50% in comparison to non-RU-treated controls ($P<0.0001$, log rank test). Induced expression of Aβ40 did not shorten lifespan at all when compared to non-RU-treated *UAS-Aβ40/+;elavGS/+* flies ($P = 0.48$, log rank test). This demonstrated a specific lifespan-shortening effect of Arctic Aβ42 compared to the Aβ40 form of the peptide. Interestingly, the leaky expression previously detected in non-RU-treated *UAS-Arctic Aβ42/+;elavGS/+* flies did result in a slight reduction in lifespan, when compared to UAS-Aβ40/+;elavGS/+ treated flies ($P<0.01$ for both comparisons, log rank test).

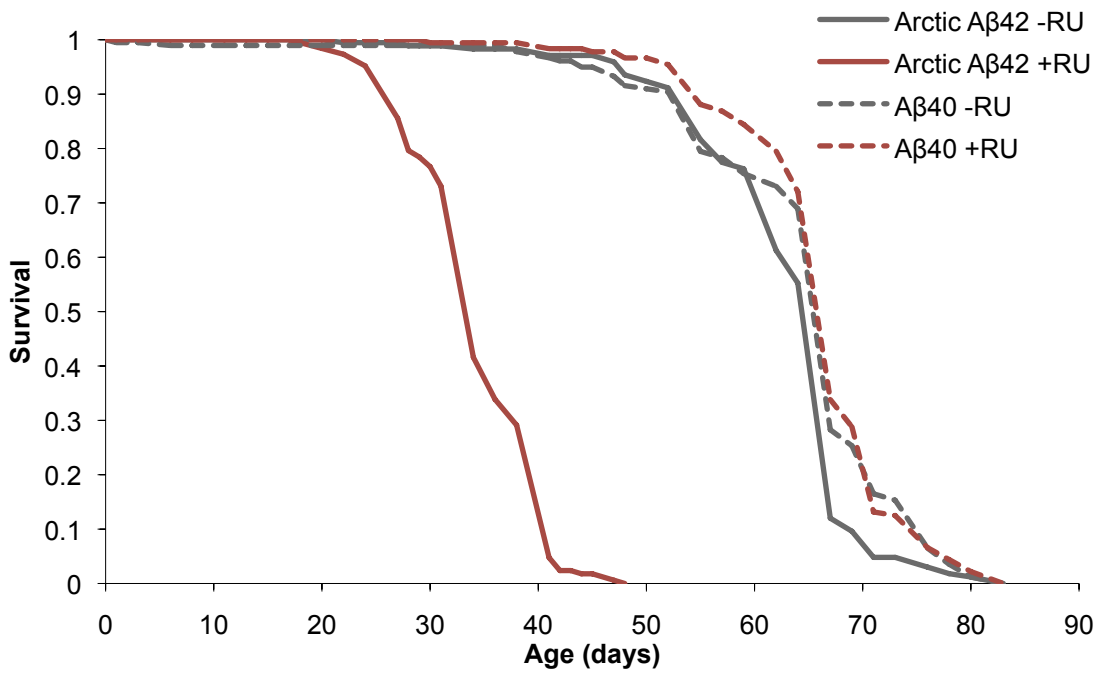

Figure 3.6. Expression of Arctic Aβ42 specifically in adult neurons shortened lifespan. Survival curves are depicted and data were compared using the log-rank test. Median lifespans are: 33 days for Arctic Aβ42 +RU, and 66 days for Arctic Aβ42 –RU, Aβ40 –RU and Aβ40 +RU. Log rank tests: Arctic Aβ42 +RU vs Arctic Aβ42-RU ($P<0.0001$), Aβ40 –RU versus Aβ40 +RU ($P = 0.48$), Arctic Aβ42 –RU versus Aβ40 –RU/+RU ($P<0.01$).

To determine whether adult-onset expression of the Arctic Aβ42 peptide caused neuronal toxicity, neuronal function was analysed directly, by recording electrophysiological responses of the *Drosophila* giant fibre system (GFS) and indirectly, by measuring negative geotaxis (climbing ability).

The GFS is a neural circuit that mediates the fly's escape response (Allen *et al*. 2006). Stimulation of the giant fibre neuron in the brain results in depolarisation of the tergotrochanteral (TTM) jump muscle and the dorsal longitudinal flight muscle (DLM). Placement of stimulating electrodes in the giant fibre neuron and

recording electrodes in the TTM or DLM allows one to measure the response latency – the time taken for a given stimulation to generate depolarisation of the muscle. The electrophysiological responses of the GFS were measured to directly examine the response of neuronal function to Arctic Aβ42 (**Figure 3.7**). GFS activity was measured in *UAS-Arctic Aβ42/+;elavGS/+* flies treated with 200μM RU486 from two days post-eclosion at day 16 and day 28 into treatment. Giant fibres (GF) were stimulated via electrodes inserted inside the compound eye, and post-synaptic potentials recorded in the TTM and DLM. Parameters measured were the latency from GF stimulation to muscle response and the stability of the response to high frequency stimulation. At day 16, response latencies in the TTM, DLM and the TTM to high frequency stimulation were comparable between *UAS-Arctic Aβ42/+;elavGS/+* flies on +RU and -RU. However, at day 28, expression of Arctic Aβ42 peptide significantly increased the response latency measured in both the TTM and DLM, and inhibited the stability of the TTM response to high frequency stimulation (at 100, 200 and 250 Hz) in comparison to untreated control flies (see figure for statistics). This indicated a progressive neuronal dysfunction following adult-onset induction of Arctic Aβ42, with young flies exhibiting no dysfunction in the GFS, while older flies showed obvious defects in response to both a single stimulus and to high-frequency stimuli.

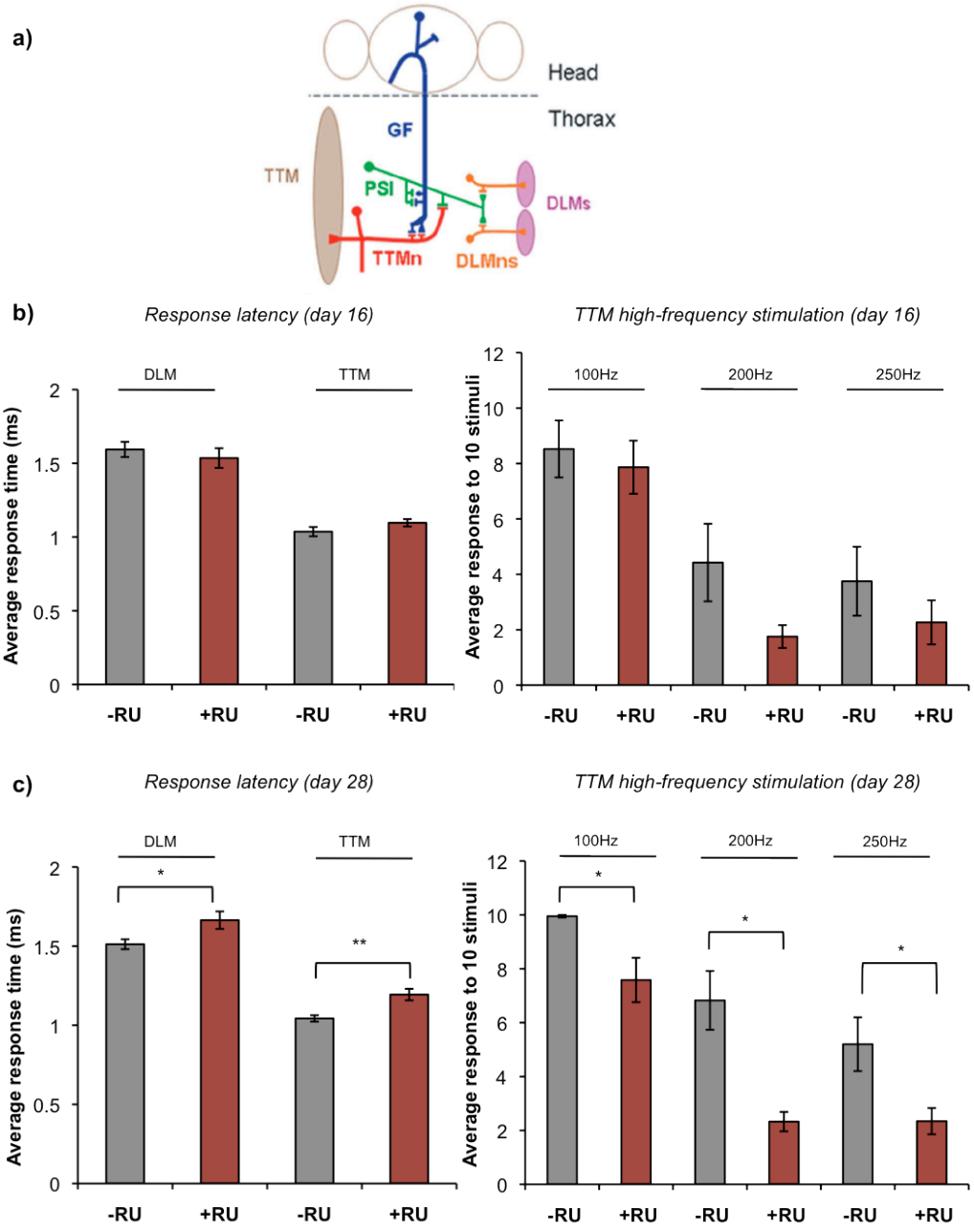

Figure 3.7. Arctic Aβ42 peptides induced progressive, adult-onset neuronal defects in *Drosophila*. (a) A schematic illustration of the *Drosophila* giant fibre system [GFS; adapted from Allen *et al*. (2006)]. Giant fibres (GFs; blue) relay signals from the brain to the thoracic musculature via mixed electrochemical synapses with the motorneurons (TTMn, red) of the tergotrancheral muscle (TTM; left), and the peripherally synapsing interneuron (PSI; green), which subsequently forms chemical synapses with the motorneurons (DLMn; orange) of the dorsal longitudinal muscles (DLM; right). Note only one of the TTMn

axons is shown exiting the nervous system and contacting the muscle on the left hand side and one set of the DLMns and corresponding neuromuscular junctions are depicted on the right hand side. GFS activity was measured in *UAS-Arctic Aβ42/+;elavGS/+* at (b) 16 days and (c) 28 days post-RU486 treatment; parameters measured were the latencies from GF stimulation to muscle response (response latency DLM and TTM) and the stability of the response to high frequency stimulation at 100, 200 and 250 Hz (high frequency stimulation TTM). Data are presented as the mean response +/- SEM (n = 8) and were analysed by Student's t-test, at each time point, on log-derived data. *P<0.05, **P<0.01 comparing response latency or response to high frequency stimulation of UAS-ArcAβ42/+;elavGS/+ +RU flies to -RU controls at 28 days post-induction. Note: H. Augustin performed all electrophysiology work.

As a behavioural, indirect measure of neuronal dysfunction, locomotor activity was assessed using a negative geotaxis (climbing) assay. Numerous labs have demonstrated that negative geotaxis declines with age in wild type flies (Cook-Wiens and Grotewiel. 2002). However, flies expressing Aβ peptides show a further decline in climbing ability (Iijima *et al*. 2004; Crowther *et al*. 2005).

Negative geotaxis was measured in *UAS-ArcAβ42/+;elavGS/+* and *UAS-ArcAβ40/+;elavGS/+* flies treated with 200μM RU486 from two-days post-eclosion (**Figure 3.8**). Non-RU-treated flies from both genotypes were used as controls. As stated earlier, *Drosophila* display an age-related decline in climbing behaviour, and this was apparent in the non-RU-treated and UAS-*ArcAβ40/+;elavGS/+* +RU control flies. However, flies expressing Arctic Aβ42 displayed a reduced negative geotaxis in comparison to their -RU control flies and the Aβ40 +RU and -RU flies from day 14 onwards (P<0.05, two-way

ANOVA). The climbing behaviour of the Arctic Aβ42 flies had declined to a level by ~ day 12 that was reached by the control flies only by day 28.

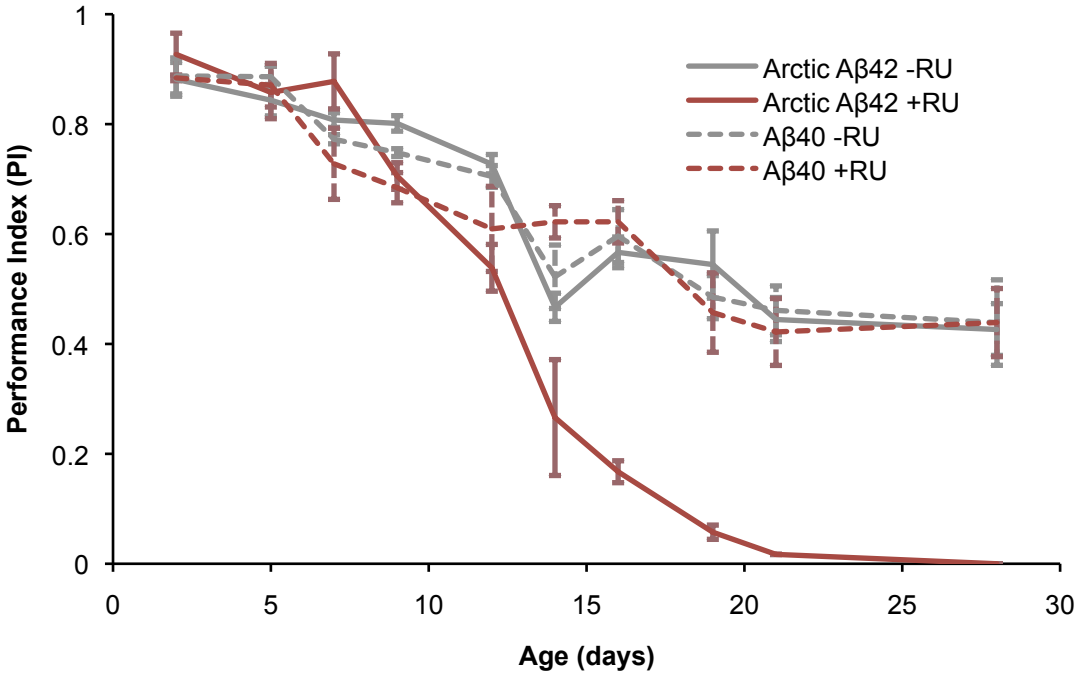

Figure 3.8. Expression of Arctic Aβ42 peptides in the adult fly nervous system caused locomotor dysfunction. Climbing ability of UAS-*ArcAβ42/+;elavGS/+* and *UAS-Aβ40/+;elavGS/+* flies on + and - RU486 SY medium was assessed at the indicated time-points. Data are presented as the average performance index (PI) +/- SEM (n = 3, number of flies per group = 39-45) and were compared using two-way ANOVA and Tukey's honestly significant difference (HSD) post-hoc analyses. The PI of *UAS-Arctic Aβ42/+;elavGS/+* +RU flies to that of untreated and Aβ40 over-expressing controls was significantly lower from day 14 onwards ($P<0.05$ all timepoints, two-way ANOVA).

To assess whether the effects of induced Arctic Aβ42 over-expresion on lifespan, neuronal function and locomotor function resulted from neuronal death, neuronal loss was quantified at day 21 in *UAS-Arctic Aβ42/+;elavGS/+* treated with + and – RU from two-days post eclosion. Interestingly, there was no evidence of neuronal loss in the brains of flies overexpressing Aβ42 peptide (**Figure 3.9**).

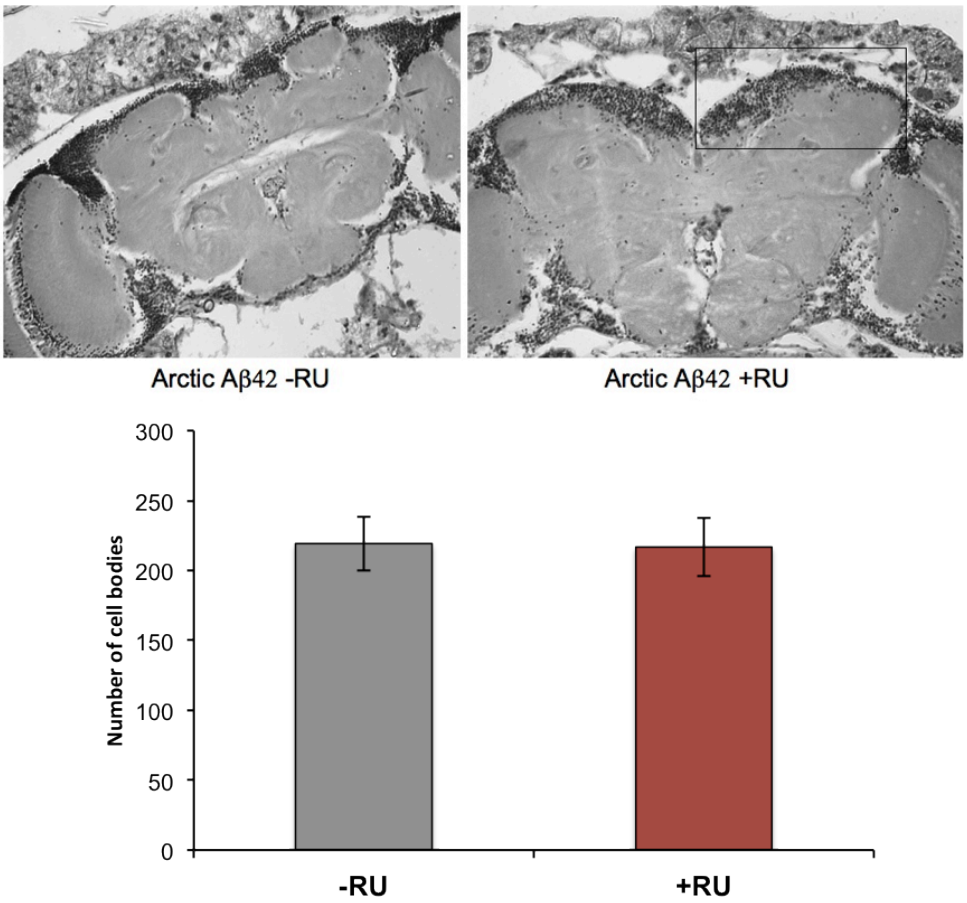

Figure 3.9. Neuronal cell loss was not evident in flies over-expressing Arctic Aβ42 peptide in adulthood. Cell loss was quantified at day 21 in UAS-Arctic Aβ42/+;elavGS flies, fed with + or – RU from two-days post-eclosion. Flies were maintained at 27ºC and neuronal loss was quantified by counting the number of cell bodies per brain hemisphere. Cell bodies were counted double blind. Data are presented as the means +/- SEM (n = 7 per genotype). No significant difference in the number of cell bodies was observed when comparing

+RU and –RU (Student's t-test). This work was a collaborative effort with Dr. Oyinkan Sofola.

3.3 *Discussion*

3.3.1 Induction with the GeneSwitch system is robust but declines with age

First and foremost, the results in this chapter reaffirm that the GeneSwitch system is an effective platform for inducing UAS-transgene overexpression in the adult fly. Induction was achieved by dissolving the inducer, RU486, in SY media (prior to dispensing and polymerisation) at a final concentration of 200μM or ~86ug/ml (method developed by Giannakou *et al*. 2004). It is interesting to note that other delivery methods have been used, such as adding RU486-supplemented yeast paste to the food (Hwangbo *et al*. 2004) or adding a single drop of RU486 solution to soak into the food ('on-food' method) (Ford *et al*. 2007). All delivery methods have been shown to be effective in inducing expression (Poirier *et al*. 2008), with the 'on food' method considered the most dose-responsive and consistent between genders (Poirier *et al*. 2008). Despite this, I decided to use 'in food' delivery because it was the most practical (when preparing many vials of SY) and because gender differences in expression were not important, since only females were used. Furthermore, dissolving RU486 into the food ensured the flies were given no choice between drug and drug-free food when feeding.

The 'in-food' method proved to be rapid and robust. In *UAS-lacZ/+;elavGS/+* flies significant beta-gal activity (compared to uninduced levels) was detected 8-12 hours following RU exposure. Similarly, elevated Aβ42 transcript and protein levels were detected after two-days of RU treatment (although this may have been sooner if earlier timepoints were assayed). This kinetic data agrees with

other studies where induction was detected 5 hours (Osterwalder *et al*. 2001) and one-day (Poirier *et al*. 2008) following RU exposure. The disparity in the induction times is probably a reflection of the different protocols, drivers and delivery methods used. For instance, Ostweralder *et al* (2001) used larvae bathed in RU486, whereas Poirier *et al* (2008) used the 'on-food' delivery method. In any case, the issue here is not the differences in the response time to RU486 but the obvious sensitivity of the GeneSwitch system to different protocols. Thus, these differences highlighted the necessity to keep drug dose and delivery consistent between experiments.

The results in this chapter also demonstrate that the level of expression driven with elavGS declines over time. There was a significant decline in Aβ42 and Aβ40 mRNA expression from four-days to 21-days of age. This was most likely due to a reduction in the amount of RU486 ingested as feeding behaviour has been shown to decrease with age in *Drosophila melanogaster* (Wong *et al*. 2009). This is an inevitable drawback of using the in-food delivery method. Direct injection of a known concentration of RU486 solution into each individual fly might offer the best way of avoiding this problem but it is not practical for large experiments.

Temporal variation in transgene expression with the GAL4/UAS system is common and has been seen with standard GAL4 (Seroude. 2002) and GeneSwitch drivers (Poirier *et al*. 2008). Interestingly, Poirier *et al* (2008) observed a steady increase in gene expression, using beta-gal activity as a proxy measure of UAS-lacZ expression, with the elavGS302.1 driver in female flies.

Although this may appear to contradict the data discussed above, it does agree with the protein data, which also indicated an increase in Aβ42 expression over time. However, using protein expression as a proxy of gene expression is flawed because protein perdurance can bias data interpretation. Extremely stable proteins might imply gene expression was constant or increasing, when in fact, transcripts were decreasing (as in the case of the inducible model). Beta-gal and Arctic Aβ42 are incredibly stable, and in the latter's case, aggregation-prone proteins. Thus, the relative perdurance of Aβ42 protein likely explains the opposite movement of Aβ42 mRNA and protein expression levels over time.

3.3.2 Transgene expression in the absence of RU486 is a feature of the GeneSwitch system

A key criterion for any conditional system is the absence of expression in the absence of the inducer (control group). The results in this chapter demonstrate that the GeneSwitch system is not truly conditional. β-gal activity and Aβ42 mRNA and protein expression was evident in non-RU-treated control *UAS-lacZ/+;elavGS* and *UAS-Arctic AB42/+;elavGS/+* flies, respectively. Because whole fly homogenates were used in the β-gal assay, it is possible that β-galactosidase present in the fly's gut bacteria were contributing to this signal. This agrees with that observation that uninduced β-gal activity did not change over time (48 hours). However, in the case of Aβ42 expressing flies, there was no other possible source of the human Aβ42 peptide. In non-RU-treated flies, Aβ42 expression was clearly evident at the transcript and protein level. Although Aβ42 transcript levels did not change between the two timepoints assayed, there was an accumulation of Aβ42 protein.

Expression in the absence of RU486 seems to be a common and unavoidable feature of the GeneSwitch system. In the original work by Osterwalder *et al* (2001), very low expression of reporter genes was detected in the absence of RU486. Furthermore, this feature has been observed in many studies since (Giannakou *et al*. 2007; Ford *et al*. 2007; Poirier *et al*. 2008). The problem of 'leaky' expression in the non-RU-treated control groups raises the question of whether GeneSwitch is really suitable for the development of conditional, adult-onset models of age-related disease as outlined in this chapter. I think the answer to this question is a resounding 'yes'. The leakiness of the GeneSwitch system does render it unsuitable for studying the effect of gene expression at a specific timepoint (e.g. during L1 phase) since it would be difficult to determine if any effects were due to expression at the specified timepoint or leaky expression at some other timepoint. However, in the case of modelling AD the main concern was whether the induced and leaky domains of expression would overlap, and whether the leaky expression was below the threshold required for toxicity. In the first instance, leaky expression was very low relative to induced levels and secondly, had no effect on climbing ability and only a slight effect on lifespan. In any case, the comparisons made in this chapter and the remainder of this thesis were always relative to the non-RU-treated controls rather than the wild-type background.

3.3.3 The inducible AD model in relation to other fly models of Aβ42 toxicity

This study extended the characterisation of fly AD models by examining the effect of AB42 expression exclusively in adulthood by using the inducible

GeneSwitch system. Since there are a large number of pre-existing models of AD in the fly, particularly models of Aβ42 toxicity, it will be relevant to discuss the findings of this chapter in relation to other models of AD in the fly.

Induced over-expression of the Arctic Aβ42 peptide in adult fly neurons led to a marked reduction in lifespan, neuronal dysfunction, as seen directly in the GFS, and behaviourial impairments. On the other hand, induced over-expression of the Aβ40 peptide had no effect on these phenotypes. These findings are in agreement with previously reported studies (Finelli *et al*. 2004; Iijima *et al*. 2004; Crowther *et al*. 2005). Of particular interest to this thesis are comparisons between the inducible model and the Crowther model since they both used the same UAS-reagents. In general, the phenotypes presented in this model were much less severe. For instance, Crowther *et al* (2005) reported that flies expressing one copy of the UAS-Arctic Aβ42 transgene had a median lifespan of six-days at 29°C, and were completely immobile by two-days post eclosion. Compare this with 33 days and 25 days respectively, in this model. Furthermore, Crowther *et al* (2005) observed a marked rough eye phenotype (mild developmental abnormality of the corneal lens of the compound eye) at eclosion. With this model, a rough eye phenotype was never observed at any age during experiments

These striking differences are most likely a consequence of the extreme experimental conditions used by Crowther *et al* (2005). Apart from the quantification of neuronal loss (**Figure 3.9**), all experiments in this chapter were carried out at 25°C, whereas in the comparative study flies were raised and maintained at 29°C. This was to ensure high levels of transgene expression.

Drosophila are ectotherms, which means they are too small to regulate their own temperature and are thus forced to adopt ambient temperature. In *Drosophila*, lowered temperature increases lifespan entirely by lowering the slope of the mortality trajectory, with no effect on the initial mortality rate (Mair *et al*. 2003). In other words, lowering the temperature decreases the rate of ageing in *Drosophila*. This explains why flies expressing Aβ42 in the inducible model were longer lived. This is exemplified by the fact even w^{1118} wild-type flies had a median lifespan of 20 days in the Crowther study. Furthermore, since negative geotaxis is also a function of ageing, the difference in experimental temperature underpins the relatively slower decline in negative geotaxis seen in these results.

Interestingly, when Crowther *et al* (2005) performed lifespan assays at 25°C rather than 29°C, flies with one copy of UAS-Arctic Aβ42 exhibited a median lifespan of 10 days. This is still significantly shorter than the results seen in this chapter. This difference cannot be due to differences in temperature. It is possible that expression with the $elav^{c155}$ driver is much greater than that with *elavGS* and RU486. Alternatively, this could be due to the accumulation of Aβ42-mediated damage during the development process. The latter point certainly fits in with the fact Crowther *et al* (2005) observed a marked rough eye phenotype at eclosion, which was absent in flies from this study. Further studies, directly comparing the expression levels and their consequences on lifespan and negative geotaxis would be useful in exploring this issue.

Although the phenotypic characterisation of the inducible model paralleled other reports, there was one major difference; no neuronal loss was observed in the

brains of flies over-expressing Aβ42. This finding contrasts with previous reports that flies over-expressing Arctic Aβ42, using the constitutive neuronal driver, *elav*^{c155}, develop vacuoles (Iijima *et al*. 2004; Crowther *et al*. 2005). These contrasting results could be reconciled if neuronal loss upon Aβ42 over-expression is a consequence of developmental abnormalities in the *Drosophila* brain or if neuronal loss represents an end-stage event in response to Aβ42 toxicity, since vacuolation has been reported only under the most extreme conditions of expression, age and temperature, while neuronal toxicity in these models is already apparent under less stringent conditions (Crowther *et al*. 2005). Importantly, these findings agree with those of other studies demonstrating that neuronal loss is generally not evident in murine models of amyloidosis, such as in mice transgenic for the amyloid precursor protein (McGowan *et al*. 2006).

Chapter 4 Testing the interaction between ageing and AD using an inducible model of AD

4.1 *Introduction*

One of the major unresolved questions in AD research and the neurodegenerative field in general, asks why does neurodegeneration occur late in life? More specifically, why do totally distinct disorders, defined by different sets of clinical and neuropathological descriptors, share similar temporal emergence patterns (Cohen & Dillin. 2008)?

The mechanisms linking protein aggregation and the appearance of disease to age remain to be identified. One possibility is that protein aggregation is a stochastic process requiring many years to accumulate to toxic levels, so that neurons would start to lose function when toxic proteins reach a certain threshold concentration. Another suggestion is that the duration of exposure or cumulative exposure to a pathogenic protein is what leads to neuronal dysfunction. This would lead to the prediction that the total length of exposure, or the area under the curve of toxic protein concentration over time, would predict the age at which neuronal function starts to decline. A third possibility is that the ageing process itself increases vulnerability of neurons to protein toxicity, so that a fixed exposure is more likely to lead to dysfunction in old age (Cohen *et al*. 2006). All of these factors could be important – they are not mutually exclusive.

One approach to investigating the mechanisms leading to late-onset neurodegeneration is to alter the rate of ageing in transgenic animal models of AD to see whether these interventions ameliorate pathology. Modulating ageing in model organisms can be achieved in many ways: genetically, via the downregulation of evolutionary conserved nutrient-sensing pathways such as the

IIS or TOR pathway; pharmacologically, with drugs such as rapamycin and resveratrol; or with dietary restriction. All these interventions have been shown to extend lifespan, and remarkably, have all been shown to suppress pathology in a range of AD disease models (for review see Douglas & Dillin. 2010). Collectively, these studies support an active role for the ageing process in the development of neurodegenerative disease.

An alternative approach to investigating the mechanisms leading to late-onset neurodegeneration is to induce expression of a toxic protein to different levels, or for different lengths of time and at different ages, to disentangle the mechanisms at work. This approach differs in that it makes no assumptions about the ageing process and what genes or pathways may be important in modulating it. Rather, it aims to measure effect the effect of normal physiological ageing. If ageing were to play an active mechanistic role in enabling neurodegeneration then one would expect that standardised exposure of older neurons to a toxic protein would lead them to develop pathology at a faster rate, or to a greater extent, than young neurons. In the few studies that have addressed this issue, older organisms have been found to be more vulnerable. Brewer et al., (1998) isolated neurons from embryonic, young and old-aged rat hippocampus and exposed them to toxic Aβ fragments (25-35). Toxicity as measured by cell death was found to be age, dose and time-dependent. The maximum toxicity in cells treated for 1 day with 25 μM Aβ (25-35) was 16%, 24% and 33% for embryonic, young and old cells respectively. In another study, Guela et al., (1998) demonstrated that aged rhesus monkeys are more vulnerable to injected plaque-equivalent concentrations of fibrillar Aβ when compared to young rhesus monkeys, which developed no

pathology at all. However, these two studies used either extracellular application of Aβ fragments or microinjection of fibrillar Aβ to induce toxicity at different ages, a drawback of which is that it makes assumptions about the nature of Aβ toxicity. Moreover, these studies may not truly reflect the human disease since it is increasingly believed that intracellular (Laferla *et al*. 2007), soluble oligomers of Aβ are pathogenic (Walsh & Selkoe. 2007), rather than extracellular, fibrillar forms of the peptide. A more accurate model of the disease process may, therefore, be achieved by inducing protein expression using conditional transgenic systems, so that Aβ originates intracellularly and aggregates under physiological conditions.

This approach was used in the preceding chapter, whereby expression of the FAD-associated Arctic Aβ42 isoform was induced in adult neurons of the fruit fly *Drosophila melanogaster*. Induction of Aβ42 in young adult flies resulted in age-dependent locomotor and electrophysiology deficits and shortened lifespan. The aim of this chapter was to further characterise the flexibility of the inducible AD model with the overall aim of investigating the effect of ageing as a risk factor for Aβ toxicity. First, the dynamics of Arctic Aβ expression with the elavGS-UAS system were evaluated. I then sought to exploit these dynamics to investigate the role of ageing in response to Aβ42-mediated toxicity. In particular I aimed to induce Arctic Aβ42 expression at progressively later ages in adult fly neurons and then measure the time to develop, and extent of, known markers of toxicity such as survival.

4.2 *Results*

4.2.1 Dynamics of Arctic Aβ42 transcript and protein expression using the elavGS-UAS system

I previously characterised an adult-onset fly model of Alzheimer's disease, generated by expressing the Arctic Aβ42 peptide under the control of an RU486-inducible pan-neuronal driver. In the current study I aimed to investigate the effects of standardised Aβ42 induction on toxicity at different ages, and so it was important to firstly understand the dynamics of transgene and protein expression and repression using this inducible system.

My previous study demonstrated that Arctic Aβ42 is expressed, at both the RNA and protein level, within four days following induction with RU486. Aβ42 RNA expression declined with age, most likely reflecting a lower intake of the inducer RU486 due to an age-dependent reduction in feeding behaviour (Wong *et al*. 2010). Aβ42 protein levels, however, increased with age, either reflecting a time-dependent accumulation of the peptide or an age-dependent reduction in protein turnover. This suggests that both the concentration of RU486 and the length of induction would need to be controlled for in order to standardise the level of Aβ42 expression at varying ages.

It was first necessary to confirm RU486 removal represses UAS-transgene expression with the GeneSwitch system. This was assessed in two ways. First, as in the previous chapter, β-galactosidase activity was used as a proxy for gene expression. *UAS-lac/+;elavGS/+* flies were treated with 200μM RU486 from 2-

days post-eclosion for seven days, and then transferred to RU486-free food SY food for 4, 12, 24 and 48 hours. Flies maintained on –RU486 and +RU486 for the entirety of each experiment were used as controls (**Figure 4.1**).

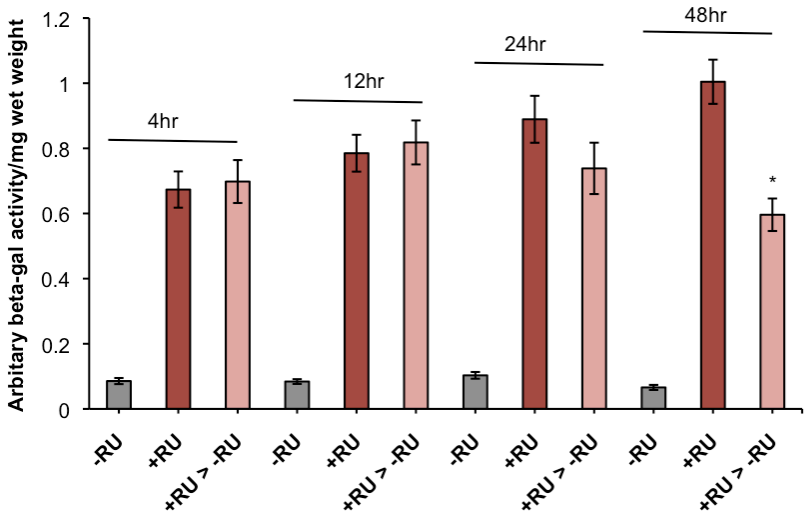

Figure 4.1. The effect of RU486 removal on β-galactosidase activity. Liquid β-galactosidase assays were carried out on once-mated female *UAS-lacZ/+;elavGS* flies. Flies were exposed to +/- RU486 at day 2 for 7 days, and then transferred to –RU486 1.0 SY food for 4, 12, 24 and 48 hours. Data are presented as means +/- SEM (n = 5 for each condition). *P<0.05 comparing beta-gal activity in flies switched to –RU486 for 48 hours to flies maintained on +RU486 (Student's t-test)

In chapter 3 it was shown that application of RU486 led to a significant increase in transgene expression (using beta-gal activity as a proxy for gene expression) within 8-12 hours. The kinetics of repression were much slower. A significant drop in β-galactosidase activity was only seen 48 hours (P<0.01, Student's t-test) after the switch to –RU486. This drop only amounted to a 40% reduction in beta-gal activity. Thus, these results highlighted a difference in the kinetics of

induction and repression with the GeneSwitch system and were in agreement with other studies reporting a relatively slower suppression of GFP expression following RU486 removal (Osterwalder *et al*. 2001). This difference could have been attributable to the perdurance of β-galactosidase. Therefore, to fully assess repression dynamics in the context of modelling AD, switch off experiments were performed using Q-PCR to profile the level of Arctic Aβ42 mRNA following RU486 removal.

UAS-Arctic Aβ42/+;elavGS/+ flies were treated with 200μM RU486 from two-days post-eclosion for 7 days, and then transferred to RU486-free SY. In contrast to the β-galactosidase data, Arctic Aβ42 transcript returned to baseline, un-induced levels within 24 hours of RU486 removal (**Figure 4.2**). Thus, at the transcript level repression is rapid. On the other hand, no significant reduction in Arctic Aβ42 protein concentration was observed over several weeks following removal of RU486 under similar induction conditions (see below; **Figure 4.8**). These data suggest that, although Aβ42 production could be rapidly switched-off using the GeneSwitch system, the Arctic Aβ42 peptide was highly resistant to degradation in these flies.

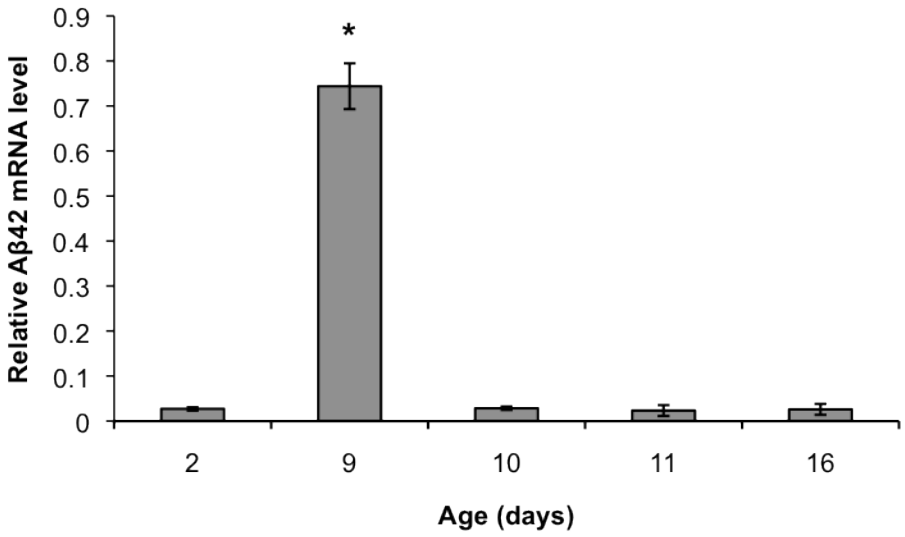

Figure 4.2. Removal of RU486 results in a robust decline in UAS-Arctic Aβ42 mRNA expression. Arctic Aβ42 mRNA expression levels in the heads of *UAS-Arctic Aβ42/+;elavGS/+* once-mated females treated with 200μM RU486 from two-days post eclosion for one-week. mRNA levels were assayed at 2-days prior to RU486 treatment (day 2), at the end of RU486 treamtment (day 9) and 24hrs (day 10), 48hrs (day 11) and a week (day 16) following the switch to RU486-free food. *P<0.05 when comparing the level of Arctic Aβ42 mRNA at day 9 to all other timepoints (ANOVA).

4.2.2 Aβ42-mediated toxicity correlates with total Arctic Aβ42 concentration in young flies

As Aβ42 peptide concentration accumulates with age, I next investigated the relationship between the length of induction, at a given age, and the extent of toxicity in the fly. UAS-Arctic Aβ42/+;elavGS/+ once-mated females were treated with 200μM RU486 SY from two-days post eclosion before being switched back to RU486-free SY at progressively later ages. This 'switch-on, switch-off' regime will be from hereon in known as a RU486 pulse. Flies were 'pulsed' for two, four and seven days, as outlined below (Table 2) and

subsequently assayed for Aβ42 protein expression (**Figure 4.3**), negative geotaxis (**Figure 4.4**) and survival (**Figure 4.5**). Flies maintained chronically on –RU486 and 200μM RU486 media were used as negative and positive controls, respectively.

Treatment	Day switched-on	Day switched to –RU
-RU	n/a	n/a
+2d RU	2	4
+4d RU	2	6
+1wk RU	2	9
+RU (chronic)	2	n/a

Table 2. The various RU486 pulses used in switch-off experiments. Note that these days are 'post-eclosion and that all flies were treated with RU486 at the same age (2-days post-eclosion).

Aβ42 protein levels increased in correlation with the length of RU486 treatment (**Figure 4.3**). Hence, at the protein level Aβ42 appeared to accumulate with longer periods of transgene expression, possibly as a consequence of the high stability of the peptide. An increase in RU486 exposure also correlated with enhanced negative geotaxis (**Figure 4.4**) and shortened lifespan (**Figure 4.5**). Chronic, one-week and four-day RU486 treatments produced significant declines in climbing ability compared to untreated controls (60%, 50% and 29% respectively). However, two-day treated flies displayed an ageing-related decline that did not differ from controls (**Figure 4.3**), suggesting that this induction

condition was below the threshold to cause neuronal dysfunction in response to Aβ42. Similarly, chronic RU486 treatment produced the largest (56%), and two-day treatment the smallest (11%), reduction in median lifespan compared to non-RU-treated controls (**Figure 4.5**). As this two-day pulse was sufficient to induce a reduction in lifespan, it suggests that survival was more sensitive to changes in RU486 exposure time than climbing ability.

Since the Arctic Aβ42 peptide was highly resistant to degradation for up to three weeks following 'switch-off' of RNA production (see below; **Figure 4.8**), varying the length of RU486 exposure may be viewed as inducing a dose-response to Aβ42 at a given time. This data, therefore, indicated that inducing Aβ42 expression in young flies leads to pathogenic phenotypes later in life that are dependent on the dose of Aβ42. These findings were important because they indicated that to induce the equivalent level of toxicity at different ages it would be necessary to induce the same Arctic Aβ42 dose at those ages.

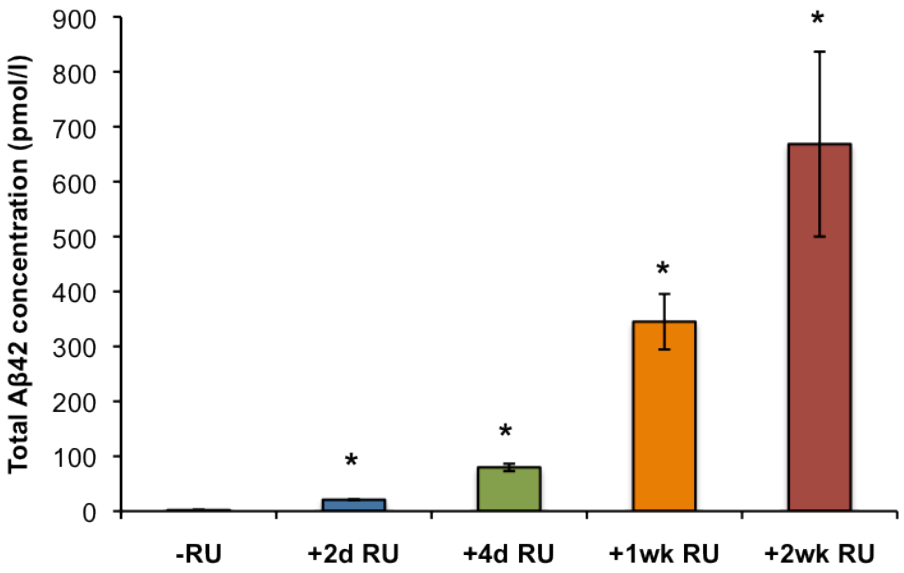

Figure 4.3. Total Aβ42 protein load increases with RU486 exposure time. Total Arctic Aβ42 protein levels were quantified at the end of each RU486 pulse in *UAS-Arctic Aβ42/+;elavGS* females. Data are presented as the mean total Arctic Aβ42 concentration (pmoles/g total protein) +/- SEM (n = 3 for each group). Total Arctic Aβ42 protein levels were significantly different between all treatments. *P<0.05 when comparing highlighted treatment with preceding e.g. +1wk RU versus +4d RU (Student's t-test).

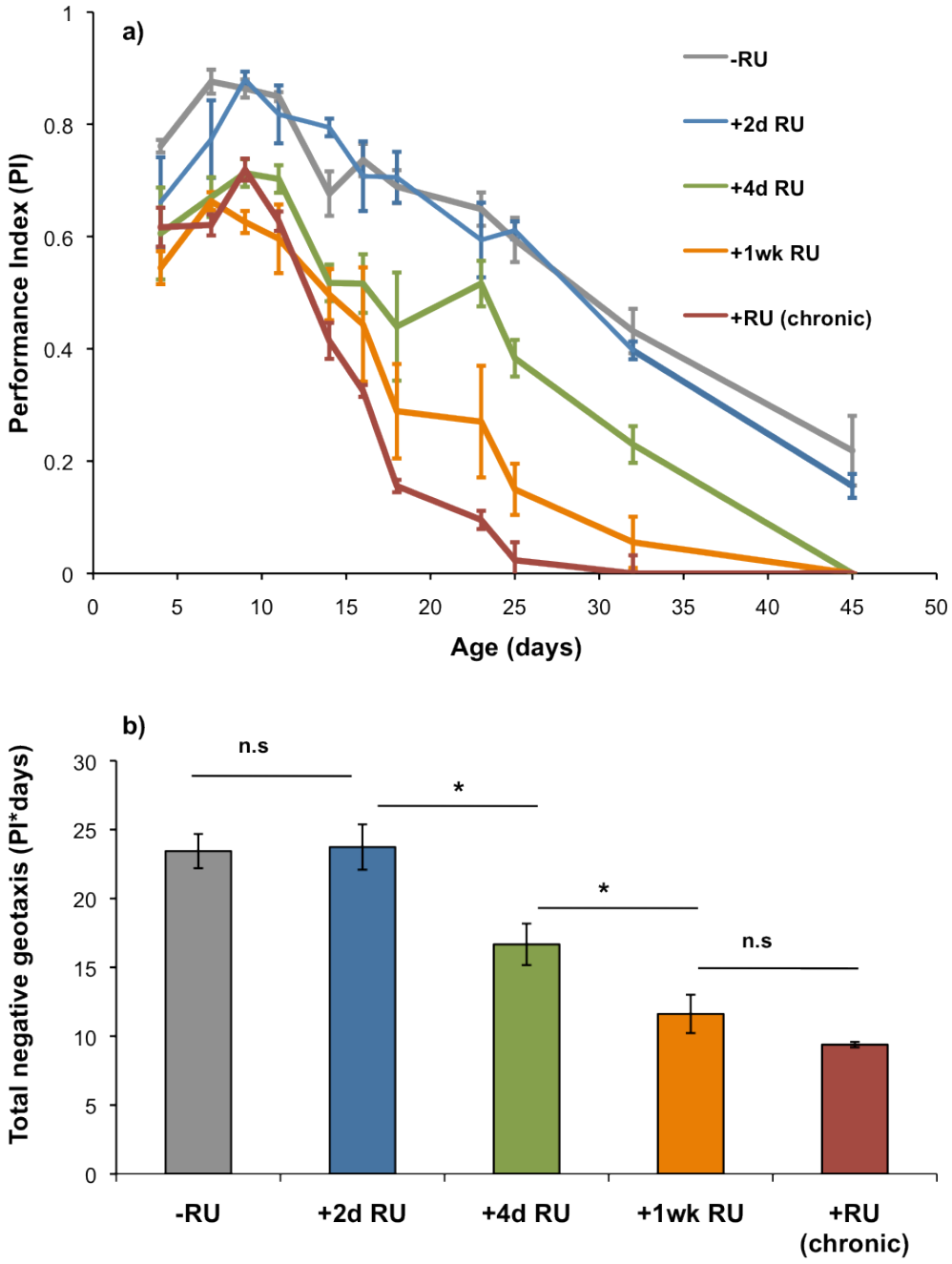

Figure 4.4. Locomotor dysfunction increases with RU486 exposure time. Climbing ability of *UAS-ArcAβ42/+;elavGS/+* females pulsed with RU486 for 2,4 and 7 days was assessed at the indicated time-points. Flies maintained on –RU486 (-RU) and 200µM RU486 (+RU chronic) were used as negative and positive controls, respectively. Data are presented as (a) the average performance index (PI) +/- SEM (n = 3, number of flies per group = 39-45) over time and (b) the average total negative geotaxis/area under the curve (PI*days) +/- SEM (n = 3) *P<0.05 when comparing total negative geotaxis between the indicated

groups, n.s. represents non-significant differences between groups (Student's t-test).

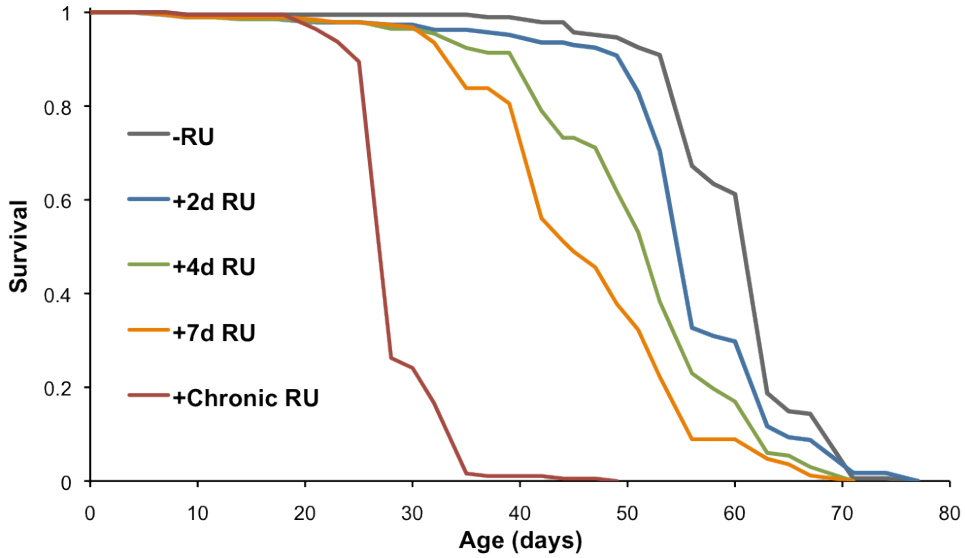

Figure 4.5. Mortality increases with RU486 exposure time. Survival curves of *UAS-Arctic Aβ42/+;elavGS/+* females pulsed with 200µM RU486 from two-days post-eclosion for 2, 4 and 7 days before being transferred to non-RU-treated SY. Flies permanently maintained on –RU486 (-RU) and 200µM RU486 (+RU chronic) were used as negative and positive controls, respectively. Median lifespans are as follows: 62 days for –RU, 55 days for +2d RU, 52 days for +4d RU, 45 days for +1wk RU and 27 days for +chronic RU. All survival curves were significantly different from each other ($P<0.001$, log rank test).

4.2.3 The challenges of measuring the effect of ageing on Arctic Aβ42-mediated toxicity

To assess the effects of age on the vulnerability of flies to Aβ42, I aimed to induce toxicity at progressively later ages and then to measure the delay to, and extent of, resultant pathological phenotypes. Although survival and negative geotaxis are useful surrogate markers of Aβ42 toxicity, they are also directly affected by ageing and this presented a technical challenge for such investigations. It was important that at all ages of induction RU486 treatment resulted in phenotypes that were significantly different from their respective untreated controls, with induction at a time-point prior to the onset of ageing-related decline. However, the ages of induction needed to be far enough apart to resolve any effect of the ageing process. Consequently two to five and 20 days post-eclosion were selected as young and old flies respectively, although these labels are somewhat arbitrary and serve only to highlight the difference in age. Since survival appeared to be more sensitive to alterations in the level of Aβ42 as described above, I continued to use this as a marker of toxicity for subsequent studies.

4.2.4 Arctic Aβ42 transcript expression equalisation in young and old flies

My first attempt at inducing equivalent levels of Arctic Aβ42 protein toxicity was largely unsuccessful. To induce an equivalent level of Arctic Aβ42-mediated toxicity, I first sought to equalise Arctic Aβ42 mRNA expression between young (5d) and old (20d) *UAS-Arctic Aβ42/+;elavGS/+* flies. As RNA expression declines with age, most likely reflecting a lower intake of RU486 due to reduced

feeding behaviour, and protein levels increase with age, in correlation with the length of the induction period, I hypothesised that Aβ42 expression could be normalised at different ages by regulating both of these parameters. In particular I predicted that a relatively higher dose of RU486 would be required to induce equivalent levels of expression in older flies to compensate for reduced food intake.

To ascertain what combination of RU486 doses in young and old flies would result in equivalent transgene expression levels 5-day and 20-day old *UAS-Arctic Aβ42/+;elavGS/+* flies were treated with a range of RU486 concentrations (0-200μM) for one week. At the end of treatment, Arctic Aβ42 mRNA levels in fly heads were quantified by Q-PCR (**Figure 4.6**). Hence, the data below represents transcripts levels at the end of the RU treatment, i.e. day 12 and day 27 respectively.

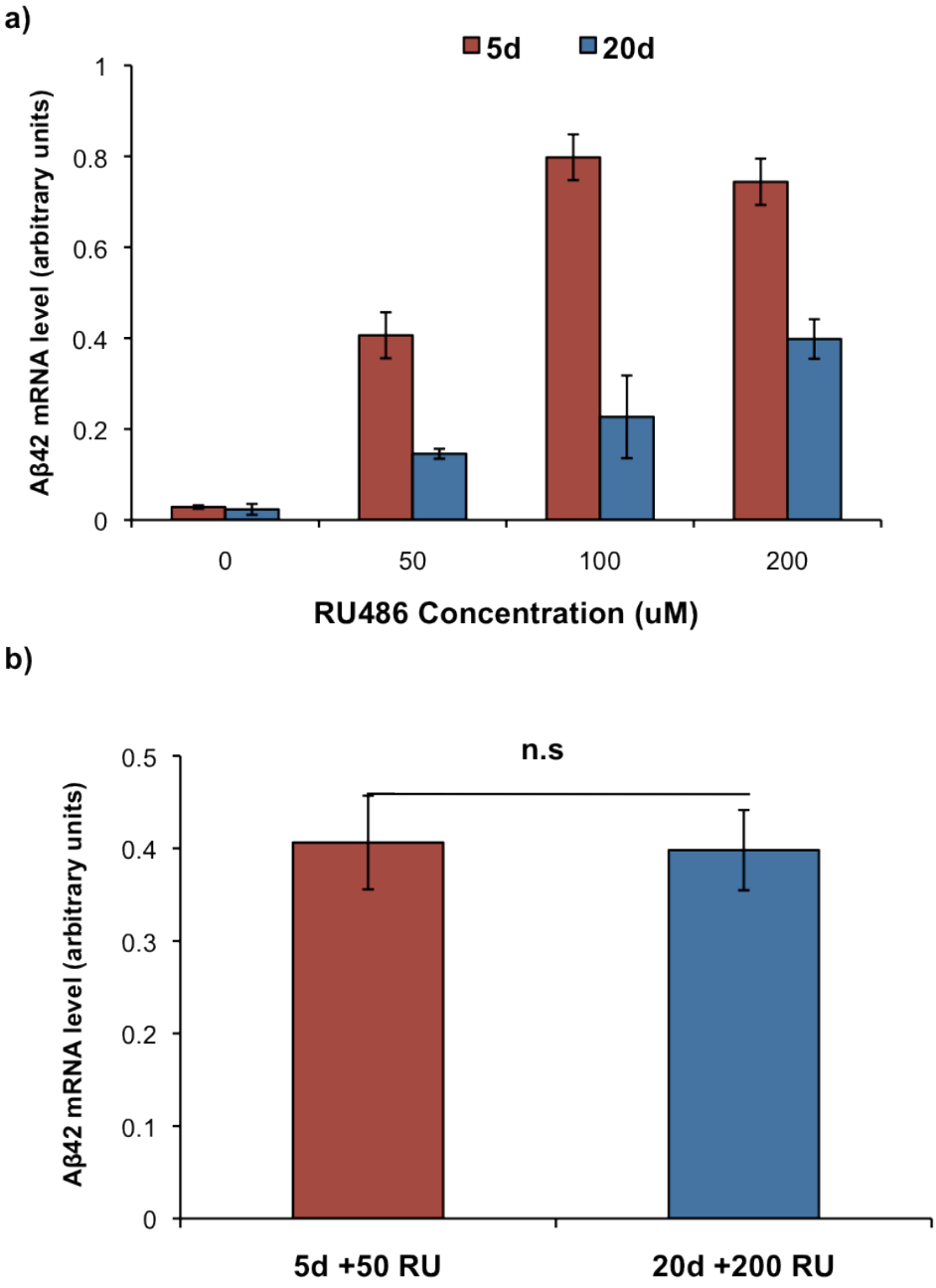

Figure 4.6. Arctic Aβ42 mRNA expression equalisation in young and old flies. (a) Arctic Aβ42 mRNA expression levels (calculated relative to w^{1118}*)* in the heads of *UAS-Arctic Aβ42/+;elavGS/+* once-mated females treated with 0, 50, 100 and 200µM RU486 for one week from 5-days and 20-days post-eclosion, as measured by Q-PCR. (b) Aβ42 mRNA expression levels were equivalent in 5 day-old and 20 day-old *UAS-Arctic Aβ42/+;elavGS/+* flies treated with 50µM and 200µM RU486, respectively (this data represents a replicate of the

concentrations used in (a). Data are presented as means +/- SEM (n = 5 for each group). Data were compared using Student's t-test.

RU486 treatment in both young and old flies resulted in Arctic Aβ42 mRNA overexpression at all doses. In both groups transcript levels were significantly higher at all concentrations, when compared to their respective age-matched non-RU-treated (0μM RU) controls ($P<0.05$). This indicated that doses as low as 50μM RU486 were sufficient to induce expression.

As has been observed previously, mRNA transcripts were detected in non-RU-treated controls, however these were negligible and did not accumulate with age. At all doses, Arctic Aβ42 mRNA expression was higher in young flies when compared to old ($P<0.05$ for all doses). This was consistent with a reduced feeding behaviour in older flies.

Comparisons within each age group revealed that expression correlated with RU486 dose but to varying degrees. There was no significant difference in Arctic Aβ42 mRNA levels in young flies treated with 100μM and 200μM RU486, although they were significantly higher than levels using 50μM RU ($P<0.05$, Student's t-test). When comparing doses in older flies, no significant difference was found between 50μM and 100μM RU486 but levels were significantly higher in 200μM RU486-treated flies.

When comparing doses between young and old flies, equivalent levels of Aβ42 mRNA were seen using RU treatments of 50μM and 200μM, respectively (**Figure 4.6b**). Notably, these were the only two conditions across age where

expression was equivalent. The fact a higher dose was required to generate the same level of expression in older flies fitted nicely with the original prediction that higher doses could compensate reduced feeding behaviour.

4.2.5 Ageing increases Aβ42 peptide accumulation and toxicity when Arctic Aβ42 transgene expression is normalised between young and old flies

Next I measured the effect of normalised Arctic Aβ42 gene expression on lifespan as a measure of toxicity at different ages (**Figure 4.7**). 5 day-old (young) and 20 day-old (old) *UAS-Arctic Aβ42/+;elavGS/+* flies were respectively pulsed with 50μM and 200μM RU486 for one week, before switching back to RU486-free food. Un-treated flies were used as controls as this had a negligible effect on lifespan (see **Figure 3.6**). Despite expressing the same level of Aβ42 mRNA at the end of their respective RU treatments (**Figure 4.6b**), only older-induced flies displayed a shortened lifespan in response to Aβ42-mediated toxicity (**Figure 4.7**). However, to determine whether this was due to an age-dependent increase in neuronal vulnerability, it was important to establish whether Arctic Aβ42 protein levels were also equivalent between young and old flies.

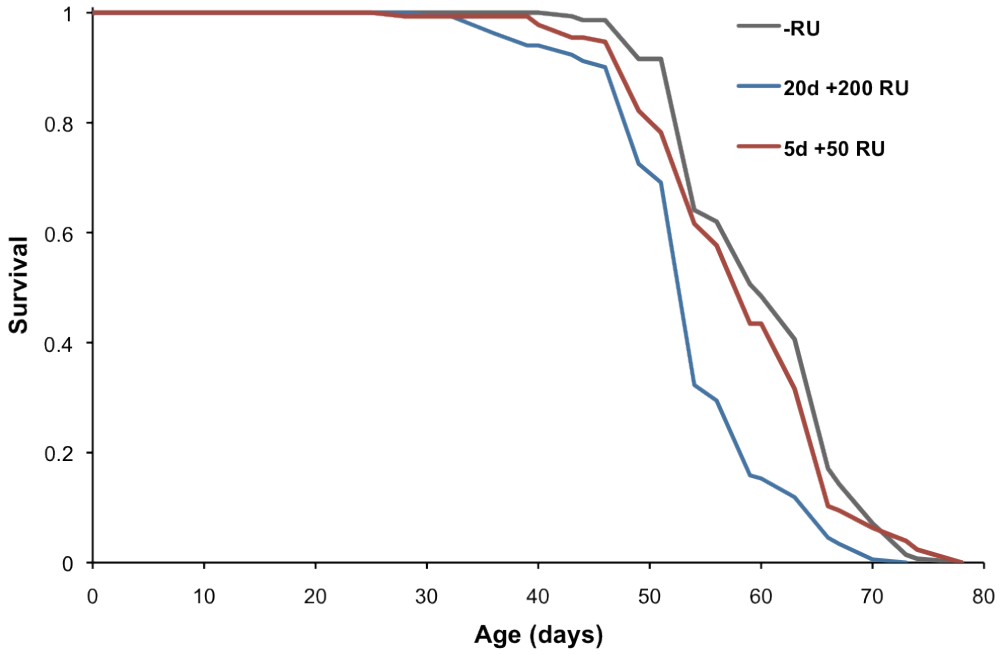

Figure 4.7. Aβ42 transcript equalisation reduces lifespan in old flies only. Survival curves of once-mated female *UAS-Arctic Aβ42/+;elavGS/+* flies conditionally (one-week RU pulse) treated with 50µM, and 200µM from 5-days and 20-days post-eclosion, respectively. Median lifespans: 60 days for -RU, 58 days for 5d +50 RU, and 53 days for 20d +200 RU. Log rank tests and p values: -RU versus 5d+50 RU ($p = 0.18$), -RU versus 20d +200 RU ($p<0.0001$).

Again flies were pulsed with RU486 for one week under the RNA equalisation conditions described above for young and old flies. Flies were frozen for protein extraction at the end of the one-week pulse (0d) and one, two and three weeks following the switch-off of transgene expression to assess the perdurance of Aβ42 peptide. Aβ42 peptide levels were measured by ELISA and normalised at each age of induction to their respective non-RU486-treated controls (**Figure 4.8**), since the peptide accumulates with age even in un-induced flies (see **Figure 3.4b**). Considerable levels of Arctic Aβ42 peptide were detected in both young and old-induced flies, but no significant reduction in Aβ42 was seen for up to three weeks following the switch to RU486-free food in either age group (**Figure**

4.8). This suggested that the Arctic Aβ42 isoform is highly resistant to degradation. Of further interest, Aβ42 levels were significantly higher in old-induced compared to young-induced flies at all timepoints assayed ($P<0.05$, Student's t-test). A greater concentration of Aβ42 peptide could, therefore, explain the relatively increased mortality observed upon induction in old flies.

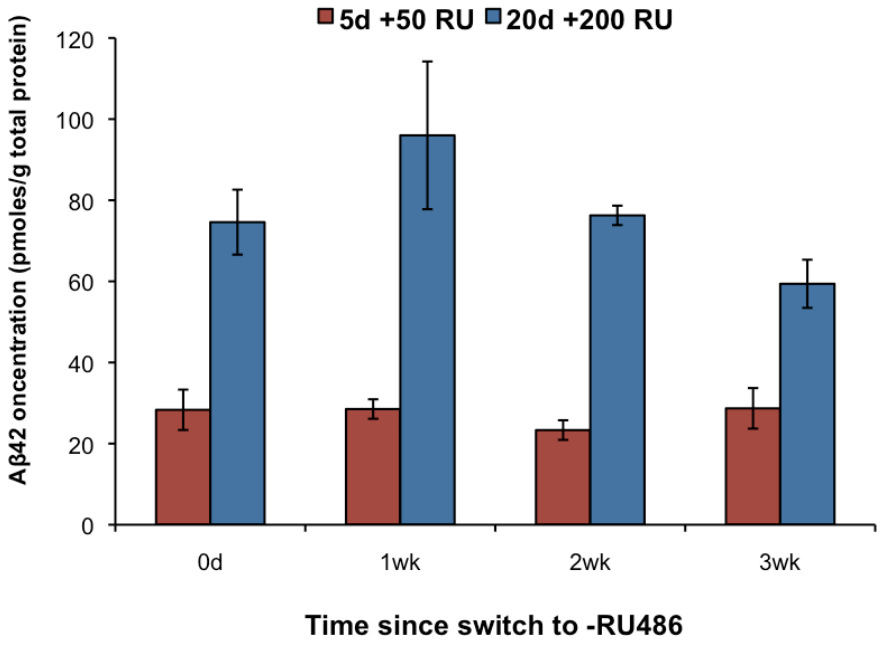

Figure 4.8. Arctic Aβ42 transcript equalisation has differential effects on protein expression in young and old flies. Arctic Aβ42 protein levels in the heads of once-mated female *UAS-Arctic Aβ42/+;elavGS/+* flies conditionally treated (one week RU pulse) with 50µM and 200µM RU from 5-days and 20-days post-eclosion as quantified by Aβ42-specific sandwich ELISA. Arctic Aβ42 protein levels were assayed immediately after the pulse (0d) and up to 3 weeks following the switch to -RU. Data are presented as means +/- SEM (n = 4 for each group). Groups were compared using Student's t-test.

Hence, at the protein level Aβ42 appears to accumulate faster in aged flies. Since mRNA levels were equivalent in old and young flies under these conditions, and protein turnover has been shown to decline with age in several organisms (Rattan. 1996), I hypothesised that this difference in Arctic Aβ42 peptide level was due to age-dependent effects on protein synthesis or degradation. As a measure of the rate of translation, ^{35}S-methionine incorporation was assessed in in 5 day-old and 20-day old *UAS-Arctic Aβ42/+;elavGS/+* flies (**Figure 4.9**). ^{35}S-methionine incorporation was significantly lower in older flies indicating a reduced rate of translation. An increase in protein synthesis was, therefore, unlikely to explain the accumulation of Aβ42 peptide in old flies. Hence, it was possible that the rate of degradation of Aβ42 was reduced with age and may have accounted for the higher levels of the peptide observed following induction in old flies.

Together this data suggested that the ageing process enhances the accumulation of Aβ42, possibly by altering the rate of protein degradation, and that this increased level of the peptide exacerbates toxicity in older flies. However, to measure the vulnerability of older neurons to protein toxicity it would be necessary to control for changes in the rate of protein turnover with age.

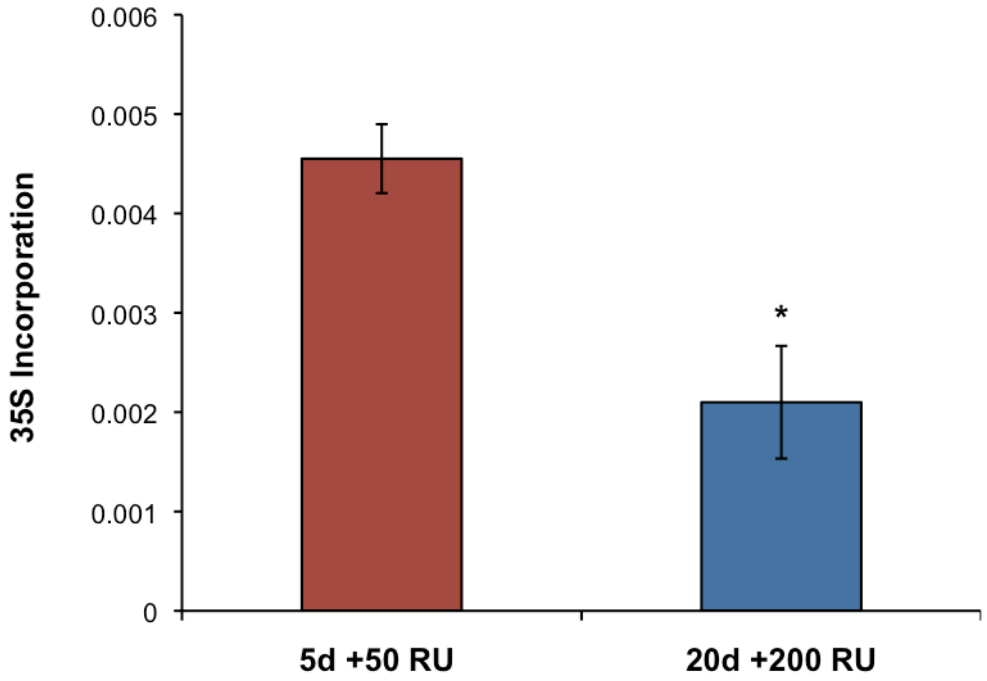

Figure 4.9. Protein translation decreases with age. ^{35}S-methionine incorporation in *UAS-Arctic Aβ42/+;elavGS/+* flies conditionally treated with 50μM and 200μM RU486 for one week from 5-days and 20-days post-eclosion, respectively. Data are presented as mean +/- SEM (n = 5 for each group). Groups were analysed using Student's t-test (*P<0.05).

4.2.6 Ageing increases neuronal vulnerability to equivalent concentrations of Arctic Aβ42 peptide in young versus old flies

As the concentration of Aβ42 peptide induced differed greatly between young and old flies (**Figure 4.8**), and the toxic response to the peptide at a given age appeared to be dose-dependent (**Figure 4.3**), I aimed to obtain a more direct measure of the effects of ageing upon neuronal vulnerability to Aβ42 by inducing a standard concentration of the peptide at different ages. I first optimised conditions to induce equivalent levels of Arc Aβ42 peptide in young

and old flies using an unbiased approach where *UAS-Arctic Aβ42/+;elavGS* flies were treated to a range of RU486 concentrations (25-400μM RU) for varying exposure times (four days to two-weeks) from 5, 20 and 30 days of age, representing young, middle and old-aged flies, respectively (**Figure 4.10**). An extra induction at 30-days was included to increase the odds of finding equivalent expression and to provide more options when comparing the toxicity response.

At the end of the induction period Aβ42 was measured at the protein level, by ELISA **(Figure 4.10)**, in order to control for age-dependent differences in mRNA expression and protein turnover.

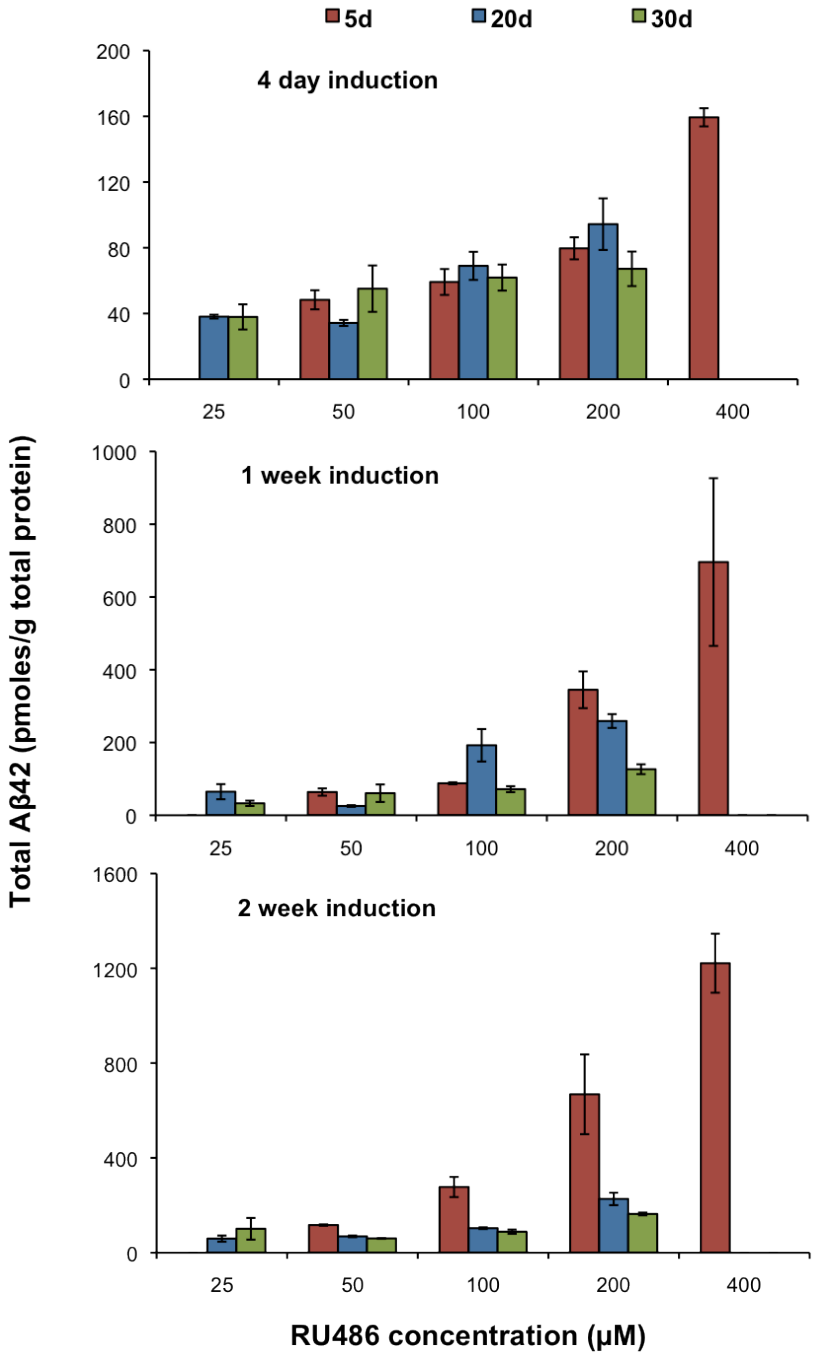

Figure 4.10. Arctic Aβ42 protein expression levels with age following conditional RU486 treatments. Arctic Aβ42 protein levels in the heads of *UAS-Arctic Aβ42/+;elavGS/+* once-mated females maintained on a variety of RU486 SY food concentrations (25μM-400μM) for 4-days, 1-week and 2-weeks from 5-days, 20-days and 30-days post-eclosion. Prior to RU486 treatment flies were maintained on RU486-free food. Arctic Aβ42 protein levels were quantified at the end of each treatment using Aβ42-specific sandwich ELISA. Data are

presented as means +/- SEM (n = 5 for each group). Please note the change in scale in each graph. Groups and conditions were compared using Student's t-test.

As expected, Aβ42 expression was dependent on the RU486 dose and exposure time. Hence, the largest doses with the longest exposures resulted in the highest levels of expression. Interestingly, within this range of RU486 concentrations and exposure times, there seemed to be no plateau effect on the level of Arctic Aβ42 expression. However, it is possible that induction periods greater than 2 weeks would not yield higher levels of expression. Expression levels were typically higher in younger flies and, as would be expected with a decline in feeding behaviour, invariably lowest in the oldest induced flies (30d). Furthermore, older flies seemed less sensitive to changes in RU486 dose.

Differences in the level of expression between different groups were not the main concern at this point. In fact, what was really interesting were the treatments that showed minimal or no difference in UAS-Arctic Aβ42 levels across age. These treatments were as follows: (1) a one week pulse of 200 μM RU in five-day versus 20-day old flies, (2) a one week pulse of 100 μM RU in 20-day old flies versus 200 μM RU in 30-day old flies and (3) a two week pulse of 100 μM RU in five-day old flies versus 200 μM RU in 20-day and 30-day old flies. The four-day induction treatments were not of interest since they produced the lowest levels of Arctic Aβ42 whereas I required high levels of equivalent expression to ensure a robust phenotype.

Arctic Aβ42 toxicity was then profiled by measuring survival under the conditional RU486 treatment conditions described in (1) (**Figure 4.12**), (2) (**Figure 4.13**) and (3) above (**Figure 4.14**). Although negative geotaxis is a more apt measure of Arctic Aβ42 toxicity since it indirectly measures neuronal dysfunction, survival was shown to be more sensitive to changes in Arctic Aβ42 toxicity. Thus, survival was used to assay Arctic Aβ42 toxicity because it was more likely to resolve subtle differences in ageing effects. Furthermore survival can be measured, by definition, over a fly's entire lifespan whereas climbing ability in control flies is significantly reduced by 30-40 days. It was important I could see a relative difference between experimental and control flies.

Two outcomes of this experiment were predicted:

1) **Ageing does not increase the vulnerability to Arctic Aβ42 toxicity (Figure 4.11a)**

In this instance, the time-to-death of of young and old-aged flies in response to equivalent Arctic Aβ42 expression would be the same. The survival from the start of RU486 treatment would not be significantly different (the survival curves would overlap). In other words, Arctic Aβ42 would take the same time to exert its effects in young and old flies.

2) Ageing increases vulnerability to Arctic Aβ42 toxicity (Figure 4.11b)

If older flies were more vulnerable to the same level of Arctic Aβ42 toxicity, then these flies would be theoretically unable to 'withstand' the proteotoxicity for as long as younger flies. Thus, older flies would exhibit reduced survival (in a

normal survival curve). This might occur if the effects of ageing were large since older flies are much more likely to die of natural causes. More probable would be the scenario where older flies showed an increased time-to-death following RU486 treatment

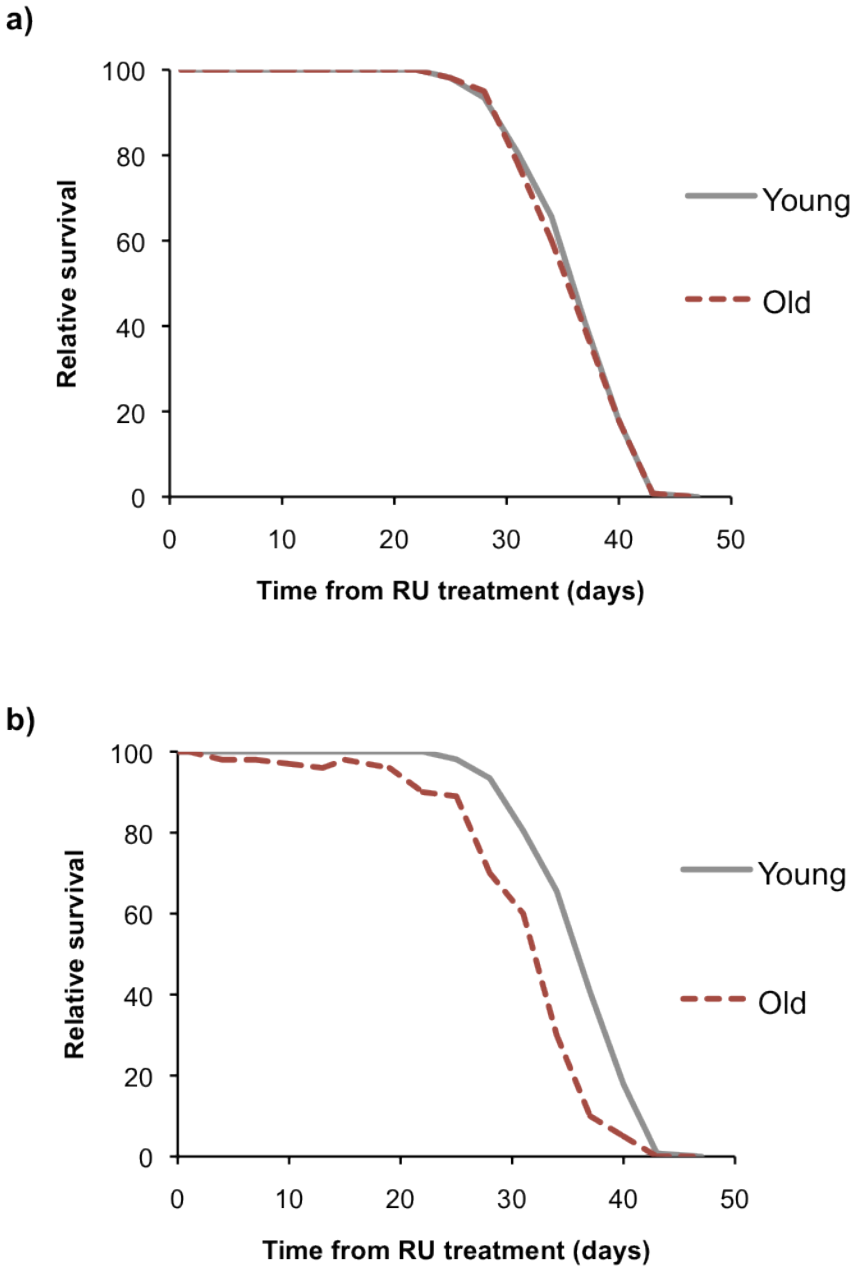

Figure 4.11. Hypothetical plots illustrating the possible effects of ageing on Arctic Aβ42 toxicity. (a) Expected survival from RU486 treatment (expressed as

a % of control flies) when ageing has no effect. (b) Expected survival from RU486 treatment if ageing rendered flies more vulnerable to Arctic Aβ42 toxicity.

Equivalent levels of Aβ42 peptide expression were again confirmed at the end of the induction period in young-induced and older-induced flies (**Figure 4.12a**). Aβ42 peptide was stable one week after switch-off of transgene expression, further confirming the resistance of the peptide to degradation. In both five-day and 20-day treated flies, survival was reduced relative to non-RU-treated controls indicating that Arctic Aβ42 was toxic when induced at both ages (**Figure 4.12b**). This amounted to a 12% reduction in median lifespan in five-day treated flies and a 7% reduction in median lifespan in 20-day treated flies, when compared to non-RU-treated controls. The difference in survival between five-day and 20-day treated flies was significant ($P<0.05$, log rank test). This implied that younger flies were more vulnerable to Arctic Aβ42 since they exhibited a relatively reduced survival compared to older flies. However, this interpretation did not take into account the fact that younger flies were exposed to Arctic Aβ42 for longer. Although RU486 was removed after one week in both 5-day and 20-day treated flies, it was likely that peptide remained in the fly due to its high stability. Therefore, we plotted survival as a function of the time from RU486 treatment (**Figure 4.12c**), from day five and day 20 respectively.

This analysis revealed that older day-20-treated flies were significantly shorter lived from the time of RU486 treatment than younger day-5-treated flies, with median lifespans of 45 days and 58 days, respectively. However, the median survival for non-RU-treated flies from 20-days and five-days was 50 days and 65

days respectively. This demonstrated that flies treated with RU486 at 20-days have a reduced survival simply because they are older or 'closer to death'. Therefore, the survival of both experimental groups were normalised to the survival of their respective non-RU treated controls at every timepoint (**Figure 4.12d**). This generated a new plot that represented the survival of each treatment expressed as a % of their respective non-RU-treated control survival. This provided a means of controlling for Arctic Aβ42 independent effects on survival and it also prevented a bias in data interpretation – because older flies are more likely to die than younger flies, the reduced time to death of older flies could be misinterpreted as an increase in vulnerability to Arctic Aβ42. Interestingly, this normalisation step had little effect on the data. The normalised survival of day-20 treated flies was still reduced when compared to flies treated at day-five ($P<0.05$, Wilcoxin rank test) (**Figure 4.12d**). This demonstrated that at a fixed concentration, Arctic Aβ42 protein was more toxic when induced in older flies compared to younger flies.

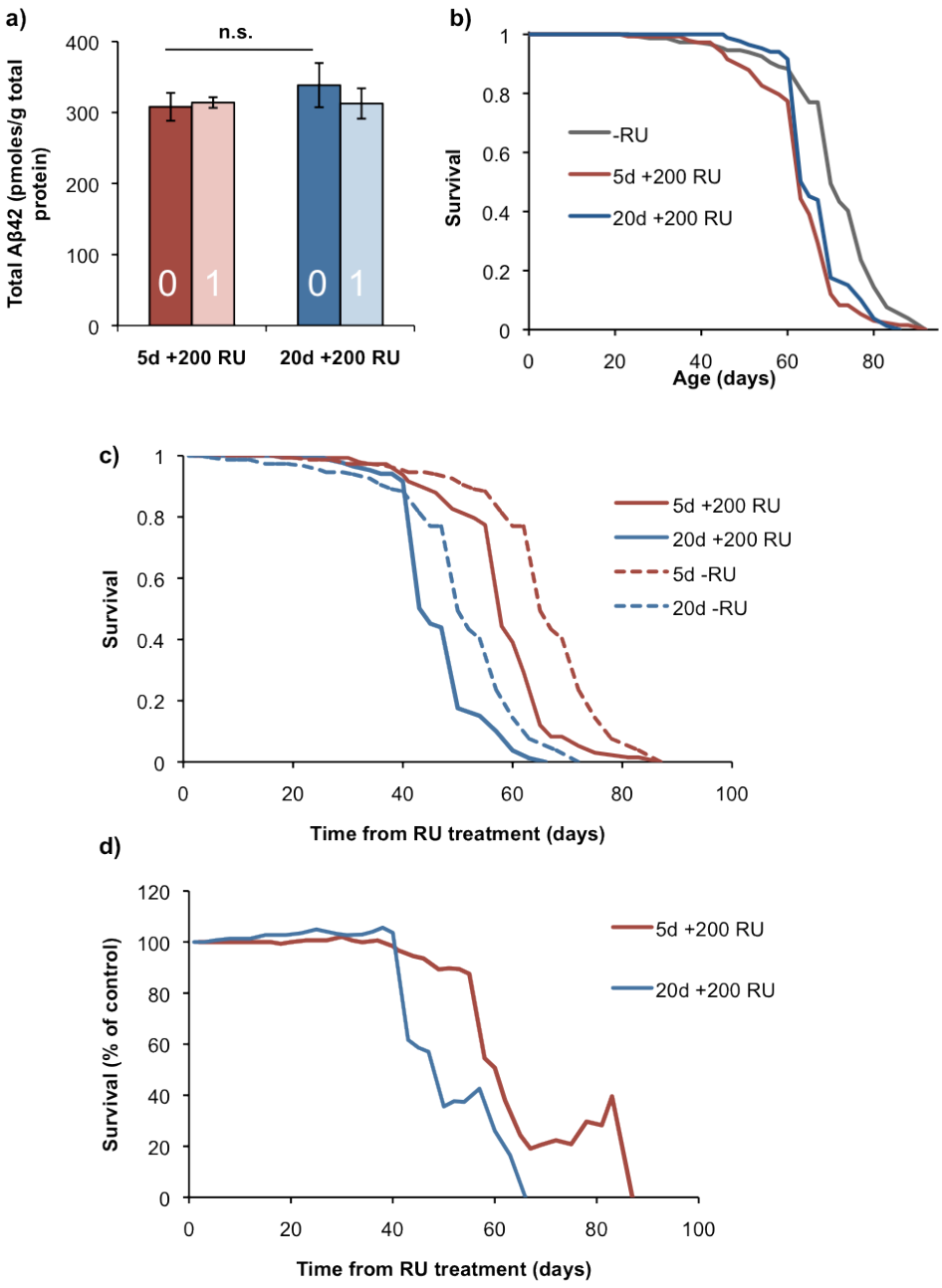

Figure 4.12. Older flies are more vulnerable when comparing the effect of equalised Arctic Aβ42 expression in 5-day and 20-day treated flies. *UAS-Arctic Aβ42/+;elavGS/+* once-mated females were conditionally treated with 200µM RU486 (RU) from 5-days and 20-days post-eclosion for one week only, and were maintained on -RU prior to and following the RU pulse. (a) Arctic Aβ42 protein expression levels were equivalent (non-significantly different) when quantified at the end of each RU pulse (0) and 1 week after the switch to –RU (1). Data expressed as mean +/- SEM (n = 5 for each group). Means

compared using Student's t-test. (b) Survival curves of conditionally treated flies. Median lifespans are: 69 days for -RU, 61 days for 5d +200 RU and 64 days for 20d +200 RU. Log rank test and p values: -RU versus 5d+ 200 RU ($p<0.0001$), -RU versus 20d +200 RU ($P<0.0001$) and 5d +200 RU versus 20d +200 RU ($p = 0.043$). (c) These curves represent the survival or time-to-death of conditionally treated flies from the first day of RU treatment i.e. 5-days and 20-days, respectively. Median lifespans are: 65 days for –RU from 5-days, 50 days for –RU from 20-days, 58 days for 5d +200 RU and 45 days for 20d +200 RU. Log rank tests: 5d+ 200 RU versus 20d+ 200 RU ($p<0.0001$). (d) When these survival curves are plotted as a percentage of their respective non-RU-treated controls, 20d +200 RU flies exhibit a significant reduction in relative survival following RU treatment ($P<0.05$, Wilcoxon rank test).

This result was then confirmed using the other equalised Arctic Aβ42 protein expression protocols previously determined (**Figure 4.13 and Figure 4.14**).

Arctic Aβ42 protein levels in flies treated with 100μM RU486 from 20-days and 200μM RU486 from 30-days post eclosion for one week only were equivalent at the end of the induction period (**Figure 4.13a**). As before, suppression of Arctic Aβ42 expression, following a week on RU486-free food, had no effect on Arctic Aβ42 levels in either age group. In both 20-day and 30-day treated flies, survival was reduced relative to non-RU-treated controls (**Figure 4.13b**). This amounted to an 8% reduction in median lifespan in 20-day treated flies and remarkably, a 14% reduction in median lifespan in flies treated at 30 days of age. The difference in survival between flies treated at 20-days and 30-days was significant ($P<0.001$, log rank test) and demonstrated that 30-day treated flies were more vulnerable to Arctic Aβ42 toxicity. Further analysis, comparing time

to death and relative survival etc., effectively amplified this effect (**Figure 4.13c and 4.13d**).

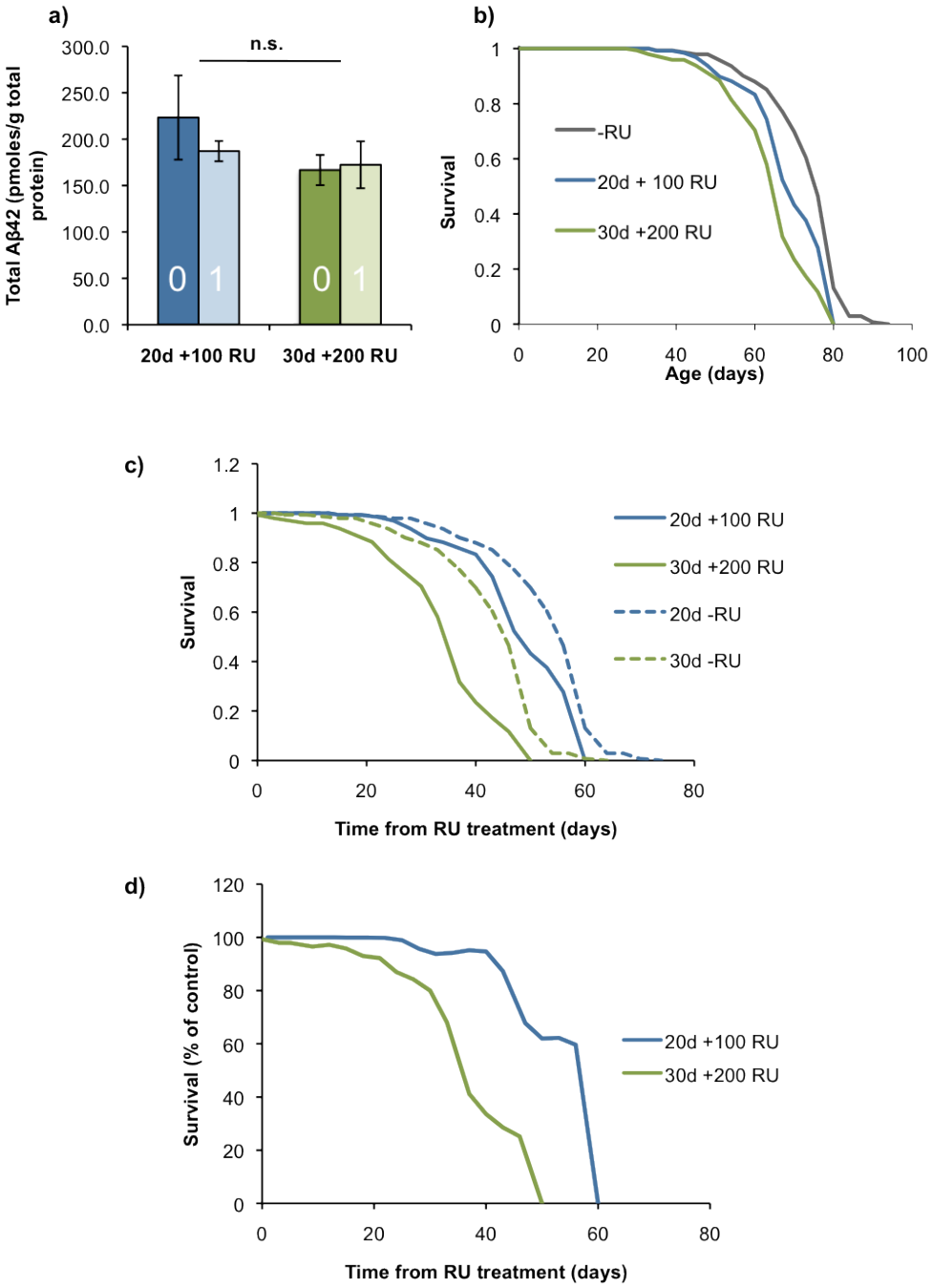

Figure 4.13. Older flies are more vulnerable to Arctic Aβ42 when comparing the effect of equalised Arctic Aβ42 protein expression in 20-day and 30-day treated flies. *UAS-Arctic Aβ42/+;elavGS/+* once-mated females were conditionally treated with 100µM RU486 (RU) from 20-days and 200µM RU486

from 30-days post-eclosion for one week only, and were maintained on -RU prior to and following the RU pulse. (a) Aβ42 protein expression levels were equivalent (non-significantly different) when quantified at the end of the RU pulse (0) and 1 week after the switch to –RU (1). Data expressed as means +/- SEM (n = 5 for each group). Means compared using Student's t-test. (b) Survival curves of conditionally treated flies. Median lifespans are: 75 days for -RU, 69 days for 20d +100 RU and 65 days for 30d +200 RU. Log rank test and p values: -RU versus 20d+ 100 RU ($P<0.0001$), -RU versus 30d +200 RU ($P<0.0001$) and 20d +100 RU versus 30d +200 RU ($p <0.0001$). (c) These curves represent the survival or time-to-death of conditionally treated flies from the first day of RU treatment i.e. 20-days and 30-days, respectively. Median lifespans from RU treatment are: 56 days for –RU from 20-days, 46 days for –RU from 30-days, 50 days for 20d +100 RU and 37 days for 30d +200 RU. Log rank tests: 20d+ 100 RU versus 30d+ 200 RU ($p<0.0001$). (d) When these survival curves were plotted as a percentage of their respective controls, 30d +200 RU flies exhibited a significant reduction in relative survival following RU treatment ($P<0.05$, Wilcoxon rank test).

Next the effect of equivalent Arctic Aβ42 expression at three different ages was assayed (**Figure 4.14**). In this experiment a two-week RU pulse was used at five, 20 and 30 days post-eclosion. The results agreed with the two previous one-week induction studies. All RU-treated flies showed a reduction in median lifespan when compared to non-RU-treated controls: 27% for five-days, 24% for 20-days and 14% for 30-days (**Figure 4.14b**). This progressive reduction was consistent with the fact younger flies are exposed to Arctic Aβ42 for longer. The normalised survival from RU treatment was inversely related with age. That is, the youngest day-5 treated flies exhibited the longest relative survival following RU486 treatment/Arctic Aβ42 induction (**Figure 4.14d**).

Overall these data clearly show that ageing renders *Drosophila* more vulnerable to a fixed amount of Arctic Aβ42. In all three equalised protein expression trials, the older fly cohort, whether comparing 20-day old flies with 5-day old or 30-day old flies with 20-day old exhibited a significant reduction in relative survival, even after normalising for differences in survival caused by normal ageing. The fact this was independently shown in three different experiments increased the confidence of the interpretations made.

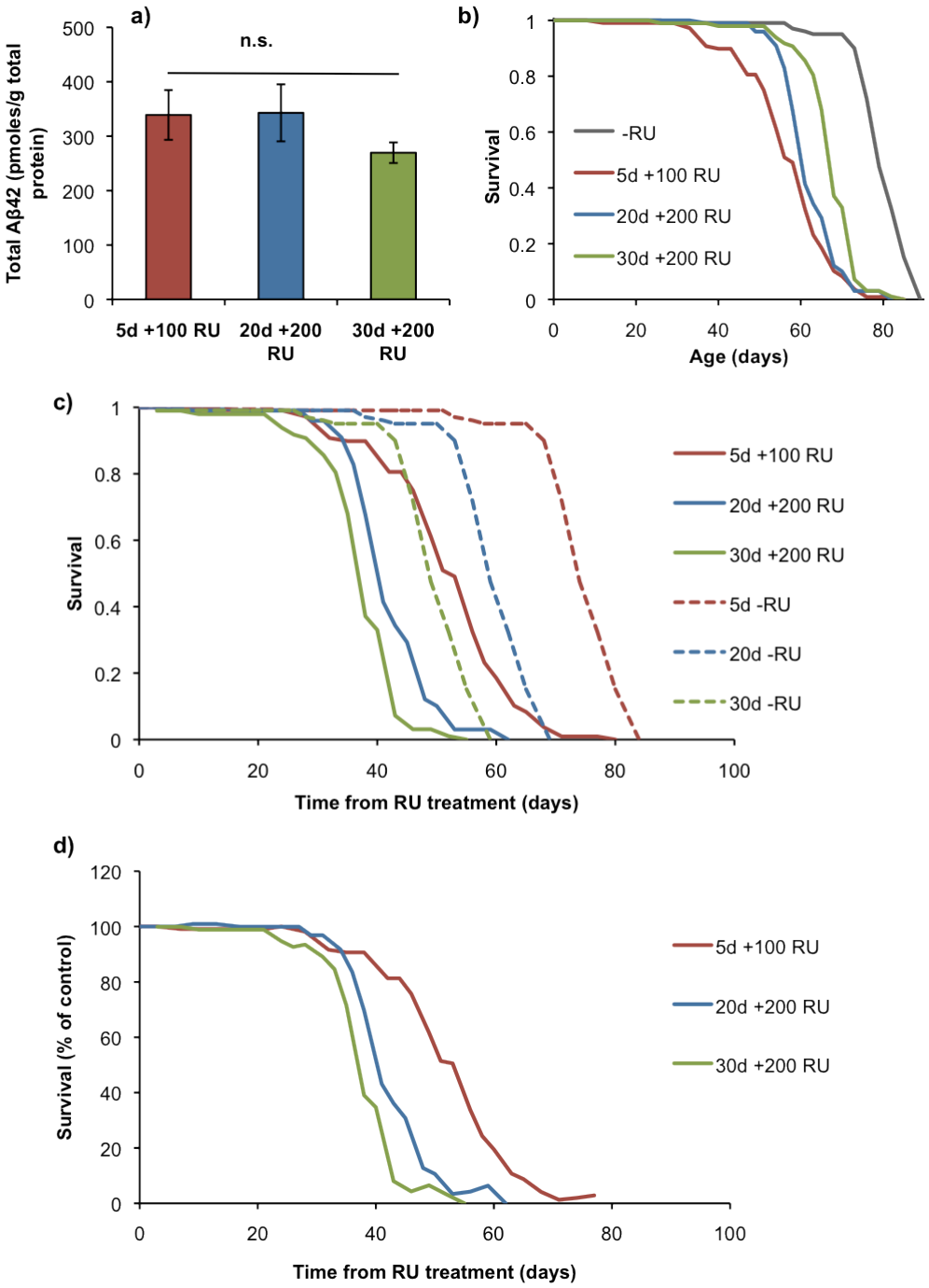

Figure 4.14. Older flies are more vulnerable when comparing the effect of equalised Arctic Aβ42 expression in 5-day, 20-day and 30-day treated flies. *UAS-Arctic Aβ42/+;elavGS/+* once-mated females were conditionally treated with 100µM RU486 (RU) from 5-days and 200µM RU486 from 20- and 30-days post-eclosion for two weeks only, and were maintained on -RU prior to and following the RU pulse. (a) Aβ42 protein expression levels were equivalent when quantified at the end of the RU pulse. Data expressed as mean +/- SEM (n

= 5 for each group). Means compared using Student's t-test. (b) Survival curves of conditionally treated flies. Median lifespans are: 78 days for -RU, 57 days for 5d +100 RU, 60 days for 20d +200 RU and 67 days for 30d +200 RU. Log rank test and p values: -RU versus 5d+ 200 RU ($p<0.0001$), -RU versus 20d +200 RU ($P<0.0001$), -RU versus 30d +200 RU ($P<0.0001$), 5d +100 RU versus 20d +200 RU. (c) These curves represent the survival or time-to-death of conditionally treated flies from the first day of RU treatment i.e. 5-days, 20-days and 30-days, respectively. Median lifespans from RU treatment are: 74 days for –RU from 5-days, 59-days for –RU from 20 days and 49 days for –RU from 30-days. For RU treated flies, median lifespans from RU treatment are: 53 days for 5d +100 RU, 41 days for 20d +200 RU and 38 days for 30d +200 RU. (d) When these survival curves are plotted as a percentage of their respective controls, older flies exhibit a significant reduction in relative survival following RU treatment ($P<0.05$ comparing 20d and 30d with 5d and 20d with 30d, Wilcoxon rank test).

4.2.7 Older flies are more vulnerable to chronic Arctic Aβ42-mediated toxicity

To further assess the vulnerability of older flies to Aβ toxicity, the effect of chronic Arctic Aβ42 expression was also measured in young and old flies. This approach made no attempt to neither induce equivalent levels of expression with different RU486 concentrations nor ensure RU exposure times were equivalent. Simply, *UAS-Arctic Aβ42/+;elavGS/+* flies were chronically treated with 200μM RU486 from two-days and 20-days post eclosion. Arctic Aβ42 protein levels were then assayed every 3-5 days until flies started to die (**Figure 4.15**). Survival was again used to measure Arctic Aβ42 toxicity (**Figure 4.16**). In essence, this experiment was exactly the same as those presented in the previous section. The main difference is that by not controlling for the level of toxicity induced at each age, Arctic Aβ42 levels had to be assayed much more frequently.

Two-day treated flies displayed a robust accumulation of Arctic Aβ42 which reached a plateau at around 15-days of age (**Figure 4.15a**). Arctic Aβ42 also accumulated following induction in older flies, but at a slower rate with the concentration continuing to increase at the end of the 25-day assay period (25-45 days; **Figure 4.15a**). Arctic Aβ42 levels were significantly higher in young-induced compared to old-induced flies at all corresponding time-points assayed ($P<0.05$, Student's t-test). Thus, the lifetime Arctic Aβ42 load (calculated from the total area under each curve) was higher in flies chronically treated with RU486 from two days compared to those treated from 20 days (**Figure 4.15b**).

Survival analysis initially indicated that induction of Aβ42 in young flies was more toxic than induction in older flies (**Figure 4.16a**), suggesting a positive correlation between the lifetime exposure to Aβ42 and toxicity. In both two-day and 20-day treated flies survival was reduced compared to untreated controls, with a 45% reduction in young-treated flies and a 25% reduction in older-treated flies. Moreover, the difference in survival between two-day and 20-day treated flies was significant ($P<0.05$, log rank test). However, this interpretation did not account for the fact that younger flies were exposed to Aβ42 for longer. I, therefore, plotted survival as function of the time from the first day of Aβ42 exposure, in other words from two-days in young flies and 20 days in old flies (**Figure 4.16b**). This analysis revealed that older flies were significantly shorter lived from the time of induction than young flies ($P<0.0001$), with median lifespans of 40 days and 37 days respectively. However, the median lifespan for non-RU-treated flies plotted from two days and 20 days was also reduced using this analysis (74 and 56 days respectively). To control for Arctic Aβ42-independent effects of normal ageing on lifespan, therefore, the survival of both experimental groups were normalised to their respective untreated controls at each timepoint (**Figure 4.16c**). Remarkably, older flies exhibited a significantly reduced relative survival when compared to younger flies ($P<0.05$, Wilcoxin rank test).

Overall these results suggest that older flies are more vulnerable to chronic Arctic Aβ42 protein expression, despite a significantly lower lifetime exposure to the peptide. However, this approach made no attempt to normalise the level of Aβ42 expression or to ensure equivalent lengths of induction at different ages

and so does not provide a direct measure of the effects of ageing on neuronal susceptibility to Aβ42 toxicity.

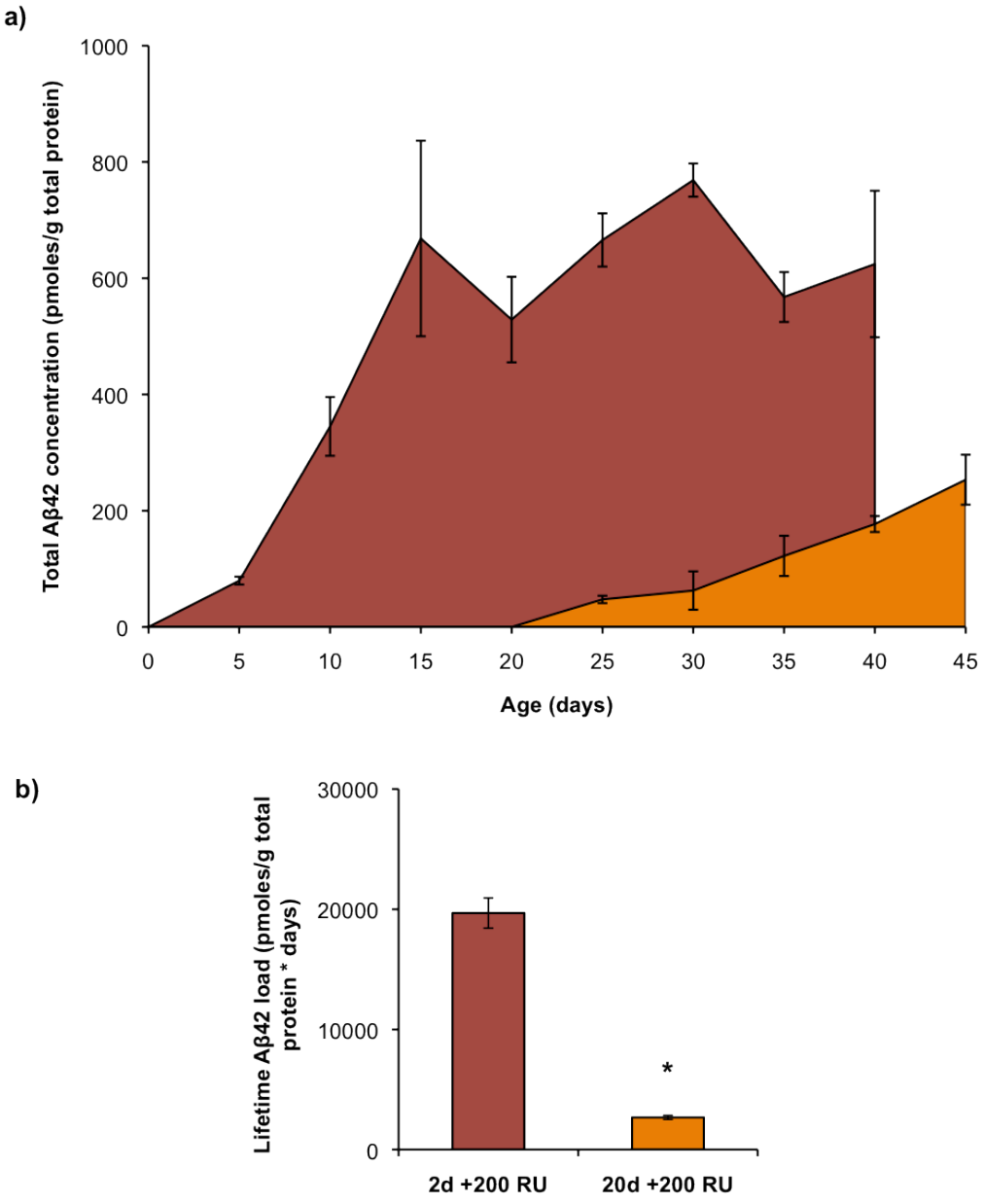

Figure 4.15. Arctic Aβ42 expression levels in response to chronic RU486 treatment in young and old flies. *UAS-Arctic Aβ42/+;elavGS/+* once-mated females were chronically treated with 200µM RU486 from two-days and 20-days post eclosion. (a) Arctic Aβ42 protein levels were assayed every 3-5 days until flies started dying. Data are presented as means +/- SEM (n = 3) with age (days). (b) The lifetime Arctic Aβ42 load was significantly lower in 20-day treated flies.

This data is a crude representative of the lifetime Arctic Aβ42 load in young and old flies, and was determined by calculating the area under the curves in (a). Data are presented as the mean lifetime Arctic Aβ42 load (pmoles/g total protein*days) +/- SEM (n = 3). *P<0.05 when comparing levels in 20d treated flies with that of 2-day treated flies.

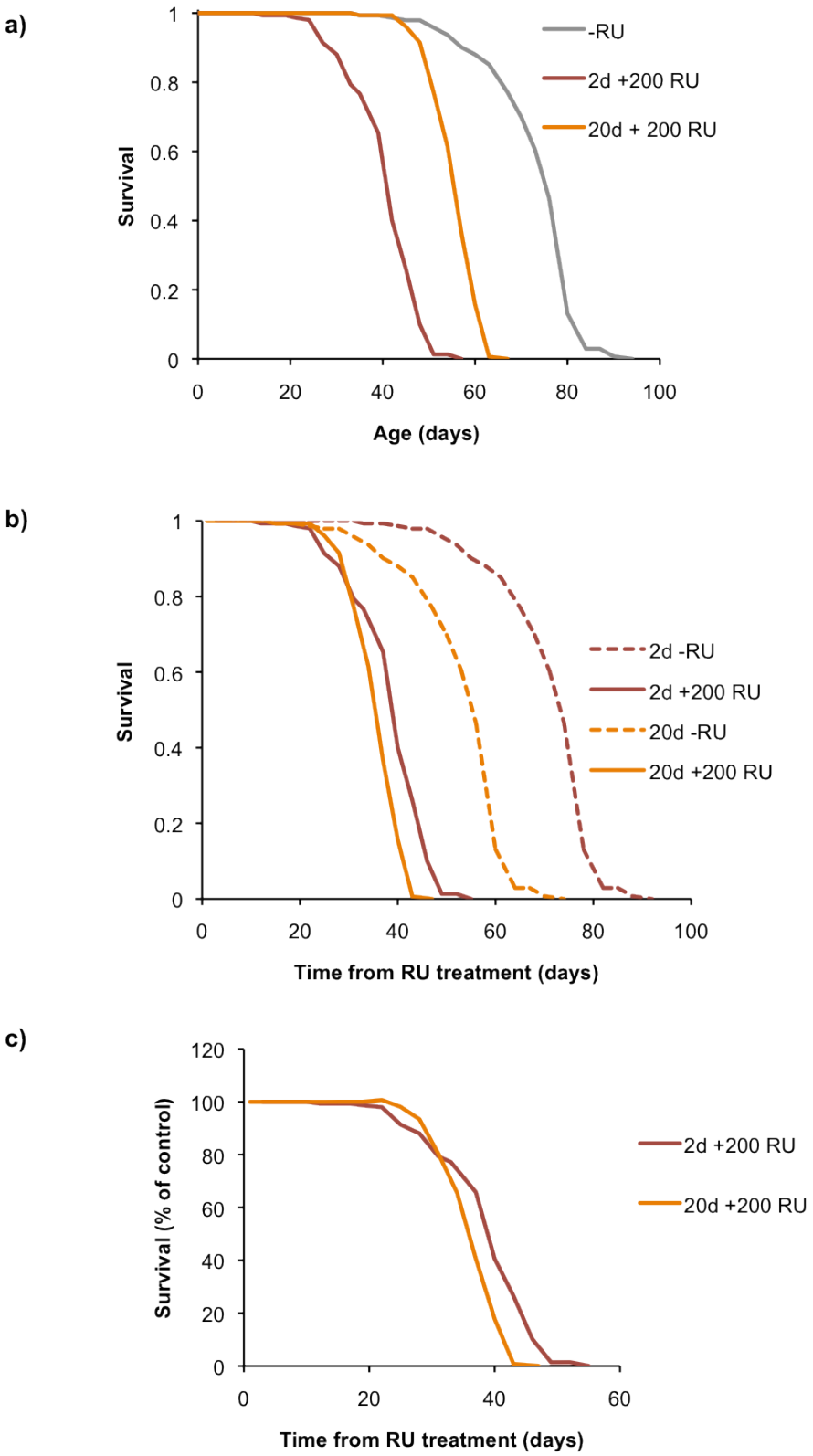

Figure 4.16. Older flies are more vulnerable to chronic Arctic Aβ42-expression. (a) Survival curves of once-mated female *UAS-Arctic Aβ42/+;elavGS/+* flies chronically treated with 200uM RU486 from two-days

and 20-days post eclosion. Median lifespans are: 75 days for -RU, 41 days for 2d +200 RU and 56 days for 20d +200 RU. Log rank test and p values: -RU versus 2d+ 200 RU ($P<0.0001$), -RU versus 20d +200 RU ($P<0.0001$) and 2d +200 RU versus 20d +200 RU ($p <0.0001$). (b) These curves represent the survival or time-to-death of conditionally treated flies from the first day of RU treatment i.e. 2-days and 20-days, respectively. Median lifespans from RU treatment are: 74 days for –RU from 2-days, 56 days for –RU from 20-days, 40 days for 2d +200 RU and 37 days for 20d +200 RU. Log rank tests: 2d+ 200 RU versus 20d+ 200 RU ($p<0.0001$). (d) When these survival curves were plotted as a percentage of their respective controls, 20d +200 RU flies exhibited a significant reduction in relative survival following RU treatment ($P<0.05$, Wilcoxon rank test).

4.3 *Discussion*

Many neurodegenerative diseases, including Alzheimer's disease, share in common the accumulation of toxic proteins and a late age of onset (Mattson. 2006). However, the mechanisms linking protein aggregation and the onset of disease symptoms to age remain unclear. Ageing may either represent a measure of the time required for the accumulation of damaged proteins to cause neuropathology, or the ageing process itself may increase the vulnerability of neurons to protein toxicity. This study aimed to address this issue by inducing expression of the toxic Arctic Aβ42 peptide to the same level and duration at different ages and to measure the delay to and extent of pathology.

4.3.1 The dynamics of Aβ42 expression

Drosophila melanogaster provides a useful model organism for such investigations, due to their short lifespan and the availability of inducible systems that enable both spatial and temporal control of protein expression (Osterwalder *et al*. 2001). The inducible GeneSwitch (GS) system has been widely used to study both ageing (Giannakou *et al*. 2004; Giannakou *et al*. 2007; Hwangbo *et al*. 2004) and neurodegeneration (Latouche *et al*. 2007); however, most studies have examined the effects of chronic induction from specific time-points, during development or adulthood, without reporting on the kinetics and subsequent effects of transgene suppression. A further analysis of the dynamics of Aβ42 suppression using my inducible AD model (developed in chapter 3) was, therefore, required.

It was found that the kinetics of mRNA and protein suppression differed upon removal of the inducer mifepristone (RU486). A rapid reduction in mRNA expression was observed within 24 hours but the 'off-response' at the protein level was much slower with Aβ42 peptide remaining for several weeks after suppression of transcription. Importantly, switching-off transgene expression in young flies did not reverse Aβ42 toxicity in this model, since climbing ability did not return to control levels following removal of RU486 and even short exposure times resulted in slight reductions in median lifespan.

This lack of reversibility is most likely to be due to the high stability of the Aβ42 peptide in these flies, which has been reported in other studies. Jankowsky *et al*. (2005) generated a mouse model that mimics the arrest of Aβ production. These mice overexpress mutant APP from a vector that can be regulated by doxycycline. Under normal conditions, APP overexpression resulted in amyloid pathology. Administration of doxycycline inhibited APP expression by >95% and reduced Aβ production to levels found in non-transgenic mice. Although this suppression halted the progression of amyloid pathology, these mice retained a considerable Aβ load 6 months after suppression, with little sign of clearance. This result is analogous to the effect seen in *Drosophila*. Removal of RU486 effectively halted the further accumulation of Arctic Aβ42 and worsening of climbing ability and lifespan but did not result in a reduction in the Arctic Aβ42 load. Furthermore, intracerebral injection of Aβ antibodies failed to clear pre-existing amyloid plaques in a mouse model of AD where APP suppression was suppressed and only led to a limited reduction of amyloid burden in mice constitutively expressing APP (Tucker *et al*. 2008). In both these studies APP

cDNA encoding the Sewdish mutation was expressed. This familial AD-associated mutation results in increased Aβ production. It does not increase the peptide's propensity to aggregate as with the Arctic mutation. Therefore, it seems the stability of Aβ42 aggregates is not specific to particular isoforms of the peptide.

The high stability of Aβ42 in this model may be related to the ability of the Arctic mutation to promote rapid aggregation (Nilsberth *et al*. 2001). Indeed most of the Aβ42 present in this model is insoluble (see **Figure 3.5**). The $Z_{Aβ3}$ Affibody, a conformation-specific Aβ binding protein that prevents Aβ42 aggregation, clears Aβ42 and rescues toxicity when co-expressed with Arctic Aβ42 in *Drosophila* neurons (Luheshi *et al*. 2010). This suggests that the aggregation state of Aβ42 can alter its stability and impact on neuropathological phenotypes in the fly. Further analyses of the solubility of Aβ42 in this model over time would be required to elucidate the role of aggregation in altering the stability and toxicity of the peptide in this inducible model system.

4.3.2 Aβ42 toxicity is a dose-dependent in *Drosophila*

One possibility for the relationship between protein toxicity and the age of onset of AD is that aggregation is a stochastic process requiring many years to accumulate toxic proteins to a threshold concentration at which neurons become dysfunctional. This study provides some evidence that Aβ42 toxicity is indeed related to the concentration of the peptide produced. Aβ42 peptide concentration correlated with the duration of induction in young flies, and as the peptide

remains stable for several weeks, this may be viewed as inducing a dose-response to Aβ42 at a given time. This resulted in negative geotaxis and shortened lifespan phenotypes in later life that were Arctic Aβ42 dose-dependent. Interestingly, survival was found to be more sensitive to changes in RU486 dose. A two-day RU486 pulse had no effect on negative geotaxis, when compared to controls but did result in small but significant reduction in lifespan. This difference could possibly be explained by the fact there is much less noise when assaying for survival. The phenotype is easy to score; the fly is dead, alive or censored. With negative geotaxis, one must count how many flies there are at the top and bottom of 25-ml pipette filled with 15 flies, once 45-seconds has passed. The problem with performing this assay manually (as throughout this thesis) is that flies can be scored incorrectly, or can change their position in the pipette suddenly i.e. falling to the bottom.

The relationship between dose and toxicity is in agreement with previous studies in cells showing that toxicity is dependent upon the dose and duration of exposure to Aβ42 (Brewer *et al*. 1998). Furthermore, in studies where Aβ42 mRNA levels were equalised at different ages of induction, it was observed that Aβ42 peptide accumulated to higher levels in older-induced flies compared to young-induced flies, and this resulted in a shortened lifespan of older flies. Hence, higher concentrations of the peptide do appear to result in stronger pathological phenotypes in this model.

However, the association between age and the onset of toxicity does not appear to be due to the time required for Aβ42 to accumulate to a toxic concentration.

At equal levels of transgene expression I found that the Aβ42 peptide accumulated more rapidly in older flies compared to young flies. This may reflect an alteration in protein turnover, the combined rates of protein synthesis and degradation, with age (Niedzwiecki & Fleming. 1990). Measurement of ^{35}S-methionine incorporation showed that general protein translation was reduced in old-induced versus young-induced Aβ42-expressing flies. This finding is consistent with published studies showing that the rate of protein synthesis decreases with age in a wide variety of cells, tissues, organs and organisms, including humans (reviewed in Rattan. 1996). Particularly, in *Drosophila*, Webster and Webster (1979) showed that the incorporation of radiolabelled amino acids in microsomal preparations declines by 70% over the first 14 days of adult life and continues to decline thereafter. They also demonstrated that the rate of protein synthesis in the thorax declines the most between 1 and 35 days of age (96%), followed by the abdomen (33%) and the head (15%). (Webster *et al,* 1980). Similar declines in the synthesis of mitochondrial proteins also occur between 6 and 38 days of age (Fleming *et al,* 1986).

As there is no pronounced reduction in protein mass with age (Ryazanov & Nefsky. 2002), this reduction in protein synthesis is likely to be accompanied by a reduction in protein degradation and this may reflect the increase in Aβ42 peptide in aged flies. Interestingly, it has been shown that younger flies show faster protein turnover rates than older flies (Niedzwiecki & Fleming, 1990). In old flies (35-37 days), labelled proteins reached a peak of radioactivity 5 hours following treatment, but no decrease was seen in this peak for up to 30 hours, indicating a very low rate of degradation.

Since Aβ42 is highly stable in these flies, directly measuring the rate of its degradation with age has proven to be difficult. A further analysis of potential Aβ42 clearance mechanisms, including proteasome activity, autophagy and the activity of Aβ42-degrading enzymes such as insulin degrading enzyme (Farris *et al*. 2003; Miller *et al*. 2003) and neprilysin (Iwata *et al*. 2001) may provide an indication as to whether the age-related accumulation of the peptide is indeed caused by alterations in its degradation. Hence, an intrinsic property of the ageing process itself may cause the accumulation of toxic proteins in older neurons and subsequently the development of dose-dependent pathologies.

Moreover, the susceptibility of older flies to Aβ42 toxicity, in comparison to young flies, does not appear to be related to the duration of exposure to the peptide. Older flies were more vulnerable to chronic induction of Arctic Aβ42, with a shortened relative lifespan from the point of exposure to RU486 compared to young flies, despite experiencing a lower lifetime exposure to the Aβ42 peptide. Under these chronic induction conditions the lower level of Aβ42 accumulated in older flies is likely to reflect a reduction in the level of the transcript produced with age as previously observed (see **Figure 3.4a**). This is probably due to a reduced intake of the inducer RU486 via an age-dependent reduction in feeding behaviour (Wong *et al*. 2010).

4.3.3 Older neurons are more vulnerable to Aβ42 toxicity

Together the above data suggest that, although Aβ42 toxicity is dose-dependent, the degree of toxicity with age does not to relate to the length of time required

for the protein to accumulate to toxic levels or to the duration of toxic protein exposure. Rather the ageing process itself may increase the susceptibility of older neurons to Aβ42 toxicity. To test this hypothesis directly I aimed to induce a standard concentration of Aβ42 peptide at different ages and measure the delay to and extent of pathology. This study highlights several technical challenges in performing such investigations using inducible models. Firstly, although negative geotaxis and lifespan serve as useful markers of Aβ42 toxicity in the fly, they are themselves directly affected by ageing. Hence, the ages of induction must be carefully chosen so that (1) peptide over-expression results in phenotypes that are significantly different from non-expressing controls at each time-point analysed and (2) they are far enough apart to resolve any effect of the ageing process. Secondly, the concentration of Aβ42 is affected by the age of induction, as older flies ingest less RU486 due to reduced feeding behaviour, and the length of exposure to RU486, with increasing concentrations correlating with longer exposures. Moreover, normalising mRNA levels at different ages does not result in equivalent levels of protein expression at each time-point of induction. Hence, to effectively measure the consequences of proteotoxicity at different ages one must systematically equalise protein expression by altering the both concentration and the length of exposure to the inducer and measuring the level of protein subsequently produced. Using this approach, I achieved normalised Arctic Aβ42 peptide levels across three ages (five, 20 and 30 days) in my inducible fly model of AD. This demonstrates that the GeneSwitch system offers sufficient flexibility to perform these studies.

In three independent trials comparing different ages of induction or different RU exposure times, older flies exhibited a faster time to death following RU treatment, even when correcting for their decreased life expectancy. This was evident by their reduced relative survival following RU486 treatment. As described above, chronic over-expression of Arctic Aβ42 was also more toxic to older flies, despite a significantly lower lifetime Arctic Aβ42 burden. Thus, in all instances, either the equivalent or a lower Arctic Aβ42 load resulted in relatively higher levels of toxicity in older flies demonstrating that ageing does increase vulnerability to protein-mediated toxicity. These results agree with other studies demonstrating that older neurons are more vulnerable to extracellularly applied Aβ42 fibrils both in cell culture (Brewer. 1998) and in the brain of rhesus monkeys (Geula *et al*. 1998). This work builds upon these findings by providing the first evidence that this is the case *in vivo* under physiological conditions of Aβ42 expression and aggregation.

4.3.4 Discussion of the Ling *et al*. (2011) study

One other study, using a similar experimental design to investigate the effects of ageing on Aβ42 toxicity in *Drosophila* (Ling *et al*. 2011), has reported findings that contrast with those in this study. Although Ling et al. (2011) used the elavGS driver in conjunction with a UAS-Aβ42 line and induction via delivery of RU486 in the food medium, they reported no difference in Aβ42 mRNA levels between young and old flies when equivalent doses of inducer were used. However, higher doses of RU486 were used and experiments performed at a higher temperature in comparison to my study, thus inducing higher levels of

expression at which subtle differences might not have been observed. Moreover, Ling et al. (2011) measured transcript levels during the induction period and I measured levels at the end of induction, which may also account for the difference in expression observed. At equivalent levels of mRNA expression in young-induced and old-induced flies Ling et al. (2011) observed a shorter maximum lifespan in young-induced flies compared to old-induced flies, concluding that younger flies were more vulnerable to Aβ42 toxicity. Aβ42 protein levels were not measured, however, and so the age-dependent effects of protein turnover on toxicity were not controlled for in their study. Moreover, the effects of normal ageing on lifespan must be accounted for by analysing the survival from the time of induction compared to non-Aβ42-expressing controls. For example, at equivalent protein expression levels I also observed that young-induced flies displayed a shorter median lifespan compared to older-induced flies, but further analysis of the survival from the time of induction revealed that in fact older flies were more vulnerable to toxicity than young flies. The varying conclusions between these two studies, therefore, highlights the importance of controlling for both the effects of protein turnover with age and the effects of normal ageing on pathology, when investigating the relationship between ageing and protein toxicity.

Overall this study demonstrates that the GeneSwitch system can be effectively manipulated to equalise both Arctic Aβ42 mRNA and protein expression at different ages. Thus, this conditional system is flexible enough, through RU486 dose compensation, to control for age-dependent effects on feeding behaviour and protein turnover. This has enabled an investigation, for the first time, in to

the effects of ageing on neuronal vulnerability to Aβ42 toxicity under physiological conditions. Although my data demonstrate that Aβ42 toxicity in the fly is dose-dependent, overall these findings strongly suggest that the ageing process increases neuronal vulnerability to protein toxicity.

Chapter 5 TOR pathway inhibition delays ageing but not neuronal dysfunction in an adult-onset model of Alzheimer's Disease

5.1 *Introduction*

The target or rapamycin (TOR) pathway is a highly conserved nutrient-sensory pathway that functions in such distinct organisms as yeast and mammals to regulate growth and metabolism in response to growth factors, amino acids, various stresses and changes in cellular status. It has also been implicated in the control of protein translation and ribosome biogenesis – up-regulation of which is required for growth (for detailed review see Wullschleger *et al*. 2006).

Central to the pathway is a serine/threonine protein kinase known as TOR kinase, which participates in two different multiprotein complexes known as TORC (TOR complex) 1 and TORC2. TORC1 regulates translation and growth via phosphorylation of two downstream effectors, the ribosomal subunit S6 kinase (S6K) and a repressor protein of the cap-binding eukaryotic initiation factor 4E (eIF4E) termed eIF4e-binding protein (4E-BP). Phosphorylated S6K functions to promote cellular and organismal growth (Montagne *et al*. 1999; Um *et al*. 2006). Phosphorylation of 4E-BP disrupts its association with eIF4E, resulting in up-regulation of cap-dependent translation.

In addition, TORC1 inhibits autophagy, the sole pathway for organelle turnover in the cell that is not only vital for reallocation of nutrients and energy, but also for degrading normal and aggregated proteins, particularly under stress or injury (Nixon. 2007). Thus, under favourable conditions for growth, such as an amino acid-rich diet, TORC1 is active and promotes cell growth through up-regulation of translation (through activation of S6K and eIF4E) and inhibition of autophagy. During times of stress, when nutrients are scarce, TORC1 inactivity results in

inhibition of protein translation (by inhibition of S6K and activation of 4E-BP) and upregulation of autophagy, which helps to reallocate energy reserves within the cell. This is exemplified by the fact S6K-deficient animals are smaller with metabolism resembling that on a low-calorie diet (Um *et al*. 2006). In contrast to the many roles of TORC1, the TORC2 complex seems to be mainly involved in cytoskeletal remodelling and up-regulating the IIS pathway through phosphorylation of Akt, the main kinase in the IIS pathway (Wullschleger *et al*. 2006).

TOR kinase is inhibited by rapamycin, a naturally occurring non-antibiotic macrolide compound first discovered over 30 years ago as a product of the bacterium *Streptomyces hygroscopius* in a soil sample from Rapa Nui, otherwise known as Easter Island (Vézina *et al*. 1975). Rapamycin is the most specific TOR inhibitor known, and acts by forming an inhibitory tri-molecular complex with TORC1 and the intracellular protein FKBP12. Inhibition of TORC1 with rapamycin reduces phosphorylation of the downstream targets S6K and 4E-BP, resulting in a reduction in protein translation (Grolleau *et al*. 2002; Bjedov *et al*. 2010) and up-regulation of autophagy (Ravikumar *et al*. 2004). On the other hand, TORC2 is thought to be rapamycin insensitive (Wullschleger *et al*. 2006), although evidence from cell culture suggests that chronic rapamycin exposure can inhibit TORC2 (Sarbassov *et al*. 2006).

Increasing evidence has pointed to a link between TOR signalling and AD. First, studies in a diverse range of model organisms have shown that reducing TOR signalling can extend lifespan, a major risk factor for AD. For instance, both

chronological (Powers *et al*. 2006) and replicative (Kaeberlein *et al*. 2005) lifespans are extended in the yeast tor1 mutant. Nematode worms carrying mutations in genes encoding the worm homolog of TOR (let-363) and S6K (rsks-1), along with components of the translational machinery (Vellai *et al*. 2003; Hansen *et al*. 2007) are long-lived, as are flies over-expressing either a dominant-negative form of S6K or negative regulators of the TOR pathway (Kapahi *et al*. 2004). Completing the set of model organisms is the recent study showing that genetic deletion of S6K1 in mice also extends lifespan (Selman *et al*. 2009). Furthermore, pharmacological down-regulation of the TOR pathway by rapamycin has been shown to increase lifespan in yeast, flies (Bjedov *et al*. 2010) and mice (Harrison *et al*. 2009), which, incredibly, were 600-days-old when first treated. This latter study indicated that pharmacological interventions initiated in middle age might still be effective in increasing lifespan.

The second major link between TOR signalling and AD is that rapamycin is a known activator of autophagy, a process that has been implicated in the neurodegeneration of AD (Nixon. 2007). Third, there is some evidence that TOR signalling is altered in Alzheimer's-disease brain tissue and transgenic models of AD. However, there is a serious lack of consensus on this issue. For instance, studies examining human tissue report increased activation of the TOR pathway in affected brain areas in Alzheimer's-diseased brains compared to non-diseased control tissue (Li *et al*. 2005). Furthermore, it has been recently demonstrated in two independent studies that rapamycin can benefit mouse models of AD. In 3xTG mice (Caccamo *et al*. 2010) and PDAPP mice (Spilman *et al*. 2010) rapamycin treatment resulted in a reduction in Aβ levels and plaque load, which

led to reduced pathology and rescue of memory impairments. Both studies claimed this rescue was dependent on autophagy upregulation.

Ma *et al.,* (2010) reported a slightly different picture, observing that TOR signalling was in fact reduced in the Tg2576 transgenic mouse and that this correlated with impaired synaptic plasticity, as measured by long-term potentiation in hippocampal slices. By up-regulating TOR signalling via GSK3 inhibition (with LiCl) they were able to prevent Aβ-induced impairments in synaptic plasticity. They also demonstrated that intraneuronal Aβ42 co-localises with TORC1 and S6K. This study was consistent with the earlier work showing that TOR signalling is down-regulated in neuroblastoma cells treated with Aβ42, and also in PSEN mice (Lafay-Chebassier *et al*. 2005).

In this chapter I set out to investigate the link between TOR signalling and AD by using the TOR inhibitor rapamycin in conjunction with a previously developed inducible model of AD. The aim was to measure the toxicity associated with Arctic Aβ42 over-expression in response to rapamycin administration.

5.2 *Results*

To determine whether inhibition of the TOR pathway would delay or prevent Aβ42 toxicity in *Drosophila*, RU486 and rapamycin were simultaneously administered to *UAS-Arctic Aβ42/+;elavGS/+* flies. Survival and negative geotaxis were then measured following drug treatment, to see whether rapamycin would ameliorate Aβ42-mediated toxicity. To avoid developmental effects, flies were reared on normal SY food and then permanently moved to food supplemented with both RU486 and rapamycin, from two-days post-eclosion.

In total, four different food combinations were used in all experiments:

-RU486 SY (-RU)

-RU486 and 200μM rapamycin (-RU/rapa)

+200μM RU486 (+RU)

+200μM RU486 and 200μM rapamycin (+RU/rapa)

The different food types were necessary to control for any non-specific or synergistic effects of the presence of two different drugs in the fly food. As before in chapter 3, RU486 was added to SY to a final concentration of 200μM. Similarly, rapamycin was dissolved in SY to a final concentration of 200μM. This dose was chosen because it was previously shown to cause the biggest increase in median lifespan without toxicity (Bjedov *et al*. 2010).

5.2.1 Rapamycin has no effect on lifespan or neuronal dysfunction in *UAS-Arctic Aβ42/+;elavGS/+* flies in the w^{1118} genetic background.

As seen previously in Chapter 3, induced Aβ42 overexpression resulted in a significant decline in locomotor function (**Figure 5.1**) and lifespan (**Figure 5.2**). *UAS-Arctic Aβ42/+;elavGS/+* flies treated with RU486 demonstrated a significant decline in climbing ability by day 13, when compared to non-RU-treated controls. The same flies treated with rapamycin (+RU/Rapa) failed to show any relative improvement in climbing ability, when compared to non-RU-treated flies. Rapamycin also had no effect on the climbing ability of non-RU-treated flies.

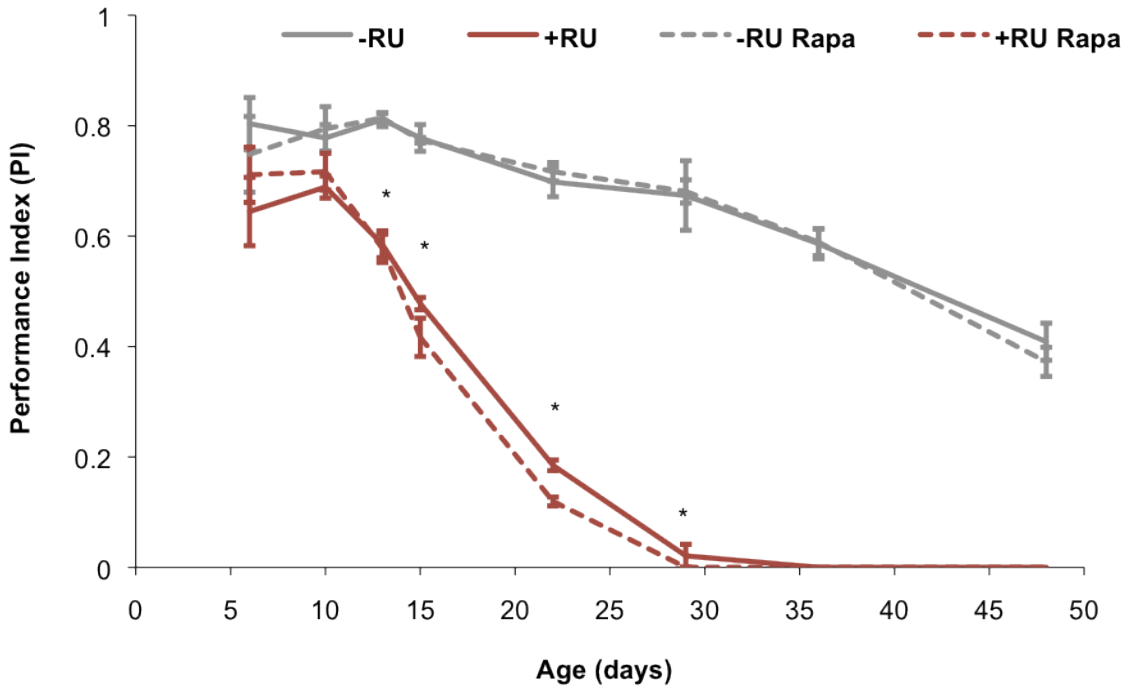

Figure 5.1. Rapamycin has no effect on Aβ42-mediated neuronal dysfunction. Negative geotaxis behaviour of w1118 UAS-Arctic Aβ42;elavGS/+ flies treated with RU486 and Rapamycin from two-days post-eclosion. Climbing ability was assessed at the indicated time-points. Data are presented as the average performance index (PI) +/- SEM (n = 3, number of flies per group = 39-45) and were compared using two-way ANOVA and Tukey's honestly significant difference (HSD) post-hoc analyses. *P<0.05 comparing PI of +RU or +RU/Rapa treatments to that of both –RU and –RU/Rapa control flies at the indicated timepoints. No significant difference was seen between –RU and –RU/Rapa at any timepoint nor was any difference observed between +RU and +RU/Rapa.

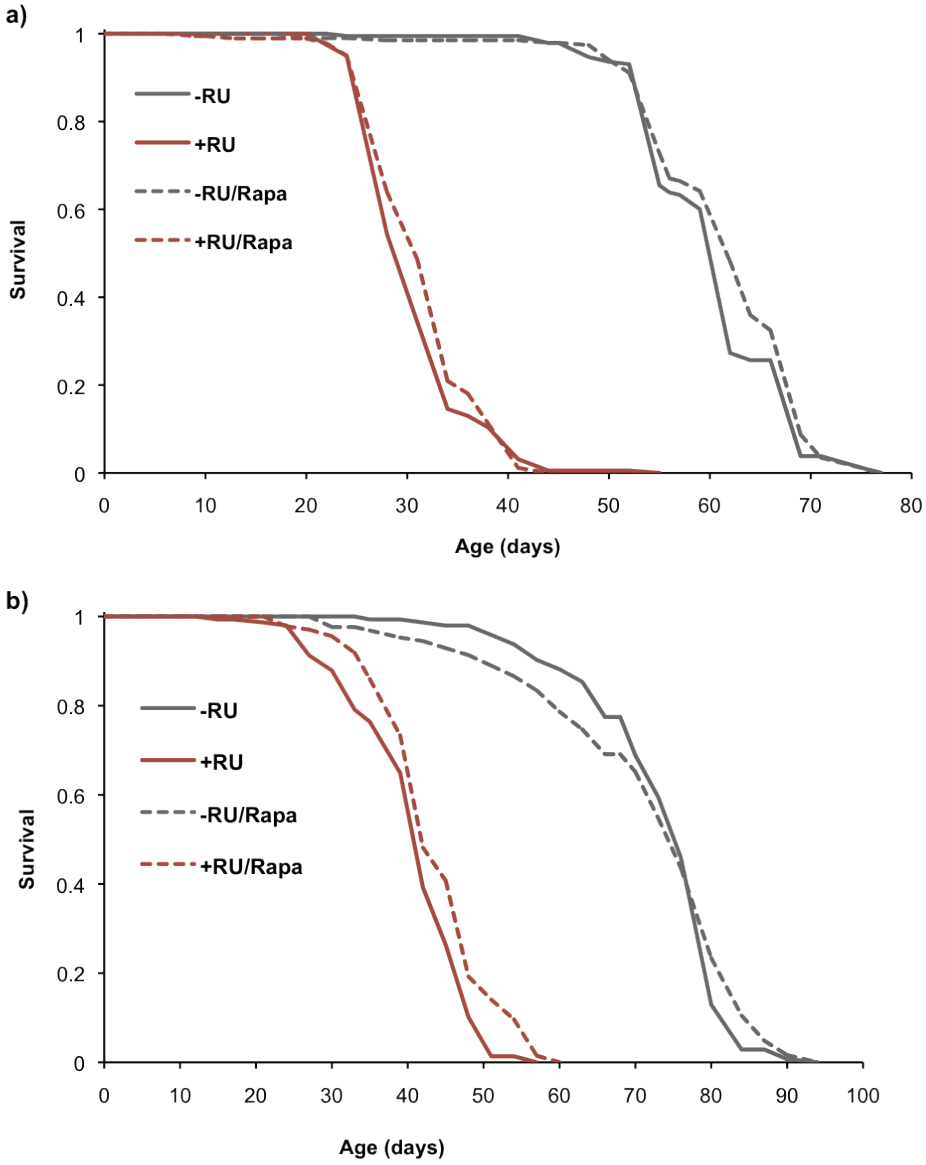

Figure 5.2. Rapamycin treatment may delay ageing in flies overexpressing Aβ42. Survival curves of *UAS-Arctic Aβ42/+;elavGS/+* flies treated with RU486 and rapamycin from two-days post-eclosion. (a) and (b) represent two individual experiments. (a) Median lifespans are as follows: 61 days for –RU and –RU/Rapa and 30 days for +RU and +RU/Rapa. No significant difference in survival was detected between +RU and +RU/Rapa ($p = 0.13$, log rank test), and –RU and –RU/Rapa ($P = 0.11$). The survival of +RU and +RU/Rapa were significantly different to their respective controls ($P<0.001$ for both comparisons). (b) Median lifespans are as follows: 75 days for –RU and –RU/Rapa and 40 days for +RU and +RU/Rapa. A significant difference in

survival was detected between +RU and +RU/Rapa (p = 0.0006, log rank test) but not between –RU and –RU/Rapa (P = 0.57). The survival of +RU and +RU/Rapa were significantly different to their respective controls (P<0.001 for both comparisons).

In two independent assays, survival was significantly reduced in *UAS-Arctic Aβ42/+;elavGS/+* flies treated with RU486 (**Figure 5.2**). In both trials median lifespan was reduced by ~50% compared to non-RU-treated controls. In the first trial, rapamycin had no effect the lifespan of RU- and non-RU-treated flies. In the second trial rapamycin did slightly increase the survival of RU-treated flies but the effect was almost neglibile (median lifespans were the same for these two treatments).

5.2.2 Rapamycin delays ageing but has no effect on neuronal dysfunction in *UAS-Arctic/+;elavGS/+* flies in the w^{Dah} genetic background

It has been previously shown that the extension of lifespan seen with rapamycin in *Drosophila* is more robust in the w^{Dah} wild-type genetic background (Bjedov *et al*. 2010). This, coupled with the negative results observed in a w^{1118} prompted a parallel study of the effect of rapamycin on Aβ42-toxicity in the w^{Dah} genetic background. All transgenes used to develop the inducible model in Chapter 3 were backcrossed (see methods) into the w^{Dah} background for at least 6 generations. Lifespan and climbing ability were then assayed in w^{Dah};*UAS-Arctic Aβ42/+;elavGS/+* flies by repeating the experiments under the same conditions as those used previously in w^{1118}.

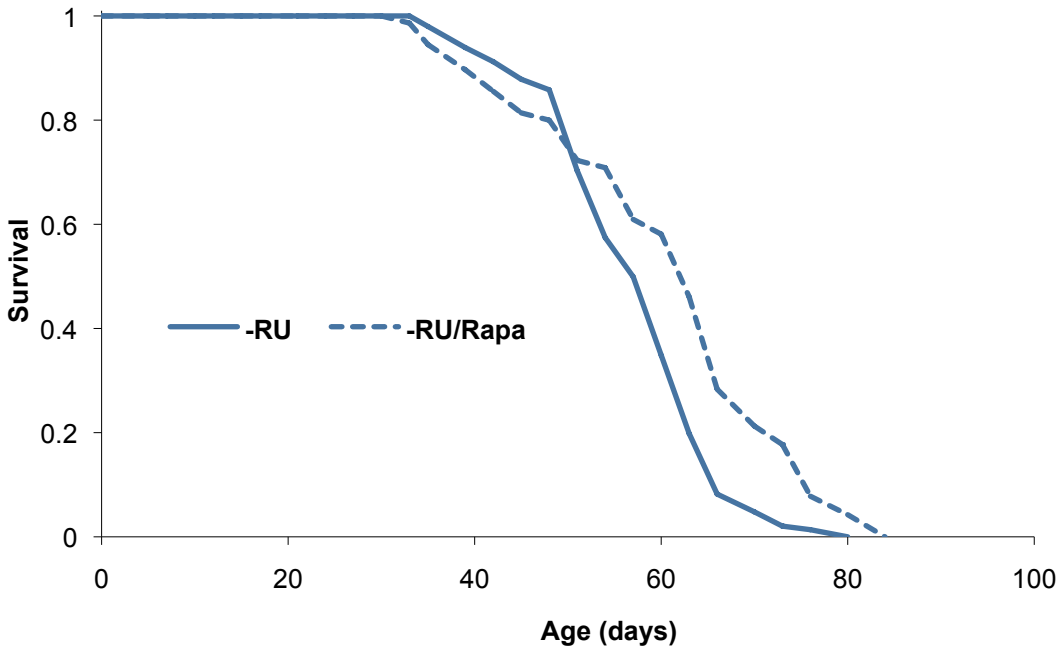

Figure 5.3. Rapamycin extends lifespan in w^{Dah} wild-type female flies. Survival curves of w^{Dah} female flies treated with 200µM rapamycin from two-days post-eclosion. Median lifespans: 56 days for –RU and 62 days for –RU/Rapa. The survival of –RU and –RU/Rapa treated flies was significantly different (P<0.0001, log rank test).

To ensure rapamycin worked in my hands, I first attempted to repeat the finding by Bjedov *et al* (2010) that w^{Dah} wild-type female flies fed 200µM rapamycin causes increased lifespan (**Figure 5.3**). In my hands, rapamycin increased median lifespan by ~11%, from 56 days to 62 days. This extension was similar in magnitude reported in Bjedov *et al* (2010). Confident that the rapamycin was biologically active, I then treated w^{Dah}*;UAS-Arctic Aβ42/+;elavGS/+* flies with 200µM RU486 and 200µM rapamycin from two-days post eclosion, whilst measuring negative geotaxis (

Figure 5.4) and survival (**Figure 5.5**).

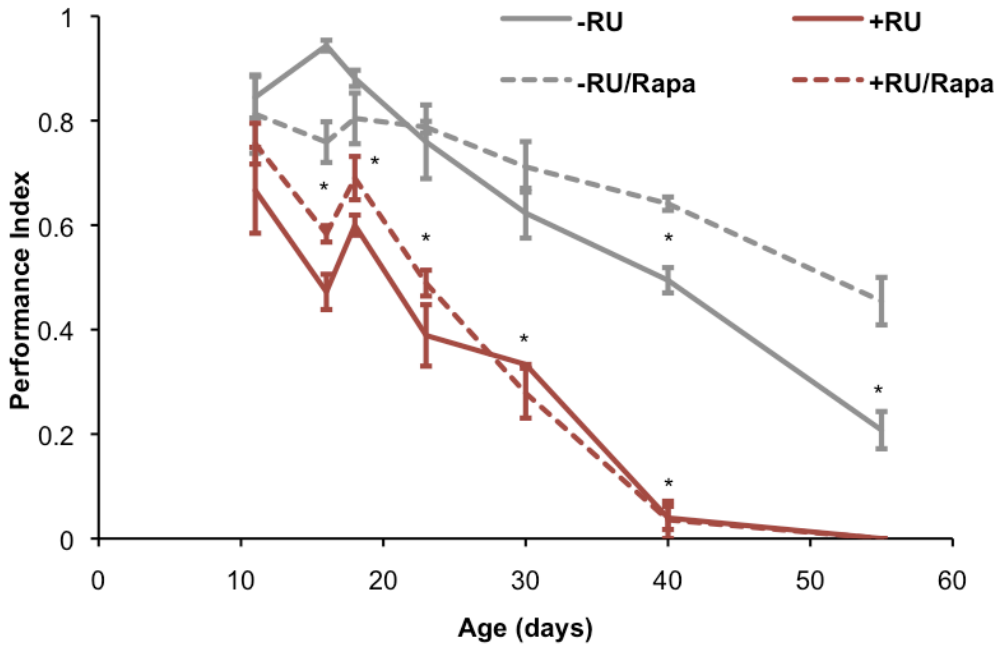

Figure 5.4. Rapamycin has no effect on Aβ42-mediated neuronal dysfunction but does delay senescent-related decline in locomotor function. Negative geotaxis behaviour of w^{Dah};*UAS-Arctic Aβ42;elavGS/+* flies treated with RU486 and Rapamycin from two-days post eclosion. Climbing ability was assessed at the indicated time-points. Data are presented as the average performance index (PI) +/- SEM (n = 3, number of flies per group = 39-45) and were compared using two-way ANOVA and Tukey's honestly significant difference (HSD) post-hoc analyses. *P<0.05 comparing PI of +RU or +RU/Rapa treatments to that of both –RU and –RU/Rapa control flies at the indicated timepoints or comparing PI or –RU treatments to that of –RU/Rapa (day 44 and 55 only). No significant difference was seen between +RU and +RU/Rapa flies. In addition, no significant difference was seen between –RU and –RU/Rapa flies until day 40, from which point, -RU/Rapa treated flies showed a higher level of climbing ability compared to –RU treated flies.

Rapamycin did not improve the climbing ability of flies expressing Aβ42 suggesting that rapamycin does not improve Aβ42-mediated neuronal

dysfunction in this model. Interestingly, non-RU-treated flies treated with rapamycin did have higher negative geotaxis scores at advanced ages (after 40 days). This supports the fact that rapamycin extended lifespan in these flies.

The effects of rapamycin on Aβ42 expressing flies were more pronounced and robust in the w^{Dah} background. In two independent assays, survival was significantly reduced in *UAS-Arctic Aβ42/+;elavGS/+* flies treated with RU486 when compared to non-RU-treated controls. In the first trial, Aβ42 overexpression resulted in a 21% decrease in lifespan compared to non-RU-treated controls. In the second trial, there was a 45% decrease in median lifespan. This effect had already been observed many times in w^{1118} so it was to be expected. However, this was the first time it had been seen in the w^{Dah} background, indicating that the model was compatible with other genetic backgrounds, consequently strengthening its reliability.

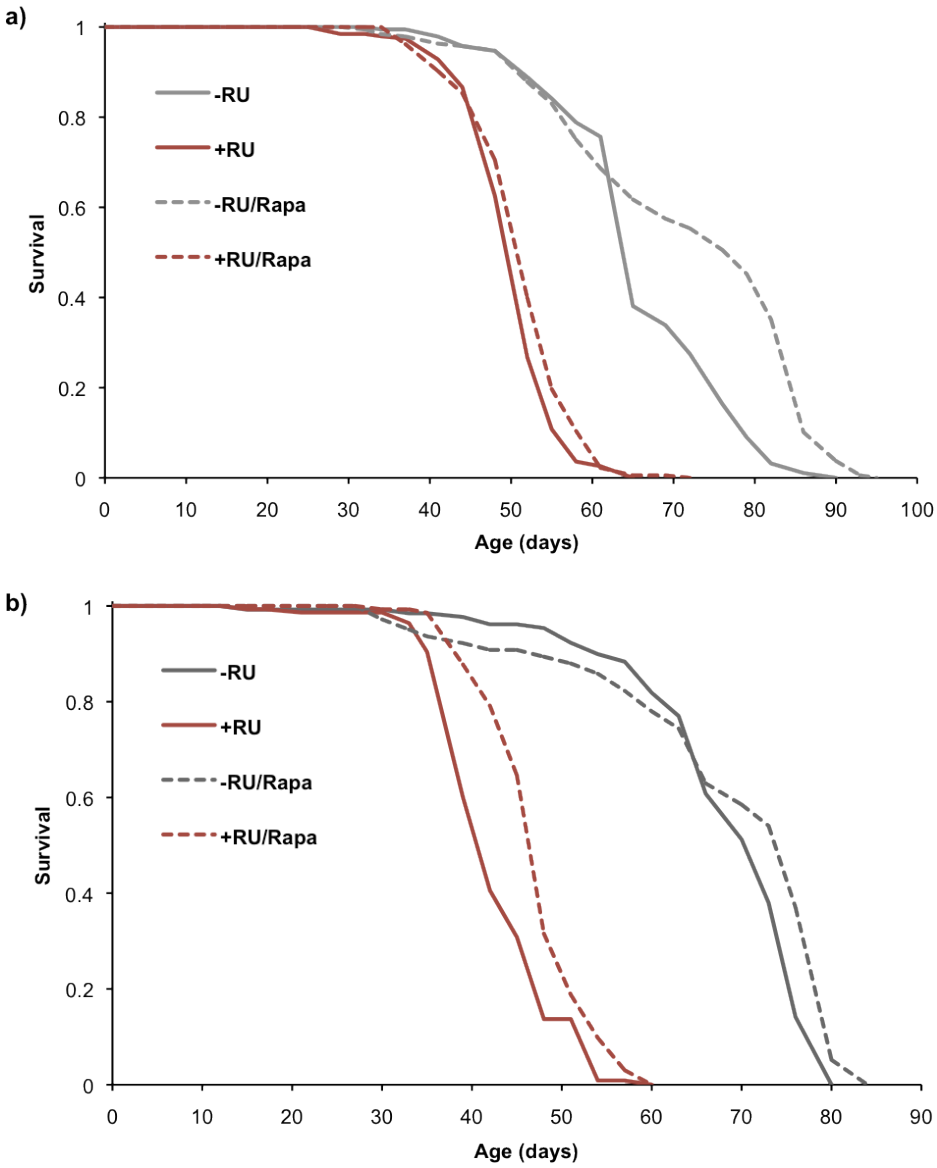

Figure 5.5. Rapamycin treatment delays ageing in flies overexpressing Aβ42. Survival curves of *UAS-Arctic Aβ42/+;elavGS/+* flies treated with RU486 and Rapamycin from two-days post-eclosion. (a) and (b) represent two individual experiments. (a) Median lifespans are as follows: 63 days for –RU, 78 days for –RU/Rapa and 50 days for +RU and +RU/Rapa. There was significant difference in survival between +RU and +RU/Rapa ($p = 0.01$, log rank test), and –RU and –RU/Rapa ($P < 0.0001$). The survival of +RU and +RU/Rapa were significantly different to their respective controls ($P<0.001$ for both comparisons). (b) Median lifespans are as follows: 72 days for –RU, 75 days for –RU/Rapa, 40 days for

+RU and 47 days for +RU/Rapa. A significant difference in survival was detected between +RU and +RU/Rapa ($P < 0.0001$, log rank test) –RU and –RU/Rapa ($P = 0.0016$). The survival of +RU and +RU/Rapa were significantly reduced when compared to their respective controls ($P<0.001$ for both comparisons).

The differences in lifespan reduction between the trials were unexpected. The 45% reduction in median lifespan was similar in magnitude seen in w^{1118}. However, in the first trial the reduction was only 21%. This could be attributable to the fact these stocks had not been recently backcrossed or that there were some problems in rearing/development or the quality of the food. Nonetheless, rapamycin increased the lifespan of flies treated with RU486 in both trials. In the first trial, this effect was very slight (median lifespans between +RU and +RU/Rapa) were actually the same) but significant ($P = 0.01$, log rank test). However, in the second trial rapamycin extended median lifespan of RU-treated flies by 15%. Of further importance was the fact, in both trials, rapamycin extended the lifespan of non-RU-treated *UAS-Arctic AB42/+;elavGS/+* flies, by 19% and 4% respectively. These large differences again could be attributed to the reasons given above. It is likely there was something amiss with the first trial, quite possibly that for some reason the flies were not feeding as well. This would explain the longer lifespan in Aβ42 over-expressing flies and the smaller extension in rapamycin-treated controls.

Because rapamycin inhibits protein translation in *Drosophila* (Bjedov *et al*. 2010), it was important to determine whether the increases in lifespan were simply a consequence of reduced Arctic Aβ42 expression. As has been shown in Chapter 4, survival is very sensitive to total Arctic Aβ42 dose. It was previously

shown that rapamycin has no effect on feeding behaviour (Bjedov *et al*. 2010), therefore any differences the amount of Aβ42 were likely to be due to changes in protein turnover. To assess Aβ42 levels, *UAS-Arctic Aβ42/+;elavGS/+* flies were treated with RU486 and rapamycin from two-days post eclosion. Total Arctic Aβ42 was then quantified at 15 days of age (**Figure 5.6**).

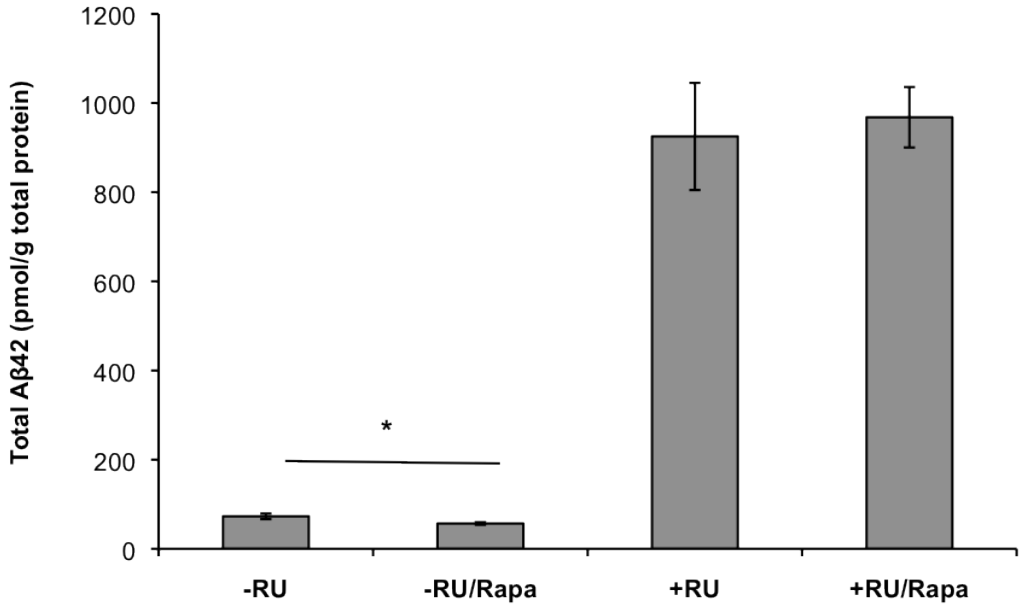

Figure 5.6. Rapamycin has no effect on total Aβ42 protein levels. Total Aβ42 protein levels were quantified at 15-days into-RU486/Rapamycin treatment in w^{Dah}*;UAS-Arctic Aβ42/+;elavGS/+*. Data are presented as means +/- SEM (n = 4 for each group) and were analysed by Student's T-test. There was no significant difference in total Aβ42 between +RU and +RU/Rapa groups. Although there was a significant different between –RU and –RU/Rapa ($P < 0.05$, Student's t-test)

Both groups of RU-treated flies exhibited significantly elevated levels of Arctic Aβ42 when compared to their respective non-RU-treated controls ($P<0.01$,

Student's t-test). However, rapamycin appeared to have no effect on the total level of Arctic Aβ42. Arctic Aβ42 was also detected in non-RU-treated controls, confirming again that there is a low level of leaky expression in this system. Interestingly, the level of leaky expression was significantly lower in flies treated with rapamcyin ($P<0.05$).

5.3 *Discussion*

Drosophila melanogaster has proven to be a valuable model organism for studying the molecular mechanisms involved in both the ageing process and in various neurodegenerative diseases. Increasing evidence suggests a link between TOR signalling and AD: down-regulation of TOR signalling extends lifespan, a well-established risk factor for AD and upregulates autophagy, which has also been implicated in the development of the disease. Furthermore, TOR signalling is altered in AD brain tissue and animal models. To investigate the link between TOR signalling and AD, I examined the effect of the TOR inhibitor, rapamycin, which extends lifespan in wild-type flies and ameliorates AD pathology in mouse models of AD, on lifespan and neuronal dysfunction in a previously developed inducible *Drosophila* model of AD (see chapter 3).

5.3.1 The effects of rapamycin were inconclusive in the w^{1118} genetic background

In the w^{1118} background the effects of rapamycin were inconclusive. Negative geotaxis was used as an indirect measure of neuronal dysfunction, and although this was compromised by Arctic Aβ42 overexpression, rapamycin did not ameliorate this effect. Arctic Aβ42 overexpression also resulted in a large reduction in lifespan (~50% reduction in median lifespan) as expected in this background. However, rapamycin treatment failed to improve the survival of Arctic Aβ42 expressing flies. In one trial rapamycin did extend the lifespan of these flies but the effect was very weak (no difference in median lifespan).

Furthermore, rapamycin had no effect on non-RU-treated controls. Because of these largely negative results further studies were not pursued.

5.3.2 Rapamycin delays ageing but not neuronal dysfunction in the w^{Dah} genetic background

Given that rapamycin was shown to have the greatest effect on lifespan in the w^{Dah} background (Bjedov *et al*. 2010), the largely negative data seen in w^{1118} prompted a repeat in *w^{Dah};UAS-Arctic AB42/+;elavGS/+ flies*. This necessitated backcrossing of the driver and UAS-lines to the w^{Dah} background for at least 6 generations.

In w^{Dah}, Arctic Aβ42 overexpression also resulted in a reduction in negative geotaxis and survival relative to non-RU-treated controls. Although these effects were to be expected, this was the first time they had been recorded in a different background. Hence, this result alone helped to increase the reliability and confidence of the inducible model first presented in Chapter 3 because it demonstrated that it was viable in more than one genetic background.

Results in w^{Dah} were more interesting. As in w^{1118}, rapamycin did not suppress the effects of Arctic Aβ42 overexpression on negative geotaxis, suggesting no rescue of neuronal dysfunction in these flies. Interestingly, it did improve the performance of non-RU-treated controls at advanced ages (from day 40 onwards). This effect has also been reported when using genetic interventions to increase lifespan. For example, homozygous $chico^{1}$ mutants exhibited elevated

negative geotaxis scores at advanced ages than their isogenic controls (Gargano *et al*. 2005).

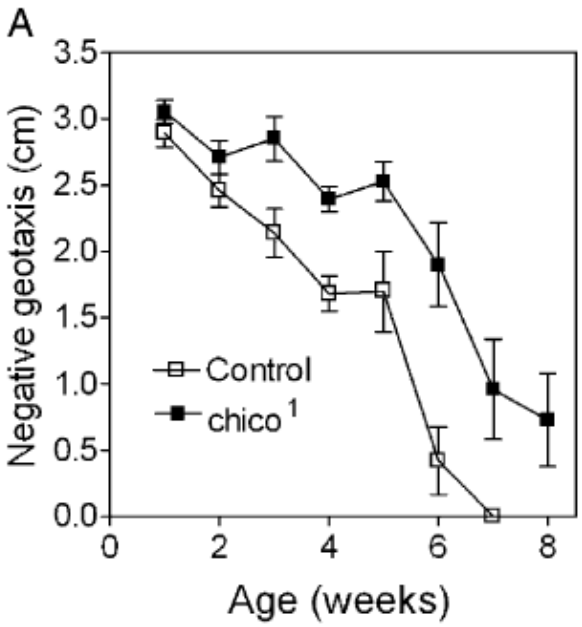

Figure 5.7. Delayed senescence of negative geotaxis in *chico*^{1} homozygous mutants. Figure taken from (Gargano *et al*. 2005).

This effect was seen earlier in this study (by 3 weeks) but they used a much more sensitive, automated method that records the height each individual fly climb (RING method; see Gargano *et al*. 2005) and thus, were more likely to detect subtle changes in negative geotaxis. What this study and the data presented in this chapter demonstrate is that interventions that extend lifespan can also delay behavioural senescence (in this case, negative geotaxis). However, this is not a general rule applicable to all functions that senesce. For example, studies on behavioural senescence in *Drosophila methusela* mutants, which are long-lived, suggest that extension of lifespan does not delay behavioural senescence (Cook-Wiens & Grotewiel. 2002). Similarly, lifespan in flies that overexpress either the

Drosophila insulin receptor (*dInR*) or its downstream signalling target dFOXO in cardiac tissue are indistinguishable, yet cardiac senescence is delayed only in flies overexpressing dFOXO (Wessells *et al*. 2004).

Although rapamycin had no effect on the Arctic Aβ42-mediated decline in negative geotaxis it did extend lifespan of flies expressing Arctic Aβ42. In one trial, a 15% increase in median lifespan was observed. Similarly, rapamycin extended the lifespan of non-RU-treated w^{Dah}*;UAS-Arctic Aβ42/+;elavGS/+* controls and w^{Dah} wild-type flies. Thus, rapamycin slowed ageing in all treatments and genotypes studied in the w^{Dah} background. The magnitude of lifespan extension was similar in RU and non-RU-treated w^{Dah}*;UAS-Arctic Aβ42/+;elavGS/+* flies, suggesting that slowing the ageing process in this manner did not ameliorate the reduction in lifespan induced by Arctic Aβ42. This interpretation is consistent with the observation that rapamycin had no effect on total Arctic Aβ42 levels. On the other hand, the fact protein levels were unaltered is inconsistent with the fact rapamycin reduces protein translation in *Drosophila* (Bjedov *et al*. 2010). It might be that the reduction in GeneSwitch expression (if translation of this gene is affected by rapamycin) was not significant to result in a reduction in UAS-transgene expression.

Given that rapamycin affects all tissues in the fly, but Arctic Aβ42 is mediating its effects predominantly from nervous system, it is likely the extension in lifespan seen in Arctic Aβ42 expressing flies was mediated from tissues outside of the nervous system and thus was independent to the effects of Arctic Aβ42 toxicity.

These results also demonstrate that the processes regulating mortality and neurodegeneration can be uncoupled, since rapamycin extended lifespan without ameliorating the neuronal dysfunction associated with Arctic Aβ42 overexpression. This finding is consistent with other studies. Kerr *et al* (2009) reported that dietary restriction (DR), an intervention known to extend lifespan in *Drosophila*, delays ageing but similarly not neuronal dysfunction in a *Drosophila* model of Aβ42 toxicity (Kerr *et al*. 2009). Furthermore, flies expressing a mutation in the ADAR (Adenosine Deaminase Acting on RNA) gene display severe, progressive neuro-behavioural impairments, but are not short-lived (Palladino *et al*. 2000).

5.3.3 The effects of rapamycin in other AD models

These findings, particularly the lack of neuronal dysfunction rescue, apparently conflict with published studies demonstrating that rapamycin abolishes cognitive deficits and reduces Aβ42 levels and deposition in PDAPP transgenic mice (Spilman *et al*. 2010) and in 3xTg mice (Caccamo *et al*. 2010). The conflicting data in this chapter could be reconciled if rapamycin were acting upstream of Aβ toxicity at the APP processing level since the fly model does not model this process. However both mouse studies reported no change in APP, C99, C83 or Aβ40 protein levels ruling out reduced amyloidgenic processing as a mechanism of rescue.

Both studies also reported an induction of autophagy in both PDAPP and 3xTg mice, and demonstrated that the reduction and disagggregation of Aβ42 was

dependent on this process. Similarly, rapamycin has been shown to reduce levels and toxicity of a variety of different aggregation-prone proteins in *Drosophila* including wild-type and mutant human tau (Berger *et al*. 2006) and Huntington protein fragments (with a 120-residue polyglutamine tail) (Ravikumar *et al*. 2004). These were also found to be dependent on autophagy.

The level of autophagy was not measured in the fly AD model so it is difficult to suggest whether a lack of autophagy induction was to account for the conflicting results. However, when using the same rapamycin dose and genetic background, Bjedov *et al* (2010) demonstrated that chronic rapamycin administration does indeed induce autophagy in *Drosophila*. It is a possibility that the high concentration of the highly aggregate-prone Arctic Aβ42 isoform was averse to disaggregation, even after autophagy had been apparently induced. This idea is consistent with the fact that a small reduction in Arctic Aβ42 levels was seen in the non-RU-treated controls where expression levels are very low, owing to leakiness of the UAS-transgene.

Thus, in future work it would be interesting to measure the effects of rapamycin on flies expressing lower levels of Arctic Aβ42. This could be simply achieved by lowering the dose of RU486 (chapter 4 demonstrated that a wide range of Arctic Aβ42 expression levels can be achieved by using different RU486 doses for varying exposures). Moreover, one could use the wild-type form of Aβ42, which is less aggregation prone and less toxic to *Drosophila* (Crowther *et al*. 2005). The only problem with these approaches is that by lowering the RU486 dose or the level of toxicity, the phenotypes will become less severe. It might be

that a combination of a much higher RU486 dose and wild-type Aβ42 would be more suitable in modelling the subtle effects of rapamycin. However, this could be complicated by the fact RU486 is toxic at high doses.

The literature concerning the effects of rapamycin in AD remains very controversial. Although this drug has been shown to alleviate toxicity and aggregation in mouse AD models, others have demonstrated that rapamycin exacerbates Aβ production and Aβ-induced cell death (Lafay-Chebassier *et al*. 2006), and can promote amyloidogenic processing and Aβ production via ADAM10 inhibition (Zhang *et al*. 2010). The data presented in this chapter only adds to this controversy. It illustrates a rather benign effect of rapamycin on Aβ42-toxicity, and a beneficial effect on lifespan that is likely independent of Aβ42. There appears to be enough evidence to suggest the mTOR pathway is certainly affected in AD. However, determining its exact role is confounded by the use of different models of AD, different age or developmental stage of the organism/cell studied, and most likely, the different concentrations and dosages of rapamycin administered. Since these all vary between different studies it is very difficult to get a grasp on what actually is going on. The data presented in this chapter only serve to highlight this difficulty since even using a different genetic background yielded alternative results. Thus, more studies must be done to clarify the role of mTOR as well as the potential therapeutic effects of rapamycin in AD. This clarification will be aided by the development of an AD model that everyone can agree accurately represents the human disease. If this is not possible, groups using different models should aim to use similar

experimental designs and behavioural paradigms to make comparisons of experiments more relevant.

Chapter 6 Investigating the interaction between reduced insulin signalling and Aβ42 toxicity in *chico*^{1} mutants

6.1 *Introduction*

Because of the strong association between ageing and neurodegenerative disease, many studies have investigated whether interventions that reduce ageing might also delay neurodegeneration in transgenic disease models (for review see (Douglas & Dillin. 2010). In particular, there has been much focus on the specific role of the IIS pathway, since this is the most prominent and best-studied pathway known to regulate ageing. Results have been mixed and have led to what some have labelled the 'insulin paradox' (Cohen & Dillin. 2008). This paradox concerns the protective nature of IIS signalling, since it has been demonstrated that both reduced and increased IIS signalling can be neuroprotective.

In worm models of HD and AD it was demonstrated that reduced IIS signalling, by AGE-1 and DAF-2 RNAi respectively, ameliorates toxicity, Furthermore, this was confirmed in various mouse models of AD, where it was shown that deficiencies in IRS-2, neuronal IGF and the neuronal insulin receptor delayed pathology (Freude *et al*. 2009); as did IRS-2 null (Killick *et al*. 2009) and IGF-1 receptor heterozygous mice (Cohen *et al*. 2009). Conversely, infusion of IGF1 into ageing rats was reported to enhance the clearance of brain Aβ resulting in levels similar to those found in the brains of young rats (Carro *et al*. 2002). More recently, the same group demonstrated that injection of IGF-1 into AD-model mice reduced the typical behavioural impairments that are associated with increased Aβ levels. Furthermore, there is now evidence to suggest that IIS signalling is compromised in the neurons of patients with AD and that the specific neurons that degenerate in AD may, in fact, be resistant to IIS signalling

(Moloney *et al*. 2010). It is unclear, however, whether this represents an active neuroprotective response or a secondary manifestation of the neurodegenerative process. Nonetheless, these studies point towards the IIS pathway as a major mechanistic candidate linking ageing, proteotoxicity and late-onset neurodegenerative disease.

This chapter sets out to further explore the link between the IIS pathway and proteotoxicity in an inducible model of AD in *Drosophila*. Interestingly, the effect of reduced IIS on a fly model of AD has yet to be reported. This is somewhat surprising since there are a variety of AD model reagents and well-characterised IIS mutants available in *Drosophila*. To assess the effect of reduced IIS on AD phenotypes, Arctic Aβ42 was pan-neurally expressed in adult flies homozygous for $chico^{1}$, a null mutation in the *Drosophila* insulin receptor substrate gene, *chico* (Böhni *et al*. 1999) that has been shown to extend median and maximum lifespan in both homozygotes and heterozygotes (Clancy *et al*. 2001).

The $chico^{1}$ mutation was shown to extend life-span by up to 48% in homozygotes and 36% in hetereozygotes, when compared to wild-type flies (Clancy *et al*. 2001). In addition, homozygous $chico^{1}$ flies have a dwarf phenotype, owing to fewer and smaller cells despite relatively higher lipid levels (Böhni *et al*. 1999).

6.2 *Results*

6.2.1 Stock generation

In previous chapters, the inducible model was established by crossing homozygous elavGS flies with homozygous *UAS-Arctic Aβ42* to generate *UAS-Arctic Aβ42/+;elavGS/+* heterozygotes. These flies were then treated with RU486, typically at two-days post-eclosion, to induce Arctic Aβ42 protein expression in adult fly neurons. In this chapter I wished to do the same but in a *chico*^{1} homozygous background. The cross that was required to achieve this is outlined below (**Figure 6.1**).

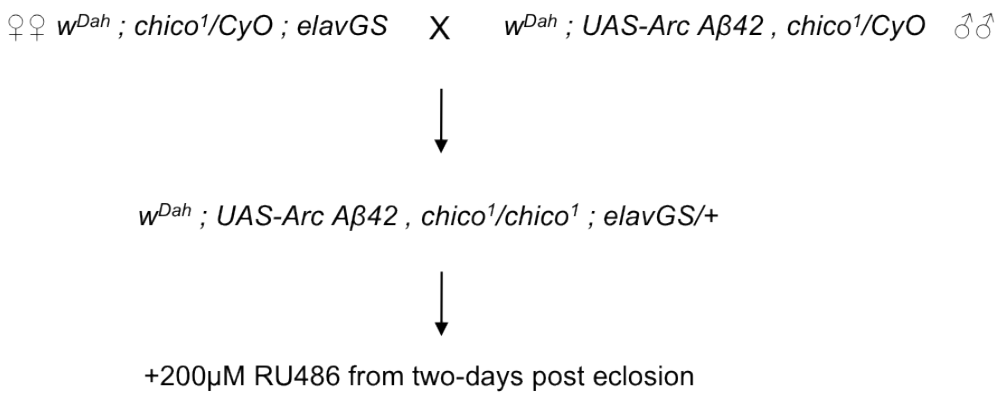

Figure 6.1. Crossing scheme used to establish the inducible AD model in a *chico*^{1} homozygous genetic background. Note: 'Arc' stands for Arctic, Dah stands for Dahomey and all females (♀) were virgins.

As evident in the above figure, this cross required the generation of new *UAS-Arctic Aβ42* and *elavGS* stocks that were heterozygous for the *chico*^{1} mutation. This ensured a proportion of the resulting offspring would be *chico*^{1} homozygotes, whilst also carrying copies of *UAS-Arctic Aβ42* and *elavGS*. Furthermore, because *chico*^{1} homozygotes are sterile (Clancy *et al*. 2001), *chico*^{1}

had to be maintained in a heterozygous state, otherwise no progeny would be generated from this cross. It is also important to note that these stocks were all in w^{Dah} genetic background. This is because *chico*^{1} was originally shown to increase lifespan in this background.

Generating the two new stocks outlined above (**Figure 6.1**) required the use of several *Drosophila* genetic techniques. Generating *chico*^{1}*/CyO;elavGS* flies was relatively straightforward because these two genes reside on different chromosomes; *chico*^{1} is located on the second chromosome whereas the *elavGS* insertion is found on the third . However, because the *UAS-Arctic Aβ42* insertion is also found on chromosome 2, it was necessary to recombine chromosomes carrying *chico*^{1} and *UAS-Arctic Aβ42*. The crossing schemes for developing these two stocks are outlined in **Figure 6.2** and **Figure 6.3**, respectively.

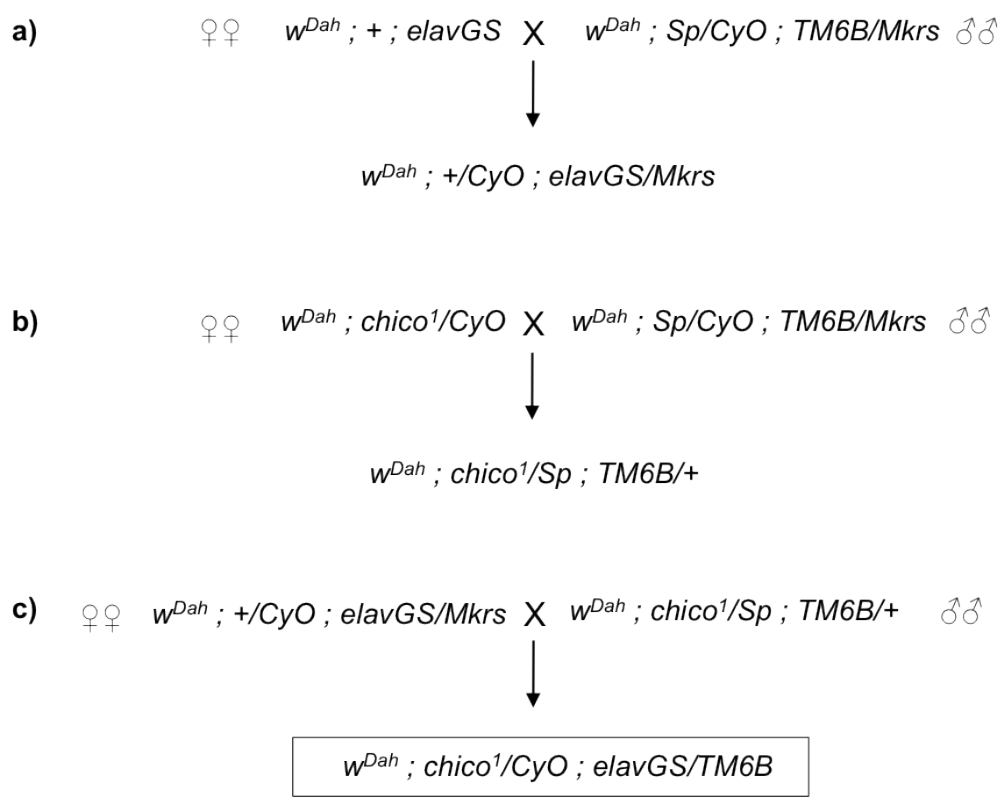

Figure 6.2. Crossing scheme used to generate *chico*^{1}/Cy*O*; elavGS/+ flies. It was first necessary to balance elavGS (a) and *chico*^{1} (b). These balanced stocks were then crossed (c) to generate progeny carrying both genes on chromosomes 2 and 3, respectively. The *w*^{Dah}*;chico*^{1}*/CyO;elavGS/TM6B* progeny were then crossed to each other to generate a stock. In subsequent generations, *TM6B* was selected against to make elavGS homozygous. However, because *chico*^{1} homozygotes are sterile, *chico*^{1} was kept balanced over *CyO*. Thus, these flies were red-eyed with curly wings.

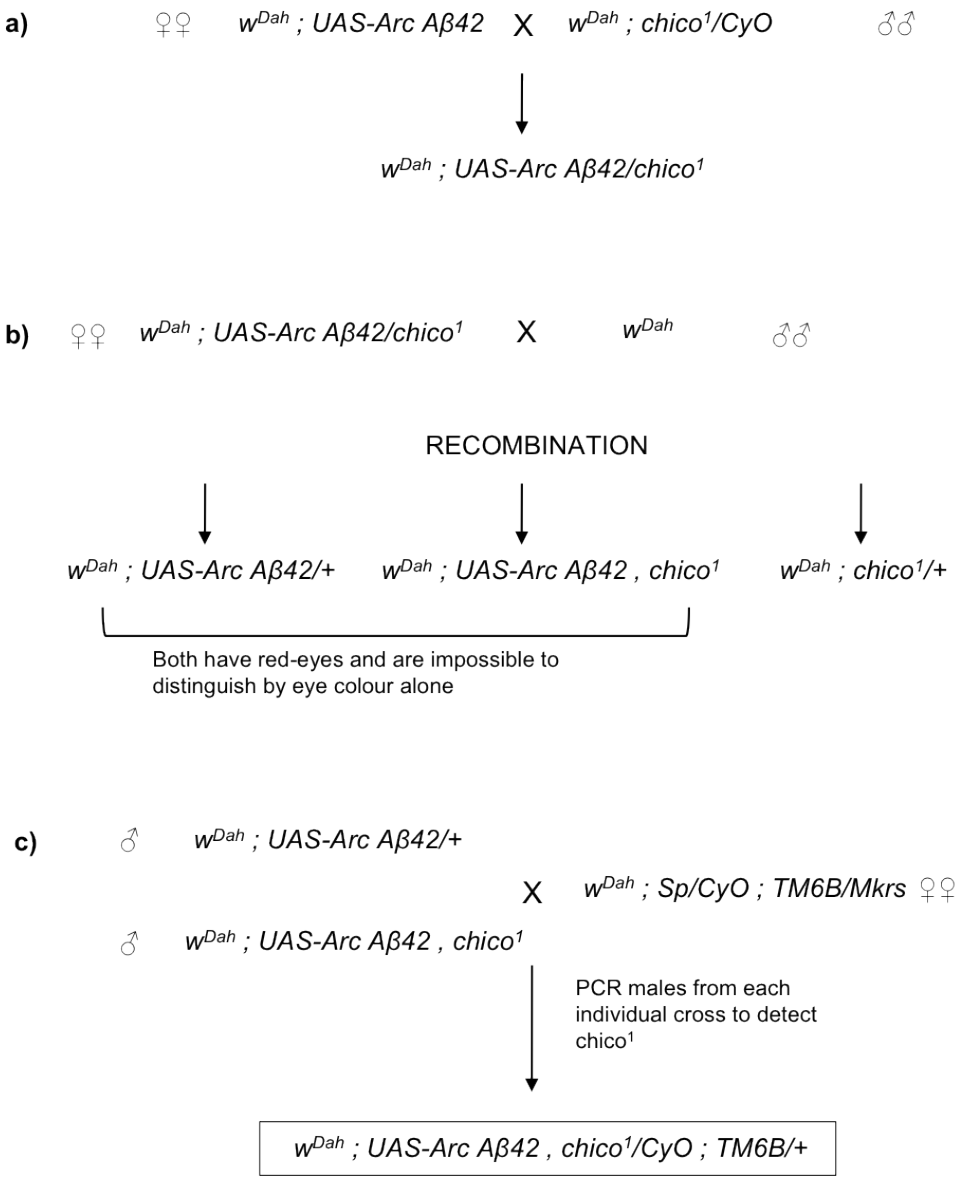

Figure 6.3. Crossing scheme for generating *UAS-Arctic Aβ42, chico^{1}* recombinants. The first step required crossing *UAS-Arctic Aβ42* homozygotes with *chico^{1}/cyo* (a). All the resulting offspring were either UAS-Arctic *Aβ42/chico^{1}* or *UAS-Arctic AB42/CyO*. Thus, flies with curly wings were selected against at this stage. *UAS-Arctic Aβ42/chico^{1}* females were then crossed to *w^{Dah}* males (b). It was important to use females in this cross because no recombination occurs in male *Drosophila* (under normal conditions). If the insertions were far enough apart on the second chromosome then a number of this progeny would have both insertions on the same chromosome following

recombination. Because it was impossible to tell the difference between *UAS-Arc Aβ42/+ and UAS-Arc Aβ42,chico^{1} flies* (they both have a red eye colour) all red-eye male flies from this cross were individually paired with double balancer virgins (c). Once these flies had mated, each individual male was subject to genomic DNA extraction, after which PCR was used to detect the presence of *chico^{1}*. One ♂ symbol represents single pair crosses.

Crossing *UAS-Arctic Aβ42,chico^{1}/CyO* flies with *chico^{1}/CyO;elavGS* yielded viable *UAS-Arctic Aβ42,chico^{1}/chico^{1};elavGS/+* offspring. As has been reported previously for *chico1* homozygotes, development was delayed by approximately two-days and they exhibited an obvious dwarf phenotype, which corresponded with a 55% reduction in mean body weight.

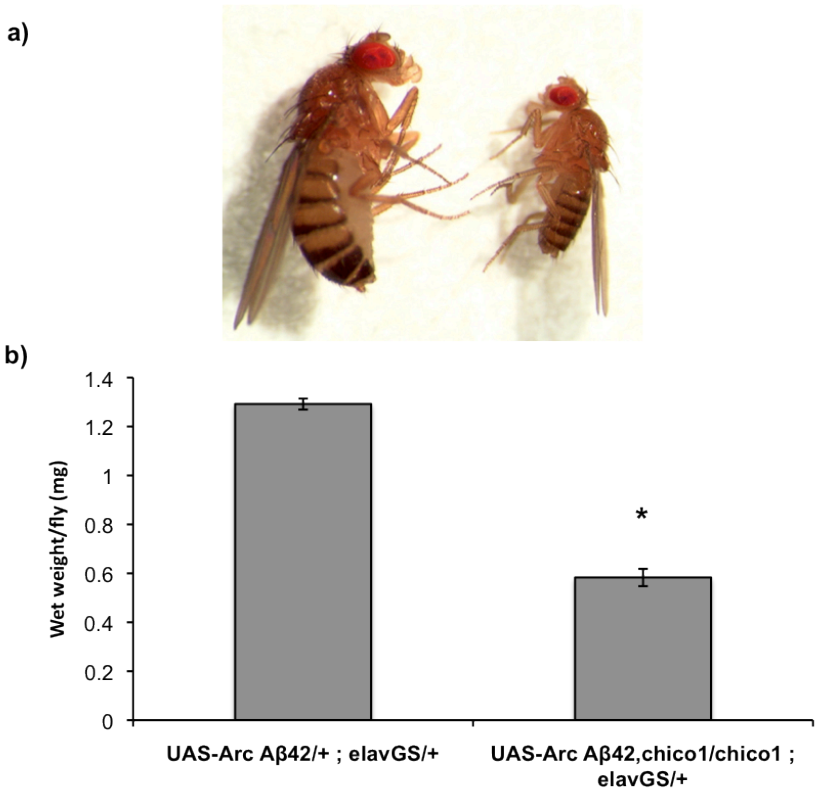

Figure 6.4. Body size reduction in *chico1* homozygotes. *UAS-Arctic Aβ42,chico^{1}/chico^{1};elavGS/+* females displayed (a) a visible dwarf phenotype that corresponded with (b) reduced body weight at eclosion. In (b) data are presented as the mean (n = 10) wet weight (mg) per fly. *chico^{1}* homozygotes were significantly smaller in body size than wild-type flies.* P<0.05, Student's t-test.

6.2.2 Arctic Aβ42-mediated toxicity is suppressed in *chico^{1}* homozygotes

Following generation and confirmation of my stocks, my first aim was to measure the effect of the loss of *chico* on Aβ42-mediated toxicity. In chapter 3, it was demonstrated that induced Arctic Aβ42 overexpression shortens lifespan; causes locomotor dysfunction (as measured by negative geotaxis) and neuronal dysfunction as measured by Giant Fibre electrophysiology. Although the GFS

phenotype offers the most direct marker of Aβ42 toxicity and neuronal dysfunction, it was not a practical method for assaying the effect of the *chico*^{1} mutation on Aβ42-mediated toxicity because this work was very tiem consuming and required a specialised lab (Dr. Hrvoje Augustin). Therefore, lifespan and negative geotaxis were chosen as markers of toxicity as they are robust, easy-to-score phenotypes.

It was important to have a suitable control for the presence of the *chico*^{1} mutation, therefore all experiments were also carried out in *UAS-Arctic Aβ42/+;elavGS* flies which have normal IIS signalling. It is important to note that because of the developmental delay present in *chico*^{1} homozygotes, these crosses were set up two-days after the *chico*^{1} crosses to ensure all progeny emerged on the same day.

I first measured the effect of Arctic Aβ42 expression in *chico*^{1} homozygotes by measuring negative geotaxis (**Figure 6.5**). Age-matched *UAS-Arctic Aβ42,chico*^{1}*/chico*^{1}*;elavGS/+* and *UAS-Arctic Aβ42/+;elavGS/+* females were chronically treated with 200μM RU486 from two-days post eclosion. Non-RU-treated flies of each genotype were used as controls.

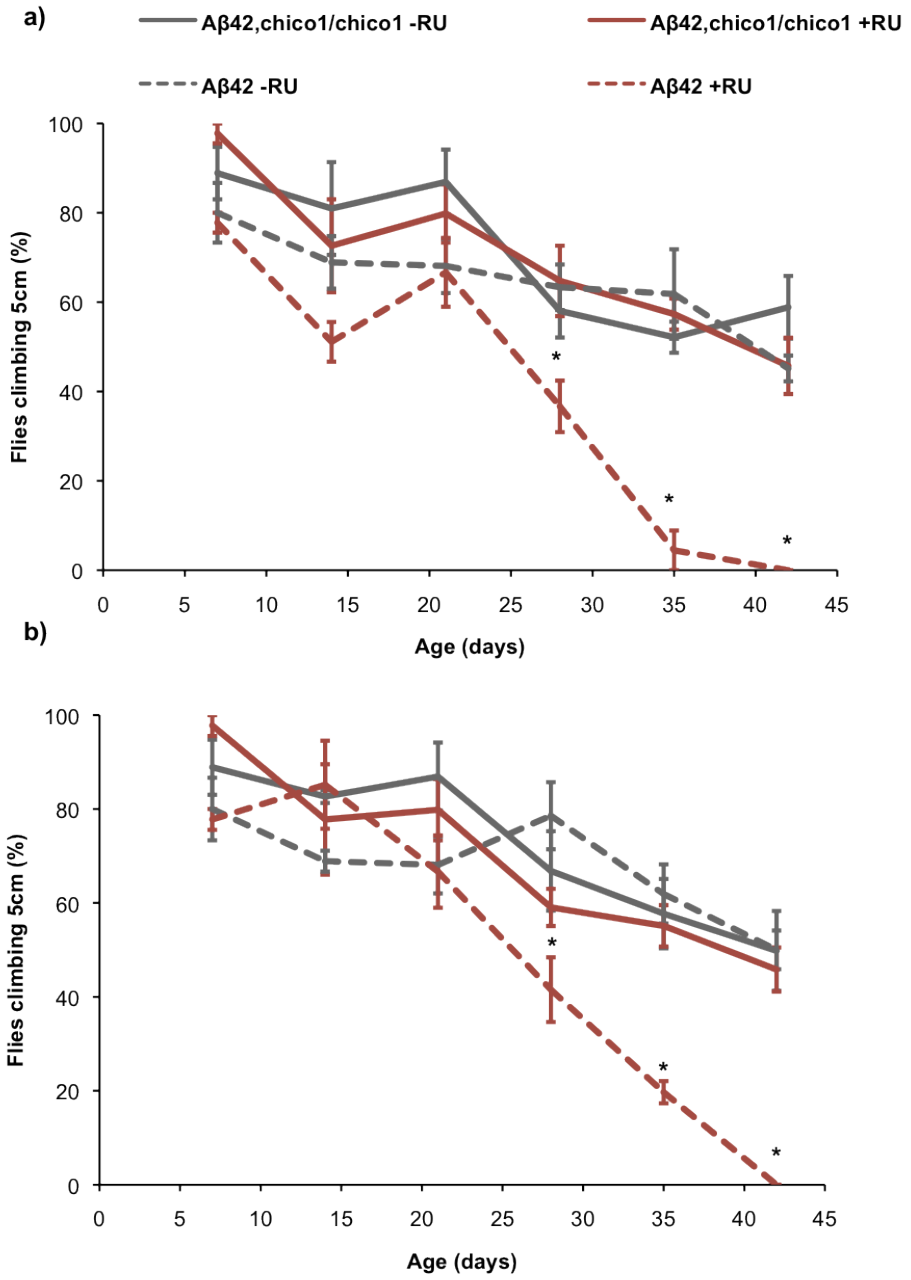

Figure 6.5. Aβ42-mediated neuronal dysfunction is ameliorated in flies homozygous for *chico*^{1}. Climbing ability of *UAS-Arctic Aβ42,chico*^{1}*/chico*^{1}*;elavGS/+* (*Aβ42,chico*^{1}*/chico*^{1} in figure) and *UAS-Arctic Aβ42/+;elavGS/+* (*Aβ42* in figure) females treated with + (200µM) and - RU486 SY medium was assessed at the indicated time-points, (a) and (b) represent two independent experiments. Data are presented as the mean percentage climbing performance (ability to climb 5cm in 18s) of flies +/- SEM (n = 3, number of flies per group = 45) and were compared using two-way ANOVA and Tukey's

honestly significant difference (HSD) post-hoc analyses. *P<0.05 comparing climbing performance of UAS-Arctic Aβ42/+;elavGS +RU to all other groups at the indicated timepoints. A significant difference was seen from day 28 onwards in both trials.

It is important to note that a slightly different negative geotaxis assay was used in this chapter. Rather than using the 25-ml pipettes, climbing performance was measured by the ability of flies to climb 5cm (in a plastic vial with no food) after 18s. The number of flies reaching the 5cm mark was expressed as a percentage of the total number of flies (15 per vial). This is a less stringent version of the climbing assay because the ability of flies to climb is distinguished over a much shorter distance. Consequently, this assay is less sensitive to subtle differences in climbing ability. However, I simply wanted to see whether the climbing phenotype could be rescued in a *chico*^{1} homozygous background so sensitivity was not such a priority. Furthermore, the use of the 25-ml pipette was likely to skew the data; due to the fact flies homozygous for *chico*^{1} would have to climb almost twice the distance, owing to their dwarf phenotype.

In two independent trials, it was found that loss of *chico* reduced the Arctic Aβ42 climbing dysfunction. *UAS-Arctic Aβ42,chico*^{1}*/chico*^{1}*;elavGS/+* flies treated with RU486 exhibited no relative decline in climbing ability when compared to non-RU-treated controls (P<0.05). On the other hand, *UAS-Arctic Aβ42/+;elavGS/+* flies treated with RU486 did show a progressive decline in climbing ability, that was significantly different to non-RU-treated controls from day 28 onwards in both trials. As expected, all flies demonstrated an age-dependent decline in climbing ability over the assay period.

Next the effect of Arctic AB42 overexpression on survival was measured in flies homozygous for *chico*^{1} (**Figure 6.6**). As before, age-matched *UAS-Arctic Aβ42,chico*^{1}*/chico*^{1}*;elavGS/+* and *UAS-Arctic Aβ42/+;elavGS/+* females were chronically treated with 200µM RU486 from two-days post eclosion. Non-RU-treated flies of each genotype were used as controls.

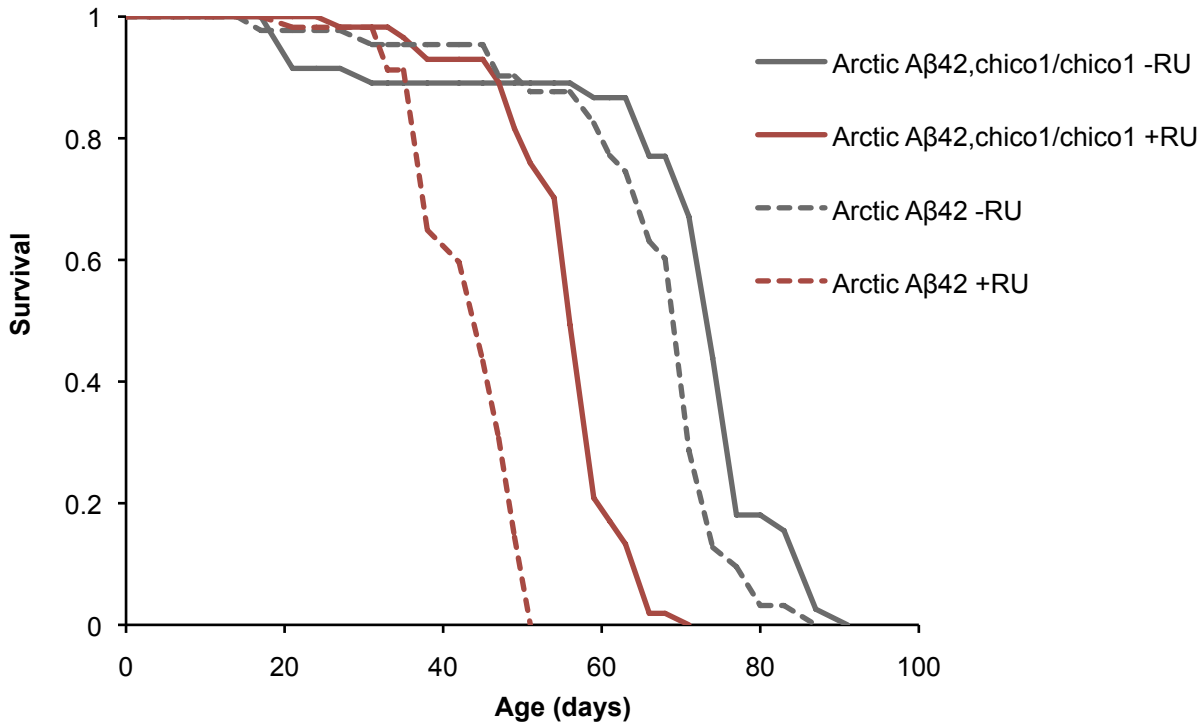

Figure 6.6. Aβ42-mediated ageing is delayed in a *chico*^{1} homozygous background. Survival curves of *Aβ42,chico*^{1}*/chico*^{1}*;elavGS/+ and UAS-Arctic Aβ42/+;elavGS* females treated with +/-RU486 from two-days post-eclosion. Median lifespans: 73 days for *Arctic Aβ42,chico/chico;elavGS/+* -RU and 55 days for +RU. 70 days for *Arctic Aβ42, chico/+;elavGS/+* -RU and 44 days for +RU.

RU486 treatment reduced lifespan in both *Aβ42,chico^{1}/chico^{1};elavGS/+* and *UAS-Arctic Aβ42/+;elavGS* flies, when compared to their respective non-RU-treated controls. Interestingly, the extent of this reduction differed between the two genotypes. In *chico^{1}* homozygotes, RU treatment resulted in a 25% reduction in median lifespan from 73 days to 55 days (P<0.001, log rank test). In flies expressing Aβ42 in a wild-type background, there was a larger 37% reduction in median lifespan, from 70 days to 44 days. When comparing both RU-treated cohorts, *chico^{1}* homozygotes exhibited a 20% extension in median lifespan over flies solely expressing Arctic Aβ42 (55 days compared with 44 days, P<0.001). A smaller extension in median lifespan of 4% was observed when comparing non-RU-treated *chico^{1}* homozygotes with controls (73 days compared with 70 days, P<0.005). These data indicated that although loss of *chico* could not fully rescue the Aβ42-mediated reduction in lifespan, it could suppress it. Furthermore, the difference in median lifespan between the RU-treated groups (20%) was greater than that seen between non-RU-treated controls (4%), indicating that IIS signalling was playing an active role in modulating Aβ42-mediated toxicity rather than extending lifespan through some unrelated independent mechanism (as was the case with rapamycin).

6.2.3 Arctic Aβ42 expression is reduced in *chico^{1}* homozygotes

To further investigate the role of reduced IIS signalling in this model, Arctic Aβ42 protein and mRNA levels were assayed in *chico^{1}* homozygotes (**Figure 6.7**). Age-matched *UAS-Arctic Aβ42,chico^{1}/chico^{1};elavGS/+* and *UAS-Arctic Aβ42/+;elavGS/+* females were chronically treated with 200μM RU486 from two-days post eclosion. Total Arctic Aβ42 protein and mRNA levels were then

assayed 12-days into RU486 treatment using Aβ42-specific ELISA and Q-PCR, respectively. Non-RU-treated flies were used as controls.

Because *chico*^{1} homozygotes are over half the size of wild-type flies it was essential to normalize total Aβ42 levels to the total level of protein in each sample. Interestingly, following this normalization, Aβ42 levels were significantly lower in *chico*^{1} homozygotes ($P<0.05$, Student's t-test). Similarly, Aβ42 mRNA levels were also significantly reduced in *chico*^{1} homozygotes ($P<0.05$, Student's t-test). Thus, these data indicated that the apparent amelioration of toxicity, as observed in survival and negative geotaxis assays, was actually a consequence of reduced Aβ42 expression rather than a direct consequence of reduced IIS signaling. IIS obviously had an effect but it was not acting at the level of Arctic Aβ42 protein turnover, which has been shown to be the case in a worm model of AD (Cohen *et al*. 2006).

The efficacy of induction with the GeneSwitch system is largely dependent on the amount of RU486 ingested during feeding. The fact *chico*^{1} homozygotes are both dwarves and sterile hinted that these flies were actually feeding less and therefore ingesting less RU486. This is because it has been reported that sterile *ovo*^{D1} flies feed less than fertile flies (Barnes *et al*. 2008).

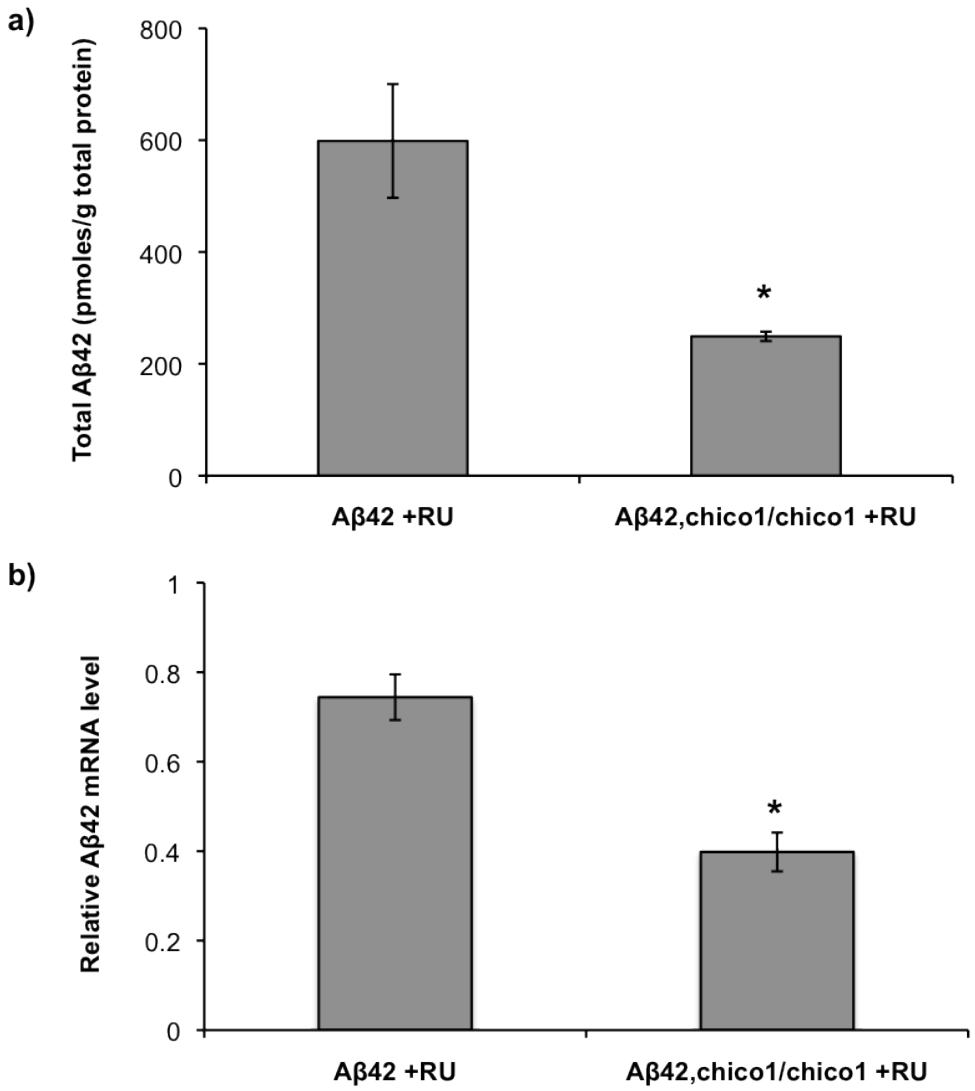

Figure 6.7. Arctic Aβ42 expression is reduced in *chico*^{1} homozygotes. Total Arctic Aβ42 protein levels (a) and mRNA levels (b) were quantified 12-days into-RU486 treatment in *Aβ42,chico*^{1}*/chico*^{1}*;elavGS/+* and *UAS-Arctic Aβ42/+;elavGS* females. Data are presented as means +/- SEM (n = 3 for each group). *P<0.05 comparing total Aβ42 between the two groups (Student's t-test)

This would explain the reduced levels of transcription, which consequently would account for the reduced Aβ42 load and corresponding suppression in Aβ42-mediated toxicity. Therefore, feeding behaviour was assayed at seven days post-eclosion in *UAS-Arctic Aβ42,chico*^{1}*/chico*^{1}*;elavGS/+* and *UAS-Arctic*

Aβ42/+;elavGS/+ females using the proboscis extension assay. It has been demonstrated that this method is an effective and accurate measure of feeding behaviour (Wong *et al*. 2009). Consequently, *chico*^{1} homozygotes exhibited a significant reduction in feeding behaviour over the assay period .

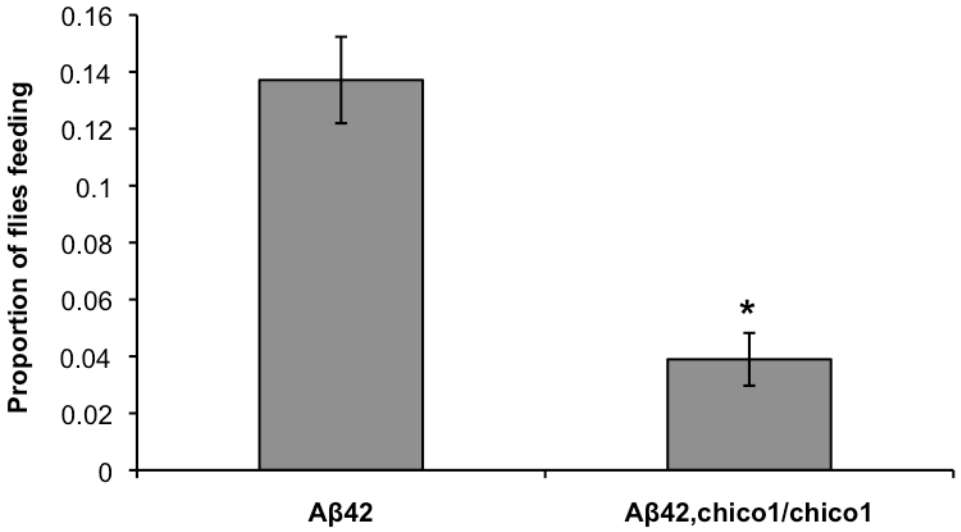

Figure 6.8. Feeding frequency is reduced in *chico*^{1} homozygotes. The proportion of time spent feeding of 7-day old *UAS-Arctic Aβ42,chico*^{1}*/chico*^{1}*;elavGS/+* (Aβ42,*chico*^{1}*/chico*^{1} in figure) and *UAS-Arctic Aβ42/+;elavGS/+* (Aβ42 in figure) females over a 2-hour period. Data are presented as means +/- SEM (N = 10 for each group). *P<0.001 when comparing the two genotypes.

6.3 *Discussion*

The aim of this chapter was to investigate the effect of reduced IIS signalling on Arctic Aβ42-mediated toxicity. This was of particular interest to this thesis since reduced IIS signalling extends lifespan in a diverse range of model organisms ranging from worms and flies to mice. Moreover, reduced IIS has been shown to alleviate toxicity in worm models of AD (and HD) and various mouse models of AD. Interestingly, this effect was yet to be observed in a *Drosophila* model of AD. The availability of well-characterised inducible model of Aβ-toxicity (see chapters 3 and 4) and various fly IIS mutants ensured this would be relatively straightforward to test.

6.3.1 The suppression of Arctic Aβ42-mediated toxicity in *chico*^{1} homozygotes is an artefact of reduced feeding

The generation of w^{Dah}*;UAS-Arctic Aβ42, chico/chico;elavGS/+* flies was successful and yielded viable, sterile, dwarf flies that were developmentally delayed (by ~2 days). This was consistent with previously reported studies on w^{Dah}*;chico*^{1} flies (Böhni *et al*. 1999; Clancy *et al*. 2001). RU486 treatment in these flies resulted in a robust induction of Arctic Aβ42 mRNA and protein expression. Initially, it appeared that Arctic Aβ42-mediated toxicity was suppressed in *chico*^{1} flies since survival and negative geotaxis were both improved, although not completely rescued, when compared to flies expressing Arctic Aβ42 in a wild-type background.

Comparison of Arctic Aβ42 mRNA and protein expression levels revealed that expression of both mRNA and protein was significantly lower in *chico*^{1} homozygotes when compared to wild-type w^{Dah} background controls. Thus, it was apparent that the suppression in toxicity was in fact due to a reduction in Arctic Aβ42 expression. This in turn prompted an investigation into the feeding behaviour of *chico*^{1} homozygotes. The rate of feeding is the major limiting factor for UAS-transgene expression when using the RU486 'in-food' delivery method. If flies feed less, they ingest less RU486 and UAS-transgene induction is likely to be reduced. Using a proboscis-extension assay, it was clear that feeding behaviour in *chico*^{1} homozygotes was reduced. Interestingly, this disagrees with a previous study showing feeding behaviour is unaltered in long-lived *chico*^{1} heterozygotes (Wong *et al*. 2009). This difference is probably due to the fact *chico*^{1} homozygotes are sterile. For instance, it has been suggested that females feed more than males because of their high nutrient-usage in egg production (Wong *et al*. 2009). Thus, the fact *chico*^{1} homozygotes are sterile suggests their lower demand for nutrients resulted in reduced feeding and therefore, reduced RU486 ingestion, in turn leading to reduced induction. This is consistent with the observation that sterile ovo^{D1} females (in which egg production is arrested) feed less during long-term undisturbed conditions than fertile females (feeding also measured by proboscis-extension assay in this study) (Barnes *et al*. 2008).

6.3.2 The pitfalls of the GeneSwitch system and possible future resolutions

Although this study set out to investigate the effects of reduced IIS signalling on Aβ-mediated toxicity in *Drosophila*, it was more effective in highlighting one of

the technical drawbacks of the GeneSwitch system, in particular, the RU486 'in-food' delivery method. Because UAS-transgene expression is dependent on amount of RU486 ingested, controlling for the rate of feeding is essential for measuring the equal effects of protein-mediated toxicity in different mutants. This is especially so when the level of toxicity in the model is a function of the toxic protein dose. This study highlighted that if feeding behaviour is not controlled for, data can be misinterpreted. For instance, if feeding behaviour was not assayed in this study I may have concluded IIS was affecting the transcription of UAS-Arctic Aβ42, when this evidently was not so.

With the benefit of hindsight it is easy to see how the real effect of *chico*^{1} on Aβ toxicity could be measured. This would require controlling for the different level of feeding between wild-type and *chico*^{1} mutant flies. There are many ways in which this could be achieved. One could use different concentrations of RU486 in wild-type and *chico*^{1} flies. This is the same approach used in chapter 4 to equalise transcript expression at different ages. Thus, a higher RU486 dose fed to *chico*^{1} flies would compensate for their reduced feeding. Although this approach has been shown to be effective, it is impractical and complex. First, a variety of RU486 food concentrations would have to be trialled to find those that result in equivalent levels of Arctic Aβ42 expression. Further complicating this is the fact that feeding behaviour declines with age. Hence, the doses might have to be changed accordingly (if using chroninc induction). Alternatively, the flies could be subject to conditional RU486 treatment as in chapter 4.

One approach that would remove the need to control for feeding behaviour would be to inject a known dose of RU486 into individual experimental flies. Although hardly practical for large experiments this technique has been shown to be effective. Bjedov *et al.* (2010) used this technique to inject a known concentration of paraquat, a compound that causes oxidative stress in *Drosophila*, into flies to check that flies are not more/less stress resistant simply because they are eating less/more of the paraquat food. Similarly, Cocheme *et al.* (2010) used the same technique to inject a mitochondrial targeted antioxidant, MitoQ, into flies and found that the compound was almost completely cleared after 12 hours. Thus, with this approach, wild-type and *chico*^{1} Arctic Aβ42-expressing flies could be pulsed with an injection of the same dose of RU486 (after accounting for difference in body weight etc.). In this way, the effect of reduced IIS could be measured in the absence of feeding differences. This would then reveal if loss of *chico* really was involved in the suppression of Aβ toxicity in this model system.

A final more radical approach would be to use a different conditional system all together. In particular, to use one that does not rely on feeding as a method of inducer delivery but still is compatible with the catalogue of existing, well-characterised GAL4 and UAS transgenic lines. Such a system has recently been developed, based on a temperature sensitive GAL80 protein and is called the temporal and regional gene expression targeting (TARGET) system (McGuire *et al*. 2003; McGuire *et al*. 2004. In yeast, GAL80 functions as a repressor of GAL4 activity only in the absence of galactose. When galactose is present, repression is relieved and GAL4 can activate the transcription of target genes.

The TARGET system uses a temperature sensitive variant of GAL80 (GAL80ts) that represses GAL4 activity at 18°C, but which is relieved when flies are moved to 30°C (**Figure 6.9**). GAL80ts is ubiquitously expressed under the control of a tubulin 1a (Tub) promoter.

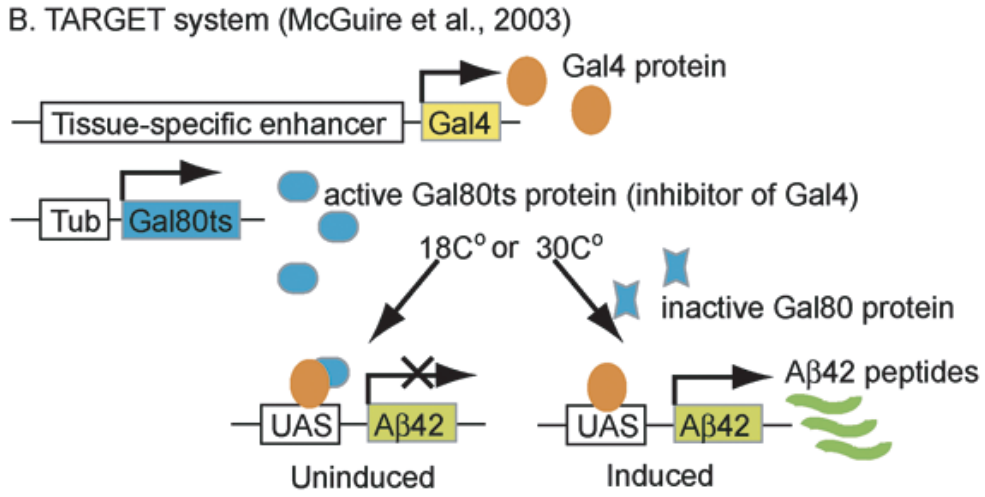

Figure 6.9. The TARGET system. A fly carrying GAL80ts and a promoter-specific GAL4 is crossed with a fly carrying a UAS-transgene (shown here as UAS-Aβ42). At the permissive temperature (18°C, uninduced) GAL80ts suppresses GAL4 activity and prevents transcription of UAS-Aβ42. When flies are moved to the restrictive temperature (30°C, induced) GAL80ts is inactivated and GAL4 can activate UAS-Aβ42 expression. Figure taken from (Iijima & Iijima-Ando. 2008).

This system would be ideal for investigating the effect of loss of *chico* because it does not rely on feeding for induction of UAS-Arctic Aβ42 transgene expression. A future study employing this system would be very interesting although it would necessitate complete re-characterisation of the inducible model. A potential downfall of this system though is that it would require the existence of

another insertion (GAL80ts), which would complicate matters, especially when using multiple gene insertions as in the case of this *chico*^{1} study.

Overall, this study provides a cautionary tale on the limitations and pitfalls of the GeneSwitch system, particularly in modelling neurodegenerative disease.

Chapter 7 Overall conclusions and future work

7.1 *Summary of findings*

The overall aims of this thesis were to investigate the role of ageing as a risk factor for Alzheimer's Disease. The fruit fly *Drosophila melanogaster* is well suited for this type of investigation for several reasons. Firstly, fruit flies are practical, with short generation times and relatively short lifespans suitable for studying age-related neurodegenerative disease. Second, a variety of genetic tools are available. Of particular importance to this thesis was the use of the conditional GeneSwitch system, that allows UAS-linked transgenes to be turned on or off at any time. This system was essential for investigating the effect of Aβ toxicity at different ages because it allowed Arctic Aβ42 expression to be induced at progressively later ages in the adult fly. Third, there are many well-characterised *Drosophila* models of AD, with freely available reagents, that reproduce many of the features of human disease. Fourth, there are a variety of assays available in the fruit fly for measuring toxicity including survival, negative geotaxis and Giant Fibre electrophysiology amongst many others not used in this thesis.

The data in chapter 3 and 4 demonstrated that the GeneSwitch system is an effective platform for developing conditional or adult-onset models of neurodegenerative disease. RU486 induction resulted in robust Aβ42 expression and age-dependent accumulation and aggregation of Arctic Aβ42, which in turn resulted in reduced survival, a progressive decline in climbing ability (locomotor function) and an impairment of Giant Fibre function. The fact these direct and surrogate markers of toxicity presented were consistent and in agreement with the literature indicated that they were all modelling the same thing i.e. Aβ

toxicity. Furthermore, the fact no neuronal loss was observed in this model, despite using some of the same reagents from studies where Arctic Aβ42-mediated neuronal loss was apparent (Crowther *et al*. 2005), highlighted the possible problems with constitutively expressing Aβ peptides during development.

Chapter 4 clearly illustrated the flexibility of the GeneSwitch system and the inducible AD model. Modulation of RU486 dose or removing it completely allowed the study of the dynamics of Aβ toxicity and investigation into the direct effects of ageing on Aβ toxicity. These latter experiments required careful calibration of Aβ dose at different ages to control for differences in RU486 ingestion and protein turnover with age. These calibration steps will be essential for studying the effect of ageing in other models neurodegenerative disease models. Failure to calibrate could lead to misinterpretation of data, as exemplified by the study by Ling *et al.* (2011).

The switch-off studies in chapter 4 demonstrated that Aβ is highly resistant to degradation in *Drosophila*. This finding was consistent with studies of Aβ suppression in mouse models of AD (Jankowsky *et al*. 2005). These studies imply that to effectively treat AD with drugs that reduce the Aβ load it will be imperative to treat the plaques as early as possible otherwise they will be very difficult to clear. Chapter 4 also demonstrated that ageing increases the vulnerability to Aβ toxicity. This conclusion was reached independently using both equalised and chronic Aβ42 induction in young and old flies and the effect was very clear. This was particularly so when measuring the effect of chronic

induction in young and old flies where the lifetime Arctic Aβ42 load was considerably lower in older flies. This provided further evidence that older flies are more sensitive or vulnerable to Aβ. The exact mechanism underlying the increased vulnerability in older flies is yet to be fully elucidated. This would be the main goal of future work and the model developed in this study provides a suitable platform to contine from.

This thesis also highlighted the problem of comparing models that are defined by different conditions (i.e. temperature, level of expression etc). This was exemplified in the study on the effects of rapamycin (chapter 5). This study produced results that were inconsistent with the literature. This was likely due to the many differences in experimental design such as the type of AD model used (APP versus Aβ overexpression), the dose of rapamycin, the behavioural or toxicity markers used, and the age at which the animals were assayed. The data in chapter 5 also demonstrated that some toxicity phenotypes such as survival and climbing could be uncoupled.

Finally, this thesis draws attention to some of the drawbacks of the GeneSwitch system. The first is that UAS-transgene expression occurs in the absence of RU486. Thus, this system is not truly inducible. In every experiment measuring UAS-linked transgene expression, a low basal level of expression was detected in all non-RU86-treated controls. This appears to be an unavoidable feature of this and has been reported elsewhere in the literature (Poirier *et al*. 2008). In the case of the experiments presented in this thesis, this leaky expression was not important since all comparisons were made to uninduced controls.

The other major flaw identified in this thesis is that the GeneSwitch system is highly dependent on the level of feeding behaviour, which complicates the study of mutations or treatments where feeding behaviour altered. This was especially evident in chapter 6 when examining the effects of the *chico*^{1} mutation on Aβ toxicity. Although it was shown in chapter 4 that modulating the RU486 dose can possibly rectify this problem, other conditional systems such as the TARGET system may be more suitable for such experiments. It would be of great interest to repeat the *chico*^{1} experiments and controlling for reduced feeding or using the TARGET system since it remains to be seen whether reduced IIS can ameliorate protein-mediated toxicity in *Drosophila*.

7.2 *Future work*

The development and extensive characterisation of this inducible model of AD provides a framework from which to develop other models of neurodegenerative disease. There are now models of AD, PD, polyglutamine and prion disease in the fly. It would be of great interest to see whether older flies were more vulnerable to these other forms of proteotoxicity. This could be achieved using the same experimental design outlined in this thesis since the experiments and protocols used are easily transferrable. This is helped immensely by the popularity and universality of the GAL4/UAS system.

This work really only scratches on the surface on the role of ageing in neurodegenerative disease. Thus future work focused on the mechanism of 'increased vulnerability' with age would be of much interest. There are several ways this could be investigated. It has been suggested that ageing decreases the

cell's ability to degrade aggregates (Cohen & Dillin. 2008). The Arctic Aβ42 isoform was incredibly stable so it was difficult to track its degradation following Arctic Aβ42 suppression. Future pulse-chase studies using less aggregatory prone proteins such as wild-type Aβ42 or even Aβ40 might provide further insight into the relative rates of degradation at different ages.

Moreover, one could induce equivalent levels of Aβ42 expression in young and old flies (using the protocols developed in this thesis) and then use microarrays to assess the relative changes in gene expression. This could potentially identify key targets or pathways that are down-regulated in older flies. Genetic or pharmacological upregulation of these target genes could then be used in an attempt to rescue the older flies increased vulnerability.

References

Allen, M. *et al*., 2006. Making an escape: development and function of the Drosophila giant fibre system. *Seminars in Cell and Developmental Biology*, 17(1), pp.31-41.

Allen, M.J. *et al*., 1999. Targeted expression of truncated glued disrupts giant fiber synapse formation in Drosophila. *Journal of Neuroscience*, 19(21), pp.9374-9384.

Amaducci, L. & Tesco, G., 1994. Aging as a major risk for degenerative diseases of the central nervous system. *Current opinion in neurology*, 7(4), pp.283-286.

Arriagada, P.V. *et al*., 1992. Neurofibrillary tangles but not senile plaques parallel duration and severity of Alzheimer's disease. *Neurology*, 42(3 Pt 1), pp.631-639.

Asai, M. *et al*., 2003. Putative function of ADAM9, ADAM10, and ADAM17 as APP alpha-secretase. *Biochemical and biophysical research communications*, 301(1), pp.231-235.

Askanas, V. & Engel, W.K., 2001. Inclusion-body myositis: newest concepts of pathogenesis and relation to aging and Alzheimer disease. *Journal of Neuropathology and Experimental Neurology*, 60(1), pp.1-14.

Austad, S.N., 2005. Diverse aging rates in metazoans: targets for functional genomics. *Mechanisms of ageing and development*, 126(1), pp.43-49.

Barnes, A.I. *et al*., 2008. Feeding, fecundity and lifespan in female *Drosophila melanogaster*. *Proceedings of the Royal Society B: Biological Sciences*, 275(1643), pp.1675-1683.

Bello, B. & Resendez-Perez, D., 1998. Spatial and temporal targeting of gene expression in Drosophila by means of a tetracycline-dependent transactivator system. *Development,* 125, pp.2193-2202.

Berger, Z. *et al*., 2006. Rapamycin alleviates toxicity of different aggregate-prone proteins. *Human Molecular Genetics*, 15(3), pp.433-442.

Bieschke, E.T., Wheeler, J.C. & Tower, J., 1998. Doxycycline-induced transgene expression during Drosophila development and aging. *Molecular & general genetics : MGG*, 258(6), pp.571-579.

Billings, L.M. *et al*., 2005. Intraneuronal Abeta causes the onset of early Alzheimer's disease-related cognitive deficits in transgenic mice. *Neuron*, 45(5), pp.675-688.

Bjedov, I. *et al*., 2010. Mechanisms of life span extension by rapamycin in the fruit fly Drosophila melanogaster. *Cell metabolism*, 11(1), pp.35-46.

Blüher, M., Kahn, B.B. & Kahn, C.R., 2003. Extended longevity in mice lacking the insulin receptor in adipose tissue. *Science*, 299(5606), pp.572-574.

Böhni, R. *et al*., 1999. Autonomous control of cell and organ size by CHICO, a Drosophila homolog of vertebrate IRS1-4. *Cell*, 97(7), pp.865-875.

Braak, H. & Braak, E., 1991. Demonstration of Amyloid Deposits and Neurofibrillary Changes in Whole Brain Sections. *Brain Pathology*, 1, pp.213-216.

Brand, A.H. & Perrimon, N., 1993. Targeted gene expression as a means of altering cell fates and generating dominant phenotypes. *Development*, 118(2), pp.401-415.

Brenner, S., 1974. The genetics of *Caenorhabditis elegans*. *Genetics,* 77(1), pp.71-94.

Brewer, G.J., 1998. Age-related toxicity to lactate, glutamate, and beta-amyloid in cultured adult neurons. *Neurobiology of Aging*, 19(6), pp.561-568.

Brookmeyer, R. *et al*., 2007. Forecasting the global burden of Alzheimer's disease. *Alzheimer's & Dementia: The Journal of the Alzheimer's Association*, 3(3), pp.186-191.

Broughton, S.J. et al., 2005. Longer lifespan, altered metabolism, and stress resistance in Drosophila from ablation of cells making insulin-like ligands. *Proceedings of the National Academy of Sciences of the United States of America*, 102(8), pp.3105–3110.

Brouwers, N., Sleegers, K. & van Broeckhoven, C., 2008. Molecular genetics of Alzheimer's disease: An update. *Annals of Medicine*, 40(8), pp.562-583.

Burns, M. *et al*., 2003. Presenilin redistribution associated with aberrant cholesterol transport enhances beta-amyloid production in vivo. *Journal of Neuroscience*, 23(13), pp.5645-5649.

Busciglio, J. & Gabuzda, D., 1993. Generation of beta-amyloid in the secretory pathway in neuronal and nonneuronal cells. *Proceedings of the National Academy of Sciences of the United States of America*, 90, pp.2092-2096.

Busciglio, J., Lorenzo, A. & Yankner, B.A., 1992. Methodological variables in the assessment of beta amyloid neurotoxicity. *Neurobiology of Aging*, 13(5), pp.609-612.

Buxbaum, J.D. *et al*., 1998. Evidence that tumor necrosis factor alpha converting enzyme is involved in regulated alpha-secretase cleavage of the Alzheimer amyloid protein precursor. *The Journal of biological chemistry*, 273(43), pp.27765-27767.

Caccamo, A. *et al*., 2010. Molecular interplay between mammalian target of

rapamycin (mTOR), amyloid-beta, and Tau: effects on cognitive impairments. *Journal of Biological Chemistry*, 285(17), pp.13107-13120.

Cambridge, S.B., Davis, R.L. & Minden, J.S., 1997. Drosophila mitotic domain boundaries as cell fate boundaries. *Science*, 277(5327), pp.825–828.

Cao, W. et al., 2008. Identification of novel genes that modify phenotypes induced by Alzheimer's beta-amyloid overexpression in Drosophila. *Genetics*, 178(3), pp.1457-1471.

Carmine-Simmen, K. et al., 2009. Neurotoxic effects induced by the Drosophila amyloid-beta peptide suggest a conserved toxic function. *Neurobiology of Disease*, 33(2), pp.274–281.

Carro, E. *et al*., 2002. Serum insulin-like growth factor I regulates brain amyloid-beta levels. *Nature Medicine*, 8(12), pp.1390-1397.

Carrotta, R. *et al*., 2005. Protofibril formation of amyloid beta-protein at low pH via a non-cooperative elongation mechanism. *The Journal of biological chemistry*, 280(34), pp.30001-30008.

Carthew, R.W., 2001. Gene silencing by double-stranded RNA. *Current Opinion in Cell Biology*, 13(2), pp.244-248.

Cataldo, A.M. *et al*., 2004. Abeta localization in abnormal endosomes: association with earliest Abeta elevations in AD and Down syndrome. *Neurobiology of Aging*, 25(10), pp.1263-1272.

Chapman, P.F. et al., 1999. Impaired synaptic plasticity and learning in aged amyloid precursor protein transgenic mice. *Nature Neuroscience*, 2(3), pp.271-276.

Chen, G. et al., 2000. A learning deficit related to age and beta-amyloid plaques in a mouse model of Alzheimer's disease. *Nature*, 408(6815), pp.975-979.

Citron, M. *et al*., 1992. Mutation of the β-amyloid precursor protein in familial Alzheimer's disease increases β-protein production. *Nature*.

Clancy, D.J. *et al*., 2001. Extension of life-span by loss of CHICO, a Drosophila insulin receptor substrate protein. *Science*, 292(5514), pp.104-106.

Cochemé, H.M. *et al*., 2011. Measurement of H2O2 within living Drosophila during aging using a ratiometric mass spectrometry probe targeted to the mitochondrial matrix. *Cell metabolism*, 13(3), pp.340-350.

Cohen, E. & Dillin, A., 2008. The insulin paradox: aging, proteotoxicity and neurodegeneration. *Nature Reviews Neuroscience*, 9(10), pp.759-767.

Cohen, E. *et al*., 2006. Opposing activities protect against age-onset proteotoxicity. *Science*, 313(5793), pp.1604-1610.

Cohen, E. *et al*., 2009. Reduced IGF-1 Signaling Delays Age-Associated

Proteotoxicity in Mice. *Cell*, 139(6), pp.1157-1169.

Cook-Wiens, E. & Grotewiel, M.S., 2002. Dissociation between functional senescence and oxidative stress resistance in Drosophila. *Experimental gerontology*, 37(12), pp.1347-1357.

Corder, E.H. *et al*., 1993. Gene dose of apolipoprotein E type 4 allele and the risk of Alzheimer's disease in late onset families. *Science*, 261(5123), pp.921-923.

Corder, E.H. *et al*., 1994. Protective effect of apolipoprotein E type 2 allele for late ons*et Al*zheimer disease. *Nature genetics*, 7(2), pp.180-184.

Crowther, D.C. *et al*., 2005. Intraneuronal Abeta, non-amyloid aggregates and neurodegeneration in a Drosophila model of Alzheimer's disease. *Neuroscience*, 132(1), pp.123-135.

Daigle, I. & Li, C., 1993. apl-1, a Caenorhabditis elegans gene encoding a protein related to the human beta-amyloid protein precursor. *Proceedings of the National Academy of Sciences of the United States of America*, 90(24), pp.12045-12049.

Delaere, P. *et al*., 1990. Large amounts of neocortical βA4 deposits without neuritic plaques nor tangles in a psychometrically assessed, non-demented person. *Neuroscience letters*, 116(1-2), pp.87-93.

Douglas, P.M. & Dillin, A., 2010. Protein homeostasis and aging in neurodegeneration. *The Journal of cell biology*, 190(5), pp.719-729.

Drachman, D.A., 2006. Aging of the brain, entropy, and Alzheimer disease. *Neurology*, 67(8), pp.1340-1352.

Drake, J., 2003. Oxidative stress precedes fibrillar deposition of Alzheimer's disease amyloid β-peptide (1–42) in a transgenic Caenorhabditis elegans model. *Neurobiology of Aging*, 24(3), pp.415-420.

Dulin, F. *et al*., 2008. P3 peptide, a truncated form of A beta devoid of synaptotoxic effect, does not assemble into soluble oligomers. *FEBS letters*, 582(13), pp.1865-1870.

Farkas, E. & Luiten, P.G., 2001. Cerebral microvascular pathology in aging and Alzheimer's disease. *Progress in neurobiology*, 64(6), pp.575-611.

Farris, W., Mansourian S, Chang Y, Lindsley L, Eckman EA, et al., 2003. Insulin-degrading enzyme regulates the levels of insulin, amyloid beta-protein, and the beta-amyloid precursor protein intracellular domain in vivo. *Proceedings of the National Academy of Sciences of the United States of America,* 100. pp.4162-4167.

Fay, D.S. et al., 1998. In vivo aggregation of beta-amyloid peptide variants. *Journal of Neurochemistry*, 71(4), pp.1616–1625.

Ferri, C.P. *et al*., 2005. Global prevalence of dementia: a Delphi consensus study. *Lancet*, 366(9503), pp.2112-2117.

Finelli, A. *et al*., 2004. A model for studying Alzheimer's Abeta42-induced toxicity in Drosophila melanogaster. *Molecular and cellular neurosciences*, 26(3), pp.365-375.

Fleming, J.E. et al., 1986. Age dependent changes in the expression of Drosophila mitochondrial proteins. *Mechanisms of ageing and development*, 34(1), pp.63-72.

Ford, D. *et al*., 2007. Alteration of Drosophila life span using conditional, tissue-specific expression of transgenes triggered by doxycyline or RU486. *Experimental gerontology*, 42(6), pp.483-497.

Fossgreen, A. et al., 1998. Transgenic Drosophila expressing human amyloid precursor protein show gamma-secretase activity and a blistered-wing phenotype. *Proceedings of the National Academy of Sciences of the United States of America*, 95(23), pp.13703–13708.

Fowler, K. & Partridge, L., 1989. A cost of mating in female fruitflies. *Nature*, 338(6218), pp.760–761.

Freude, S. *et al*., 2009. Neuronal IGF-1 resistance reduces Abeta accumulation and protects against premature death in a model of Alzheimer's disease. *The FASEB Journal*, 23(10), pp.3315-3324.

Furukawa, K. *et al*., 1996. Increased activity-regulating and neuroprotective efficacy of alpha-secretase-derived secreted amyloid precursor protein conferred by a C-terminal heparin-binding domain. *Journal of Neurochemistry*, 67(5), pp.1882-1896.

Games, D. *et al*., 1995. Alzheimer-type neuropathology in transgenic mice overexpressing V717F beta-amyloid precursor protein. *Nature*, 373(6514), pp.523-527.

Gargano, J.W. *et al*., 2005. Rapid iterative negative geotaxis (RING): a new method for assessing age-related locomotor decline in Drosophila. *Experimental gerontology*, 40(5), pp.386-395.

Geula, C. *et al*., 1998. Aging renders the brain vulnerable to amyloid beta-protein neurotoxicity. *Nature Medicine*, 4(7), pp.827-831.

Giannakou, M.E. & Partridge, L., 2007. Role of insulin-like signalling in Drosophila lifespan. *Trends in Biochemical Sciences*, 32(4), pp.180-188.

Giannakou, M.E. *et al*., 2007. Dynamics of the action of dFOXO on adult mortality in Drosophila. *Aging Cell*, 6(4), pp.429-438.

Giannakou, M.E. *et al*., 2004. Long-lived Drosophila with overexpressed dFOXO in adult fat body. *Science*, 305(5682), p.361.

Glenner, G.G. & Wong, C.W., 1984a. Alzheimer“s disease and Down”s syndrome: sharing of a unique cerebrovascular amyloid fibril protein. *Biochemical and biophysical research communications*, 122(3), pp.1131-1135.

Glenner, G.G. & Wong, C.W., 1984b. Alzheimer's disease: initial report of the purification and characterization of a novel cerebrovascular amyloid protein. *Biochemical and biophysical research communications*, 120(3), pp.885-890.

Goate, A. *et al*., 1991. Segregation of a missense mutation in the amyloid precursor protein gene with familial Alzheimer's disease. *Nature*, 349(6311), pp.704-706.

Götz, J. *et al*., 2001. Formation of neurofibrillary tangles in P301l tau transgenic mice induced by Abeta 42 fibrils. *Science*, 293(5534), pp.1491-1495.

Greeve, I. *et al*., 2004. Age-dependent neurodegeneration and Alzheimer-amyloid plaque formation in transgenic Drosophila. *Journal of Neuroscience*, 24(16), pp.3899-3906.

Grolleau, A. *et al*., 2002. Global and specific translational control by rapamycin in T cells uncovered by microarrays and proteomics. *The Journal of biological chemistry*, 277(25), pp.22175-22184.

Grotewiel, M.S. *et al*., 2005. Functional senescence in Drosophila melanogaster. *Ageing research reviews*, 4(3), pp.372-397.

Grönke, S. *et al*., 2010. Molecular evolution and functional characterization of Drosophila insulin-like peptides. *PLoS genetics*, 6(2), p.e1000857.

Grundke-Iqbal, I., Iqbal, K. & Quinlan, M., 1986. Microtubule-associated protein tau. A component of Alzheimer paired helical filaments. *Journal of Biological Sciences*, 261(13), pp.6084-6089.

Gunawardena, S. & Goldstein, L.S., 2001. Disruption of axonal transport and neuronal viability by amyloid precursor protein mutations in Drosophila. *Neuron*, 32(3), pp.389-401.

Haass, C. & Selkoe, D.J., 2007. Soluble protein oligomers in neurodegeneration: lessons from the Alzheimer's amyloid β-peptide. *Nature Reviews Molecular Cell Biology*, 8(2), pp.101-112.

Haass, C *et al*., 1992. Targeting of cell-surface beta-amyloid precursor protein to lysosomes: alternative processing into amyloid-bearing fragments. *Nature*, 357(6378), pp.500-503.

Hansen, M. *et al*., 2007. Lifespan extension by conditions that inhibit translation in Caenorhabditis elegans. *Aging Cell*, 6(1), pp.95-110.

Hardy, J. & Selkoe, D.J, 2002. The amyloid hypothesis of Alzheimer's disease: progress and problems on the road to therapeutics. *Science*, 297(5580), pp.353-356.

Harrison, D.E. *et al*., 2009. Rapamycin fed late in life extends lifespan in genetically heterogeneous mice. *Nature*, 460(7253), pp.392-395.

Holcomb, L.A. *et al*., 1999. Behavioral changes in transgenic mice expressing both amyloid precursor protein and presenilin-1 mutations: lack of association with amyloid deposits. *Behavior genetics*, 29(3), pp.177-185.

Holzenberger, M. *et al*., 2003. IGF-1 receptor regulates lifespan and resistance to oxidative stress in mice. *Nature*, 421(6919), pp.182-187.

Hsu, A., Murphy, C.T. & Kenyon, C., 2003. Regulation of aging and age-related disease by DAF-16 and heat-shock factor. *Science*, 300(5622), pp.1142-1145.

Hutton, M. *et al*., 1998. Association of missense and 5'|-splice-site mutations in tau with the inherited dementia FTDP-17. *Nature*, 393(6686), pp.702-705.

Hwangbo, D.S. *et al*., 2004. Drosophila dFOXO controls lifespan and regulates insulin signalling in brain and fat body. *Nature*, 429(6991), pp.562-566.

Iijima, K. & Iijima-Ando, K., 2008. Drosophila models of Alzheimer's amyloidosis: the challenge of dissecting the complex mechanisms of toxicity of amyloid-beta 42. *Journal of Alzheimer's disease: JAD*, 15(4), pp.523-540.

Iijima, K. *et al*., 2004. Dissecting the pathological effects of human Abeta40 and Abeta42 in Drosophila: a potential model for Alzheimer's disease. *Proceedings of the National Academy of Sciences of the United States of America*, 101(17), pp.6623-6628.

Irizarry, M C *et al*., 1997a. Abeta deposition is associated with neuropil changes, but not with overt neuronal loss in the human amyloid precursor protein V717F (PDAPP) transgenic mouse. *The Journal of neuroscience : the official journal of the Society for Neuroscience*, 17(18), pp.7053-7059.

Irizarry, Michael C *et al*., 1997b. APPSW transgenic mice develop age-related Abeta deposits and neuropil abnormalities, but no neuronal loss in CA1. *Journal of neuropathology and experimental neurology*, 56(9), p.965.

Irizarry, M.C. et al., 2004. Apolipoprotein E modulates gamma-secretase cleavage of the amyloid precursor protein. *Journal of Neurochemistry*, 90(5), pp.1132–1143.

Iwata, N. et al., 2001. Metabolic regulation of brain Abeta by neprilysin. *Science*, 292. pp.1550-1552.

Iwatsubo, T. *et al*., 1995. Amyloid β protein (Aβ) deposition: Aβ42(43) precedes Aβ40 in down Syndrome. *Annals of neurology*, 37(3), pp.294-299.

Iwatsubo, T. *et al*., 1994. Visualization of Aβ42(43) and Aβ40 in senile plaques with end-specific Aβ monoclonals: Evidence that an initially deposited species is Aβ42(43). *Neuron*, 13(1), pp.45-53.

Jacobsen, K.T. & Iverfeldt, K., 2009. Amyloid precursor protein and its homologues: a family of proteolysis-dependent receptors. *Cellular and molecular life sciences : CMLS*, 66(14), pp.2299-2318.

Jankowsky, J.L. *et al*., 2005. Persistent amyloidosis following suppression of Abeta production in a transgenic model of Alzheimer disease. *PLoS medicine*, 2(12), p.e355.

Jarrett, J.T., Berger, E.P. & Lansbury, P.T., 1993. The carboxy terminus of the beta amyloid protein is critical for the seeding of amyloid formation: implications for the pathogenesis of Alzheimer's disease. *Biochemistry*, 32(18), pp.4693–4697.

Joachim, C.L., Morris, J.H. & Selkoe, D.J., 1989. Diffuse senile plaques occur commonly in the cerebellum in Alzheimer's disease. *The American journal of pathology*, 135(2), pp.309-319.

Kaeberlein, M. *et al*., 2005. Regulation of yeast replicative life span by TOR and Sch9 in response to nutrients. *Science*, 310(5751), pp.1193-1196.

Kang, J. *et al*., 1987. The precursor of Alzheimer's disease amyloid A4 protein resembles a cell-surface receptor. *Nature*, 325(6106), pp.733-736.

Kapahi, P. *et al*., 2004. Regulation of lifespan in Drosophila by modulation of genes in the TOR signaling pathway. *Current biology : CB*, 14(10), pp.885-890.

Katzman, R., Terry, R. & DeTeresa, R., 1988. Clinical, pathological, and neurochemical changes in dementia: A subgroup with preserved mental status and numerous neocortical plaques. *Annals of Neurology*, 23(2), pp.138-144.

Kayed, R. *et al*., 2003. Common structure of soluble amyloid oligomers implies common mechanism of pathogenesis. *Science*, 300(5618), pp.486-489.

Kennington, W., 2001. *Drosoph Inf Serv*.

Kenyon, C. *et al*., 1993. A C. elegans mutant that lives twice as long as wild type. *Nature*, 366(6454), pp.461-464.

Kerr, F. *et al*., 2009. Dietary restriction delays aging, but not neuronal dysfunction, in Drosophila models of Alzheimer's disease. *Neurobiology of Aging*, 32 (2011), pp.1977–1989.

Killick, R. *et al*., 2009. Deletion of Irs2 reduces amyloid deposition and rescues behavioural deficits in APP transgenic mice. *Biochemical and biophysical research communications*, 386(1), pp.257-262.

Kinghorn, K.J. et al., 2006. Neuroserpin binds Abeta and is a neuroprotective component of amyloid plaques in Alzheimer disease. *The Journal of biological chemistry*, 281(39), pp.29268–29277.

Kirkwood, T.B.L. & Austad, S.N., 2000. Why do we age? *Nature*, 408(6809), pp.233-238.

Klass, M.R., 1983. A method for the isolation of longevity mutants in the nematode Caenorhabditis elegans and initial results. *Mechanisms of ageing and development*, 22(3-4), pp.279-286.

Koepsell, T.D. *et al*., 2007. Education, cognitive function, and severity of neuropathology in Alzheimer disease. *Neurology*, 70(Iss 19, Part 2), pp.1732-1739.

Koike, H. *et al*., 1999. Membrane-anchored metalloprotease MDC9 has an alpha-secretase activity responsible for processing the amyloid precursor protein. *The Biochemical journal*, 343 Pt 2, pp.371-375.

Kosik, K. & Joachim, C., 1986. Microtubule-associated protein tau (tau) is a major antigenic component of paired helical filaments in Alzheimer disease. *Proceedings of the National Academy of Sciences of the United States of America,* 83 (11), pp.4044-4048.

Lafay-Chebassier, C. *et al*., 2005. mTOR/p70S6k signalling alteration by Abeta exposure as well as in APP-PS1 transgenic models and in patients with Alzheimer's disease. *Journal of Neurochemistry*, 94(1), pp.215-225.

Lafay-Chebassier, C. *et al*., 2006. The immunosuppressant rapamycin exacerbates neurotoxicity of Abeta peptide. *Journal of neuroscience research*, 84(6), pp.1323-1334.

LaFerla, F.M. et al., 1995. The Alzheimer's A beta peptide induces neurodegeneration and apoptotic cell death in transgenic mice. *Nature genetics*, 9(1), pp.21-30.

Laferla, F.M., Green, K.N. & Oddo, S., 2007. Intracellular amyloid-beta in Alzheimer's disease. *Nature Reviews Neuroscience*, 8(7), pp.499-509.

Lambert, M.P. *et al*., 1998. Diffusible, nonfibrillar ligands derived from Abeta1-42 are potent central nervous system neurotoxins. *Proceedings of the National Academy of Sciences of the United States of America*, 95(11), pp.6448-6453.

Lammich, S. *et al*., 1999. Constitutive and regulated alpha-secretase cleavage of Alzheimer's amyloid precursor protein by a disintegrin metalloprotease. *Proceedings of the National Academy of Sciences of the United States of America*, 96(7), pp.3922-3927.

Latouche, M. *et al*., 2007. A Conditional Pan-Neuronal Drosophila Model of Spinocerebellar Ataxia 7 with a Reversible Adult Phenotype Suitable for Identifying Modifier Genes. *Journal of Neuroscience*, 27(10), pp.2483-2492.

Lesné, S., Kotilinek, L. & Ashe, K.H., 2008. Plaque-bearing mice with reduced levels of oligomeric amyloid-β assemblies have intact memory function. *Neuroscience*, 151(3), pp.745-749.

Lewis, J. *et al*., 2001. Enhanced neurofibrillary degeneration in transgenic mice expressing mutant tau and APP. *Science*, 293(5534), pp.1487-1491.

Li, X. *et al*., 2005. Levels of mTOR and its downstream targets 4E-BP1, eEF2, and eEF2 kinase in relationships with tau in Alzheimer's disease brain. *The FEBS journal*, 272(16), pp.4211-4220.

Ling, D. & Salvaterra, P.M., 2011. Brain aging and $A\beta_{1-42}$ neurotoxicity converge via deterioration in autophagy-lysosomal system: a conditional Drosophila model linking Alzheimer's neurodegeneration with aging. *Acta Neuropathologica*, 121(2), pp.183-191.

Link, C.D., 1995. Expression of human beta-amyloid peptide in transgenic Caenorhabditis elegans. *Proceedings of the National Academy of Sciences of the United States of America*, 92 (20), pp.9368-9372.

Link, C D, 2005. Invertebrate models of Alzheimer's disease. *Genes, Brain and Behavior*, 4(3), pp.147-156.

Link, C.D. *et al*., 2003. Gene expression analysis in a transgenic Caenorhabditis elegans Alzheimer's disease model. *Neurobiology of Aging*, 24(3), pp.397-413.

Lu, B. & Vogel, H., 2009. Drosophila models of neurodegenerative diseases. *Annual review of pathology*, 4, pp.315-342.

Lue, L.F. *et al*., 1999. Soluble amyloid beta peptide concentration as a predictor of synaptic change in Alzheimer's disease. *The American journal of pathology*, 155(3), pp.853-862.

Luheshi, L.M. *et al*., 2010. Sequestration of the Abeta peptide prevents toxicity and promotes degradation in vivo. *PLoS Biology*, 8(3), p.e1000334.

Luo, Y. *et al*., 2001. Mice deficient in BACE1, the Alzheimer's β-secretase, have normal phenotype and abolished β-amyloid generation. *Nature Neuroscience*, 4(3), pp.231-232.

Ma, T. et al., 2010. Dysregulation of the mTOR pathway mediates impairment of synaptic plasticity in a mouse model of Alzheimer's disease. *PLoS ONE*, 5(9).

Mair, W. & Dillin, A., 2008. Aging and survival: the genetics of life span extension by dietary restriction. *Annual review of biochemistry*, 77, pp.727-754.

Mair, W. *et al*., 2003. Demography of dietary restriction and death in Drosophila. *Science*, 301(5640), pp.1731-1733.

Martínez, D., 1998. Mortality Patterns Suggest Lack of Senescence in Hydra. *Experimental gerontology*, 33(3), pp.217-225.

Masters, C.L. *et al*., 1985. Amyloid plaque core protein in Alzheimer disease and

Down syndrome. *Proceedings of the National Academy of Sciences of the United States of America*, 82(12), pp.4245-4249.

Mattson, M.P., 2004. Pathways towards and away from Alzheimer's disease. *Nature*, 430(7000), pp.631–639.

Mattson, M.P. & Magnus, T., 2006. Ageing and neuronal vulnerability. *Nature reviews Neuroscience*, 7. pp.278-294.

Matsui, T. *et al*., 2007. Expression of APP pathway mRNAs and proteins in Alzheimer's disease. *Brain research*, 1161, pp.116-123.

McGowan, E., Eriksen, J. & Hutton, M., 2006. A decade of modeling Alzheimer's disease in transgenic mice. *Trends in genetics*, 22(5), pp.281-289.

McGowan, E. et al., 2005. Abeta42 is essential for parenchymal and vascular amyloid deposition in mice. *Neuron*, 47(2), pp.191-199.

McGuire, S.E., Mao, Z. & Davis, R.L., 2004. Spatiotemporal gene expression targeting with the TARGET and gene-switch systems in Drosophila. *Science's STKE : signal transduction knowledge environment*, 2004(220), p.pl6.

McGuire, S.E. *et al*., 2003. Spatiotemporal rescue of memory dysfunction in Drosophila. *Science*, 302(5651), pp.1765-1768.

Meyer-Luehmann, M. *et al*., 2008. Rapid appearance and local toxicity of amyloid-beta plaques in a mouse model of Alzheimer's disease. *Nature*, 451(7179), pp.720-724.

Meziane, H. *et al*., 1998. Memory-enhancing effects of secreted forms of the beta-amyloid precursor protein in normal and amnestic mice. *Proceedings of the National Academy of Sciences of the United States of America*, 95(21), pp.12683-12688.

Miller, B.C. *et al*., 2003. Amyloid-beta peptide levels in brain are inversely correlated with insulysin activity levels in vivo. *Proceedings of the National Academy of Sciences of the United States of America,* 100. pp.6221-6226.

Minati, L. *et al*., 2009. Reviews: Current Concepts in Alzheimer's Disease: A Multidisciplinary Review. *American Journal of Alzheimer's Disease and Other Dementias*, 24(2), pp.95-121.

Moloney, A.M. *et al*., 2010. Defects in IGF-1 receptor, insulin receptor and IRS-1/2 in Alzheimer's disease indicate possible resistance to IGF-1 and insulin signalling. *Neurobiology of Aging*, 31(2), pp.224-243.

Morley, J.F. *et al*., 2002. The threshold for polyglutamine-expansion protein aggregation and cellular toxicity is dynamic and influenced by aging in Caenorhabditis elegans. *Proceedings of the National Academy of Sciences of*

the United States of America, 99(16), pp.10417-10422.

Mott, R.T. & Hulette, C.M., 2005. Neuropathology of Alzheimer's Disease. *Neuroimaging clinics of North America*, 15(4), pp.755-765.

Mucke, L. *et al*., 2000. High-Level Neuronal Expression of Aβ1–42 in Wild-Type Human Amyloid Protein Precursor Transgenic Mice: Synaptotoxicity without Plaque Formation. *The Journal of Neuroscience*, 20(11), pp.4050-4058.

Mullan, M. *et al*., 1992. A pathogenic mutation for probable Alzheimer's disease in the APP gene at the N-terminus of beta-amyloid. *Nature genetics*, 1(5), pp.345-347.

Murakami, K. *et al*., 2002. Synthesis, aggregation, neurotoxicity, and secondary structure of various A beta 1-42 mutants of familial Alzheimer's disease at positions 21-23. *Biochemical and biophysical research communications*, 294(1), pp.5-10.

Näslund, J. *et al*., 2000. Correlation between elevated levels of amyloid beta-peptide in the brain and cognitive decline. *JAMA :The Journal of the American Medical Association*, 283(12), pp.1571-1577.

Niedzwiecki, A. & Fleming, J.E., 1990. Changes in protein turnover after heat shock are related to accumulation of abnormal proteins in aging Drosophila melanogaster. *Mechanisms of ageing and development*, 52(2-3), pp.295–304.

Nikolaev, A. *et al*., 2009. APP binds DR6 to trigger axon pruning and neuron death via distinct caspases. *Nature*, 457(7232), pp.981-989.

Nilsberth, C. *et al*., 2001. The 'Arctic‘ APP mutation (E693G) causes Alzheimer’s disease by enhanced Abeta protofibril formation. *Nature Neuroscience*, 4(9), pp.887-893.

Nixon, R., 2007. Autophagy, amyloidogenesis and Alzheimer disease. *Journal of Cell Science*.

Nordstedt, C. *et al*., 1993. Identification of the Alzheimer beta/A4 amyloid precursor protein in clathrin-coated vesicles purified from PC12 cells. *The Journal of biological chemistry*, 268(1), pp.608-612.

Nukina, N., 1986. One of the antigenic determinants of paired helical filaments is related to tau protein. *Journal of biochemistry*.

Oddo, S. *et al*., 2003. Triple-transgenic model of Alzheimer's disease with plaques and tangles: intracellular Abeta and synaptic dysfunction. *Neuron*, 39(3), pp.409-421.

Olson, M. & Shaw, C., 1969. Presenile Dementia and Alzheimers Disease in Mongolism. *Brain*, 92, pp.147-156.

Osterwalder, T. *et al*., 2001. A conditional tissue-specific transgene expression

system using inducible GAL4. *Proceedings of the National Academy of Sciences of the United States of America*, 98(22), pp.12596-12601.

Ownby, R.L. *et al*., 2006. Depression and risk for Alzheimer disease: systematic review, meta-analysis, and metaregression analysis. *Archives of general psychiatry*, 63(5), pp.530-538.

Partridge, Linda, 2010. The new biology of ageing. *Philosophical Transactions of the Royal Society B: Biological Sciences*, 365(1537), pp.147-154.

Partridge, Linda & Gems, D., 2006. Beyond the evolutionary theory of ageing, from functional genomics to evo-gero. *Trends in ecology & evolution (Personal edition)*, 21(6), pp.334-340.

Parvathy, S. *et al*., 1999. Cleavage of Alzheimer's amyloid precursor protein by alpha-secretase occurs at the surface of neuronal cells. *Biochemistry*, 38(30), pp.9728-9734.

Pasternak, S.H., Callahan, J.W. & Mahuran, D.J., 2004. The role of the endosomal/lysosomal system in amyloid-beta production and the pathophysiology of Alzheimer's disease: reexamining the spatial paradox from a lysosomal perspective. *Journal of Alzheimer's disease: JAD*, 6(1), pp.53-65.

Pimplikar, S.W., 2009. Reassessing the amyloid cascade hypothesis of Alzheimer's disease. *International Journal of Biochemistry & Cell Biology*, 41(6), pp.1261-1268.

Poirier, Luc *et al*., 2008. Characterization of the Drosophila gene-switch system in aging studies: a cautionary tale. *Aging Cell*, 7(5), pp.758-770.

Powers, R.W. *et al*., 2006. Extension of chronological life span in yeast by decreased TOR pathway signaling. *Genes & Development*, 20(2), pp.174-184.

Prasher, V.P. *et al*., 1998. Molecular mapping of Alzheimer-type dementia in Down's syndrome. *Annals of neurology*, 43(3), pp.380-383.

Priest, N. *et al*., 2002. The role of parental age effects on the evolution of aging. *Evolution*, 56(5), pp. 927-935.

Rattan, S., 1996. Synthesis, modifications and turnover of proteins druing aging. pp.1-15. *Experimental Gerontology*, 31(1), pp. 33-47.

Ravikumar, B. *et al*., 2004. Inhibition of mTOR induces autophagy and reduces toxicity of polyglutamine expansions in fly and mouse models of Huntington disease. *Nature genetics*, 36(6), pp.585-595.

Reiter, L.T. *et al*., 2001. A systematic analysis of human disease-associated gene sequences in Drosophila melanogaster. *Genome research*, 11(6), pp.1114-1125.

Rival, T. et al., 2009. Fenton chemistry and oxidative stress mediate the toxicity of the beta-amyloid peptide in a Drosophila model of Alzheimer's disease. *The European journal of neuroscience*, 29(7), pp.1335-1347.

Roberts, D.B., 1998. *Drosophila*, Oxford University Press, USA.

Roman, G. et al., 2001. P{Switch}, a system for spatial and temporal control of gene expression in Drosophila melanogaster. *Proceedings of the National Academy of Sciences of the United States of America*, 98(22), pp.12602-12607.

Rosen, D.R. *et al*., 1989. A Drosophila gene encoding a protein resembling the human beta-amyloid protein precursor. *Proceedings of the National Academy of Sciences of the United States of America*, 86(7), pp.2478-2482.

Rovelet-Lecrux, A. *et al*., 2006. APP locus duplication causes autosomal dominant early-ons*et Al*zheimer disease with cerebral amyloid angiopathy. *Nature genetics*, 38(1), pp.24-26.

Ryazanov, A.G. & Nefsky, B.S., 2002. Protein turnover plays a key role in aging. *Mechanisms of ageing and development*, 123(2-3), pp.207-213.

Santacruz, K. *et al*., 2005. Tau suppression in a neurodegenerative mouse model improves memory function. *Science*, 309(5733), pp.476-481.

Sarasa, M. & Pesini, P., 2009. Natural non-trasgenic animal models for research in Alzheimer's disease. *Current Alzheimer Research*, 6(2), pp.171-178.

Sarbassov, D.D. *et al*., 2006. Prolonged rapamycin treatment inhibits mTORC2 assembly and Akt/PKB. *Molecular cell*, 22(2), pp.159-168.

Selkoe, D J, 2001. Alzheimer's disease: genes, proteins, and therapy. *Physiological reviews*, 81(2), pp.741-766.

Selman, C. *et al*., 2009. Ribosomal protein S6 kinase 1 signaling regulates mammalian life span. *Science*, 326(5949), pp.140-144.

Seroude, L., 2002. GAL4 drivers expression in the whole adult fly. *Genesis*, 34(1-2), pp.34-38.

Seubert, P. *et al*., 1992. Isolation and quantification of soluble Alzheimer's β-peptide from biological fluids. *Nature*, 359, pp.325-327.

Sgrò, C.M. & Partridge, L, 2001. Laboratory adaptation of life history in Drosophila. *The American Naturalist*, 158(6), pp.657-658.

Shoji, M. *et al*., 1992. Production of the Alzheimer amyloid beta protein by normal proteolytic processing. *Science*, 258(5079), pp.126-129.

Skorokhod, A. *et al*., 1999. Origin of insulin receptor-like tyrosine kinases in marine sponges. *The Biological bulletin*, 197(2), pp.198-206.

Small, S.A. & Duff, K., 2008. Linking Abeta and tau in late-onset *Alz*heimer's disease: a dual pathway hypothesis. *Neuron*, 60(4), pp.534-542.

Sofola, O. *et al*., 2010. Inhibition of GSK-3 ameliorates Abeta pathology in an adult-onset Drosophila model of Alzheimer's disease. *PLoS genetics*, 6(9). p.e1001087,

Spilman, P. *et al*., 2010. Inhibition of mTOR by rapamycin abolishes cognitive deficits and reduces amyloid-beta levels in a mouse model of Alzheimer's disease. *PLoS ONE*, 5(4), p.e9979.

Stebbins, M., 2001. Adaptable doxycycline-regulated gene expression systems for Drosophila. *Gene*, 270(1-2), pp.103-111.

Steinkraus, K.A. *et al*., 2008. Dietary restriction suppresses proteotoxicity and enhances longevity by an hsf-1-dependent mechanism in Caenorhabditis elegans. *Aging Cell*, 7(3), pp.394-404.

Suzuki, N. *et al*., 1994. An increased percentage of long amyloid beta protein secreted by familial amyloid beta protein precursor (beta APP717) mutants. *Science*, 264(5163), pp.1336-1340.

Tagliavini, F. *et al*., 1988. Preamyloid deposits in the cerebral cortex of patients with Alzheimer's disease and nondemented individuals. *Neuroscience letters*, 93(2-3), pp.191-196.

Takahashi, R.H. *et al*., 2004. Oligomerization of Alzheimer's beta-amyloid within processes and synapses of cultured neurons and brain. *Journal of Neuroscience*, 24(14), pp.3592-3599.

Tamaoka, A. *et al*., 1994. APP717 missense mutation affects the ratio of amyloid beta protein species (Abeta 1-42/43 and abeta 1-40) in familial Alzheimer's disease brain. *The Journal of biological chemistry*, 269(52), pp.32721-32724.

Tanzi, R.E. *et al*., 1987. Amyloid beta protein gene: cDNA, mRNA distribution, and genetic linkage near the Alzheimer locus. *Science*, 235(4791), pp.880-884.

Tatar, M. *et al*., 2001. A mutant Drosophila insulin receptor homolog that extends life-span and impairs neuroendocrine function. *Science*, 292(5514), pp.107-110.

Terry, R.D. *et al*., 1991. Physical basis of cognitive alterations in Alzheimer's disease: synapse loss is the major correlate of cognitive impairment. *Annals of neurology*, 30(4), pp.572-580.

Tokuda, T. *et al*., 1997. Plasma levels of amyloid beta proteins Abeta1-40 and Abeta1-42(43) are elevated in Down's syndrome. *Annals of neurology*, 41(2), pp.271-273.

Torroja, L., Chu, H., *et al*., 1999a. Neuronal overexpression of APPL, the

Drosophila homologue of the amyloid precursor protein (APP), disrupts axonal transport. *Current biology,* 9(9), pp.489-492.

Torroja, L., Packard, M., *et al*., 1999b. The Drosophila beta-amyloid precursor protein homolog promotes synapse differentiation at the neuromuscular junction. *Journal of Neuroscience*, 19(18), pp.7793-7803.

Trevitt, S. & Partridge, L., 1991. A cost of receiving sperm in the female fruitfly Drosophila melanogaster. *Journal of Insect Physiology*, 37(6), pp.471–475.

Tucker, S.M.F., Borchelt, D.R. & Troncoso, J.C., 2008. Limited clearance of pre-existing amyloid plaques after intracerebral injection of Abeta antibodies in two mouse models of Alzheimer disease. *Journal of neuropathology and experimental neurology*, 67(1), pp.30-40.

Vassar, R. *et al*., 1999. Beta-secretase cleavage of Alzheimer's amyloid precursor protein by the transmembrane aspartic protease BACE. *Science*, 286(5440), pp.735-741.

Vellai, T. *et al*., 2003. Genetics: influence of TOR kinase on lifespan in C. elegans. *Nature*, 426(6967), p.620.

Vézina, C., Kudelski, A. & Sehgal, S.N., 1975. Rapamycin (AY-22,989), a new antifungal antibiotic. I. Taxonomy of the producing streptomycete and isolation of the active principle. *The Journal of antibiotics*, 28(10), pp.721-726.

Walsh, D.M. & Selkoe, Dennis J, 2007. A beta oligomers - a decade of discovery. *Journal of Neurochemistry*, 101(5), pp.1172-1184.

Wang, J. *et al*., 1999. The levels of soluble versus insoluble brain Abeta distinguish Alzheimer's disease from normal and pathologic aging. *Experimental Neurology*, 158(2), pp.328-337.

Webster, G.C. & Webster, S.L., 1979. Decreased protein synthesis by microsomes from aging Drosophila melanogaster. *Experimental gerontology*, 14(6), pp.343-348.

Webster, G.C., Beachell, V.T. & Webster, S.L., 1980. Differential decrease in protein synthesis by microsomes from aging Drosophila melanogaster. *Experimental gerontology*, 15(5), pp.495-497.

Wentzell, J. & Kretzschmar, D., 2010. Alzheimer's Disease and tauopathy studies in flies and worms. *Neurobiology of Disease*, 40(1), pp.21-28.

Wessells, R.J. *et al*., 2004. Insulin regulation of heart function in aging fruit flies. *Nature genetics*, 36(12), pp.1275-1281.

Westerman, M. *et al*., 2002. The relationship between Abeta and memory in the Tg2576 mouse model of Alzheimer's disease. *Journal of Neuroscience*, 22(5), p.1858.

Wolfe, M.S. *et al*., 1999. Two transmembrane aspartates in presenilin-1 required for presenilin endoproteolysis and γ-secretase activity. *Nature*, 398(6727), pp.513-517.

Wong, R. *et al*., 2009. Quantification of food intake in Drosophila. *PLoS ONE*, 4(6), p.e6063.

Wullschleger, S., Loewith, R. & Hall, M.N., 2006. TOR signaling in growth and metabolism. *Cell*, 124(3), pp.471-484.

Yankner, B.A., Duffy, L.K. & Kirschner, D.A., 1990. Neurotrophic and neurotoxic effects of amyloid beta protein: reversal by tachykinin neuropeptides. *Science*, 250(4978), pp.279-282.

Zhang, S. *et al*., 2010. Rapamycin promotes beta-amyloid production via ADAM-10 inhibition. *Biochemical and biophysical research communications*, 398(3), pp.337-341.

Zheng, H. *et al*., 1995. Beta-Amyloid precursor protein-deficient mice show reactive gliosis and decreased locomotor activity. *Cell*, 81(4), pp.525-531.

Appendix

Sofola, O., Kerr, F., Rogers, I., 2010. Inhibition of GSK-3 ameliorates Abeta pathology in an adult-onset Drosophila model of Alzheimer's disease. *PLoS genetics*, 6(9).

OPEN ACCESS Freely available online

PLoS GENETICS

Inhibition of GSK-3 Ameliorates Aβ Pathology in an Adult-Onset *Drosophila* Model of Alzheimer's Disease

Oyinkan Sofola[1☯], Fiona Kerr[1,2☯], Iain Rogers[1☯], Richard Killick[3], Hrvoje Augustin[1], Carina Gandy[1,2], Marcus J. Allen[4], John Hardy[5], Simon Lovestone[3], Linda Partridge[1,2]*

1 Institute of Healthy Ageing and Research Department of Genetics, Evolution, and Environment, University College London, London, United Kingdom, **2** Max Planck Institute for Biology of Ageing, Köln, Germany, **3** Institute of Psychiatry, King's College London, London, United Kingdom, **4** School of Biosciences, University of Kent, Canterbury, United Kingdom, **5** Institute of Neurology, University College London, London, United Kingdom

Abstract

Aβ peptide accumulation is thought to be the primary event in the pathogenesis of Alzheimer's disease (AD), with downstream neurotoxic effects including the hyperphosphorylation of tau protein. Glycogen synthase kinase-3 (GSK-3) is increasingly implicated as playing a pivotal role in this amyloid cascade. We have developed an adult-onset *Drosophila* model of AD, using an inducible gene expression system to express Arctic mutant Aβ42 specifically in adult neurons, to avoid developmental effects. Aβ42 accumulated with age in these flies and they displayed increased mortality together with progressive neuronal dysfunction, but in the apparent absence of neuronal loss. This fly model can thus be used to examine the role of events during adulthood and early AD aetiology. Expression of Aβ42 in adult neurons increased GSK-3 activity, and inhibition of GSK-3 (either genetically or pharmacologically by lithium treatment) rescued Aβ42 toxicity. Aβ42 pathogenesis was also reduced by removal of endogenous fly tau; but, within the limits of detection of available methods, tau phosphorylation did not appear to be altered in flies expressing Aβ42. The GSK-3–mediated effects on Aβ42 toxicity appear to be at least in part mediated by tau-independent mechanisms, because the protective effect of lithium alone was greater than that of the removal of tau alone. Finally, Aβ42 levels were reduced upon GSK-3 inhibition, pointing to a direct role of GSK-3 in the regulation of Aβ42 peptide level, in the absence of APP processing. Our study points to the need both to identify the mechanisms by which GSK-3 modulates Aβ42 levels in the fly and to determine if similar mechanisms are present in mammals, and it supports the potential therapeutic use of GSK-3 inhibitors in AD.

Citation: Sofola O, Kerr F, Rogers I, Killick R, Augustin H, et al. (2010) Inhibition of GSK-3 Ameliorates Aβ Pathology in an Adult-Onset *Drosophila* Model of Alzheimer's Disease. PLoS Genet 6(9): e1001087. doi:10.1371/journal.pgen.1001087

Editor: Bingwei Lu, Stanford University School of Medicine, United States of America

Received August 5, 2009; **Accepted** July 23, 2010; **Published** September 2, 2010

Funding: Alzheimer's Society, the European Commission, Wellcome Trust, Eisai London Research Laboratories (UK), and the Max Planck Institute for the Biology of Ageing. The funders had no role in study design, data collection and analysis, decision to publish, or preparation of the manuscript.

Competing Interests: The authors have declared that no competing interests exist.

* E-mail: l.partridge@ucl.ac.uk

☯ These authors contributed equally to this work.

Introduction

Alzheimer's disease (AD) is the leading cause of dementia in the ageing population. Symptoms include, but are not limited to, memory loss, cognitive decline, and deterioration of language skills. The pathological hallmarks of AD are the presence of plaques and neurofibrillary tangles [1]. The tangles are composed of hyperphosphorylated tau protein while the plaques are comprised of amyloid beta (Aβ) peptides, various species of which are derived from the amyloid precursor protein (APP), the most abundant being Aβ40 and Aβ42 [2]. AD-causing mutations either increase the level of Aβ42 or the ratio of Aβ42/Aβ40, indicating that this is the more toxic form of the peptide [2].

The leading candidate explanation for the molecular basis of AD pathology is the amyloid cascade hypothesis. This states that the Aβ protein initiates the disease process, activating downstream neurotoxic mechanisms including the dysregulation of tau. Perhaps the strongest support for the amyloid cascade hypothesis is that all of the mutations implicated in early-onset, familial AD, such as the Aβ Arctic mutation, increase the aggregation or production of Aβ [1]. Although tau mutations exist, none have been linked to familial AD, but rather to fronto-temporal dementia, in which Aβ plaques are absent [3,4]. The amyloid cascade has also been tested experimentally in various ways. For example, a double transgenic mouse model expressing APP-V7171 and Tau-P301L, develops amyloid pathology similarly to mice transgenic for APP-V7171 alone, whereas tauopathy is dramatically enhanced in the double transgenic compared to mice transgenic for Tau-P301L alone. This implies that Aβ pathology affects tauopathy but not *vice versa* [5]. Also, clearance of Aβ using Aβ-specific antibodies reduced early tau burden, while elevating tau burden in transgenic mice had no effect on Aβ accumulation [6,7]. Furthermore, a reduction in tau levels rescued learning and memory impairment induced by Aβ in a mouse model expressing human APP [8].

Aβ increases the phosphorylation of tau protein and concomitantly activates glycogen synthase kinase, GSK-3 [9,10]. GSK-3 is a multi-functional kinase involved in regulating various cellular processes, including growth and differentiation [9,11]. There are two isoforms of the protein, GSK-3α and GSK-3β. They share 98% identity within their kinase domain, but are not functionally identical, although both have been suggested to be involved in AD

Author Summary

Alzheimer's disease (AD) is the leading cause of dementia in the ageing population. Symptoms include memory loss and decline in understanding and reasoning. Alois Alzheimer, who reported the first case of AD, observed plaques and tangles in the brains of patients. The plaques are made up of amyloid protein, while the tangles are of tau protein. One of the main scientific ideas about AD is that it starts with build-up of amyloid, which then alters tau protein, causing the disease. Another protein, called GSK-3, also seems to play a part. Simple invertebrates such as flies are useful for understanding human diseases. We have created an AD model in the fruit fly *Drosophila* where amyloid protein is present in the nerve cells of the adult fly; this caused the flies to be impaired in their survival, nerve function, and behavior. We found that amyloid increased the activity of GSK-3, and so we experimentally turned down its activity and found that this improved the survival and behavior of the flies. Importantly, turning down the activity of GSK-3 in flies that did not have amyloid did not seem to harm them. GSK-3 could therefore be a good target for drugs against AD.

pathogenesis [11]. GSK-3α has been implicated in the amyloidogenic processing of APP to yield Aβ peptides [12], while GSK-3β has been implicated in the tau-related pathogenesis of AD, by colocalizing with tau tangles and phosphorylating tau [9]. As yet, the exact role of GSK-3 in the generation of Aβ peptides is not known. GSK-3 itself is also regulated by phosphorylation. Phosphorylation at Ser9 of GSK-3β and the equivalent Ser21 of GSK-3α inhibits activity, while phosphorylation at Tyr216/Tyr279 of GSK-3β and GSK-3α, respectively, is thought to increase activity [13].

Remarkable similarities are seen between double transgenic mice expressing tau either with APP or with GSK-3β. This finding is consistent with the hypothesis that amyloid acts via activation of GSK-3 to modulate tau function [5,9,14]. Lithium chloride, which is used as a mood stabilizing agent in patients with bipolar disorders, inhibits GSK-3 activity, either by competing with magnesium ions [15] or by increasing Ser9 phosphorylation [16]. Lithium reduces amyloid production by altering the role of GSK-3α in APP processing/cleavage; selective inhibition of GSK-3 by siRNA or expressing a dominant negative form of GSK-3 also decreases Aβ production in cultured cells and mice [12,17]. Furthermore, lithium reduces both tau phosphorylation at several GSK-3 epitopes and tauopathy in a mouse model expressing mutant human tau [12,18]. However, in another study, lithium was seen to reduce tau phosphorylation but not to affect Aβ load in a triple mutant mouse expressing human APP_{swe}, human tau_{P301L} and with mutant presenilin 1 $PS1_{M146V}$ knock-in. The differing observations might be due to variations in the age at which the mice were treated with lithium, as suggested by the authors [19].

Fruit flies, *Drosophila melanogaster*, can provide useful invertebrate models of neurodegeneration because of their complex brains, short lifespans and relative ease of genetic manipulation. Several fly models of aspects of AD biology have been made, including ones that over-express either *Drosophila* or human tau, and show neuronal dysfunction phenotypes [20–22]. Co-expression of human tau protein with Shaggy (Sgg), the *Drosophila* homologue of GSK-3 [23], exacerbates these neurotoxic phenotypes and leads to the appearance of neurofibrillary tangles [22,24,25]. Fly models expressing Aβ peptides have also been generated, and show neurodegeneration and amyloid deposits [26,28]. Although an APP orthologue exists in flies, the Aβ sequence is not conserved, and *Drosophila* models directly expressing Aβ allow study of Aβ toxicity in the absence of any endogenous amyloid production [29].

In this study we have generated a fly model that expresses Arctic mutant Aβ42 peptide in the nervous system of adult flies, using an inducible system for gene expression, because we wished to understand the underlying mechanism of disease progression of AD in adults, without complications from developmental effects. We first characterised this model, and then used it to investigate the amyloid cascade hypothesis, by modulating the levels of endogenous fly tau and examining the effects on phenotypes consequent upon expression of Aβ. We also investigated the requirement for GSK-3 in Aβ pathology and its role in direct regulation of Aβ peptides.

Results

Arctic Aβ42 expression can be induced in adult *Drosophila* neurons

To generate an adult-onset fly model of Alzheimer's disease, we expressed Arctic mutant Aβ42 peptides using an inducible pan-neuronal driver. An elav GeneSwitch (elavGS) driver line [30–31] that has been used previously to develop an adult-onset *Drosophila* model of spinocerebellar ataxia (SCA) [32] was used to direct expression of a UAS-Arctic Aβ42 transgene [33] both spatially and temporally, to neurons of the adult fly (Figure 1A). A UAS-Aβ40 line [33] was used as a control for over-expression of non-toxic forms of Aβ in fly neurons, since this form of the peptide has previously been shown to have no detrimental effect in flies [26–28].

We measured expression of Aβ peptides in adult neurons when we treated elavGS;UAS-Arctic Aβ42 flies with the activator mifepristone (RU486;RU) from two days post-eclosion, by measuring RNA and protein levels at 4 and 21 days into treatment (Figure 1B and 1C). Aβ transcripts were clearly elevated in RU-treated elavGS;UAS-Arctic Aβ42 flies in comparison with untreated (−RU) flies at both time-points (Figure 1B). Moreover, an Aβ42-specific ELISA confirmed that Aβ42 protein was elevated in elavGS;UAS-Arctic Aβ42 (+RU) flies compared to untreated (−RU) flies and that the level of protein increased with age (Figure 1C). Since RNA transcript level decreased with age, this age-dependent accumulation of Aβ42 protein is most likely to be attributable to an increased rate of translation of the protein relative to the rate of protein degradation.

Aggregation of Aβ has been shown to be of critical importance for its pathogenicity [34]. Therefore, we assessed the state of aggregation of Aβ42 in the mutant flies by separating soluble and insoluble protein fractions from fly brain extracts. At day 15, when the first signs of pathology were observed in the Arctic Aβ42 flies (see below), we found that most of the Aβ42 protein had accumulated into an insoluble, fibrillar form (Figure 2), consistent with the aggregation-promoting effects of the Arctic mutation [35].

Overall these results confirm that the elavGS-UAS system used in this study is sufficient to induce over-expression of Aβ peptides specifically in the adult fly nervous system, and that Arctic mutant Aβ42 protein accumulates with age.

Over-expression of Arctic Aβ42 peptide in adult neurons increases mortality and induces neuronal dysfunction in *Drosophila*, without evidence of neuronal cell loss

Previously published studies have shown that constitutive expression of Arctic Aβ42 peptide in fly neurons significantly shortens lifespan, induces behavioural impairments and causes neuronal death [26–28]. To determine whether adult-onset expression of Arctic Aβ42 peptide in neurons causes similar

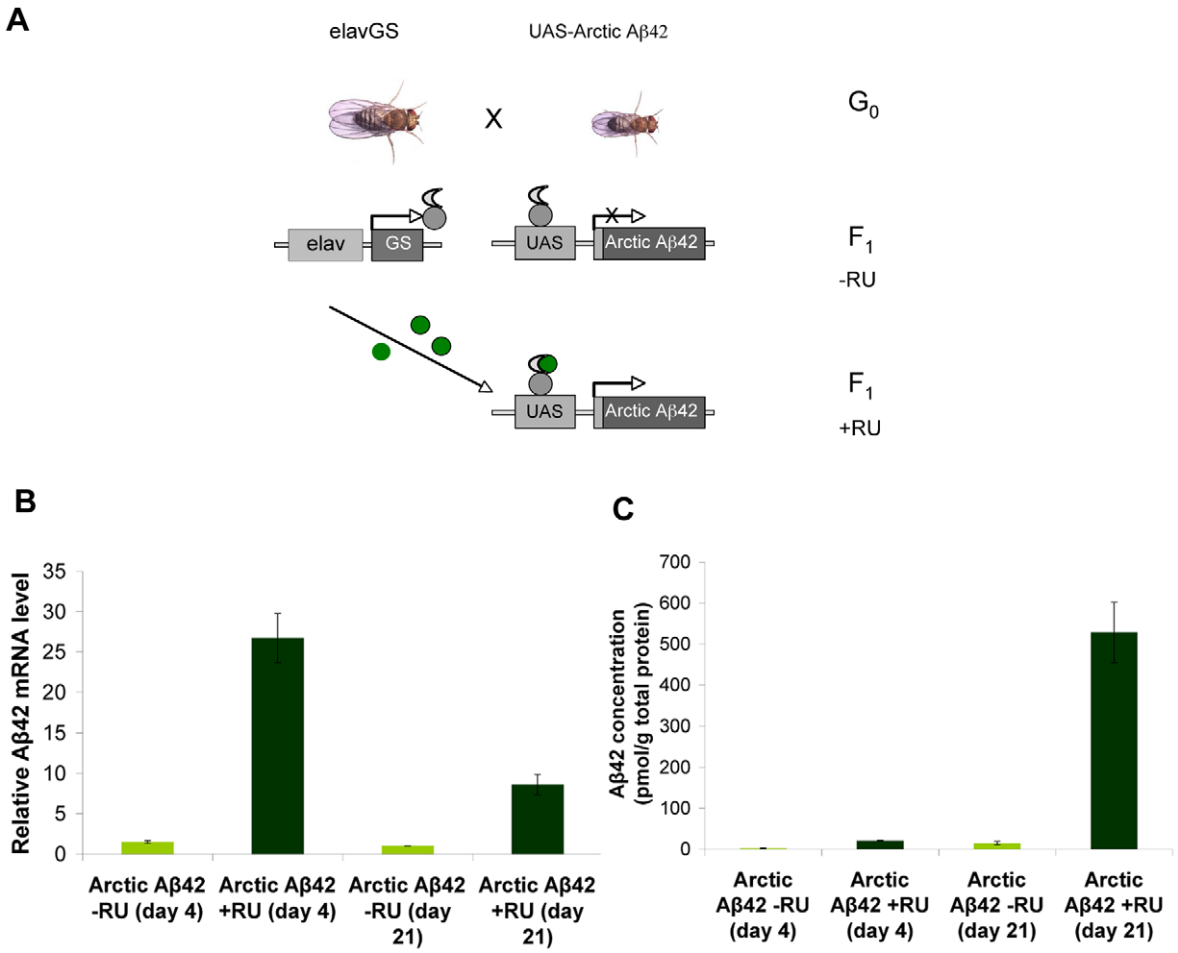

Figure 1. Adult-onset induction of Arctic Aβ42 peptide in the *Drosophila* nervous system. (A) A schematic representation of the GeneSwitch-UAS expression system (based on [30]). Driver lines expressing the transcriptional activator GeneSwitch under control of the nervous system-specific elav promoter (elavGS) are crossed to flies expressing an Aβ transgene fused to a GAL4-binding upstream activation sequence (UAS-Aβ). In the absence of the activator mifepristone (RU486; −RU), the GeneSwitch protein is expressed in neurons but remains transcriptionally silent, so that Aβ is not expressed. Following treatment with RU486 (+RU; green) the GeneSwitch protein is transcriptionally activated, binds to UAS and thus mediates expression of Aβ peptide specifically in the fly nervous system. Aβ42 RNA (B) and protein (C) levels were quantified at four days and 21 days post-RU486 treatment (see Materials and Methods). Data are presented as means ± SEM and were analysed by two-way ANOVA and Tukey's honestly significant difference (HSD) post-hoc comparisons. $P<0.05$ comparing Aβ RNA expression in RU486-treated UAS-ArcAβ42/+;elavGS/+ flies to their −RU486 controls at both time-points (Tukey's HSD). $P<0.01$ comparing Aβ42 protein levels in RU486-treated UAS-ArcAβ42/+;elavGS/+ flies to untreated controls at both time-points.
doi:10.1371/journal.pgen.1001087.g001

phenotypes, we examined survival, neuronal and behavioural dysfunction in our inducible *Drosophila* model of AD.

First, we measured the effects of Arctic Aβ42 expression on lifespan, by treating elavGS;UAS-Arctic Aβ42 and elavGS;UAS-Aβ40 flies with RU from two days post-eclosion and recording their survival. Expression of Arctic Aβ42 in adult neurons shortened median lifespan by about 50% and maximum lifespan by about 45% in comparison to non-RU-treated flies, and to Aβ40 +RU and −RU control flies (Figure 3), demonstrating a specific lifespan-shortening effect of Arctic Aβ42 compared to the Aβ40 form of the peptide.

Next, we determined whether adult-onset expression of Arctic Aβ42 peptide in fly neurons caused neuronal toxicity, by analysing neuronal function. As a direct measure of physiological activity, we examined the electrophysiological responses of the *Drosophila* giant fibre system (GFS; Figure 4A). Adult elavGS;UAS-Arctic Aβ42 flies were fed + or − RU486 media from two days post-eclosion, and GFS activity measured at day 16 and day 28 into treatment. Giant fibres (GF) were stimulated via electrodes inserted inside the compound eye, and post-synaptic potentials recorded in the tergotrochanteral muscle (TTM) and the dorsal longitudinal flight muscle (DLM) (Figure 4A); parameters measured were the latency from GF stimulation to muscle response and the stability of the response to high frequency stimulation. At day 16, response latencies in the TTM, DLM and the TTM to high frequency stimulation were comparable between elavGS;UAS-Arctic Aβ42 flies on + and − RU486 food (Figure 4B and Figure S1). However, at day 28, expression of Arctic Aβ42 peptide significantly increased the response latency measured in both the TTM and DLM, and inhibited the stability of the TTM response to high frequency stimulation (at 100, 200 and 250 Hz) in comparison to untreated control flies (Figure 4C and Figure S1). This indicates a progressive neuronal dysfunction following adult-onset induction of Arctic Aβ42, with young flies exhibiting no dysfunction in the GFS, while older flies showed obvious defects in response to both a single stimulus and to high frequency stimuli.

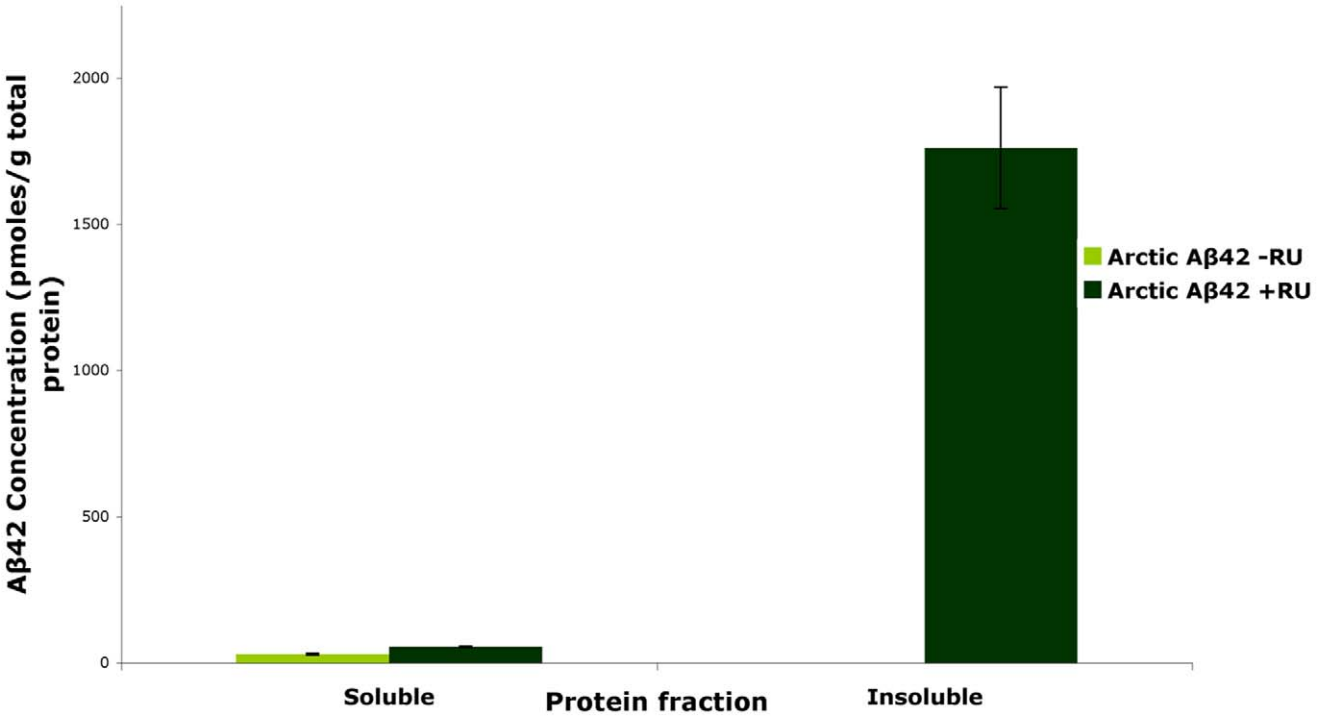

Figure 2. Arctic Aβ42 peptide in the adult *Drosophila* nervous system is mostly in an insoluble fibrillar state. In the absence of the activator mifepristone (RU486; −RU), a negligible amount of soluble protein is observed at day 15. Following treatment with RU486 (+RU; dark green) the Aβ peptide expression is seen in both soluble and insoluble fractions with a significant proportion observed in the insoluble fraction. Data are presented as means ± SEM and were analysed by ANOVA, $P<0.01$ when protein levels of soluble and insoluble fractions of Aβ42 expressing flies were compared.
doi:10.1371/journal.pgen.1001087.g002

As a behavioural measure of neuronal dysfunction in our inducible model, locomotor activity was assessed using a negative geotaxis (climbing) assay that has been used extensively to characterise fly models of neurodegenerative diseases [33,36]. *Drosophila* display an age-related decline in climbing behaviour, and this was apparent in the non-RU-treated and elavGS;UAS-Aβ40 +RU control flies used in the current study (Figure 5). We found that flies expressing Arctic Aβ42 displayed a reduced negative geotaxis in comparison to their −RU control flies and the Aβ40 +RU and −RU flies (Figure 5). The climbing behaviour of the Arctic Aβ42 flies had declined to a level by day 15 that was reached by the control flies only by day 28.

Finally, we quantified neuronal loss, as measured by the number of cell bodies in one hemisphere, in flies over-expressing Arctic Aβ42 peptide in adult neurons compared to non-expressing controls. No neuronal loss was evident in the brains of these flies (Figure S2).

Collectively, these data demonstrate that expression of Arctic Aβ42 specifically in the neurons of the adult fly leads to early death and progressive neuronal dysfunction, in the apparent absence of neuronal loss. Hence we have successfully developed an inducible *Drosophila* model of AD that will provide a useful system in which to further investigate the potential mechanisms underlying pathogenesis in Alzheimer's disease, without any confounding effects on neuronal development.

Adult-onset expression of Aβ42 increases the activity of Shaggy in the adult nervous system

Because of the described role of GSK-3 in Alzheimer's disease, we investigated the activity of the fly orthologue of GSK-3, Sgg, in the Aβ42-expressing flies. Phosphorylation at Ser9 of Sgg is important in suppressing its kinase activity. We found that expression of Arctic Aβ42 in the adult nervous system decreased the Ser9 phosphorylation level of Sgg, indicating an up-regulation of the activity of the kinase (see Figure 6). This increase in Sgg activity could have contributed to the toxicity we observed in our Aβ42 expressing flies. Lithium is a GSK-3 inhibitor, and we therefore tested its effect on Ser9 phosphorylation in the Aβ42 flies and, indeed, we found an increase in Ser9 phosphorylation compared to untreated controls (Figure 6).

Inhibition of Shaggy activity in the adult nervous system suppresses the toxicity of Arctic Aβ42

We next investigated if the increase in Sgg activity that we observed in the Artic Aβ42-expressing flies contributed to Aβ42 toxicity. To do this, we co-expressed in adult neurons a dominant negative form of Sgg, the S9E mutant, which mimics an inhibited state of the kinase [37,38] and renders it inactive. Expression of this dominant-negative Sgg increased the median and maximum lifespan of flies expressing Arctic Aβ42. Flies co-expressing Arctic Aβ42 and the dominant negative mutant S9E lived significantly longer than control flies co-expressing Arctic Aβ42 and GFP (Figure 7), to control for any titration effect of GAL4 in the presence of a second UAS-transgene. Furthermore, inactivation of Sgg, either by expressing the dominant negative mutant S9E or feeding the flies lithium in adulthood, significantly suppressed the climbing deficit of the Arctic Aβ42-expressing flies (Figure 8). Two different doses of lithium (30mM and 100mM) both rescued the climbing deficit of the Aβ42-expressing flies. These data demonstrate that inhibiting the activity of Sgg in neurons in adults suppresses the adult onset Arctic Aβ42 induced toxicity, and demonstrate experimentally a functional role of GSK-3 in mediating Aβ42 toxicity.

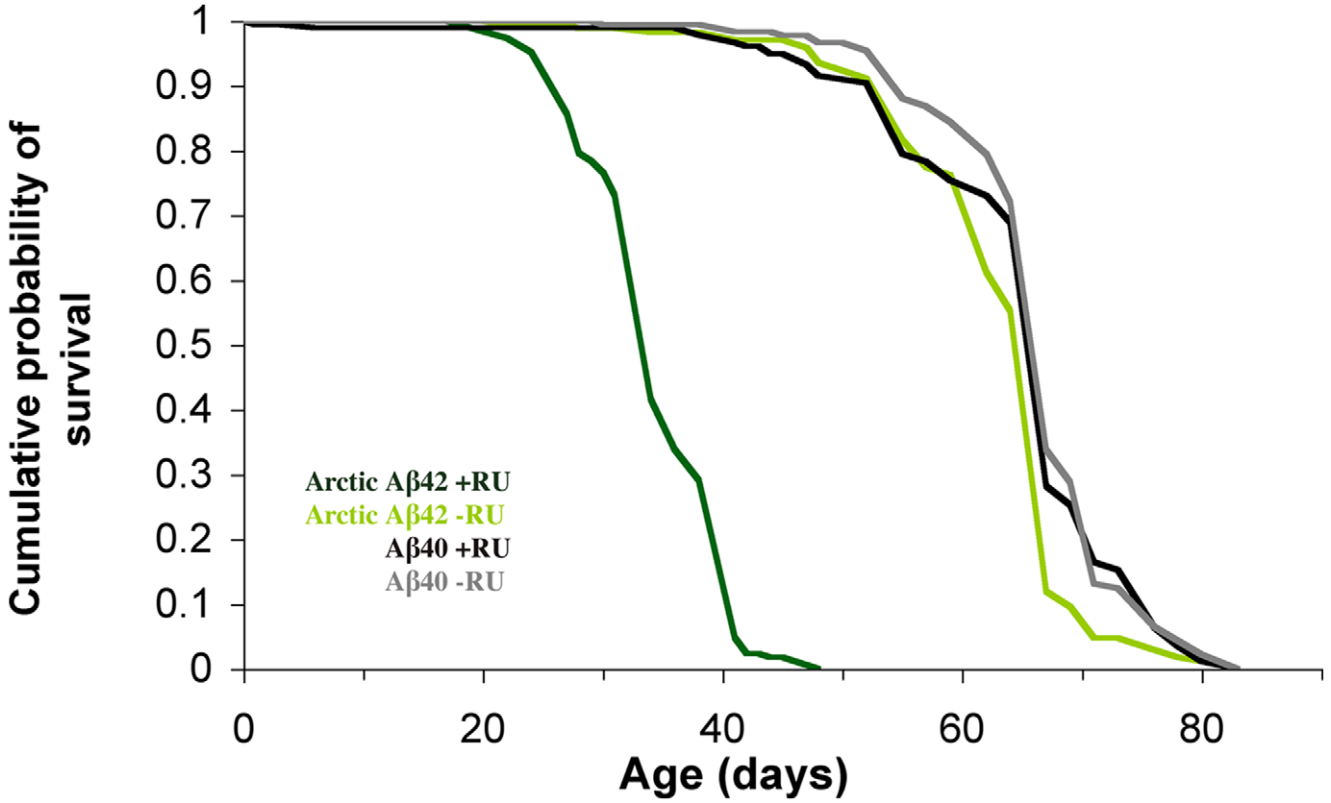

Figure 3. Expression of Arctic Aβ42 specifically in the adult nervous system shortens lifespan. Lifespans were determined as described in materials & methods. Survival curves are depicted and data were compared using the log-rank test. $P<0.01$ comparing median lifespan of UAS-ArcAβ42/+;elavGS/+ +RU flies to their −RU controls. $P<0.01$ comparing UAS-ArcAβ42/+;elavGS/+ +RU flies to UAS-Aβ40/+;elavGS/+ +RU controls. Induction of Aβ40 in the adult nervous system did not alter lifespan in comparison to non-RU486-treated controls.
doi:10.1371/journal.pgen.1001087.g003

Arctic Aβ42 toxicity, and protection by Shaggy inhibition, is not mediated predominantly through alterations in tau phosphorylation

Since GSK-3 is a well-established tau kinase, and tau is abnormally phosphorylated in AD, we next investigated whether the protective effect of Sgg inhibition on Aβ42 toxicity in our fly model is mediated via alterations in tau phosphorylation. Hence, we examined the phosphorylation of *Drosophila* tau in flies over-expressing Arctic Aβ42 peptide in the absence or presence of lithium-treatment (Figure 9).

We analysed tau phosphorylation using Phos-tag acrylamide gels, a technique for separating phosphorylated protein isoforms [39], which has been employed previously to investigate the phosphorylation of fly proteins [40]. Phos-tag is a phosphate-binding compound which, when incorporated into polyacrylamide gels, can result in an exaggerated mobility shift for phosphorylated proteins, dependent on the degree of phosphorylation. When heat-stable fly head homogenates were run on Phos-tag gels, several prominent tau bands were detected, implying that endogenous tau is phosphorylated at multiple sites in WT tissue (Figure 9A). De-phosphorylation using λ-protein phosphatase confirmed that the high molecular weight bands were due to tau phosphorylation, and that non-phosphorylated fly tau runs as a doublet (Figure 9A). This method is thus capable of detecting at least some phosphorylation changes on the endogenous fly tau. Using this method, no difference in the level of tau phosphorylation was observed in flies over-expressing Arctic Aβ42 compared to non-expressing controls or to Arctic Aβ42 flies treated with lithium chloride (Figure 9A and Figure S3A).

The phosphorylation sites on fly tau have not yet been extensively characterized. *Drosophila*-specific phosphorylation-dependent antibodies are hence not available for the examination of specific sites. However, several GSK-3 specific sites [41,42], and sites reported to be altered by Aβ42 peptide [43–45], on human tau appear to be conserved in the *Drosophila* tau sequence (Figure S4). Of these, Ser262, and Ser356 phosphorylation-dependent human tau antibodies were found to detect fly tau protein specifically (Figure 9B and Figure S3B). We therefore used these antibodies to examine the effects on tau phosphorylation at these sites. Arctic Aβ42 over-expression, or treatment of Aβ42-expressing flies with lithium, did not modify phosphorylation at the Ser262 or Ser356 homologous tau epitopes (Figure 9B). This suggests that neither Aβ42 nor GSK-3 are predominant *in vivo* regulators of the phosphorylation of these sites on fly tau.

Loss of Tau reduces adult-onset Aβ42 toxicity

Although we could not uncover a role for tau phosphorylation in Aβ42 toxicity, we investigated whether the presence of tau modulates Aβ42 pathology. We found that loss of tau reduced the Arctic Aβ42 climbing dysfunction. UAS-ArcAβ42/+;elavGS tau EP3203/tau deficiency (dfc) flies, which express Arctic Aβ42 in a genetic background homozygous mutant for tau (see Figure 10A for tau expression levels; tau antibody has previously been described [46]), had improved locomotor ability compared to UAS-ArcAβ42/+;elavGS tau EP2303/TM6 flies, which express a much greater level of tau ($P<0.0001$, two-way ANOVA; Figure 10A) and UAS-ArcAβ42/+;elavGS/+ flies, which express

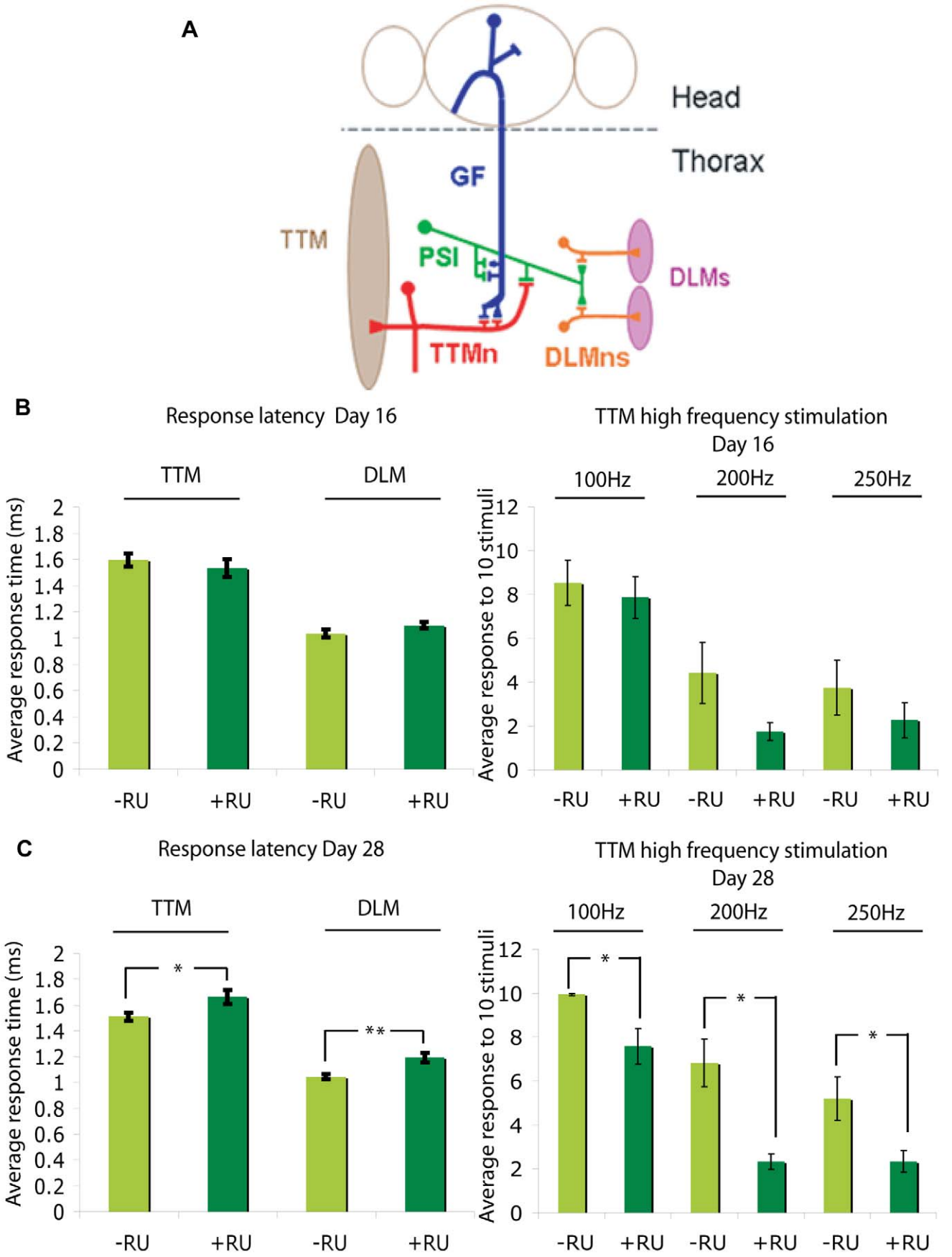
A
Head
Thorax
GF
TTM
PSI
DLMs
TTMn
DLMns
B
Response latency Day 16
TTM
DLM
Average response time (ms)
2
1.8
1.6
1.4
1.2
1
0.8
0.6
0.4
0.2
0
-RU
+RU
-RU
+RU
TTM high frequency stimulation
Day 16
100Hz
200Hz
250Hz
Average response to 10 stimuli
12
10
8
6
4
2
0
-RU
+RU
-RU
+RU
-RU
+RU
C
Response latency Day 28
TTM
DLM
Average response time (ms)
*
**
-RU
+RU
-RU
+RU
TTM high frequency stimulation
Day 28
100Hz
200Hz
250Hz
Average response to 10 stimuli
*
*
*
-RU
+RU
-RU
+RU
-RU
+RU

Figure 4. Arctic Aβ42 peptides induce progressive, adult-onset neuronal defects in *Drosophila*. (A) A schematic illustration of the *Drosophila* giant fibre system (GFS; adapted from [74]). Giant fibres (GFs; blue) relay signals from the brain to the thoracic musculature via mixed electrochemical synapses with the motorneurons (TTMn, red) of the tergotrancheral muscle (TTM; left), and the peripherally synapsing interneuron (PSI; green), which subsequently forms chemical synapses with the motorneurons (DLMn; orange) of the dorsal longitudinal muscles (DLM; right). Note only one of the TTMn axons is shown exiting the nervous system and contacting the muscle on the left hand side and one set of the DLMns and corresponding neuromuscular junctions are depicted on the right hand side. GFS activity was measured in UAS-ArcAβ42;elavGS flies at (B) 16 days and (C) 28 days post-RU486 treatment (see Materials and Methods); parameters measured were the latencies from GF stimulation to muscle response (response latency DLM and TTM) and the stability of the response to high frequency stimulation at 100, 200 and 250 Hz (high frequency stimulation TTM). Data are presented as the mean response ± SEM and were analysed by student's t-test, at each time point, on log-derived data. *$P<0.05$, **$P<0.01$ comparing response latency or response to high frequency stimulation of UAS-ArcAβ42/+;elavGS/+ +RU flies to −RU controls at 28 days post-induction.
doi:10.1371/journal.pgen.1001087.g004

wild-type tau levels ($P = 0.0002$, two-way ANOVA; Figure 10B), on +RU food. It is important to note, however, that tau loss of function flies themselves displayed some locomotor dysfunction compared to controls (Figure 10B; $P<0.0001$ comparing UAS-ArcAβ42/+;elavGS/+ to UAS-ArcAβ42/+;elavGS tau EP3203/tau dfc on −RU486, two-way ANOVA), thus potentially reducing the apparent protective effect of removing tau on Aβ42 pathology. These data parallel observations in mammals, where loss of murine Tau rescued Aβ-induced behavioural deficits in a mouse AD model [8].

We further investigated interactions between *Drosophila* tau and GSK-3 in the protection against Aβ42 pathology, to determine if they might act in the same biochemical pathway (Figure 10B). Lithium treatment alone had a greater protective effect against Aβ42 toxicity than did loss of tau function alone, although this may have been confounded by the reduced climbing ability of flies with reduced tau. Moreover, lithium treatment rescued Aβ42-induced climbing dysfunction to the same extent in the presence or absence of tau, ($P = 0.692$ comparing UAS-ArcAβ42/+;elavGS/+ and UAS-ArcAβ42/+;elavGS tau EP3203/tau dfc flies on +RU, + lithium food, two-way ANOVA) suggesting that endogenous tau is not required for the lithium effect. This suggests that a large proportion of the protective effect of GSK-3 inhibition on Aβ42 toxicity is mediated via non-tau-dependent mechanisms. We also show that tau is required for the manifestation of Aβ42 effects. Our experimental design does not address, neither excludes, the possibility that a direct interaction of GSK-3 and tau may also affect Aβ42 toxicity.

Inhibition of Shaggy in the adult nervous system reduces Aβ load in Arctic Aβ42-expressing flies

Because the amelioration of Aβ42 toxicity by reduced GSK-3 activity did not appear to be mediated mainly through tau, we next examined the direct effect of GSK-3 inhibition on Aβ42 levels. Interestingly, we found by ELISA analysis that Aβ peptide was significantly reduced in flies expressing Arctic Aβ42 when Sgg activity was reduced. Adult flies that co-expressed Arctic Aβ42 and the inactive dominant negative mutant Sgg S9E, or adult flies that expressed Arctic Aβ42 and were fed lithium, showed a major reduction in total Aβ42 levels in comparison to flies expressing Arctic Aβ42 alone and reared on food without lithium (Figure 11A). The transcript levels of Aβ42 in the presence of functional or inhibited Sgg activity were not significantly different

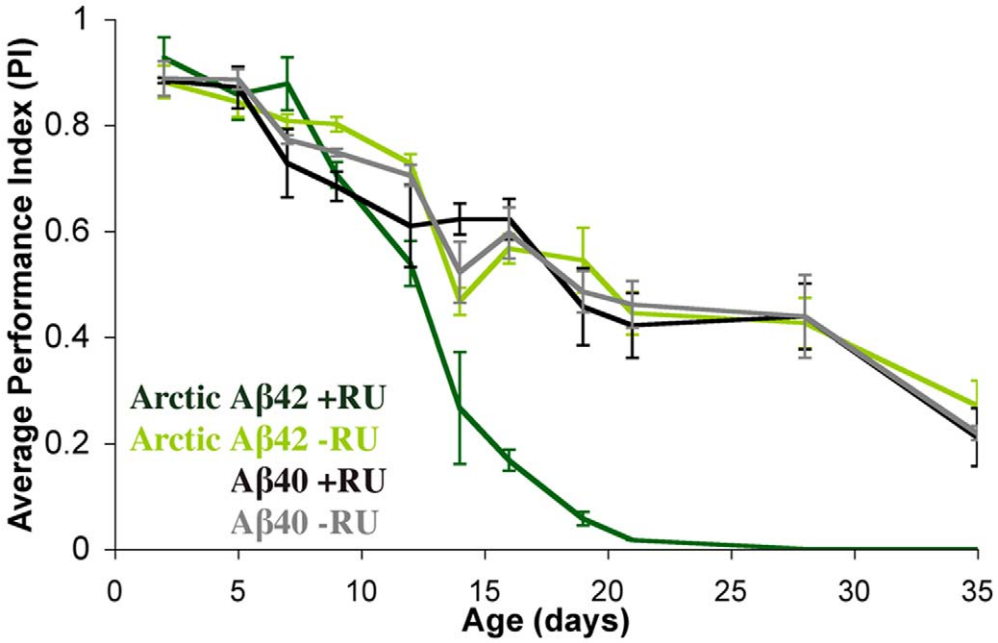

Figure 5. Expression of Arctic Aβ42 peptides in the adult fly nervous system causes locomotor dysfunction. Climbing ability of UAS-ArcAβ42/+;elavGS/+ and UAS-Aβ40/+;elavGS/+ flies on + and − RU486 SY medium was assessed at the indicated time-points (see Materials and Methods). Data are presented as the average performance index (PI) ± SEM and were compared using two-way ANOVA and Tukey's honestly significant difference (HSD) post-hoc analyses (number of independent tests (n) = 3, number of flies per group (n_t) = 39–45). *$P<0.05$ comparing PI of UAS-ArcAβ42/+;elavGS/+ +RU486 flies to that of untreated and Aβ40 over-expressing controls at the indicated time points (Tukey's HSD).
doi:10.1371/journal.pgen.1001087.g005

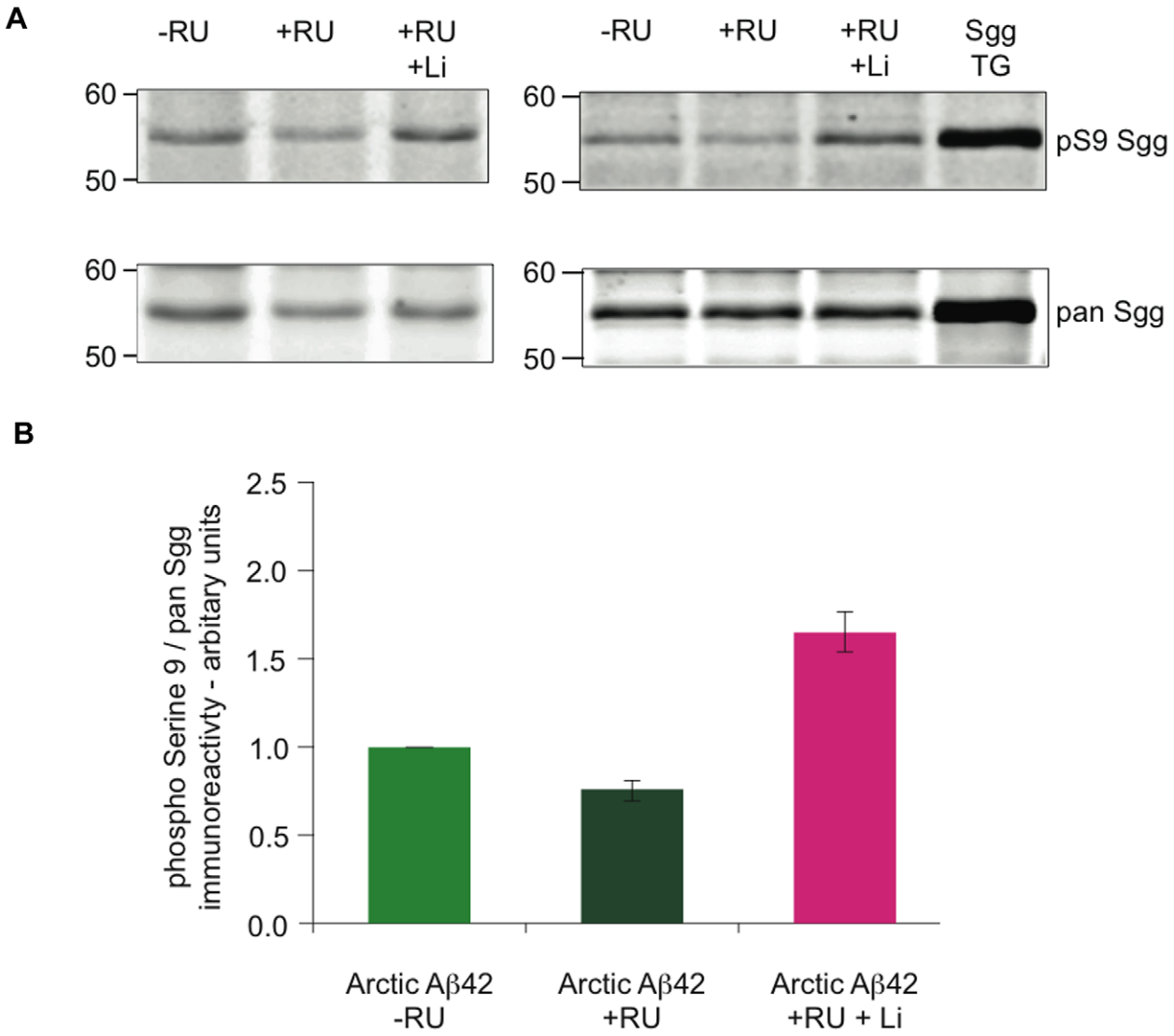

Figure 6. Flies expressing Aβ42 in adult neurons show a decrease in Shaggy inhibitory Ser9 phosphorylation. (A) Western blot analyses for pan-Sgg and phospho Ser9 Sgg revealed a decrease in Ser9 phosphorylation in flies expressing Aβ42 by RU induction for 15 days (UAS-ArcAβ42/+;elavGS/+ or UAS-ArcAβ42/GFP;elavGS/+) in comparison to their −RU controls, while an increase in Ser9 phosphorylation was observed when the Aβ42 expressing flies were fed lithium (+RU +Li). Flies over expressing Sgg were used as positive control. (B) Quantification of the western blot analysis in (A), n = 3, is depicted in the bar chart, with significant differences seen between ArcAβ42/+;elavGS/+ +RU flies to −RU controls ($P<0.01$), and between ArcAβ42/+;elavGS/+ +RU +Li flies to +RU controls ($P<0.001$).
doi:10.1371/journal.pgen.1001087.g006

(Figure 11B), suggesting that Sgg does not affect transgene expression, but rather acts directly or indirectly on Aβ degradation/sequestration. These data demonstrate for the first time a role of GSK-3 in determining the level of Aβ42 peptide, in the absence of effects on APP processing. Furthermore, this reduction in the levels of Aβ42 peptide by GSK-3 inhibition is most likely not mediated by tau, since loss of tau function partially rescued Aβ toxicity, but did not affect Aβ42 levels (Figure 10A and Figure S5). These data again suggest that GSK-3 can modify Aβ42 toxicity via tau-independent mechanisms.

Discussion

Glycogen synthase kinase-3 is increasingly thought to play a pivotal role in the pathogenesis of Alzheimer's disease, both as a regulator of the accumulation of Aβ peptide [12,17,47] and through its well-established role as a tau kinase [48–52]. Although previous studies in mice have suggested that GSK-3 alters Aβ levels via modulation of APP processing [12,17], the direct effects of the enzyme on Aβ toxicity, and in the adult nervous system, have not been examined. We therefore performed a more direct analysis of the specific role of GSK-3 in regulating Aβ42 toxicity in adult neurons *in vivo*, by modulating its activity in an adult-onset *Drosophila* model of Alzheimer's disease. Our study shows for the first time that GSK-3 inhibition ameliorates Aβ42 toxicity in adult flies, and also highlights a novel mechanism of protection by which GSK-3 directly regulates Aβ42 levels in the absence of any effects on APP processing.

We have generated an inducible *Drosophila* model of Alzheimer's disease. Over-expression of the Arctic Aβ42 peptide in adult fly neurons led to shortened lifespan, neuronal dysfunction and behavioural impairments. However, no neuronal loss was evident

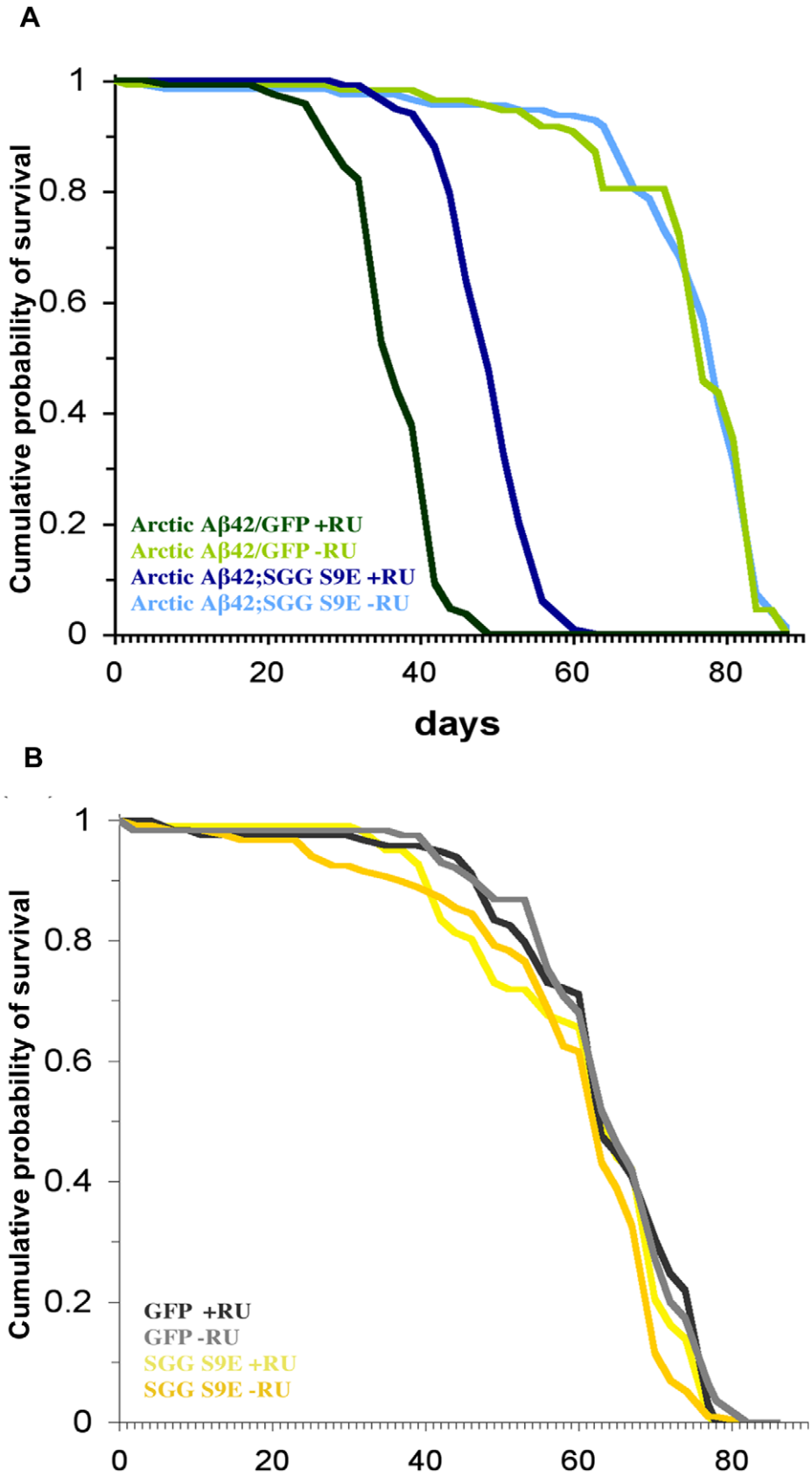

Figure 7. Expression of the dominant negative mutant Shaggy S9E in the adult nervous system extends the median and maximum lifespan of Arctic Aβ42 flies. (A). Survival curves of flies co-expressing Arctic Aβ42 and SggS9E are depicted and data were compared using the log-rank test. $P<0.001$ comparing UAS-ArcAβ42/+;elavGS/UAS-SggS9E +RU flies to UAS-ArcAβ42/UAS-gfp;elavGS/+ +RU controls. No significant

difference was seen in the −RU controls. (B). Expression of Shaggy S9E alone did not affect control lifespan. No significant difference was observed comparing elavGS/UAS-SggS9E +RU to either elavGS/UAS-SggS9E −RU, or UAS-gfp/elavGS/+ +RU control lifespans.
doi:10.1371/journal.pgen.1001087.g007

in the brains of these flies. This finding contrasts with previous reports that flies over-expressing Arctic Aβ42, using a constitutive neuronal driver, develop vacuoles [28,33], These contrasting results could be reconciled if neuronal loss upon Aβ42 over-expression is a consequence of developmental abnormalities in the *Drosophila* brain or if neuronal loss represents an end-stage event in response to Aβ42 toxicity, since vacuolation has been reported only under the most extreme conditions of expression, age and temperature, while neuronal toxicity in these models is already apparent under less stringent conditions [33]. Importantly, our findings agree with those of other studies demonstrating that neuronal loss is generally not evident in murine models of amyloidosis, such as in mice transgenic for the amyloid precursor protein [53]. Moreover, our study has provided direct evidence of neuronal dysfunction in response to Aβ42, by electrophysiological methods, at a timepoint more suitable to understanding the early events that lead to neuronal decline in AD.

GSK-3 activity was increased in our flies upon Arctic Aβ42 over-expression, as measured by reductions in phosphorylation of endogenous Sgg at the inhibitiory Ser9 site. This is consistent with previous observations showing that Aβ42 alters GSK-3 phosphorylation in cells [54] and in mice [14]. Contrary to these findings,

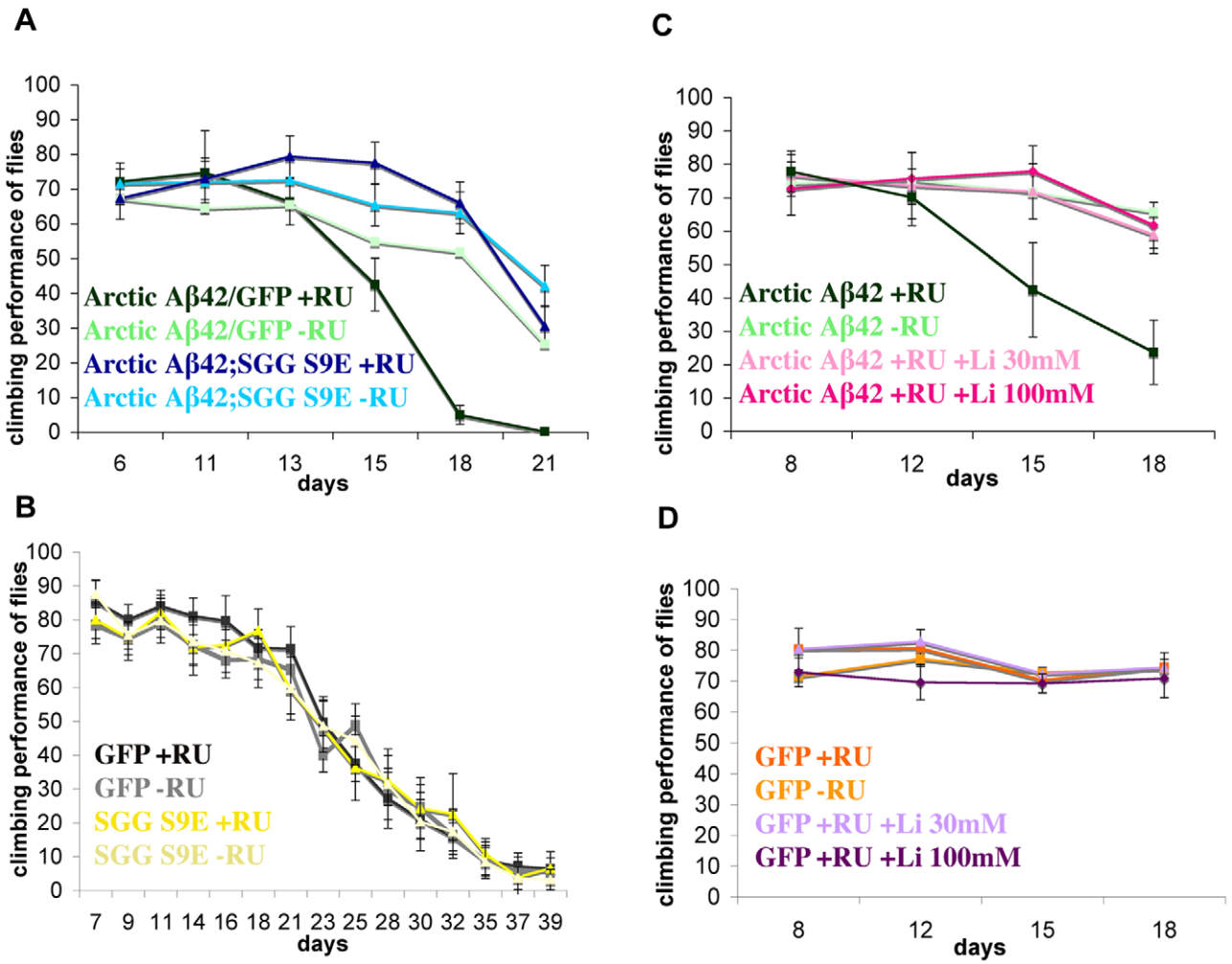

Figure 8. Inhibition of Shaggy, either by expression of SggS9E in the adult nervous system or treatment with lithium, suppresses the locomotor dysfunction phenotype of Arctic Aβ42 flies. (A) Climbing ability of UAS-ArcAβ42/UAS-gfp;elavGS/+ and UAS-ArcAβ42/+;elavGS/UAS-SggS9E flies on +RU486 SY medium was assessed at the indicated time-points (see Materials and Methods). Data are presented as the percentage climbing performance of flies ± SD. $P<0.001$ when UAS-ArcAβ42/UAS-gfp;elavGS/+ and UAS-ArcAβ42/+;elavGS/UAS-SggS9E flies are compared at day 21 (one-way ANOVA, number of independent tests (n) = 3). Graph shows one representative data of repeated experiments. (B) Expression of Shaggy S9E alone does not reduce climbing ability of control flies. elavGS/UAS-SggS9E +RU flies display a similar locomotor function compared to both elavGS/UAS-SggS9E −RU and UAS-gfp/+;elavGS/+ +RU control flies. (C) Climbing ability of UAS-ArcAβ42/+;elavGS/+ and UAS-ArcAβ42/UAS-gfp;elavGS/+ on +RU486 SY medium was assessed in the presence and absence of lithium chloride (30mM and 100mM). $P<0.001$ when UAS-ArcAβ42 flies were fed lithium and compared to flies not fed lithium at day 18 (one-way ANOVA, n = 3). Graph shows one representative data of repeated experiments. (D) Lithium had no effect on negative geotaxis of control flies. UAS-gfp/+;elavGS/+ +RU and UAS-gfp/+;elavGS/+ +RU in the presence of lithium had similar locomotor function. The crosses were performed at 27°C.
doi:10.1371/journal.pgen.1001087.g008

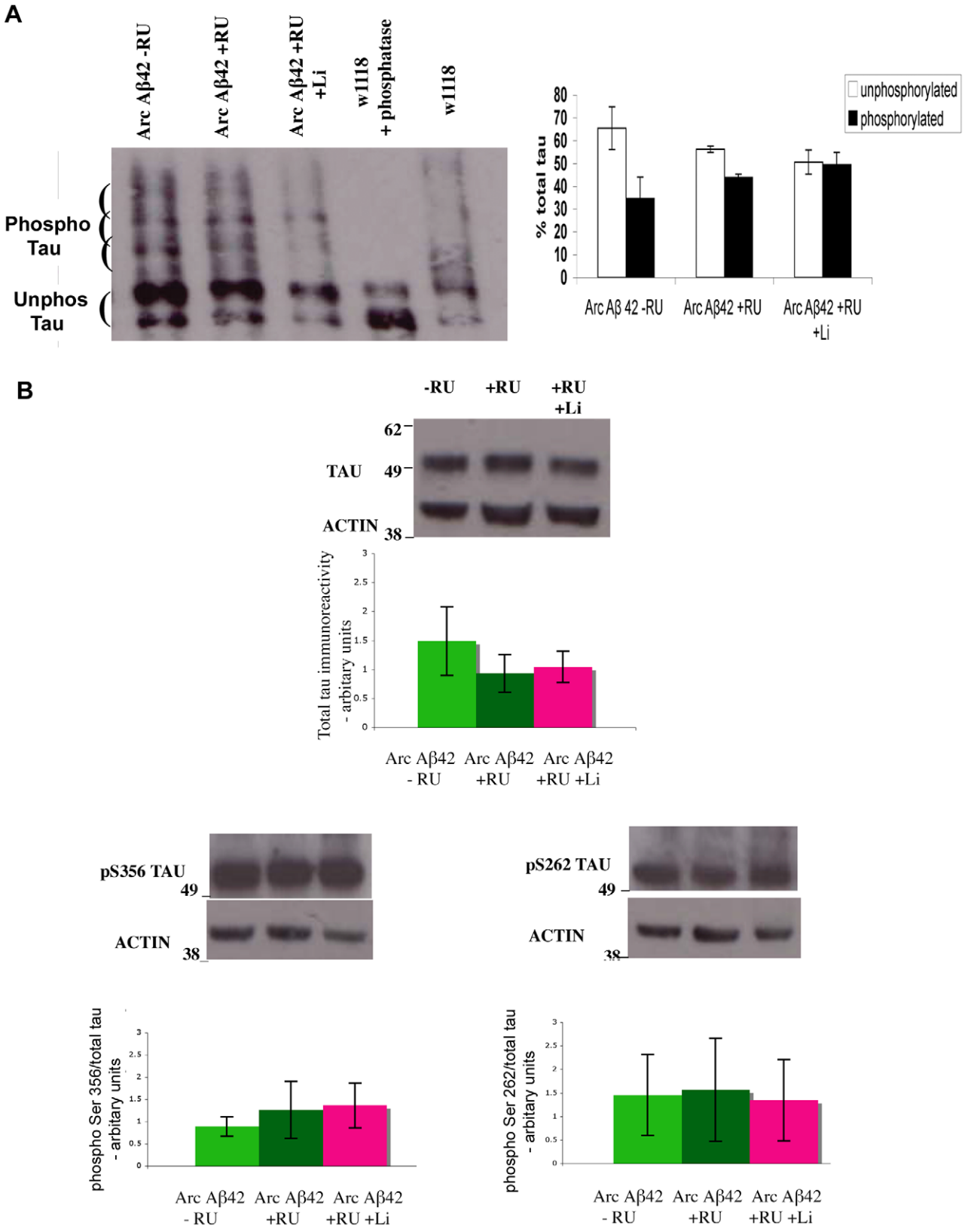

Figure 9. Flies expressing Aβ42 in adult neurons show no changes in total tau phosphorylation and at Ser 262 and Ser 356 specific epitopes. (A) Western blot analyses for total tau phosphorylation using phos-tag gels and (B) phospho Ser262 and Ser356. Tau showed no changes in phosphorylation in flies expressing Aβ42 (UAS-ArcAβ42/GFP;elavGS/+) in comparison to their −RU controls, and when the Aβ42 expressing flies were fed lithium (+RU +Li). Flies were collected 17 days post RU induction, and maintained at 27°C. Quantification of the western blot analysis in (A), phospho-tau or non-phospho-tau normalised to total tau per sample (n = 4), and in (B) n = 4 for total tau and n = 3 for the Ser sites depicted in the bar chart, showed no significant differences between ArcAβ42/+;elavGS/+ +RU flies to −RU controls or to ArcAβ42/+;elavGS/+ +RU +Li flies (one-way ANOVA).
doi:10.1371/journal.pgen.1001087.g009

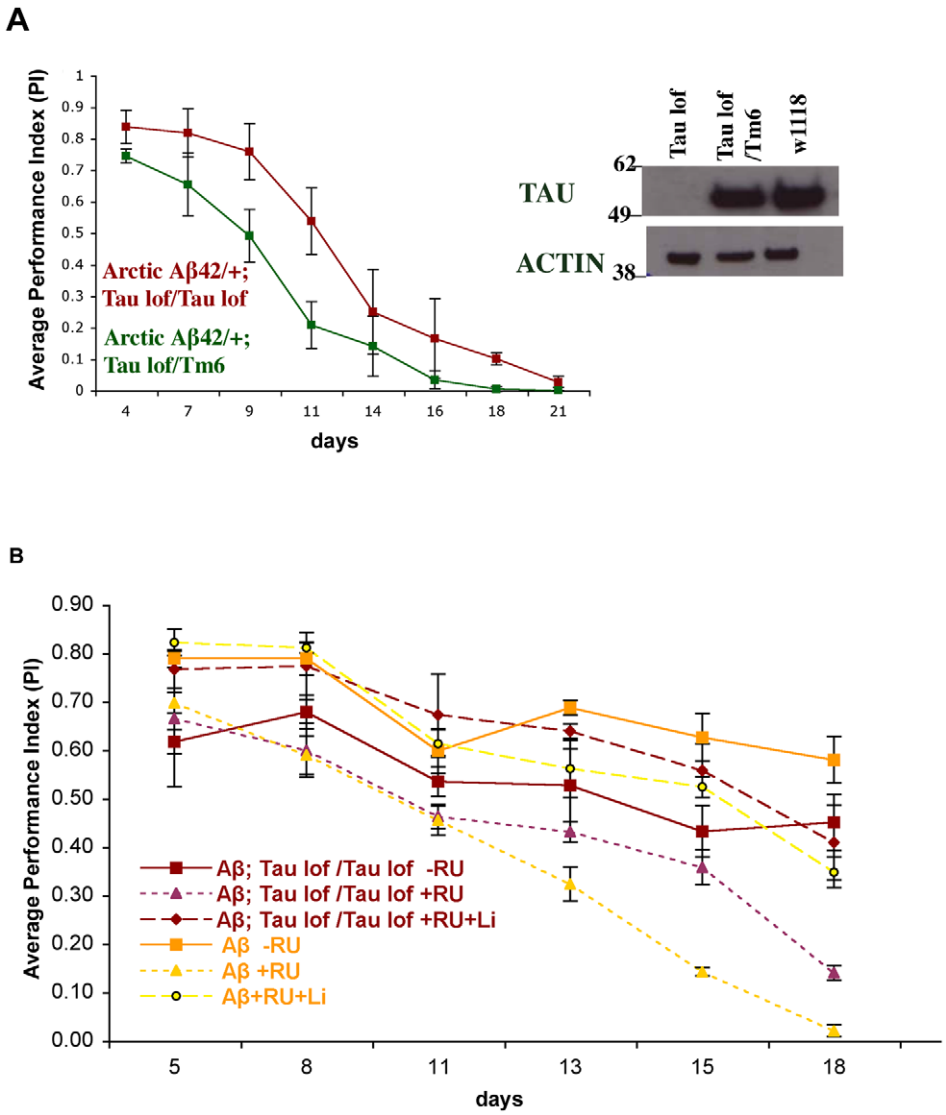

Figure 10. Lithium treatment alone has a greater protective effect against Aβ42 toxicity than loss of tau function alone. (A) Loss of tau partially suppressed the locomotor dysfunction phenotype of Arctic Aβ42 flies. Expression of Arctic Aβ42 peptide in a tau heterozygous background in the adult fly nervous system caused locomotor dysfunction. This phenotype was suppressed when Arctic Aβ42 peptide was expressed in a homozygous tau mutant background. Climbing ability of UAS-ArcAβ42/+;elavGS Tau EP3203/TM6 and UAS-ArcAβ42/+;elavGS Tau EP3203/Tau Dfc flies on +RU486 SY medium was assessed at the indicated time-points (see Materials and Methods). Data are presented as the average performance index (PI) ± SEM (number of independent tests (n) = 3, number of flies per group (n_t) = 45). $P<0.0001$ comparing the PI of UAS-ArcAβ42/+;elavGS Tau EP3203/Tau Dfc to UAS-ArcAβ42/+;elavGS Tau EP3203/TM6 flies (two-way ANOVA). The crosses were performed at 27°C. Western blotting analysis, using a non-phosphorylation dependent antibody to *Drosophila* tau, confirmed that endogenous tau protein levels were greatly reduced in UAS-ArcAβ42/+;elavGS tau EP3203/tau Dfc flies in comparison to tau heterozygous flies (UAS-ArcAβ42/+;elavGS tau EP3203/TM6) and control w1118 flies. (B) Arctic Aβ42 toxicity was suppressed when the peptide was expressed in a homozygous tau mutant background or when flies were treated with lithium. Lithium treatment alone had a greater protective effect against Aβ42 toxicity than did loss of tau function alone, and was not dependent on tau. Climbing ability of UAS-ArcAβ42/+;elavGS/+ and UAS-ArcAβ42/+;elavGS tau EP3203/tau Dfc flies on − or +RU486 SY medium, in the presence or absence of lithium, was assessed at the indicated time-points. Data are presented as the average PI ± SEM and were analysed by two-way ANOVA (number of independent tests (n) = 4, number of flies per group (n_t) = 60). Comparing PI of UAS-ArcAβ42/UAS-gfp;elavGS/+ and UAS-ArcAβ42/+;elavGS tau EP3203/tau Dfc flies on −RU, significant differences between genotypes ($P<0.0001$) were observed. $P = 0.0002$ comparing PI of UAS-ArcAβ42/UAS-gfp;elavGS/+ and UAS-ArcAβ42/+;elavGS tau EP3203/tau Dfc flies on +RU food. No significant differences were observed comparing UAS-ArcAβ42/+;elavGS/+ and UAS-ArcAβ42/+;elavGS tau EP3203/tau Dfc flies on +RU +lithium ($P = 0.692$).
doi:10.1371/journal.pgen.1001087.g010

however, one other study has shown that WT Aβ42 expression does not alter phosphorylation of Sgg in flies [55]. These differences may reflect varying mechanisms by which Arctic mutant Aβ42 and WT Aβ42 peptides modulate GSK-3 activity, or a distinction in the effect of expressing Aβ42 throughout development compared to adult-only expression. Hence, our observed increase in Sgg activity may reflect an age-dependent effect. We aimed, therefore, to further investigate the functional role of this kinase in mediating Aβ toxicity in our adult-onset AD model.

GSK-3 plays an important role in neuronal development [56,57]. Previous analyses of the role of GSK-3 in amyloid toxicity

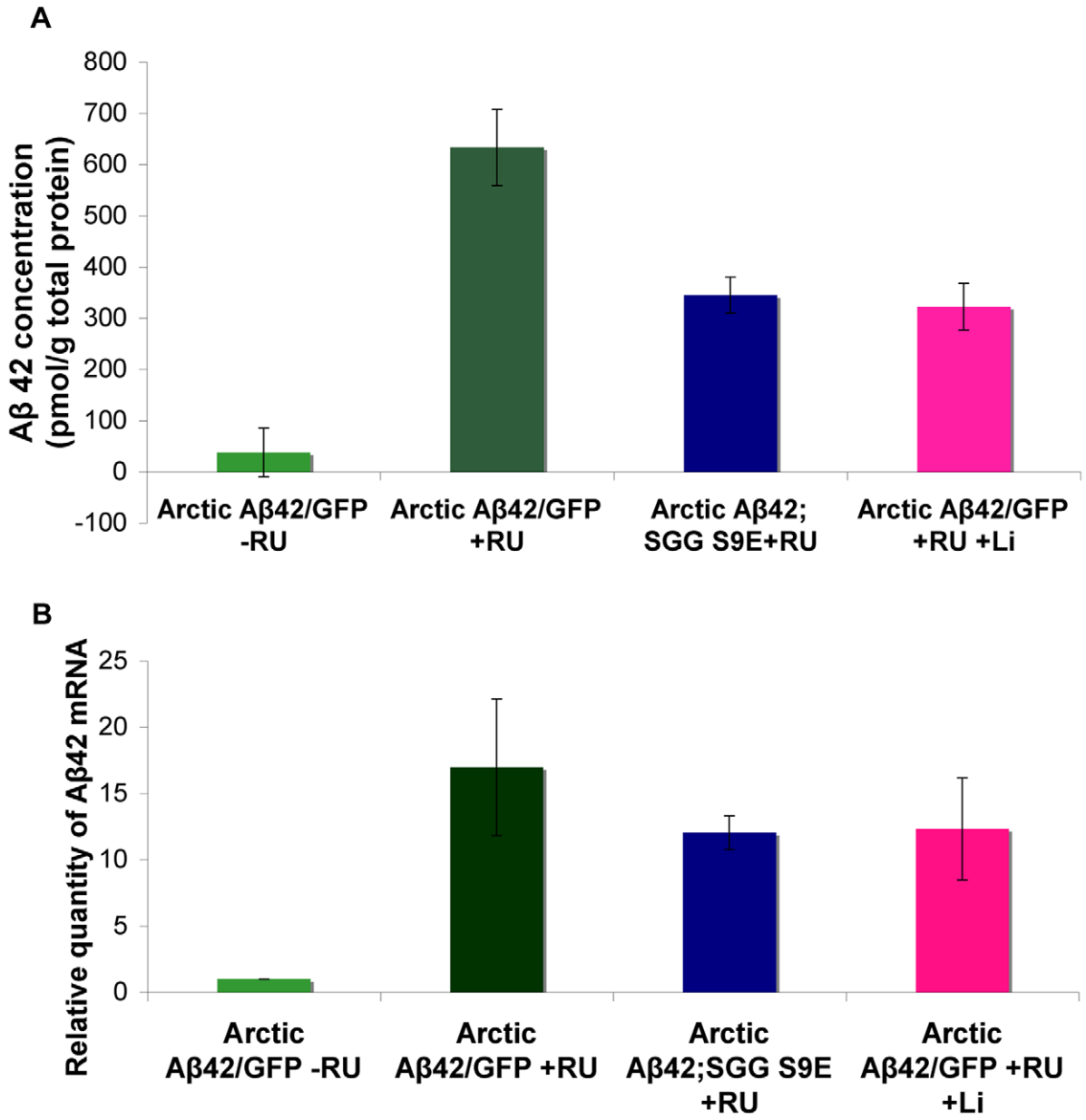

Figure 11. Inhibiting Shaggy activity reduces amyloid levels of Arctic Aβ42 flies. (A) Protein levels of UAS-ArcAβ42/UAS-gfp;elavGS/+ and UAS-ArcAβ42/+;elavGS/UAS-SggS9E flies on +RU486 SY medium, and UAS-ArcAβ42/UAS-gfp;elavGS/+ flies on +RU +Lithium (Li), were measured by ELISA at 15 days post-induction (see Materials and Methods). Data were compared using one-way ANOVA, number of independent tests (n) = 3. $P<0.01$, and $P<0.0001$ when comparing UAS-ArcAβ42/UAS-gfp;elavGS/+ to UAS-ArcAβ42/+;elavGS/UAS-SggS9E flies on +RU486 SY medium, and UAS-ArcAβ42/UAS-gfp;elavGS/+ +RU to UAS-ArcAβ42/UAS-gfp;elavGS/+ +RU +Li respectively. (B) RNA levels of UAS-ArcAβ42/UAS-gfp;elavGS/+, UAS-ArcAβ42/+;elavGS/UAS-SggS9E +RU486 SY medium and UAS-ArcAβ42/UAS-gfp;elavGS/+ +RU + lithium flies were measured at day 5. No significant difference was seen in the levels of RNA expression, number of independent tests (n) = 3.
doi:10.1371/journal.pgen.1001087.g011

using constitutive expression systems may, therefore, represent abnormal neuronal development in addition to the response to AD pathology in the adult period. Hence, we confined GSK-3 inhibition to the adult neurons of Arctic Aβ42-expressing flies, by over-expressing a dominant negative form of the *Drosophila* orthologue Sgg, using our inducible expression system, or we treated whole adult flies with the GSK-3 inhibitor, lithium. GSK-3 inhibition extended lifespan of Arctic Aβ42-expressing flies and suppressed the locomotor dysfunction caused by expression of the peptide in adult neurons. This is an important finding because it demonstrates a definitive role for GSK-3 in Aβ42 pathogenesis in adult flies. Moreover, we found that inhibiting Sgg in adulthood had no adverse effect on wild type flies. Hence, our study provides further support for the therapeutic potential of GSK-3 inhibitors in treating Alzheimer's disease. Further studies are required to test this potential in mammalian models, firstly to confirm the relevance of GSK-3 for direct regulation of Aβ42 toxicity and secondly to establish a therapeutic index for GSK-3 inhibition in the treatment of AD.

Aβ42 has been shown previously to increase tau phosphorylation in cells [45] and in mice [5,43]. Correlative evidence has suggested that GSK-3 may mediate the effects of Aβ on tau

phosphorylation, since Aβ increases GSK-3 activity [10]. Furthermore, GSK-3 and APP cause similar increases in tau phosphorylation and aggregation in tau over-expressing mice [14]. Because both tau and GSK-3 appeared to play a causal role in Arctic Aβ42 toxicity in our flies, we examined whether the protective effect of GSK-3 inhibition on Aβ toxicity might be mediated via alterations in phosphorylation of endogenous *Drosophila* tau. We found that Arctic Aβ42 over-expression and lithium treatment of Aβ42-expressing flies did not have an observable effect on overall tau phosphorylation, as revealed both by generic measures, and at two specific sites by examination of phosphorylation of fly tau at Ser262 and Ser356 epitopes. However, because the Ser 262 and 356 sites are also predominant *in vivo* substrates for MARK (microtubule-associated protein (MAP)-microtubule affinity regulating kinase) [58,59], further investigation of more specific GSK-3 sites on *Drosophila* tau, using mass spectrometric methods, would provide a more definitive analysis of the role of tau phosphorylation by GSK-3 in mediating Aβ42 toxicity in the fly.

Our data suggest that tau phosphorylation may not be the only mechanism by which Aβ42 exerts its toxic effect in *Drosophila*, since phosphorylation sites thought to be important for mediating Aβ42 effects on tau (Thr212/Ser214 [43], Thr231 [45], Ser422, Ser262 [44]) are predominantly not conserved in the fly, or are not altered by Aβ42 over-expression in our AD model. These findings seem to contradict previous studies showing that Aβ42 increases phosphorylation of human tau in *Drosophila* [55,60], and indicating that particular sites, such as Ser262, are important in mediating Aβ toxicity in the fly [60]. This disparity could reflect a lack of conservation of the mechanisms through which Aβ42 regulates human and *Drosophila* tau proteins. However, the endogenous fly tau does appear to be an important downstream mediator of Aβ42 toxicity, since loss of tau function partially reduced Aβ42 pathology in our study. This protective effect of tau against Aβ42 toxicity, however, may have been masked by the locomotor dysfunction from reducing levels of tau itself in flies that do not over-express the Aβ42 peptide. As a previous study has reported similar tau-dependent neuropathological phenotypes in an APP-overexpressing mouse model of AD [8], our findings suggest that the role of tau in amyloid toxicity is conserved over large evolutionary distances.

We further examined the epistatic interaction between GSK-3 inhibition and tau loss of function in protecting against Aβ42 toxicity in our fly model. Lithium alone had a greater protective effect against Aβ42 toxicity than loss of tau function alone, and lithium could prevent Aβ42-induced dysfunction in the presence or absence of tau. This suggests that a large proportion of the protective effect of GSK-3 inhibition on Aβ42 toxicity is mediated via non-tau-dependent mechanisms and that tau is not required for this effect. We observed no additive effect of combining lithium treatment and tau loss of function in protection against Aβ42-induced pathology; however, this could have been a consequence either of toxicity of loss of tau in the absence of Aβ42 or of the level of protection afforded by lithium, which could have produced a ceiling effect. Our findings agree with other recently published studies, showing that loss of tau only partially protects against GSK-3-induced neuronal degeneration in adult mice [61], suggesting that other non-tau-dependent mechanisms of GSK-3 neuro-toxicity exist.

Previous studies have shown a reduction in Aβ load in mice as a result of GSK-3 inhibition, but this has been explained mainly by dysregulation of APP processing, either by increasing γ-secretase activity [12] or by increasing the phosphorylation of APP and therefore directing its subcellular location to sites of secretase activity [17]. Our inducible *Drosophila* model, however, expresses the Arctic Aβ42 peptide directly, thus circumventing the requirement for APP processing. We found that inhibition of GSK-3 caused a reduction in the level of Aβ42 peptide, but not in RNA transcript levels. Hence, although previous studies have indicated that GSK-3 does not affect Aβ degradation [17], our findings demonstrate a novel effect of GSK-3 in Aβ metabolism, irrespective of APP processing, in the adult nervous system. Furthermore, this observation may, partially, explain the non-tau-dependent effect of GSK-3 in protecting against Aβ toxicity in our flies.

Our study, therefore, implies that GSK-3 may increase Aβ degradation or clearance. Candidate *in vivo* Aβ degrading enzymes include neprilysin (NEP) [62], insulin degrading enzyme (IDE) [63–64] and to a lesser extent endothelin converting enzymes (ECE-1,2) [65] and plasmin [66]. Mice deficient in IDE [63,64] or NEP [62] display increased levels of Aβ peptides in the brain. Conversely, increasing expression and activity of NEP or IDE reduces the cerebral amyloid plaque burden observed in APP over-expressing mice [67], further implying that these are predominant *in vivo* Aβ degrading enzymes. Direct interactions between GSK-3 and IDE or neprilysin activities in relation to Aβ degradation, however, have not been extensively investigated. Studies examining the effects of reduced insulin signalling on amyloid toxicity in APP over-expressing mice have reported either increased GSK-3 activity, reduced IDE activity and increased amyloidosis [68] or decreased GSK-3 activity, increased IDE expression and reduced amyloidosis [69] in the brain, suggesting an inverse correlation between GSK-3 and IDE activities in relation to Aβ metabolism. Other studies have reported no correlation between inhibition of GSK-3 activity and neprilysin levels in relation to reduced Aβ load in mice [17], but NEP activity was not measured and may provide a more accurate indication of the role of this enzyme in Aβ metabolism downstream of GSK-3. As most information from mouse models is correlative, however, further work is required to determine whether these degrading enzymes are direct mediators of Aβ degradation in response to GSK-3 inhibition, by modulating their activities in our inducible *Drosophila* model. *Drosophila* homologues of both IDE and NEP exist, and over-expression of both NEP [26,70] and IDE [71] have been shown to reduce Aβ induced neurotoxicity in flies. This suggests that these degradation mechanisms may be generally conserved, and that the fly is a valuable model for the direct analysis of these genetic interactions with respect to the role of GSK-3 in AD.

The more general proteosome degradation pathway could also play a role in regulating Aβ degradation or sequestration. Heat shock protein 90 (Hsp90), a protein chaperone involved in the proteosome degradation pathway, is thought to phosphorylate GSK-3 and regulate its activity [13]. In addition, an increase in levels of GSK-3 down-regulates the transcriptional activity of Heat shock factor-1 (HSF-1) and Hsp70 [72]; thus a decrease in GSK-3 activity could lead to an increase in levels/activity of these chaperone molecules and augment the levels of Aβ. In a *Caenorhabdits elegans* worm model of AD, the aggregation-mediated Aβ42 toxicity was regulated by modulating the levels of hsf-1; a reduction in hsf-1 increased paralysis in these worms, suggesting a role of hsf-1 in the dis-aggregation of Aβ toxic oligomers [73]. Thus, any of these pathways/molecules could play a role in affecting Aβ load in our fly model and will require detailed exploration in the future.

Our data highlight that this fly model is suitable for the study of AD pathology, since we observe neuronal dysfunction and toxicity that are particular to the expression of Aβ42 peptide. Furthermore, we have been able to test the amyloid cascade hypothesis in

part, to show that tau is acting downstream of Aβ pathology. This inducible model of AD will also open the way to understanding the role of events at different ages and of the ageing process itself in the biological pathway leading to this ageing related disease. We have shown the involvement of GSK-3, particularly in adulthood, in AD pathogenesis, and also uncover a novel mechanism by which GSK-3 could be acting directly or indirectly on Aβ, by reducing Aβ load. These results raise new potential therapeutic benefits of GSK-3 in AD pathology.

Materials and Methods

Fly stocks and maintenance

All fly stocks were maintained at 25°C or 27°C on a 12:12-h light:dark cycle at constant humidity on a standard sugar-yeast (SY) medium ($15gl^{-1}$ agar, 50 gl^{-1} sugar, 100 gl^{-1} autolysed yeast, $100gl^{-1}$ nipagin and $3ml\ l^{-1}$ propionic acid). Adult-onset neuronal-specific expression of Arctic mutant Aβ42 peptide or constitutively active Sgg was achieved by using the elav GeneSwitch (elavGS)-UAS system [GAL4-dependant upstream activator sequence; [30]]. ElavGS was derived from the original elavGS 301.2 line [30] and obtained as a generous gift from Dr H. Tricoire (CNRS, France). UAS-ArcAβ42 and UAS-SggS9E were obtained from Dr D. Crowther (University of Cambridge, UK) and the Bloomington Drosophila Stock Centre respectively. Tau dfc (9530) and EP line 3203 (17098) were received from Bloomington Drosophila stock centre. The EP line orientation is opposite to tau expression and causes a reduction in tau expression [46]. elavGS and UAS-lines used in all experiments were backcrossed six times into the w1118 genetic background. Male flies expressing UAS-constructs were crossed to female flies expressing elavGS, and adult-onset neuronal expression induced in female progeny by treatment with mifepristone (RU486;200mM) added to the standard SY medium.

Lithium treatment protocol

Lithium Chloride was made at 1M concentration and added to 200mM RU486 standard SY medium at a final concentration of 30mM or 100mM.

Lifespan analyses

For all experiments, flies were raised at a standard density on standard SY medium in 200 mL bottles. Two days after eclosion once-mated females were transferred to experimental vials containing SY medium with or without RU486 (200mM) at a density of 10 flies per vial. Deaths were scored almost every other day and flies were transferred to fresh food three times a week. Statistical analyses were performed using JMP (version 7.0) software (SAS Institute, Cary, NC, USA). Data are presented as survival curves and analysis was performed using log-rank tests to compare between groups.

Negative Geotaxis Assays

To characterise the adult-onset behavioural effects of Arctic Aβ42 peptide on neuronal function, climbing assays were initially performed at 25°C according to previously published methods [75]. Climbing ability was analysed every 2–3 days post-RU486 treatment. Briefly, 15 adult flies were placed in a vertical column (25cm long, 1.5cm diameter) with a conic bottom end, tapped to the bottom of the column, and their subsequent climb to the top of the column was analysed. Flies reaching the top and flies remaining at the bottom of the column after a 45 sec period were counted separately, and three trials were performed at 1 min intervals for each experiment. Scores recorded were the mean number of flies at the top (n_{top}), the mean number of flies at the bottom (n_{bottom}) and the total number of flies assessed (n_{tot}). A performance index (PI) defined as $\frac{1}{2}(n_{tot}+n_{top}-n_{bottom})/n_{tot}$) was calculated. Data are presented as the mean PI ± SEM obtained in three independent experiments for each group, and analysis of variances (ANOVA) and post hoc analyses were performed using JMP 7.0 software.

To assess various modifiers of the adult-onset neuronal dysfunction in Arctic Aβ42 over-expressing flies, a less stringent climbing assay was performed at 27°C. Thirty flies expressing Arctic Aβ42 with or without co-expressing modifiers in the neurons (elav-GAL4GS) were used for the climbing assay, adapted from Ganetzky *et al.* [76]. Climbing performance (ability to climb past a 5cm mark in 18s) was assessed after eclosion post RU486 treatment.

Electrophysiology

Recordings from the GFS of adult flies were made essentially as described in [77]; a method based on those described by Tanouye and Wyman (1980) [78] and Gorczyca and Hall (1984) [79]. Flies were anaesthetized by cooling on ice and secured in wax, ventral side down, with the wings held outwards in the wax. A tungsten earth wire (ground electrode) was placed into abdomen; tungsten electrodes were pushed through the eyes and into the brain to deliver a 40V pulse for 0.03ms using a Grass S48 stimulator. Recordings were made from the TTM and contralateral DLM muscle using glass microelectrodes (resistance: 40–60 MΩ). The electrodes were filled with 3M KCl and placed into the muscles through the cuticle. Responses were amplified using Getting 5A amplifiers (Getting Instruments, USA) and the data digitized using an analogue-digital Digidata 1320 and Axoscope 9.0 software (Axon Instruments, USA). For response latency recordings, at least 5 single stimuli were given with a 5s rest period between each stimulus; trains of 10 stimuli, at either 100Hz, 200 Hz or 250Hz, were given a 5s rest interval between each train.

Histology

For neuronal cell loss, adult heads were fixed, dehydrated and transverse sections were stained with Toluidine blue. Cell bodies were then counted blind for each genotype.

Quantitative RT–PCR

Total RNA was extracted from 20–25 fly heads using Trizol (GIBCO) according to the manufacturers' instructions. The concentration of total RNA purified for each sample was measured using an *eppendorf biophotometer*. 1μg of total RNA was then subjected to DNA digestion using DNAse I (Ambion), immediately followed by reverse transcription using the Super-script II system (Invitrogen) with oligo(dT) primers. Quantitative PCR was performed using the PRISM 7000 sequence-detection system (Applied Biosystems), SYBR Green (Molecular Probes), ROX Reference Dye (Invitrogen), and Hot Star Taq (Qiagen, Valencia, CA) by following manufacturers' instructions. Each sample was analysed in triplicate with both target gene (Arctic Aβ42) and control gene (RP49) primers in parallel. The primers for the Aβ transgenes were directed to the 5′ end and 3′ end of the Aβ coding sequence: forward GATCCTTCTCCTGCTAACC; reverse CACCATCAAGCCAATAATCG. The RP49 primers were as follows: forward ATGACCATCCGCCCAGCATCAGG; reverse ATCTCGCCGCAGTAAACG.

Quantification of total, soluble, and aggregated Aβ42

To extract total Aβ42, five fly heads were homogenised in 50 μl GnHCl extraction buffer (5 M Guanidinium HCl, 50 mM Hepes pH 7.3, protease inhibitor cocktail (Sigma, P8340) and 5mM

EDTA), centrifuged at 21,000 g for 5 min at 4°C, and cleared supernatant retained as the total fly Aβ42 sample. Alternatively, soluble and insoluble pools of Aβ42 were extracted using a protocol adapted from previously published methods [80]: 200 fly heads were homogenised in 200 µl tissue homogenisation buffer (250mM sucrose, 20mM Tris base, 1mM EDTA, 1mM EGTA, protease inhibitor cocktail (Sigma) then mixed further with 200µl DEA buffer (0.4% DEA, 100mM NaCl and protease inhibitor cocktail). Samples were centrifuged at 135,000 g for 1 hour at 4°C (Beckman Optima Max centrifuge, TLA120.1 rotor), and supernatant retained as the cytosolic, soluble Aβ42 fraction. Pellets were further resuspended in 400µl ice-cold formic acid (70%), and sonicated for 2×30 sec on ice. Samples were re-centrifuged at 135,000 g for 1 hour at 4°C, then 210 µl of supernatant diluted with 4ml FA neutralisation buffer (1M Tris base, 0.5M Na_2HPO_4, 0.05% NaN_3) and retained as the insoluble, formic acid-extractable Aβ42 fraction.

Total, soluble or insoluble Aβ42 content was measured in Arctic mutant Aβ42 flies and controls using the hAmyloid β42 ELISA kit (HS) (The Genetics Company, Switzerland). Total Aβ42 samples were diluted 1:100, and soluble versus insoluble Aβ42 samples diluted 1:10 in sample/standard dilution buffer, then ELISA performed according to the manufacturers' instructions. Protein extracts were quantified using the Bradford protein assay (Bio-Rad protein assay reagent; Bio-Rad laboratories Ltd (UK)) and the amount of Aβ42 in each sample expressed as a ratio of the total protein content (pmoles/g total protein). Data are expressed as the mean ± SEM obtained in three independent experiments for each genotype. ANOVAs and Tukey's-HSD post-hoc analyses were performed using JMP 7.0 software.

Analysis of tau phosphorylation by Phos-tag SDS-PAGE

Fly heads were homogenised in Mes buffer (100 mM Mes, pH 6.5, 1 M NaCl, 0.5 mM $MgCl_2$, 1 mM EGTA, 10 mM NaF, Protease inhibitor cocktail [Sigma, P8340] and Phosphatase inhibitor cocktail 2 [Sigma, P5726]), centrifuged at 20,000 g for 30 minutes at 4°C, then supernatants adjusted to 0.5% β-mercaptoethanol, boiled for 5 minutes and re-centrifuged. Cleared supernatants were then retained as heat-stable soluble tau. Control samples were dephosphorylated by incubating with λ-protein phosphatase (NEB, P0753) for 3 hours at 30°C.

To detect phosphorylated and non-phosphorylated tau, samples were separated by SDS-PAGE, using Phos-tag AAL-107 (FMS laboratory) according to the manufacturers' instructions. Western blotting was then performed using a non-phosphorylation dependent *Drosophila* rabbit anti-tau antibody (1:5000). Quantitation was performed using Image J software (National Institutes of Health). Phosphorylated and non-phosphorylated tau was expressed as a percentage of the total amount of tau present in each sample. ANOVA and Tukey's-HSD post-hoc analyses were performed using JMP 7.0 software.

Western blotting

Drosophila heads were pooled and homogenised in 2×Laemmli sample buffer containing β-mercaptoethanol and boiled for 10 mins. Proteins were separated on SDS polyacrylamide gels and blotted onto nitrocellulose. Membranes were incubated in a blocking solution containing 5% milk proteins either in TBST for 1hr at room temperature for Tau blot or in PBST for 20 min for Sgg blot, then probed with primary antibodies overnight at 4°C. Mouse anti-actin antibody (Santacruz) was used at a 1 in 1000 dilution. Tau antibody (rabbit) was a kind gift from Nick Lowe, and used at a 1 in 2000 dilution. Rabbit anti-phospho S262 and S356 (Abcam) were used at a dilution of 1:1000 in 5% BSA TBST. Quantitation was performed using Image J software. Rabbit anti-phospho S9/S21 GSK-3 antibody (AB 9331 Cell Signaling) at a 1 in 250 dilution was detected using an anti-rabbit 800 nm flourophore conjugate (Rockland, USA). Monoclonal antibody, pan Sgg mouse monoclonal (4G1G) at a 1 in 2000 dilution was a kind gift from Marc Bourouis, which was subsequently detected using a 680 nm anti-mouse flourophore conjugate (Invitrogen, UK). Membranes were sequentially scanned at 700 and 800 nm using a Licor Odyssey infrared scanner. Densitometric measurements were taken in both wavelengths. Relative phospho-serine 9 Sgg levels were determined by dividing the signal at 800 nm by that obtained at 700 nm. Details of secondary antibodies and Odyssey analysis have been previously described in [69].

Supporting Information

Figure S1 Neuronal electrophysiology of flies over-expressing Arctic Aβ42 peptide in adulthood. Representative traces for (A) TTM and DLM response latencies and (B) TTM responses to high frequency stimulation (100 Hz) measured in elavGS/+;UAS-ArcAβ42/+ flies fed with + or − RU486 medium at days 16 and 28. TTM and DLM response latency was increased in Arctic Aβ42 over-expressing flies at day 28, but not at day 16 (marked with arrows). Vertical scale bars, 50 mV (TTM) and 60mV (DLM) for response latencies, 20 mV for following at 100Hz; horizontal, 2 ms for response latencies, 20ms for following at 100 Hz.
Found at: doi:10.1371/journal.pgen.1001087.s001 (0.11 MB DOC)

Figure S2 Neuronal cell loss is not evident in flies over-expressing Arctic Aβ42 peptide in adulthood. Cell loss was quantified at day 21 in elavGS/+;UAS-ArcAβ42/+ flies, fed with + or − RU486 medium and maintained at 27 degrees, by counting the number of cell bodies per brain hemisphere. No significant difference was observed when the two genotypes were compared (student's t-test), N = 7 per genotype.
Found at: doi:10.1371/journal.pgen.1001087.s002 (0.22 MB DOC)

Figure S3 Investigating tau phosphorylation. (A) Western blot analyses of tau phosphorylation using phos-tag polyacrylamide gels. Tau showed no changes in phosphorylation in flies expressing Aβ42 (UAS-ArcAβ42/GFP;elavGS/+) in comparison to their −RU controls, and when the Aβ42 expressing flies were fed lithium (+RU +Li). (B) Phospho-Ser262 and Ser356 human tau antibodies specifically detect tau in fly head homogenates. The 55 kDa tau band is reduced in tau lof/TM6 and absent in tau lof/tau lof flies compared to w1118 controls.
Found at: doi:10.1371/journal.pgen.1001087.s003 (1.23 MB DOC)

Figure S4 Full-length Tau (P10636), the longest CNS Tau isoform (P10636-8) and *Drosophila* Tau were aligned by Clustal W alignment. *Shaded in sky and light blue are sites conserved between human and Drosophila tau that are phosphorylated by GSK-3 in vitro. The two Ser sites 262 and 356 (light blue) had available human tau antibodies that detect those conserved sites in *Drosophila*. ** Shaded in red are likely GSK-3 sites and Abeta sites (212 and 214 for Abeta) that we had available antibodies for and tested in *Drosophila*, but did not work since they are not conserved. ***Shaded in yellow is an Abeta site (Ser 422) that is conserved in *Drosophila*, which we had an antibody for; Ser 262 is also a likely Abeta site.
Found at: doi:10.1371/journal.pgen.1001087.s004 (0.03 MB DOC)

Figure S5 Reduction in tau levels does not affect amyloid levels of Arctic Aβ42 flies. Protein levels of UAS-ArcAβ42/+;elavGS Tau EP3203/Tau Dfc to UAS-ArcAβ42/+;elavGS Tau EP3203/

TM6 flies flies on +RU486 SY medium, were measured by ELISA at 21 days post-induction. Data are presented as the average protein concentration, ± standard error of mean, data were compared using one-way ANOVA and student t-test, number of independent tests (n) = 3. No significant difference was seen in the levels of Aβ42.

Found at: doi:10.1371/journal.pgen.1001087.s005 (0.08 MB DOC)

Acknowledgments

We thank Dr. D. Crowther (University of Cambridge) for helpful discussions and kind donation of UAS-Aβ42 fly stocks, Dr. H. Tricoire (CNRS, France) for kind donation of elavGS fly stocks, Dr. N. Lowe (University of Cambridge) for the *Drosophila* tau antibody, Dr. M. Bourouis (CNRS, France) for the pan-Sgg antibody, and Dr. J. Fitzgerald (Institute of Neurology, UCL) for advice on using the phos-tag methods.

Author Contributions

Conceived and designed the experiments: OS FK IR SL LP. Performed the experiments: OS FK IR RK HA CG MJA. Analyzed the data: OS FK IR RK HA CG MJA. Contributed reagents/materials/analysis tools: OS FK MJA. Wrote the paper: OS FK IR JH SL LP.

References

1. Spires TL, Hyman BT (2005) Transgenic models of Alzheimer's disease: learning from animals. NeuroRx 2: 423–437.
2. Selkoe DJ, Schenk D (2003) Alzheimer's disease: molecular understanding predicts amyloid-based therapeutics. Annu Rev Pharmacol Toxicol 43: 545–584.
3. Hutton M, Lendon CL, Rizzu P, Baker M, Froelich S, et al. (1998) Association of missense and 5′-splice-site mutations in tau with the inherited dementia FTDP-17. Nature 393: 702–705.
4. Rizzu P, Van Swieten JC, Joosse M, Hasegawa M, Stevens M, et al. (1999) High prevalence of mutations in the microtubule-associated protein tau in a population study of frontotemporal dementia in the Netherlands. Am J Hum Genet 64: 414–421.
5. Lewis J, Dickson DW, Lin WL, Chisholm L, Corral A, et al. (2001) Enhanced neurofibrillary degeneration in transgenic mice expressing mutant tau and APP. Science 293: 1487–1491.
6. Oddo S, Billings L, Kesslak JP, Cribbs DH, LaFerla FM (2004) Abeta immunotherapy leads to clearance of early, but not late, hyperphosphorylated tau aggregates via the proteasome. Neuron 43: 321–332.
7. Oddo S, Caccamo A, Cheng D, Jouleh B, Torp R, et al. (2007) Genetically augmenting tau levels does not modulate the onset or progression of Abeta pathology in transgenic mice. J Neurochem 102: 1053–1063.
8. Roberson ED, Scearce-Levie K, Palop JJ, Yan F, Cheng IH, et al. (2007) Reducing endogenous tau ameliorates amyloid beta-induced deficits in an Alzheimer's disease mouse model. Science 316: 750–754.
9. Muyllaert D, Kremer A, Jaworski T, Borghgraef P, Devijver H, et al. (2008) Glycogen synthase kinase-3beta, or a link between amyloid and tau pathology? Genes Brain Behav 7 Suppl 1: 57–66.
10. Wang ZF, Li HL, Li XC, Zhang Q, Tian Q, et al. (2006) Effects of endogenous beta-amyloid overproduction on tau phosphorylation in cell culture. J Neurochem 98: 1167–1175.
11. Forde JE, Dale TC (2007) Glycogen synthase kinase 3: a key regulator of cellular fate. Cell Mol Life Sci 64: 1930–1944.
12. Phiel CJ, Wilson CA, Lee VM, Klein PS (2003) GSK-3alpha regulates production of Alzheimer's disease amyloid-beta peptides. Nature 423: 435–439.
13. Lochhead PA, Kinstrie R, Sibbet G, Rawjee T, Morrice N, et al. (2006) A chaperone-dependent GSK-3beta transitional intermediate mediates activation-loop autophosphorylation. Mol Cell 24: 627–633.
14. Terwel D, Muyllaert D, Dewachter I, Borghgraef P, Croes S, et al. (2008) Amyloid activates GSK-3beta to aggravate neuronal tauopathy in bigenic mice. Am J Pathol 172: 786–798.
15. Ryves WJ, Harwood AJ (2001) Lithium inhibits glycogen synthase kinase-3 by competition for magnesium. Biochem Biophys Res Commun 280: 720–725.
16. Chalecka-Franaszek E, Chuang DM (1999) Lithium activates the serine/threonine kinase Akt-1 and suppresses glutamate-induced inhibition of Akt-1 activity in neurons. Proc Natl Acad Sci U S A 96: 8745–8750.
17. Rockenstein E, Torrance M, Adame A, Mante M, Bar-on P, et al. (2007) Neuroprotective effects of regulators of the glycogen synthase kinase-3beta signaling pathway in a transgenic model of Alzheimer's disease are associated with reduced amyloid precursor protein phosphorylation. J Neurosci 27: 1981–1991.
18. Noble W, Planel E, Zehr C, Olm V, Meyerson J, et al. (2005) Inhibition of glycogen synthase kinase-3 by lithium correlates with reduced tauopathy and degeneration in vivo. Proc Natl Acad Sci U S A 102: 6990–6995.
19. Caccamo A, Oddo S, Tran LX, LaFerla FM (2007) Lithium reduces tau phosphorylation but not A beta or working memory deficits in a transgenic model with both plaques and tangles. Am J Pathol 170: 1669–1675.
20. Mershin A, Pavlopoulos E, Fitch O, Braden BC, Nanopoulos DV, et al. (2004) Learning and memory deficits upon TAU accumulation in Drosophila mushroom body neurons. Learn Mem 11: 277–287.
21. Ubhi KK, Shaibah H, Newman TA, Shepherd D, Mudher A (2007) A comparison of the neuronal dysfunction caused by Drosophila tau and human tau in a Drosophila model of tauopathies. Invert Neurosci 7: 165–171.
22. Wittmann CW, Wszolek MF, Shulman JM, Salvaterra PM, Lewis J, et al. (2001) Tauopathy in Drosophila: neurodegeneration without neurofibrillary tangles. Science 293: 711–714.
23. Ruel L, Bourouis M, Heitzler P, Pantesco V, Simpson P (1993) Drosophila shaggy kinase and rat glycogen synthase kinase-3 have conserved activities and act downstream of Notch. Nature 362: 557–560.
24. Jackson GR, Wiedau-Pazos M, Sang TK, Wagle N, Brown CA, et al. (2002) Human wild-type tau interacts with wingless pathway components and produces neurofibrillary pathology in Drosophila. Neuron 34: 509–519.
25. Mudher A, Shepherd D, Newman TA, Mildren P, Jukes JP, et al. (2004) GSK-3beta inhibition reverses axonal transport defects and behavioural phenotypes in Drosophila. Mol Psychiatry 9: 522–530.
26. Finelli A, Kelkar A, Song HJ, Yang H, Konsolaki M (2004) A model for studying Alzheimer's Abeta42-induced toxicity in Drosophila melanogaster. Mol Cell Neurosci 26: 365–375.
27. Crowther DC, Page R, Chandraratna D, Lomas DA (2006) A Drosophila model of Alzheimer's disease. Methods Enzymol 412: 234–255.
28. Iijima K, Liu HP, Chiang AS, Hearn SA, Konsolaki M, et al. (2004) Dissecting the pathological effects of human Abeta40 and Abeta42 in Drosophila: a potential model for Alzheimer's disease. Proc Natl Acad Sci U S A 101: 6623–6628.
29. Rosen DR, Martin-Morris L, Luo LQ, White K (1989) A Drosophila gene encoding a protein resembling the human beta-amyloid protein precursor. Proc Natl Acad Sci U S A 86: 2478–2482.
30. Osterwalder T, Yoon KS, White BH, Keshishian H (2001) A conditional tissue-specific transgene expression system using inducible GAL4. Proc Natl Acad Sci U S A 98: 12596–12601.
31. McGuire SE, Mao Z, Davis RL (2004) Spatiotemporal gene expression targeting with the TARGET and gene-switch systems in Drosophila. Sci STKE 2004: pl6.
32. Latouche M, Lasbleiz C, Martin E, Monnier V, Debeir T, et al. (2007) A conditional pan-neuronal Drosophila model of spinocerebellar ataxia 7 with a reversible adult phenotype suitable for identifying modifier genes. J Neurosci 27: 2483–2492.
33. Crowther DC, Kinghorn KJ, Miranda E, Page R, Curry JA, et al. (2005) Intraneuronal Abeta, non-amyloid aggregates and neurodegeneration in a Drosophila model of Alzheimer's disease. Neuroscience 132: 123–135.
34. Bharadwaj PR, Dubey AK, Masters CL, Martins RN, Macreadie IG (2009) Abeta aggregation and possible implications in Alzheimer's disease pathogenesis. J Cell Mol Med 13: 412–421.
35. Nilsberth C, Westlind-Danielsson A, Eckman CB, Condron MM, Axelman K, et al. (2001) The 'Arctic' APP mutation (E693G) causes Alzheimer's disease by enhanced Abeta protofibril formation. Nat Neurosci 4: 887–893.
36. Feany MB, Bender WW (2000) A Drosophila model of Parkinson's disease. Nature 404: 394–398.
37. Papadopoulou D, Bianchi MW, Bourouis M (2004) Functional studies of shaggy/glycogen synthase kinase 3 phosphorylation sites in Drosophila melanogaster. Mol Cell Biol 24: 4909–4919.
38. Bourouis M (2002) Targeted increase in shaggy activity levels blocks wingless signaling. Genesis 34: 99–102.
39. Kinoshita E, Kinoshita-Kikuta E, Takiyama K, Koike T (2006) Phosphate-binding tag, a new tool to visualize phosphorylated proteins. Mol Cell Proteomics 5: 749–757.
40. Oh H, Irvine KD (2008) In vivo regulation of Yorkie phosphorylation and localization. Development 135: 1081–1088.
41. Hanger DP, Byers HL, Wray S, Leung KY, Saxton MJ, et al. (2007) Novel phosphorylation sites in tau from Alzheimer brain support a role for casein kinase 1 in disease pathogenesis. J Biol Chem 282: 23645–23654.
42. Hanger DP, Anderton BH, Noble W (2009) Tau phosphorylation: the therapeutic challenge for neurodegenerative disease. Trends Mol Med 15: 112–119.
43. Gotz J, Chen F, van Dorpe J, Nitsch RM (2001) Formation of neurofibrillary tangles in P301l tau transgenic mice induced by Abeta 42 fibrils. Science 293: 1491–1495.
44. Perez M, Ribe E, Rubio A, Lim F, Moran MA, et al. (2005) Characterization of a double (amyloid precursor protein-tau) transgenic: tau phosphorylation and aggregation. Neuroscience 130: 339–347.

45. Pennanen L, Gotz J (2005) Different tau epitopes define Abeta42-mediated tau insolubility. Biochem Biophys Res Commun 337: 1097–1101.
46. Doerflinger H, Benton R, Shulman JM, St Johnston D (2003) The role of PAR-1 in regulating the polarised microtubule cytoskeleton in the Drosophila follicular epithelium. Development 130: 3965–3975.
47. Su Y, Ryder J, Li B, Wu X, Fox N, et al. (2004) Lithium, a common drug for bipolar disorder treatment, regulates amyloid-beta precursor protein processing. Biochemistry 43: 6899–6908.
48. Hanger DP, Hughes K, Woodgett JR, Brion JP, Anderton BH (1992) Glycogen synthase kinase-3 induces Alzheimer's disease-like phosphorylation of tau: generation of paired helical filament epitopes and neuronal localisation of the kinase. Neurosci Lett 147: 58–62.
49. Mandelkow EM, Drewes G, Biernat J, Gustke N, Van Lint J, et al. (1992) Glycogen synthase kinase-3 and the Alzheimer-like state of microtubule-associated protein tau. FEBS Lett 314: 315–321.
50. Lovestone S, Reynolds CH, Latimer D, Davis DR, Anderton BH, et al. (1994) Alzheimer's disease-like phosphorylation of the microtubule-associated protein tau by glycogen synthase kinase-3 in transfected mammalian cells. Curr Biol 4: 1077–1086.
51. Brownlees J, Irving NG, Brion JP, Gibb BJ, Wagner U, et al. (1997) Tau phosphorylation in transgenic mice expressing glycogen synthase kinase-3beta transgenes. Neuroreport 8: 3251–3255.
52. Lucas JJ, Hernandez F, Gomez-Ramos P, Moran MA, Hen R, et al. (2001) Decreased nuclear beta-catenin, tau hyperphosphorylation and neurodegeneration in GSK-3beta conditional transgenic mice. Embo J 20: 27–39.
53. McGowan E, Eriksen J, Hutton M (2006) A decade of modeling Alzheimer's disease in transgenic mice. Trends Genet 22: 281–289.
54. Magrane J, Rosen KM, Smith RC, Walsh K, Gouras GK, et al. (2005) Intraneuronal beta-amyloid expression downregulates the Akt survival pathway and blunts the stress response. J Neurosci 25: 10960–10969.
55. Folwell J, Cowan CM, Ubhi KK, Shiabh H, Newman TA, et al. Abeta exacerbates the neuronal dysfunction caused by human tau expression in a Drosophila model of Alzheimer's disease. Exp Neurol 223: 401–409.
56. Joutel A, Tournier-Lasserve E (1998) Notch signalling pathway and human diseases. Semin Cell Dev Biol 9: 619–625.
57. Dierick H, Bejsovec A (1999) Cellular mechanisms of wingless/Wnt signal transduction. Curr Top Dev Biol 43: 153–190.
58. Drewes G, Ebneth A, Preuss U, Mandelkow EM, Mandelkow E (1997) MARK, a novel family of protein kinases that phosphorylate microtubule-associated proteins and trigger microtubule disruption. Cell 89: 297–308.
59. Nishimura I, Yang Y, Lu B (2004) PAR-1 kinase plays an initiator role in a temporally ordered phosphorylation process that confers tau toxicity in Drosophila. Cell 116: 671–682.
60. Iijima K, Gatt A, Iijima-Ando K (2010) Tau Ser262 phosphorylation is critical for A{beta}42-induced tau toxicity in a transgenic Drosophila model of Alzheimer's disease. Hum Mol Genet. epub ahead of print.
61. Gomez de Barreda E, Perez M, Gomez Ramos P, de Cristobal J, Martin-Maestro P, et al. Tau-knockout mice show reduced GSK-3-induced hippocampal degeneration and learning deficits. Neurobiol Dis 37: 622–629.
62. Iwata N, Tsubuki S, Takaki Y, Shirotani K, Lu B, et al. (2001) Metabolic regulation of brain Abeta by neprilysin. Science 292: 1550–1552.
63. Farris W, Mansourian S, Chang Y, Lindsley L, Eckman EA, et al. (2003) Insulin-degrading enzyme regulates the levels of insulin, amyloid beta-protein, and the beta-amyloid precursor protein intracellular domain in vivo. Proc Natl Acad Sci U S A 100: 4162–4167.
64. Miller BC, Eckman EA, Sambamurti K, Dobbs N, Chow KM, et al. (2003) Amyloid-beta peptide levels in brain are inversely correlated with insulysin activity levels in vivo. Proc Natl Acad Sci U S A 100: 6221–6226.
65. Eckman EA, Watson M, Marlow L, Sambamurti K, Eckman CB (2003) Alzheimer's disease beta-amyloid peptide is increased in mice deficient in endothelin-converting enzyme. J Biol Chem 278: 2081–2084.
66. Melchor JP, Pawlak R, Strickland S (2003) The tissue plasminogen activator-plasminogen proteolytic cascade accelerates amyloid-beta (Abeta) degradation and inhibits Abeta-induced neurodegeneration. J Neurosci 23: 8867–8871.
67. Leissring MA, Farris W, Chang AY, Walsh DM, Wu X, et al. (2003) Enhanced proteolysis of beta-amyloid in APP transgenic mice prevents plaque formation, secondary pathology, and premature death. Neuron 40: 1087–1093.
68. Ho L, Qin W, Pompl PN, Xiang Z, Wang J, et al. (2004) Diet-induced insulin resistance promotes amyloidosis in a transgenic mouse model of Alzheimer's disease. Faseb J 18: 902–904.
69. Killick R, Scales G, Leroy K, Causevic M, Hooper C, et al. (2009) Deletion of Irs2 reduces amyloid deposition and rescues behavioural deficits in APP transgenic mice. Biochem Biophys Res Commun 386: 257–262.
70. Iijima-Ando K, Hearn SA, Granger L, Shenton C, Gatt A, et al. (2008) Overexpression of neprilysin reduces alzheimer amyloid-beta42 (Abeta42)-induced neuron loss and intraneuronal Abeta42 deposits but causes a reduction in cAMP-responsive element-binding protein-mediated transcription, age-dependent axon pathology, and premature death in Drosophila. J Biol Chem 283: 19066–19076.
71. Tsuda M, Kobayashi T, Matsuo T, Aigaki T Insulin-degrading enzyme antagonizes insulin-dependent tissue growth and Abeta-induced neurotoxicity in Drosophila. FEBS Lett.
72. He B, Meng YH, Mivechi NF (1998) Glycogen synthase kinase 3beta and extracellular signal-regulated kinase inactivate heat shock transcription factor 1 by facilitating the disappearance of transcriptionally active granules after heat shock. Mol Cell Biol 18: 6624–6633.
73. Cohen E, Bieschke J, Perciavalle RM, Kelly JW, Dillin A (2006) Opposing activities protect against age-onset proteotoxicity. Science 313: 1604–1610.
74. Allen MJ, Godenschwege TA, Tanouye MA, Phelan P (2006) Making an escape: development and function of the Drosophila giant fibre system. Semin Cell Dev Biol 17: 31–41.
75. Rival T, Soustelle L, Strambi C, Besson MT, Iche M, et al. (2004) Decreasing glutamate buffering capacity triggers oxidative stress and neuropil degeneration in the Drosophila brain. Curr Biol 14: 599–605.
76. Ganetzky B, Flanagan JR (1978) On the relationship between senescence and age-related changes in two wild-type strains of Drosophila melanogaster. Exp Gerontol 13: 189–196.
77. Allen MJ, Shan X, Caruccio P, Froggett SJ, Moffat KG, et al. (1999) Targeted expression of truncated glued disrupts giant fiber synapse formation in Drosophila. J Neurosci 19: 9374–9384.
78. Tanouye MA, Wyman RJ (1980) Motor outputs of giant nerve fiber in Drosophila. J Neurophysiol 44: 405–421.
79. Gorczyca M, Hall JC (1984) Identification of a cholinergic synapse in the giant fiber pathway of Drosophila using conditional mutations of acetylcholine synthesis. J Neurogenet 1: 289–313.
80. Burns M, Gaynor K, Olm V, Mercken M, LaFrancois J, et al. (2003) Presenilin redistribution associated with aberrant cholesterol transport enhances beta-amyloid production in vivo. J Neurosci 23: 5645–5649.